Severe Slugging with Multiphase Fluid Transport and Phase Separation in Subsea Pipelines

By

© Loveday Chidozie Igbokwe

A thesis submitted to the School of Graduate Studies

in partial fulfillment of the requirements for the degree of

Doctor of Philosophy

Faculty of Engineering and Applied Science

Memorial University of Newfoundland

St. John's, Newfoundland and Labrador

January 2020

ABSTRACT

Flow assurance and separation of multiphase oil and gas flows are becoming more challenging as offshore development advances into more difficult environments. Petroleum fluids are required to be transported to processing facilities over long distances and through difficult terrain, as well as under varying temperatures and pressures. Severe slugging is a well-known flow assurance problem that limits effective offshore petroleum production. Gas-lifting and topside choking have been used for decades to mitigate this flow problem in fluid transport and processing. However, the application of these techniques has been challenged by design, cost, and footprint constraints. The introduced complexities require detailed understanding of the detailed dynamics of fluid flow in highly compact designs.

Systematic experimental and modeling investigations of severe slugging in pipeline-riser systems can provide useful information on these slugging mechanisms and characteristics. Experimental studies are conducted in this thesis to determine the mechanisms and key parameters involved in the slugging performance in fluid processing installations. Through well designed experimental tests, the impacts of actuators on slugging are examined. This thesis also focuses on control systems to suppress slugging in the pipeline-riser system using experimental analysis and control models. The research also presents new models that predict phenomena of slugging behaviour, and more importantly, fitting for control designs in offshore flow separation.

Furthermore, this thesis identifies and quantifies the process variables and conditions associated with both slugging and non-slugging regions, leading to the development of more effective solution methods and correlations. Relevant correlations (including

slugging frequency, production rates, gas injection rate, compression requirements, and operating pressures) are developed by dimensional analysis techniques. The study develops new models, data and useful information for better understanding of slugging in pipeline systems. Sensitivity analyses to assist in the selection and design of more accurate control methods are also presented. The research outcomes provide improved and more robust models and guidelines for implementing slugging mitigation measures.

ACKNOWLEDGEMENTS

I wish to express my profound gratitude to my supervisor, Prof. Greg Naterer for his patience, training, mentorship and guidance during my doctoral degree program at Memorial University. It is a great privilege to have worked under his supervision. I have greatly benefitted from his leadership and expertise in research, technical reporting, presentation, multiphase flow, and engineering analysis. I would also like to acknowledge my co-supervisor, Dr. Sohrab Zendehboudi, for his great support, training and encouragement throughout the research work. I am deeply grateful to my former supervisor Dr. Enamul Hossain for giving me the opportunity to study at Memorial University and his valuable expertise, training and instructions.

I sincerely thank my lovely wife Joan and my beautiful children, Pearl and Grace. They have been a great source of joy and motivation. Joan supported me immensely and sacrificed a lot in taking care of our children while I was away in Denmark for experimental studies and providing us with quality care, nutritious meals and emotional support. I am forever grateful to my parents and siblings, as they are irreplaceable.

I would like to also thank Memorial University (NL, Canada), Equinor Canada, and the Natural Sciences and Engineering Research Council of Canada (NSERC) for their financial support.

I am indebted to my friends, Dr. Simon Pedersen and the offshore team at the Energy Department of Aalborg University, Esbjerg Campus, for their helpful support, stimulating discussions and resources they provided. I also appreciate the team support of my

colleagues, Murtada Elhaj, Javad Kondori, Barun Maity and others. Finally, I appreciate the prayers, friendship and support of all members of the Faith Bible Chapel, St. John's.

DEDICATION

This work is dedicated to my parents, the late Mr. Michael Igbokwe and Mrs. Priscilla Igbokwe.

TABLE OF CONTENTS

NOMENCLATURE

A = Pipe cross-sectional area, m^2

D_p = Pipeline diameter, m

D_r = Riser diameter, m

ΔP = Pressure change, Pa

f_s = Slug frequency, Hz

g = Gravitational acceleration, m^2/s

h_L = Liquid film height, m

L_r = Riser length, m

L_p = Pipeline length, m

$L_{p\theta}$ = Length of inclined section of pipeline, m

L_t = Total pipeline length, m

P = Pressure, Pa

R = Universal gas constant, J/ (kg K)

T = Temperature, K

U_m = Mixture velocity, m/s

w_{mix} = Mixture flowrate, m^3/s

U_{sg} = Superficial gas velocity, m/s

U_{sl} = Superficial liquid velocity, m/s

w_l = Mass flow rate of liquid, kg/s

w_g = Mass flow rate of gas, kg/s

U_{sg} = Superficial gas velocity, m/s

U_{sl} = Superficial liquid velocity, m/s

ρ_l = Liquid density, kg/m^3

v = Characteristic velocity, m/s

θ = Inclination angle, degrees

Z = Riser-top choke opening, percent

R_e = Reynolds number

F_r = Froude number

B_e = Bejan number

Kc = Koulegan- Carpenter number

Greek symbols

α = Void fraction in the pipeline

θ = Angle of the inclined section of the pipeline to the vertical

u = Average liquid holdup in the riser

μ_l = Liquid viscosity, Pa.s

μ_g = Gas viscosity, Pa.s

ρ_g = Gas density, kg/m^3

ρ_l = Liquid density, kg/m^3

ε = Pipe roughness

Subscripts/superscripts

r = riser

p = pipeline

m = mixture

$*$ = dimensionless

List of Abbreviations

GVF = Gas volume fraction

SISO = Single-input-single-output

SIMO = Single-input-multiple-output

MIMO = Multiple-input-multiple-output

SS1 = Severe slugging type 1

SS2 = Severe slugging type 2

PI = Proportional integral

PID = Proportional integral derivative

PDR = Pressure drop ratio

LIST OF TABLES

LIST OF FIGURES

1 INTRODUCTION

1.1 Background

The offshore Newfoundland and Labrador oil and gas industry has origins dating back to the 1970*s*, with the development of its first oilfield, called Hibernia. The oilfield is located on the Grand Banks in the Jeanne d'Arc Basin, about 315 km east of St. John's and holding over 800 million barrels of oil. The platform produced its first barrel of oil in 1997 (CNOLPB, 2008; Higgins, 2009). Since then, the oil and gas industry has grown in Newfoundland offshore waters, increasingly developing more petroleum fields.

In the primary extraction phase for typical oilfield developments, the well's fluids are transported to the surface production facilities through a single flowline-riser system, but over time as more reservoirs and nearby fields are developed, subsea tie-backs become more feasible and economically efficient for fluid transport and processing. The increased oil and gas production from the multiple reservoirs and adjacent wells impact the production, transport, and separation. As a result, they strain the processing facilities and increase flow assurance problems. Figure 1.1 shows a typical configuration of a pipeline-riser system used in offshore fluid transport and processing.

The major flow assurance issues encountered in the offshore installation include slugging, hydrate formation, and wax deposition. These conditions affect safe and economical transport of the produced fluid to the downstream processing facilities.

The slugging flow regime has been characterized in several ways. A slug flow can occur when small fluid bubbles coalesce to form layers of larger-sized bubbles (Naterer, 2018).

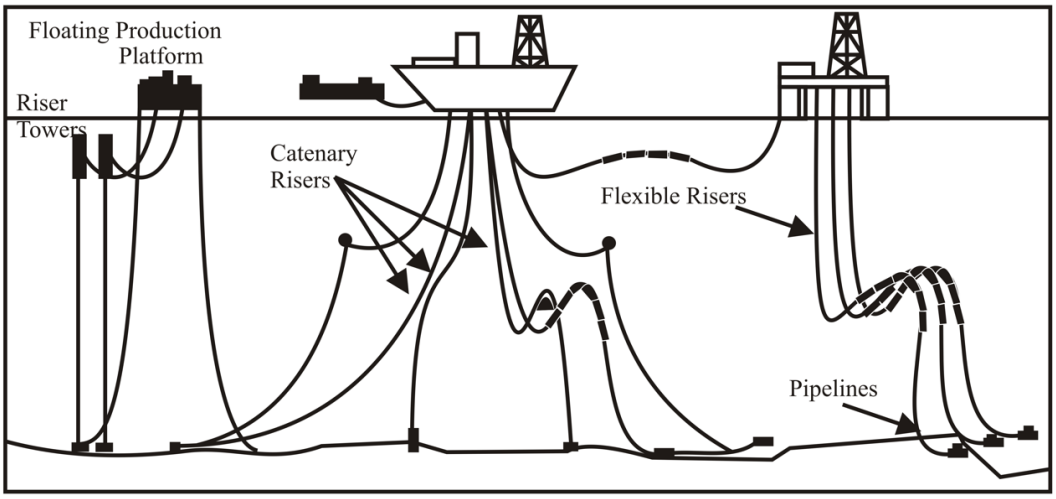

Figure 1.1 Typical offshore oil and gas production installation

Another definition is that it occurs when the gas holdup in the liquid slug is higher than 10% for an elongated flow regime (Kokal & Stanislav, 1989). Slugging occurs mostly due to fluid chemistry, topography, and flow conditions. The presence of slugs in the pipelines causes higher instabilities, limits fluid processing capacities, and strains the production equipment. Slugging flow regimes can also cause frequent shutdowns, thereby shrinking crude oil sales. For example, 50% of production losses are attributed to equipment limitations in handling production variations (Zhuo et al., 2018). Furthermore, the inherent space and weight restrictions in offshore operations cause separation prices to rise when dealing with these flow issues. Thus, the reduction of instabilities in the flow stream is preferred before oil is delivered at the receiving facilities. These issues continue to be challenging for the industry and affect offshore fluid transport and separation activities. Improving flow stability and separation capabilities has potentially major economic, safety, and environmental benefits. Motivated by these shortcomings in current technology and

applications, this study aims to develop new models and implement improved anti-slug control techniques.

1.2 Problem Formulation

This research identifies three key challenges as follows.

a) Two proven techniques for slug elimination are topside choking and gas lift. A third approach involves a combination of these schemes. Choking can be implemented by reducing the opening of the fluid outlet at the topside of the riser (Z Schmidt, Brill, & Beggs, 1979), while gas lift involves injecting gas at the bottom of the riser where the liquid loading tendency is most anticipated (Hill, 1990; Hill & Wood, 1994; Pots, Bromilow, & Konijn, 1987). Several studies have described these mechanisms and applications. Some research investigations have reported on how each technique affects other involved techniques, especially when applied simultaneously.

b) Researchers have been investigating the application of control oriented models and feedback control techniques via topside choking to eliminate slugging (Di Meglio, Kaasa, & Petit, 2009; Di Meglio, Kaasa, Petit, & Alstad, 2010a; Jahanshahi & Skogestad, 2014, 2015; Jahanshahi, Skogestad, & Helgesen, 2012; Skogestad & Postlethwaite, 2005). Analysis of the choke behaviour and the controllability analysis have also been presented (Jahanshahi & Skogestad, 2014; Jahanshahi et al., 2012; Pedersen, Durdevic, & Yang, 2017). These models have been used to gain insight into slug attenuation mechanisms. However, these models have many simplifying assumptions, particularly involving the geometry, which significantly affects the slugging process. As a result, the models often do not accurately represent the real

system (Di Meglio, Kaasa, Petit, & Alstad, 2012). Therefore, robustness of the existing models is limited in the assessment and design of slug control schemes for real systems.

c) Current designs of two-phase process facilities often aggravate slugging and prohibit the effective performance of slug control measures. More reliable prediction of slug frequency, slug velocity, and production rate are needed for more accurate characterization of flow, selection and design of appropriate mitigation methods. Slugging frequency is particularly crucial in topside process facility design. This is required as an input parameter for mechanistic models. Although there are several past research works on standard slug frequency in both horizontal and inclined pipelines, a few studies have been conducted to predict severe slugging frequency in offshore applications. In this thesis, an experimental investigation will be carried out with air-water two-phase flow in a pipeline-riser system.

1.3 Research Objectives

This study will seek to address the above challenges through meeting the following objectives.

a) This thesis will compare the performance and potential of various actuators to suppress slugging during transport of multiphase fluids in pipeline-riser systems. The comparison will be conducted based on the following criteria: the capability to control and stabilize the undesired unstable flow regime; ability to optimize fluid production; operating costs; and safety requirements for operating offshore installations.

b) This research is intended to improve the existing anti-slug models by introducing a riser geometry, which significantly affects the slugging process, and hence improves the model robustness.

c) The study will develop non-dimensional correlations for determination of vital operating parameters such as slug frequency and production flow rate for evaluation, design, and implementation of slug control. The models would be useful for controller design and system analysis.

2 LITERATURE REVIEW

2.1 Overview of Multiphase Flow in Pipes

Multiphase flow is the concurrent flow of two or more phases, liquid, solid or gas, where the motion influences the interface between the phases. The flow regime or flow pattern is a qualitative description of the phase distribution in the pipe. Three major types of flow regimes are identified in gas-liquid transportation pipelines, which include: segregated, intermittent and distributive flows. Segregated flow can be stratified smooth, stratified wavy, or annular flow regimes. The intermittent flow regimes are classified into slug flow and plug (elongated bubble) flow, while distributive flow regimes include bubble, and mist flows. In the bubble flow, gas bubbles tend to float at the top of the liquid. In the stratified flow, the gas and liquid interface is distinct due to gravitational separations. The liquid flows along the bottom of the pipe, and the gas flows at the top. Intermittent or slug flow is characterized by large frothy slugs of liquid alternating with large gas pockets; the bubbles coalesce to make layer groups of bubbles with a combined size (Naterer, 2018). In the case of annular flow, a liquid ring is attached to the pipe wall with gas rapidly blowing through the center of the pipe due to increased vapor pressure (Osman, 2001) Figure 2.1 illustrates typical flow patterns in a vertical pipe.

Multiphase flow occurs in almost all producing oil and gas wells and surface pipes that transport produced fluids. The differences in densities and viscosities of these fluids make multiphase flow much more complicated than the single-phase flow.

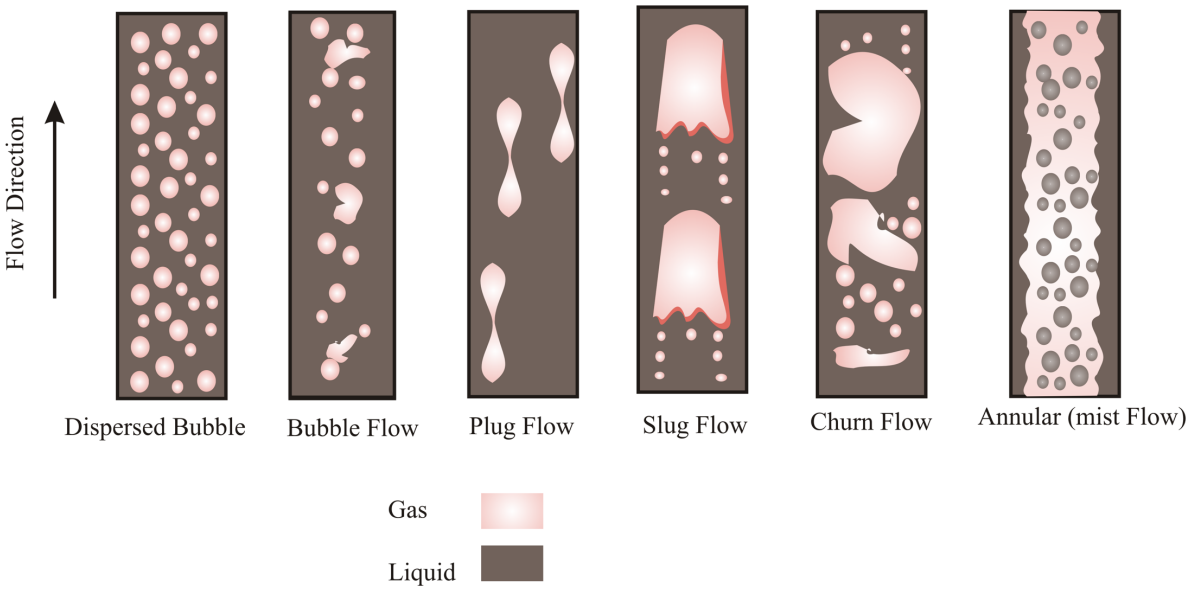

Figure 2.1. Typical flow patterns in vertical pipes

Predicting multiphase-flow behaviour in an oil and gas production system is further complicated by the geometry of the transportation path and the complex heat transfer that occurs as fluids flow through the piping system and the mass transfer that takes place among hydrocarbon fluids as pressure and temperature change. These phenomena are governed by conservation of mass, momentum, and energy, coupled with fundamental thermodynamics and heat transfer (Brill, 2010).

Flow properties such as pressure drop, flow velocities, liquid holdup, and void fractions are vital variables for multiphase process design inflow, but these variables are not readily obtained. Past researchers (e.g., Petalas et al., 2000) have examined the various flow properties for the major flow regimes, and presented empirical correlations for determining: (i) liquid/wall and liquid/gas interfacial friction, flow velocity, and slug

frequency in different slug, bubble, and stratified flows; (ii) liquid-fraction entrained, and interfacial friction in annular-mist flow; and (iii) the distribution coefficient used in the determination of holdup in intermittent flow. Typically, petroleum and chemical engineers rely on empirical correlations to calculate pressure traverses through tubing from the sand face to the wellhead (El Moniem and El-Banbi, 2015).

The prediction of flow properties such as pressure drop, flow velocity, liquid holdup, and phase distribution in risers is of great importance for accurate design and operation of surface facilities in offshore fields. Empirical steady-state correlations, mechanistic models, and dynamic models are documented for calculating the multiphase flow properties (Ruiz-Cárcel, Cao, Mba, Lao, & Samuel, 2015).

Abd El Moniem et al. (2015) presented correlations of pressure drop, fluid viscosity, and density for varied flow conditions, fluid properties, and well configuration. They analyzed an extensive database of pressure drop consisting of over 3,200 measured pressure points. The data was taken from survey and single-point measurements in over 800 wells representing significant variations of flow conditions, such as oil rate (50 to 31,000 BBL/D), water cut (0 to 98%), gas-oil ratio (0 to 20,000 SCF/STB), water gas ratio (0 to 200 BBL/MMSCF), and condensate gas ratio (0 to 200 BBL/MMSCF). They developed models for the wells and test conditions. They then analyzed the large database, and for every group, they compared the performance of the correlations. They also highlighted the parameters that mostly affect each correlation to aid engineers in decision making.

Ruiz et al. (2015) surveyed several notable multiphase flow correlations used in the petroleum industry such as Beggs and Brill (1973), Duns and Ros (1991), Govier and Aziz

(1972), Hagedorn and Brown (1965), Mukherjee and Brill (1985), and Orkiszewski (1967). Although many multiphase flow correlations cover most of the existing flow conditions, there are still no clear criteria to select appropriate correlations in the absence of flowing gradient survey data. Furthermore, the offshore petroleum production system needs new models that fit the current system upgrades and modifications.

2.2 Severe Slugging in Offshore Fluid Transport

The current offshore installations of oil and gas multiphase production and transport have serious challenges related to slugging, an unstable multiphase flow regime where the flow rates, pressures, and temperatures significantly oscillate, causing a potentially negative impact on downstream processing. Slugging in pipeline-riser systems can lead to significant fluctuations in gas and liquid flow rates (Andreolli et al., 2017; Azevedo et al., 2015; Baliño et al., 2010; Baliño, 2014; Jahanshahi et al., 2017). This can lead to severe vibrations in the riser, platform trips, reduced separation performance, reduced riser integrity, and a decrease in the overall safety. Severe slugging is usually caused by complex configurations in the installation and variations in operating conditions. The composition of the fluid can also affect the potential for slug flow. The most severe slugs are often induced in long vertical risers or production wells, where the liquid phase in the gas-liquid mixture blocks the gas at the riser base or bottom of the well, causing pressure to accumulate and consequently result in system oscillations (Carroll et al., 2005; Gudimetla et al., 2006; Jansen et al., 1996). Currently, deepwater oil and gas fields are often developed through subsea tie-backs to existing facilities (Fong et al., 2013; Hill & Wood, 1994; Pedersen et al., 2016; Pedersen et al., 2015), which increase the potential for slugging.

The various types of slugging phenomena, classifications, descriptions, and elimination methods have been documented by several researchers (Boe, 1981; Fabre et al., 1990; Jansen et al., 1996; Schmid and Henningson, 2012; Schmidt et al., 1980; Taitel, 1986; Taitel et al., 1990; Wordsworth et al., 1998). At constant inflow conditions, fluctuations in large-amplitude pressure and flow rates may occur in a pipeline-riser system operating at relatively low liquid and gas flow rates. This cyclic flow instability is called severe slugging (Alvarez et al., 2010; Azevedo, 2017; Cozin et al., 2013; Henau and Raithby, 1996; Ehinmowo et al., 2016; Malekzadeh et al., 2012; Mo, 2015; Zakarian, 2000)

Slugging is a common flow pattern in multiphase flow systems and oil and gas upstream production processes. The gas and liquid (water and oil) may not be evenly distributed throughout the production wells, transport pipelines, and risers due to a specific configuration and operating condition. The liquid and gas travel as a plugged section with a large plug of one phase medium followed by the other phase medium through the pipeline. As shown in Figure 2.1, these large plugs are often called slugs (Schmidt et al., 1980;Taitel, 1986; Taitel, Bornea et al., 1980; Taitel and Dukler, 1976). This type of irregular flow can result in very poor oil and water separation, reduced production capability, and extra fatigue loads on installations and facilities, thereby shortening device life-times, accelerating component corrosion, and even emergency shut-off of production (Taitel et al., 1990; Hassanein and Fairhurst, 1998; Havre and Dalsmo, 2001;Tengesdal et al., 2002; Eikrem et al., 2004; Eikrem, 2006; Aamo et al., 2005; Storkaas, 2005; Storkaas and Skogestad, 2004, 2007; Meglio et al., 2012). Severe slugging may lead to liquid accumulation and blowout in flow-line riser geometries (Kjeldby, Henkes, & Nydal, 2013). Naterer (2018) described how liquid slugs carried in multiphase gas-liquid flows may be

separated into regions consisting of small bubbles dispersed in the fluid system. Bubbles may coalesce to form larger sizes in layers as they are transported through the pipe.

As the petroleum industry matures and extends operations into harsher environments and deeper offshore locations, slugging in oil production systems is becoming more common and severe. Current trends of developing deepwater fields and producing from marginal fields via subsea tie-backs to existing facilities often lead to slugging. Similar problems can be seen in fields approaching their end of life, due to a decrease in gas coupled with an increase in water production. In these situations, large fluctuations in gas and liquid production may cause platform trips and riser vibrations, ultimately leading to production deferment, riser integrity/safety issue, and potential abandonment of fields operating near the end of life (Yaw et al., 2014). In riser slugging, flowrates and pressure oscillate repeatedly in an irregular manner most of the times. The irregular flow oscillations contribute to the lack of ability in achieving stability. In comparison to uncontrolled systems that would yield riser slugging, anti-slug control systems are preferred since they can stabilize the flow in pipelines at the same operating conditions, thereby limiting riser slugging (Storkaas, 2005).

Park and Nydal (2014) stated that large pressure fluctuations at the base of the riser are more severe in long riser systems, which are often used for deepwater developments. They explained that slugging in long risers can be up to 3,000 m long with high operating pressures (e.g., 130 bar to 150 bar for the first stage separator in the Gulf of Mexico) that can have significant safety implications.

Pedersen et al. (2015) reviewed some of the key challenges about slug detection, dynamic modelling, and elimination of slugging in flows. Mathematical modelling was used to

investigate the slug mechanism and anti-slug control. Most of the available models were based on mass-balance formulations, which often require sufficient data for reliable parameter tuning and identification. Slug elimination and control were investigated for many years and there exist many solutions proposed to eliminate slugging. However, some of these methods would simultaneously reduce the flow rate of oil and gas production, which is a key performance parameter in the offshore industry. Petersen et al. (2015) reported that although slugging in flow systems has been widely investigated in the past decade, many challenges remain unaddressed related to the cost-effective and optimal control and modelling of slugging.

2.2.1 Severe Slugging Experiments

Taitel et al. (1990) reviewed experimental studies on slugging in a pipeline-vertical riser to gain a better understanding of the characteristic behavior of slug flow in offshore fluid transport. The researchers measured the slug cycle time, surface velocities, and maximum penetration length of the liquid interface in a 5 degree downward-inclined flowline. From their experimental data, they classified the transient condition/regime after the gas movement into the riser as follows.

- Gas penetration followed by oscillation that leads to steady-state flow conditions (continuous gas penetration), where the gas penetration was never zero, and there is no blockage at the base of the riser.
- Gas penetration leading to a cyclic fluctuation without a liquid fallback, where there is no gas entering the riser, and the liquid interface progresses into the pipeline. However, gas is produced at the top of the riser, and the

liquid level continues to increase in the riser, thereby increasing the hydrostatic column.

- Gas penetration resulting in a cyclic process accompanied by liquid fallback, where there is gas accumulation close to the riser topside. The liquid flow rate is very low with a negative liquid velocity and a variable liquid level in the transient regime.

Malekzadeh et al. (2012) conducted experimental, theoretical, and numerical investigations of severe slugging in a relatively long pipeline-riser system. The experiments were carried out in a 65 m long, 50.8 mm diameter horizontal steel pipeline connected to a 35 m long, 50.8 mm diameter Perspex pipeline which is inclined at -2.54^0 from the horizontal, followed by a 15.5 m high, 45 mm vertical PVC riser, operating at the end at atmospheric pressure. The experimental facility also included a 250-litre gas buffer vessel, placed upstream of the pipeline, to obtain an extra pipeline compressibility. Air and water were used as the experimental fluids. They observed five types of flow regimes and characterized them based on the visual observations and the measured pressure drops over the riser. The transient slugs were generated upstream in the pipeline thereby blocking the riser base. They developed new models for the prediction of flow behaviour in the pipeline–riser system, which showed a good match with the data obtained from the experiments.

Alvarez et al. (2010) designed and constructed an experimental facility enabling acquisition of slug flow data split into parallel and looped lines. They reported 81 experimental test runs for various combinations of superficial gas and liquid velocities and acquired data on uneven split conditions by either utilizing a choke valve on one of the lines or different pipe diameters. For the symmetrical configurations of both the parallel

and looped cases with equal diameter lines, the authors showed that the phases were split equally into the lines. When the lines were subject to uneven split conditions, the phases were also split unevenly, with the gas phase preferring the line with lower flow resistance. The gas-phase flowed preferentially into the smaller resistance line. Therefore, the asymmetrical resistance configuration resulted in different gas-liquid ratios in the two lines, which were different from the gas-liquid ratio at the inlet. Their experiment led to the development of semi-analytical models for the prediction of the uneven splitting of gas and liquid. Good agreement was observed between the model predictions and the experimental data, with an average error of about 15% in the phase splitting and pressure drop.

Before the work of Xie et al. (2017), most experiments for severe slugging were conducted at atmospheric pressure. Several researchers (e.g., Guo, and Xie, 2017; Xie et al., 2017) performed experiments at elevated pressures to study the effect of topside pressure on severe slugging and also to understand the stability boundaries, amplitude and frequency of slugs formed in the pressure range of 0–50 bar. Their results showed that increased back pressure gives a reduced region of severe slugging in the flow pattern map, whereas it also mitigates pressure fluctuations and decreased the slug frequency. Based on their findings, the effect of back pressure on the stability analysis of slug flow was investigated.

Past experimental investigations focused on developing correlations for the void fractions, pressure drop, physical pipeline parameters (e.g., pipe diameters), and inclination angles to capture the sensitivities to slugging patterns (e.g., Andreussi and Bendiksen, 1989; Bendiksen, 1984).Past models have correlated: (i) the drift flow as a function of inclination angle, flow velocity, and slug frequency; and (ii) the void fraction as a function of pressure

and flow rates of fluids (e.g., air-water, stream-water, hydrocarbon, and oxygen). Most studies agree that slugging phenomenon is especially sensitive to the void fractions and phase velocities, as well as pipeline diameter, flow rate, downstream pressure and small variations in the position of the pipeline relative to the horizontal. Most models are also sensitive to surface tension and gas density. Although numerous empirical models exist for evaluating the slugging phenomenon, there is still a lack of adequate models that can predict flow parameters for offshore situations with an acceptable accuracy. Most of the past empirical correlations considered gravity-based separation capabilities, which can handle small pockets of slugs through its larger contact area within a reasonable retention time. However, the current slug mitigation methods and offshore development facilities are unequipped with large gravity-based separators. The desired compact technology, adapted for the most offshore operations, limits the application of current models and excludes the robustness of modern offshore designs.

2.2.2 Stages of Severe Slugging Development

Several researchers (Schmidt et al., 1979; Schmidt et al., 1980; Schmidt et al., 1985; Taitel, 1986; Taitel and Dukler, 1976) described the development cycle of severe slugging in terms of the following four stages: (1) slug formation; (2) slug movement into the separator; (3) blowout; and (4) liquid fall back. A study by Malekzadeh et al. (2012) highlighted the differences between all types of severe slugging and characterized the cycle of severe slugging in five stages: (1) blockage of the riser base; (2) slug growth; (3) liquid production; (4) fast liquid production; and (5) gas blow-down. Although the researchers produced a varying number of steps in developing severe slugging, the fundamental

concept is similar. The different stages of slug formation and growth in the subsea pipeline-riser system are illustrated in Figure 2.2.

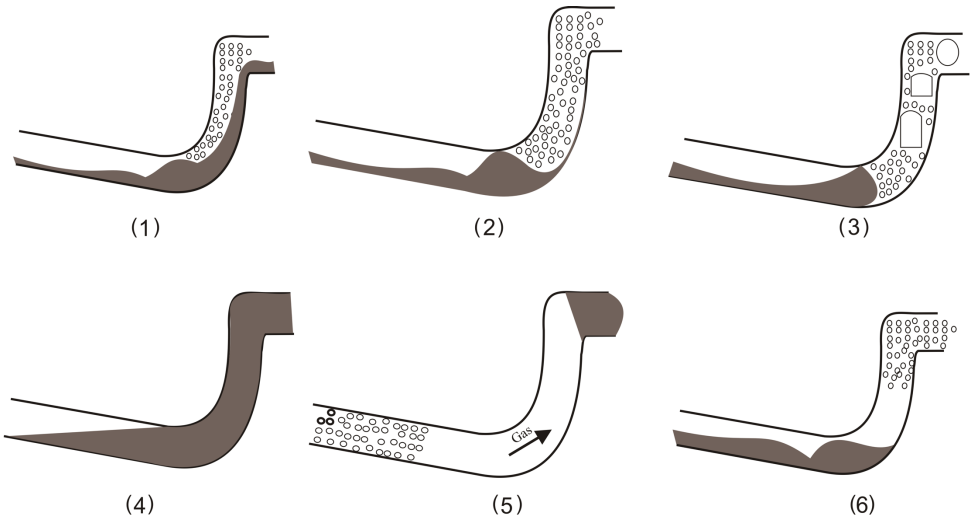

Figure 2.1. Stages of development of slugging in pipeline-riser systems: (1) liquid level riser; (2) pipeline blockage; (3) slug growth (elongated bubble in riser); (4) liquid production; (5) gas blowdown; and (6) gas production followed by liquid slugs.

2.2.3 Overview of Slug Elimination Methods

Riser induced slugging occurs in a production system when the liquid forms a blockage at the base of the riser mostly before the upward inclination. The blockage hinders the flow of gas into the riser section and gas accumulates behind the liquid, thereby decreasing downstream gas production to possible complete cessation. When the blockage occurs, downstream gas production decreases and may completely stop. The compressed gas accumulated behind the blockage eventually causes a blowout (a violet liquid production followed by large gas volume production). The violent slug production at the surface

processing facilities causes poor performance of fluid separation and stabilization. The repeated cycle of the liquid and gas surges can result in a more adverse effect on safety.

For over 20 years, several slugging elimination strategies have been developed. For any given control strategy, the aim is to maintain a constant total volumetric flow rate throughout the system to prevent blockage at the riser base. This section will briefly summarize the most common techniques for slug mitigation.

Gas lifting. Gas lift is one of the common methods for most installations and well-proven to maintain high production rates. For deepwater applications, gas lift becomes more challenging and uncontrollable. Many shortcomings arise from gas handling issues, e.g., Joule-Thompson cooling effects, cost, space, and weight constraints. Past studies (e.g., Pots et al., 1987) concluded that the volume of gas required to eliminate slugging may become unrealistic and impractical for field operations. The main results obtained from slug mitigation investigations will be briefly described in the following section.

Increasing pipeline pressure. This technique involves increasing the pipeline operating pressure. An increase in the pipeline pressure decreases the volume of gas in the pipeline, leading to an increase in the pipeline liquid holdup. Previous studies including Sarica and Tengesdal (2000) showed that the back pressure severely lowers production capacity, which is not viable for both shallow- and deepwater.

Self-gas lift. Past research work conducted by Sarica and Tengesdal (2000) proposed the transfer of pipeline gas (in-situ gas) to the riser section at the pit slightly above the riser base. It was found that the transfer process would reduce the hydrostatic head in the riser

and decrease the pipeline pressure, thereby mitigating or eliminating the slugging regime. They modified the drift flux model proposed by Zuber and Findlay (1967) and compared their results to experimental data that used the riser base as the transfer point. Their proposed method requires a by-pass to transfer gas from the pipeline to the riser base. This means that the success of the method depends on the efficiency of the gas transfer. Pressure losses in the by-pass will decrease the gas rate as well as the riser holdup. In their experimental investigation, Tengesdal et al. (2002) showed the physical mechanisms of the process and concluded that it is the best to place the injection point at the same level with the transfer point or slightly higher than the take-off point for attaining the maximum performance. The method did not require external gas injection and was shown to be insensitive to variations in both liquid and gas flow rates for a wide range of operating conditions. However, no field application has been reported to prove its effectiveness.

Riser base pressure control with surface control valve. In practice, this technique is similar to choking. It has been applied in a Dunber 16" pipeline-riser system in a Total field (Courbot,1996). The set-back reported for this application included high back pressures and an overall pressure increase in the production system. This problem makes the application of this technique unattractive, especially for deepwater applications, where a major reduction in the production rate is anticipated due to high back pressures.

Flow rate control. This approach involves the use of a control valve to maintain a constant volumetric flowrate at the choke outlet. The slugging is mitigated through the back pressures imposed by choking, whereas the production is kept at minimal limits. There are some experimental studies in the literature that have used the technique. It was found that

the back pressures are increased three times higher before the system becomes stable (Gong et al., 2014; Pots et al., 1987). A flow rate control method cannot be successfully applied in offshore installations as a result of the inherent low production and significant back pressure at the end of the flowline. Also, in offshore cases, there can be substantial delays in the response of the control system due to the expected long distance between the topside control and the bottom of the riser.

Pipe insertion. In this approach, smaller diameter pipes are inserted near the bottom of the riser system to reduce the incoming line diameter and achieve a stable flow regime. By reducing the incoming line diameter, continuous gas penetration is maintained (Tengesdal et al., 2002; Tengesdal et al., 2003). Thompson and Sarica (2003) carried out experimental work on a small water table with a slope of -3 degrees, and on oil-gas bed at inclination angles of -1, -3 and -5 degrees. According to their work, the best performance is obtained when the injection point of the bypass line is at the same level and slightly higher than the extraction point. The disadvantages of this method include additional cost and higher maintenance implications. Wax deposition, high gas velocities, and Joule Thompson cooling are also crucial concerns. Frequent plugging may be problematic, which affects the production schedule and increases maintenance costs.

Multiphase riser base lift. This technique involves the installation of multiple risers instead of the usual one riser system. A high-capacity multi-line enables some fluid productions to be diverted into other pipeline-riser production systems to eliminate the slugging or enhance start-up after the production is shut down. Previous studies (e.g., Tengesdal et al., 2002; Tengesdal et al., 2003) presented a model in a permanent regime

that permitted the evaluation of the conditions for the successful operation of the self-lifting method. A similar study by Boe (1981) predicted a considerable reduction of the unstable region using this method. The maximum and minimum values of pressure drop were deducted through the by-pass for gas-lift operation. These values were compared with experimental measurements (Tengesdal et al., 2002; Tengesdal et al., 2003). This method has been considered superior to the riser base gas lift because the lift fluids did not cause cooling (Yocum, 1973). Although no gas injection facilities are installed for this method, additional multiphase lines should be available for its application. Therefore, it is proposed as a case-specific operation.

Foaming. This technique involves the injection of foaming agents, which can attenuate the non-homogenous fluid into a homogeneous fluid by reducing the surface tension (Hassanein and Fairhurst, 1998). Although it is possible to achieve homogeneity of the multiphase flow, there is separation at the low-pressure topside that reduces the quality of the fluid (Pedersen et al., 2016). The mechanism was not described with enough details, and no field application has been reported for pipeline-riser systems.

Subsea separation. The subsea method does not impose back pressure on the system. It has the potential of fulfilling the gas use requirements, achieving zero flare regulations, and reducing gas use and costs. Two separate flowlines and a liquid pump are required to pump liquid to the surface processing facilities. Most of the gas phase is separated, which allows mostly the liquid phase to enter the separator for higher fluid recovery. One of the most successful compact technologies is the inline separator (Boschee, 2013; Chin et al., 2002; Fong et al., 2013; Frankiewicz et al., 2001; Gomez et al., 2002; Gomez et al., 2000;

Knudsen et al., 2010; Schook and Thierens, 2011; Schook and Asperen, 2005; Swanborn and Egwim, 2011).

Inline separation technology (ILS) can handle increased throughput from: (1) higher production rates; (2) third party processing; (3) new resources tied to existing facilities; and (4) first pass separation of the gas phase from the liquid flow stream (Gomez et al., 2000; Knudsen et al., 2010; Schook and Thierens, 2011; Schook and Asperen, 2005; Swanborn and Egwim, 2011). Various configurations of ILS equipment are targeted to achieve high centrifugal acceleration (Arpandi et al., 1996). The liquid dominated feed stream is passed through a low-pressure mixing element to create bubbles in the flow stream to avoid a stratified flow regime (Schook and Thierens, 2011; Schook and Asperen, 2005). A swirl turbine device stationed at the inlet initiates accelerated rotation. An inline degasser may be installed at the inlet to initiate accelerated circulation of the feed hydrocarbon (HC) mixtures. Phase separation based on density differences occurring in the system will move the gas phase to the center of the cyclone to form a stable core through a vertical scrubber section, while the liquid phase is carried through the main flowline. The inline separators, unlike their large conventional counterparts, are very sensitive towards variations in the multiphase flow to be separated.

Leskens et al. (2011) followed a model-based approach to improve the capabilities of ILS to handle minor flow variations. More specifically, they proposed a new approach for control-oriented modelling of gas/liquid (G/L) ILS. They presented a feed-forward control-based method for fast approximation of closed-loop performance limits of a G/L ILS. This enabled an acceleration in the overall G/L ILS design speed. The merits of the method were

demonstrated through a simulation-based application on a commercially available G/L ILS (Leskens et al., 2011; Swanborn and Egwim, 2011). Areas of future research include modelling the hydrodynamic behaviour of multiphase flow at the inlet of the inline separator, and specifically, the effects of the inlet geometry on the separator performance. Compact separator systems (inline separator devices) have recently been applied in offshore fields such as Trolls and Tordis, Pazflor, Marlim, Perdido and Parques das Conchas (Kristiansen et al., 2016). Under variable flow conditions, ILS performance is significantly reduced. Severe flow fluctuations, excessive liquid level rise, pressure surges, high gas velocities (re-entrainment), and high GOR have been reported in the literature (Kristiansen et al., 2016).

Choking. This method involves a manual reduction of the choke opening to induce back pressures and reduce the flow rate. Choking is a proven technique to reduce or eliminate severe slugging. Careful choking is needed to have a minimum back pressure in the production system. Excess back pressures and reduction in the production rate are reported set-backs to the choking method. For deepwater systems, the back pressure increase could even be worsened due to potential production losses.

Gas-lift and choking combination. This technique was reported to be a viable method and a field application was published for combined choking and gas lift for an offshore Nigerian field (Yaw et al., 2014). It might alleviate some of the cooling and excessive frictional pressure loss problems by requiring less injection gas. It will require injection gas and the necessary gas lift installation.

Active choking. The concept of active choking is to use the flow responses to suppress riser induced slugging. The benefits of active slug control are that it does not require additional space and weight since the choke control valve is already installed. Only localized measurements of pressures and flow rates are used by the controller as controlled variables. Both the liquid and gas surges of the fluid production are acted upon by the active choke without the need for prior separation. This advantage allows the controller to stabilize the production arriving at the processing facilities, thereby enabling production optimization and boosting. The active control technique also stabilizes the liquid level in the separator, allowing for proper separation and reduced pressure on the processing vessels. The process control allows operation of the the system stably within the unstable operating envelope due to the ability of the control loop to respond to system instabilities dynamically, even with minor variations in operating conditions.

Shell slug suppression system (smart choke). This smart choke method involves the application of feedback control to control slugs. The technology uses a single control valve, which is installed between the riser top and first stage separator. The smart choke regulates liquid and gas flow rates by manipulating the control valve opening. Compared to conventional slug management techniques which require large footprints and high capital/operating costs, a smart choke is compact and cost-efficient. Smart chokes have been installed in the Gulf of Mexico and Malaysia (Yaw et al., 2014). The smart chokes were tested in these fields and proven to be capable of suppressing riser-induced slugs and controlling slugs initiated in horizontal pipelines. Practical field applications were reported over a one-year extension in oilfield productions with about a 5% to 10% production

increase (Fong et al., 2013; Knudsen et al., 2010; Lage and Time, 2000; Yaw et al., 2014). They presented field data to demonstrate the recorded improved fluid recovery.

2.2.4 Dynamic Modelling of Severe Slugging and Stability Criteria

Prior modelling investigations on severe slugging have focused mostly on numerical modeling, simulation of steady-state flows, and stability criteria analysis (Tailtel and Duckler, 1976; Boe, 1984; Balino, 2010). Taitel and Dukler (1976) presented analytical models for the prediction of the transition between flow regimes of biphasic flow. Their study developed models for determining the transition curves and characterizing the different flow regimes (e.g., intermittent, stratified, dispersed bubble, annular, and scattered flows). Another study presented stability criteria based on the disturbance of the steady-state conditions during gas penetration in the riser (Taitel, 1986). Since the early 1990s, steady-state modelling of slugging led to several transient models based on the mass and momentum equations.

Sarica and Shoham (1991) introduced a 1-D transient model for two-phase flow in a pipeline-riser system. It was found that the flow is dominated by gravity and the effects of inertia are neglected. Their model assumed stratified flow in the pipeline with a constant void fraction. It used the continuity equations for the riser section. They included important physical characteristics of the severe slugging phenomenon, such as the discontinuity in the conduit due to the accumulation of liquid, variation of liquid level, and a void fraction in the riser. The model results were compared with the data/results from several experimental studies for vertical risers (Fabre et al., 1990). These experimental measurements were also presented on the stability maps of the past study (Boe, 1981) by

plotting their gas and liquid velocities. Some data corresponding to the severe intermittence were observed to fall outside the unstable region predicted by these maps, implying that, even for simple geometries such as vertical risers, there is no satisfactory stability criterion. The results demonstrated that the model achieved stability and could predict the slugging phenomenon. However, the results showed a systematic error in the periods of the cycle of severe slugging and lack of convergence for some cases. The authors attributed the lack of convergence to inertial effects.

Masella et al. (1998) modelled transient multiphase flows in a pipeline-riser system using a two-fluid model, a simplified drift flux model and a no-pressure wave model. They implemented the two-fluid model in OLGA commercial software. For the drift-flux approach, the researchers solved two conservation equations, one for each phase for the pipeline section and a single momentum equation for the riser section. They used an algebraic relation for the slip closure. The authors showed that the results obtained for the three different approaches were similar. Wörner (2003) summarized the major numerical simulation methods of multiphase flow in pipes. The researcher concluded that the drift flux model is widely used and more efficient based on its well-posedness for all flow conditions (Baliño et al., 2007; Baliño et al., 2010; Fabre et al., 1990; Malekzadeh et al., 2012; Sarica and Tengesdal, 2000; Sarica and Shoham, 1991).

Balino et al. (2010) presented a transient model for simulations of various transient conditions in a pipeline-riser system. They developed a dynamic model for various local riser inclination angles, capable of identifying the different types of slugging through tracking of the liquid level in the riser and the liquid accumulation length in the pipeline. The model converged and was tested with experimental data of Wordsworth et al. (1998)

for a catenary riser, showing a good match. In other work by Baliño et al. (2014), they improved the previously published transient model by including inertial effects. They used a rigid water-hammer approximation to account for the inertia term in the riser. They considered the acceleration terms in the gas and liquid phases using the momentum equation and were able to calculate the values of the pressure drop and void fraction. Their model assumed an incompressible liquid phase in the mass conservation formulation and included a valve located at the top of the riser and a gas injection line at the bottom of the riser to aid in evaluating the valve closure and gas lift as mitigating actions for severe slugging.

Nemoto and Baliño (2012) examined the dynamics of a 3-phase flow (gas, oil, and water) in the pipeline-riser system with mass transfer effects. They reported that extrapolating results from air-water models to real petroleum production systems yield unrealistic outcomes. They attributed the poor performance to the behaviour of the multi-component fluids in the operating conditions (McCain, 1990; Nemoto and Baliño, 2012), and the high-pressure ratios between the bottom and top of the riser, which lead to a higher gas-phase expansion. This interpretation invalidates the mean void fraction assumption in past investigations. The authors modelled the flowline and riser sections as lumped and distributed parameters, respectively, for two scenarios; (1) continuous gas penetration into the riser, and (2) no-gas penetrating the riser due to blockage by the accumulated liquid. They accounted for the mass transfer effect using the black oil approximation procedure and compared their outcome with simulation results from the OLGA simulation software, leading to a good match.

Other researchers such as Gavrilyuk and Fabre (1996) presented a model based on the conservation equations for slugging during two-phase flow. Similar to the hypothesis used in developing the majority of past intermittent models, they considered the gas phase evolving as a perfect gas and isothermally. However, in their model, they assumed a gravity dominated flow with a constant void fraction. The effects of inertia were also neglected.

Different numerical simulations have been presented for multiphase flow in pipeline-riser systems. Most of the simulations are based on mass, momentum, and energy conservation. Although the goal of each model differed in various cases, most focused on stability analysis and production optimization. The OLGA simulator, which is widely used for design and analysis of multiphase transport**,** was developed in 1980 (Malnes and Bendiksen, 1980). It uses five mass equations, two momentum equations, three slip relationships, and one mixture energy equation for the conservation equations (Meringdal, 2014). The simulator works by discretizing the pipeline into multiple segments. Its accuracy increases as the number of segments increases (Meringdal, 2014). Although the OLGA model is robust and can provide detailed flow information, it is not suitable for control design, because there are too many differential equations resulting from the multiple segments (Jahanshahi, 2014), and many of the variables are not available to the user.

Flow Manager by FMC Technologies is another common numerical simulator that is used for simulating several aspects of the process equipment in both steady-state and transient situations. The dynamic part is used for testing control systems, and for testing different procedures such as start-ups and system shutdowns. The multiphase simulations are built based on the OLGA simulator (Park and Nydal, 2014).

2.2.5 Review of Dynamic Slug Flow Modelling

Most of the past models assume a stratified flow regime in the pipeline and use a constant void fraction determined as a stationary state for the numerical simulations. As a result, in most cases, the momentum balance equations are not satisfied, which prevents the determination of void fraction variations in the transient state. This may explain why most of the models did not converge. Furthermore, a riser model with a simplified momentum equation that considers only the gravity force has limitations to deal with general boundary conditions. Accounting for a discontinuous pressure boundary condition, a discontinuous time variation in the void fraction distribution and a superficial distributional velocity would be necessary. A dominant gravity riser also affects the velocity profile and a discontinuous applied force. This limitation may lead to non-convergence problems reported in past literature (Taitel et al., 1990, Sirica and Shoham, 1991).

When the riser topside choke opening is altered discontinuously, a discontinuous pressure boundary is observed at the severe slugging development stage for a constant valve opening (Balino, 2014). The discontinuous superficial velocities lead to unrealistic results when the multiphase mixture reaches the top of the riser, because the pressure drop across the choke valve for a mixture flow is significant compared to cases where only gas is produced through the conduit.

2.2.6 Review of Control-Oriented Modelling

Schmidt et al. (1979a) proposed an alternative to the traditional method of attenuating riser slugging, based on feedback control. They developed an algorithm that uses a pressure

measurement located upstream of the riser, and flow measurement in the riser as inputs, to automatically adjust the topside choke valve position. Mokhatab et al. (2007) reviewed the technologies for remediating the problems associated with severe slugging in pipeline-riser systems. They also studied the feasibility and potential of applying dynamic feedback control to unstable multiphase flow such as severe slugging and casing heading (Jansen et al., 1999).

Havre et al. (2000) demonstrated the use of dynamic feedback control to solve severe slugging problems in offshore pipes, by comparing two control case studies – with feedback and without feedback. They presented field tests and dynamic multiphase flow simulation results from the OLGA simulator. The controllers applied to all cases aimed to stabilize the flow conditions by implementing feedback control and allowing a downstream processing unit to handle the slug flow. The results from simulations with feedback control provided stable process conditions both at the pipeline inlet and outlet for all cases. Pipeline profile plots of liquid volume fraction during a typical slug flow cycle were also compared against corresponding plots with applied feedback control. They used the results to justify internal stability of the pipeline, in which feedback control reduced the pipeline inlet pressure, leading to a higher production rate. In another study, Havre et al. (2001) showed that the actual minimum achievable pipeline inlet pressure, which is based on the inlet flow rate and gas-oil ratio, was much less than the corresponding pressure achieved by manual choking. It was noticed that a reduction in inlet pressure impacts wells connected to the pipeline significantly. Thus, it is clear that for wells with reduced lifting capacity, the variation in the pipeline pressure could cause the wells to stop producing.

Previous research studies (e.g., Nydal et al, 1992; Nydal et al., 2001) developed a control-oriented model for simulating slugging in the pipeline-risers system where three tuning parameters were used. They included more physics with some simplifying physical assumptions in the new model to fit the model correctly. However, their model was not able to match the results obtained from the OLGA dynamic simulator. Their proposed model did not include any physical property of the system as a tuning parameter.

Storkaas (2003) developed a simplified model based on the mass balance equations for severe slugging in the flowline-riser system. The 1-D equations are shown below:

$$\dot{m}_{g,p} = w_{g,in} - w_{g,lp} \tag{2.1}$$

$$\dot{m}_{l,p} = w_{l,in} - w_{l,lp} \tag{2.2}$$

The mass conservation equations are similarly used to describe the riser system as follows:

$$\dot{m}_{g,r} = w_{g,in} - w_{g,out} \tag{2.3}$$

$$\dot{m}_{l,r} = w_{l,in} - w_{l,out} \tag{2.4}$$

In Equations (2.1) and (2.2), $\dot{m}$ is the change in the mass flow rate from the difference between the injected (w_{in}) and the outflow mass rates (w_{out}) for the gas (Equation (2.1)) and liquid (Equation (2.2)), respectively for the pipeline section. Also $\dot{m}$ in Equations (2.3) and (2.4) is the change in the mass flow rate between the mass flow entering the riser section and the mass outflow at the topside of the riser for the gas and liquid phases, respectively, for the riser section. The subscripts p, r, g and l denote the gas and liquid phases, respectively. The model uses an orifice equation at the low point (end of the pipeline section connecting the riser section) to simulate fluid transport from the horizontal flowline into the inclined riser.

The model has four states, which identify the major characteristics of the riser slugging system, including: (1) the flow stability as expressed as a function of choke valve position, (2) the nature of the transition to instability (Hopf bifurcation), (3) the presence of an unstable steady-state solution, and (4) the amplitude of the oscillations. Jahanshahi (2012) reported that it is more important for the model to describe the (desired) steady-state flow regime than the (undesired) slug behavior, especially for control analysis. They compared their results of the model to the OLGA simulation outputs and scaled experimental laboratory data. Both the OLGA and the experimental data were in good agreement with the model results. They demonstrated the capability of the model to describe the slug flow phenomenon as well as effective system control. Consequently, high-performance anti-slug controllers have been designed based on this model and proven by reported field applications for slug suppression (Calvert and Davis, 2010; Storkaas, 2005).

Storkaas et al. (2003) fitted a model to data both from an OLGA test case and from medium-scale experiments. It was reported that both cases achieved good agreement with the data. They also reported that the simplified model was easier to fit experimental data than the more complicated PDE-based two-fluid models which included more system details. A controllability analysis, which they performed from a PDE-based two-fluid model and simplified model, led to similar results, providing additional validation of the simplified model.

Storkaas et al. (2004) designed PID anti-slug controllers for a pipeline-riser system studied previousely by Storkaas (2003). The controller parameters were optimized based on the simplified, three-state model developed in Storkaas (2003). The choice of measurements was based on the controllability findings from Storkaas (2003). The controllers were tested

with simulations on both the simplified three-state model, the two-fluid model of Storkaas (2003) and the OLGA model. The researchers noticed that control is based on manipulating the valve position. Their studies also showed that single-input-single-output (SISO) PID controllers based on an upstream pressure measurement (pipeline inlet pressure or the riser base pressure) performed well. They also investigated the use of flowrate as the primary control variable. It was found that it can stabilize the process, but yield low-frequency performance. In a cascade control loop, the flow controller generated good results (Storkaas et al., 2004). They concluded that the pipeline inlet pressure measurements perform better in a cascade control loop compared to SISO control. They also reported that the pressure drop across the choke at the topside, or the valve opening size, as a control variable, stabilizes the system.

Di Meglio et al. (2010) proposed a model to represent the slugging flow regime in vertical risers. They developed a 1-D two-phase model, which consisted of a liquid phase and a gaseous compressible phase. Their model allowed them to predict periodic regimes. It also brought new insight into the physics of the slugging phenomenon. The model was relatively easy to tune and suitable for control design. Di Meglio et al. (2011) also studied the multiphase slugging flow phenomenon in oil production wells and flowlines. They used a distributed parameter model, comprising the gas mass fraction, pressure, and gas velocity as thermodynamic states. Utilizing appropriate boundary conditions on a 1-D space domain, they formulated a mixed initial-boundary value problem for a quasilinear hyperbolic system and employed the method of characteristics for the numerical simulation. They compared their results with experimental data from past literature. It was

shown that the period of simulated oscillations and their overall model matched well with published results.

Jahanshahi et al. (2011) proposed a dynamic model for severe slugging flow in pipeline-riser systems. The model, along with five other simplified models in the literature, were compared to the results from an OLGA® simulator. They recommended an active feedback control solution to prevent a severe slugging flow regime in multiphase transport pipelines. Instead of detailed models such as CFD and OLGA®, a relatively simple dynamical model with few state variables was used in a model-based control system (Jahanshahi and Skogestad, 2011). There was a trade-off between the complexity of the models and the number of tuning parameters to correctly match the desired process. The Kaasa model (with seven parameters) and the Di Meglio model (with five parameters) demonstrated a good fit. These techniques have experienced success in various field applications (see Table 2.1).

Kjeldby et al. (2013) discussed the applicability of a slug tracking model for slug initiation in the horizontal pipeline. They examined their model capability to understand the impact of the upstream hydrodynamic slug initialization on a severe slug cycle in a riser section. Using a scaled laboratory set-up, they assessed air-water flow in a 100 m long pipeline (65 m horizontal and 35 m with a section at 2.54 degrees downwards) and a 15 m long vertical riser. Their analysis identified two flow regions: slug and bubble regions. They modelled the slug and bubble regions using drift flux and two-fluid equations, respectively. They reported that the slug initiation from unstable stratified flow can be captured directly by solving the two-fluid model on a fine grid. Based on the sensitivity analysis of hydrodynamic slug initiation in their studies, it was concluded that precise prediction of the severe slugging cycle is sensitive to the initiation of upstream hydrodynamic slugs. It

was less sensitive to the local structure of the slug flow (frequencies and lengths) in the upstream region.

Meringdal (2014) developed a six-state dynamic model for pipeline-riser slugging using MATLAB. The model development was based on mass conservation of the gas and liquid phases in the well, pipeline, and riser. The researcher provided phase equations describing steady-state and transient behaviours in pipes. The model used an integrator with variable steps for length calculations and a fixed data sampling rate, which provided the model properties a real scenario resemblance. Different control systems were tested for the topside valve. A subsea valve was also tested but it led to poor results. The model resulted in a very good performance when testing the control solutions, and the model variables were relatively easy to obtain. The researcher conducted an analysis to establish a suitable control variable. The choke valve control led to an average increased production of over 8%, while the wellhead pressure control had problems with flow spikes in the transitions every time that the setpoint changed. A control using the mass flow rate measurement at the topside choke valve handled the spike issues but was not able to stabilize the flow slugging.

Several researchers (e.g., Durdevic et al., 2016; Pedersen et al., 2016) also examined severe slugs in well-pipeline-riser systems. They reviewed existing anti-slug control strategies for robustness. They validated the major 1-D models with results obtained from a lab-scale slug testing facility. Furthermore, the controllers were studied with input disturbances and parametric variations to evaluate their robustness. It was reported that the existing anti-slug control strategies lacked robustness to handle uncertain system and operating changes. Pederson et al. (2017) also analyzed the controller development for both the low point (Pb)

and topside (Pt) measurements, to find a suitable location for control transmitter installation. They evaluated the performance of the controllers numerically both with the non-linear MATLAB program and the OLGA simulator. They showed that the topside pressure output (Pt) is inadequate for anti-slug implementation. The Pt did not increase the closed-loop bifurcation point significantly and was also sensitive to disturbances. However, Pt is still a prefered option as it is the most accessible measurement on offshore platforms. They suggested a cascaded combination of the outlet mass flow and Pt for cases where only topside transmitters are available.

2.2.7 Review of Controllers and Control Variables

Jansen et al. (1996) evaluated the effects of the choke valve and gas lift on the stability and dynamics of the pipeline-riser system by modifying the stability criterion proposed by other researchers (Taitel, 1986). They introduced a shut-off choke valve to manipulate the flowrate at the topside. The introduction of the shut-off choke valves increases the pressure at the top of the riser, while the gas inlet reduces the pressure in the column. They reported that both the choke valve and choke have a stabilizing impact on the system.

However, past studies (e.g., Schmidt et al., 1979a; Hedne et al., 1990) did not result in industrial applications. The first industrial use of an anti-slug control system was reported for the Hod-Valhall pipeline (Havre et al., 2000). The authors evaluated the performance of anti-slug systems with both simulations and actual field data. The simulation results proved that the control system stabilizes an unstable operating point. It was found that for a constant valve opening when the control system is turned off, the riser slugging will be back to the system. They obtained a steady flow in the pipeline at an unstable operating

point, where the same boundary condition as the slugging regime existed. Havre et al. (2001) later presented a detailed methodology for implementing the system control introduced in their previous study (Havre et al., 2000).

Some past control studies reported models used solely to provide an estimate of the bottom pressure, which can then be used in a PI control design to stabilize the flow (Aamo et al., 2005; Sin'egre, 2006; Eikrem et al., 2004). Other studies used detailed information provided by the observers to design more advanced control schemes, taking into account the nonlinearity of the models. They also examined several other control variables, among which are the bottom pressure, the height of liquid at the low-point, and the mass of liquid in the riser.

Hedne et al. (1990) considered the difference between the bottom and topside pressures as an alternative control variable. They showed that the differential pressure correlates well with the total mass of liquid in the system, which plays a critical role in the stability properties of slugging systems (Di Meglio et al., 2010a; Imsland, 2002; Siahaan et al., 2005).

Di Meglio (2011) reported that the differential pressure performs better than the riser-base pressure for control stabilization. It was observed that the pressure difference allowed the system to stabilize at the operating points corresponding to high production rates, even though the differential pressure measurements require the availability of a bottom pressure sensor.

Sivertsen et al. (2010) proposed a solution using topside information only. They combined various sensors, including the traditionally available measurements, namely volumetric flow rate, density, mass flow rate, and pressure. It was reported that for a cascade control

loop design, a normalized volumetric flow rate measurement gave the best results for the inner loop while for the outer loop, the valve opening had the best performance.

2.2.8 Review of Slug Control Design Experiments

Di Meglio et al. (2012) examined the various control strategies for slugging. They reviewed model-based control laws and their solution schemes. They also investigated the application of proportional-integrator (PI) controllers for different control loop designs and model-based control laws. They documented the studies reported in Courbot (1996) as the first successful stabilization experiments of real-scale slugging wells, where a PI controller was used in stabilizing the pressures at the bottom of the riser. They also reported successful implementations of these control strategies in past studies (Aamo et al.,2005; Dalsmo et al., 2002; Godhavn et al., 2005; Havre et al., 2000; Sin`egre, 2006; Storkaas et al., 2005).

Skofteland and Godhavn (2003) used conventional PID controllers to stabilize the flow in pipeline-riser systems and reported both field experiences from the Heidrun field and experimental results from a Sintef Petroleum Research Multiphase Flow Laboratory. They introduced a cascade control system, where an inner flow loop was combined with an outer pressure loop to suppress both severe and moderate slugging. Hedne and Linga (1990) also studied the use of a PI controller based on an upstream pressure measurement to prevent riser slugging, using a medium-scale experimental flow loop. The study showed the potential for using control solutions to avoid riser slugging in pipeline-riser systems. They also outlined benefits of using a control solution over conventional control methods, including: (1) relatively little equipment expenses and (2) no significant pressure drop in

the system. Other experimental and field studies (e.g., Godhavn et al., 2005; Fard et al., 2003) also reported a combined application of an anti-slug controller with model predictive control to handle slugs that enter the inlet separator. Storkaas (2005) demonstrated that a PID controller is close to an optimal case and provides good performance and robustness when a riser-base or pipeline inlet pressure are used as input measurements.

Godhavn et al. (2005) provided guidelines for tuning simplified linear models of the slugging oscillations in pipes. It was concluded that the PI controller for the riser-base pressure exhibits two significant shortcomings as follows: (1) high sensitivity at the moment where the controller is triggered (Sivertsen et al., 2010) and (2) lack of robustness to changes in operating conditions (Di Meglio, 2011). As a result, they require frequent re-tuning. They explained that the controller should be turned when the bottom pressure is in the increasing phase of its oscillations to ensure good efficiency.

Jahanshahi et al. (2013a) proposed a closed-loop Internal Model Control (IMC) design for anti-slug control, which they tested on a small-scale and medium-scale S-riser. The model parameters were estimated from a closed-loop step test. Jahanshahi et al. (2013b, 2013c) also tested four nonlinear anti-slug controllers on the same experimental platform under the same conditions. They used a mechanistic model to test two nonlinear controller designs, a nonlinear observer (linearizing feedback controller), and an IMC gain-schedule. With the IMC gain schedule module, they stabilized the slugging system at a 60% valve opening. However, they reported a time delay in measurements when they are implemented on longer pipelines,. Although the linear controller approach has exhibited success in oil field applications, the control systems rely on downhole pressure measurements which are many times unreliable or even unavailable in some cases (Scibilia et al., 2008).

Biltoft et al. (2013) emulated riser slug flow in offshore oil and gas production using a laboratory set-up to analyze and improve control methods. They validated the set-up by checking the consistency of the results obtained with some existing typical riser slug models. The theoretical analysis and experimental results showed that the set-up can recreate the key features of slugging flow phenomena with reasonable accuracy. It served as a good platform for further slug control studies. They proposed a solution based on a high gain observer for the process state. The key feature of the proposed solution was its simplicity and because it easily utilizes measurements obtained from the top of a single well. Thus, it can be applicable to multiple-well systems where one common outflow manifold is installed. However, this method presents difficulty in identifying the particular well operating in an oscillating regime from the outflow measurements. Jahanshahi et al. (2015) also used a closed-loop step test to identify an unstable linear model. They obtained a second-order internal model controller that could be implemented as a PID controller.

Pederson et al. (2016) analyzed the input-output control of pipeline-riser slugging for robustness concerning changing operating conditions. Their analysis was applied with a 1-D model of Jahanshahi (2011) and the OLGA software simulation results. They showed that a robust controller can improve the system stability without losing much of the nominal performance. Pedersen et al. (2017) also evaluated riser-induced slugging influence on a typical separation process, based on experimental tests performed on a laboratory set-up. The test facility consisted of a 3-phase gravity separator physically linked to a de-oiling hydro cyclone. They investigated different operating flow rates and separator pressures. Three PID controller coefficients were kept constant for all the tests: the separator pressure, water level, and hydro-cyclone pressure-drop-ratio (PDR) controllers. The researchers

compared uncontrolled, open-loop, and closed-loop anti-slug control configurations. They concluded that both open-loop and closed-loop anti-slug control strategies improve the water level and PDR setpoint tracking. It was found that the closed-loop strategy offered the best production rate. Furthermore, they showed that a control strategy should guarantee a stable mass inflow rate to the separator.

Jahanshahi et al. (2017) proposed a cascade control strategy for anti-slug control, based on virtual measurements on the topside choke valve. They used a frequency domain analysis to test the robustness properties of the proposed control technique. They reported that the virtual flow output is not affected by response dynamics. The properties were valid for systems with an oscillatory nature such as slugging. They tested the cascade controller successfully in OLGA simulations and experiments. Good results for both the setpoint tracking and the disturbance rejection were noticed. However, the pressure outputs depicted high sensitivities in closed-loop configurations, which signalled a robustness problem.

2.2.9 Review of Controllability and Stability Analysis

A topside choke valve is commonly used as the manipulated variable for anti-slug control of multiphase flow in offshore risers. With advances in subsea technology, it is now possible to move topside facilities to the seafloor. This presents an alternative location for the installation of actuators as manipulated variables in the system control loop. Controllability analysis is focused on evaluating the actuators and location that are most effective for process control. Some researchers have investigated other control variables beside a topside choke valve and their locations, which may be used for adequate control

(Pederson et al, 2016). Many studies considered alternative locations for the control valve and investigated how to deal with nonlinearity in the model equations (Jahanshhi et al, 2014). The studies in the following section analyzed controllability of existing simplified models when fitted to the results of lab experiments and the OLGA simulator.

Storkaas (2003) showed that riser slugging in pipelines can be stabilized with simple control systems. The researcher evaluated key control variables and measurement locations and concluded that the type and location of the measured input to the controller are critical. Among the variables considered in their work, the upstream pressure (pipeline inlet or riser base) measurement and flow measurement at the outlet were able to stabilize control. It was shown that the use of an upstream pressure measurement works well for stabilization, but is not effective for suppressing high-frequency slugs such as small hydrodynamic slugs formed in the pipeline. They also observed that using th inlet pressure as a control variable may present difficulty for long pipelines as a result of the delay in pressure wave propagation. The outlet flow measurement, on the other hand, could suppress high-frequency slugs. However, the low-frequency fluctuations were not captured, and their setpoint tracking properties were not effective. They also investigated the topside flow measurement and reported that it leads to good results in specific control designs such as cascade or single input-multiple output (SIMO) systems. Their analysis of the properties of the system demonstrated that slugging mechanics can be adequately described by a simpler model than a PDE-based model.

Storkaas et al. (2005) also presented an analysis of the system variable characteristics that are relevant to control riser slugging. The controllability analysis was conducted using two different models – the two-fluid model and the drift flux model. Their analysis showed that

slug flow control was possible by a relatively simple control system that would manipulate the valve at the top of the riser. They also concluded that the type of measurement and the location of the actuators are critical to the effectiveness of control. They concluded that the pressure at the pipeline inlet or bottom of the riser produced the best results among the control variables considered. It was recommended that a mixture flow rate at the top of the riser should only be used in combination with another measurement as the steady-state gain is close to zero. Based on their model analysis, it was revealed that a simpler model with fewer states can be used to simulate the slugging process for control purposes. Hence, they developed a simple nonlinear dynamic model with three states. The outputs of the three-state model were compared with the controllability analysis results from a more complicated two-fluid model and OLGA simulator. They obtained a similar dynamic behaviour for both the two-fluid model and OLGA. In their study, the topside choke valve was used as an input for anti-slug control.

Jahanshahi et al. (2012a) performed a controllability analysis of two cases – a well-pipeline-riser system and a gas-lifted oil well. Their studies verified previous findings that the riser bottom and the oil well bottom hole pressures are better choices for control variables in a single-input-single-output control configuration, even though those measurements may be difficult to obtain. However, their finding differed from the previous report (Storkaas et al., 2007) on the application of flow rate measurement.

Contrary to the report of Storkass et al. (2007), the study by Jahanshahi et al. (2014) reported that flow measurements provide a higher steady-state gain and better performance, compared to the pipeline-riser. They also concluded from their analysis that the bottom-hole pressure is the best-controlled variable for gas-lifted oil wells. An accurate

measurement of the outlet flow rate of the choke valve can yield stability in a SISO control scheme. They also reported that combining an upstream pressure measurement with the choke outlet flow rate leads to the best result for a well-pipeline-riser system. In situations where the subsea pressure measurements were not available as in the case for many offshore platforms, they suggested combining the top pressure and the flow rate. Furthermore, they suggested that the riser top pressure may be combined with the outlet mixture density to achieve system stability. Most of the past studies concluded that the topside riser pressure, topside riser density or liquid holdup measurements are not suitable as control variables for a SISO control but may be effectively combined with other measurements in an MIMO or SIMO configurations.

2.2.10 Review of Slugging for Different Pipe Configurations

Storkaas et al. (2005) introduced a control structure that can aid pipeline slug control by including suppression of surge waves and start-up slugs. Surge waves and start-up slugs are the multiphase phenomena that can also initiate a slugging regime in offshore pipeline-riser systems. Surge waves are large liquid waves that can occur when the production rate in a gas-condensate flow is increased, whereas start-up slugs occur when the pipeline starts up from shut-in conditions. The start-up slugs are similar to surge waves; however, they can be even more serious as they potentially can initiate riser slugs and thereby cause even larger peaks in the liquid production (Storkaas et al, 2005). The researchers designed a control system by combining a stabilizing anti-slug controller and individual flow controllers. The flow controllers used the pipeline as a buffer volume to reduce the flow

variations such that the minor slugs could be handled by the separator. The performance of the control system was illustrated with simulations of an industrial case study.

Park and Nydal (2014) carried out experimental studies on severe slugging in an S-shaped-riser. They used an air-water flow mixture in an S-shaped-riser facility. They took measurements of pressures and liquid holdup at the riser inlet and two other locations along the riser for varied flow rates. The measurements were taken for both unstable and stable flow conditions. They compared their results with predictions from the OLGA dynamic simulator. Based on the study of Park et al. (2014), the stability maps, pressure amplitudes, and slug frequencies matched closely with the OLGA results. However, the OLGA software slightly over-predicted the slug formation region in the flow-regime map in comparison to their results. Also, 5% to 9% deviations were estimated for pressure amplitudes. A maximum deviation of 26% was noticed in the slug frequencies at low flow rates.

Until the last few years, the preferred solution to avoid or reduce the problems associated with riser slugging has been to design the transport system such that the slugging potential is minimized, or change the boundary condition by reducing the topside choke valve opening (Sarica & Tengesdal, 2000). However, none of these solutions is optimal. Design changes often involve installation of expensive equipment such as slug catchers. Rreducing the topside choke valve opening introduces an extra pressure drop that will limit production when the reservoir pressure goes down as the reservoir is depleted.

In recent years, there has been renewed interest in control based solutions to avoid riser slugging. Feedback control has been proven effective and economical for attenuating slugging flow regimes in offshore oil production. In this application, the opening value of

a choke valve at the topside platform is usually used as the control input to regulate the pressure or the flow rate in the pipeline. Designing such a control system based on topside measurements, without subsea sensing devices, is preferred from a practical point of view. Controlling the topside pressure alone is difficult, and it is not robust in practice, but combining the topside pressure and the flow rate results in a robust control solution, although measuring the flow rate of a multiphase stream is challenging and requires expensive instrumentation.

2.3 Limitations of Existing Models

The simplified model of Storkaas (2003) was based on a pipeline riser system with a regular L-shaped riser. Current offshore development prefers floating systems to a fixed platform for fluid recovery and processing. The floating platforms allow for surge, sway, roll, pitch and yaw movements through dynamic positioning systems. While current control models have been proven effective for control applications, they are limited in use for platforms such as semi-submersibles and FPSO's, in which the fluid processing installations are prone to both lateral and axial displacement of the pipeline-riser systems. These are the primary conduits of the multiphase flow and current models fail to account for the dynamic geometry of the pipeline-risers.

Also, varied installation configurations are used to accommodate the terrain and flow properties of the produced fluid. As a result, different geometries other than simply vertical lines would limit the undesired flow instabilities in fluid recovery installations. Low-pressure reservoirs, medium to high viscous reservoirs, and EOR candidate wells are more prone to flow instabilities. Therefore, the integrated well-pipeline-riser model design may

lead to an improvement in robustness since the effect of flow instability in the well can be felt even in the pipeline.

Another limitation of predictive models is the assumption of constant liquid holdup in the pipeline leading into the riser, which prevent both frequency and amplitude of the oscillations to be fitted simultaneously. There is, therefore, a need for the following extensions of the simplified 3-state model to be developed:

- Other pipeline and riser configurations, including catenary and flexible risers, which accommodate lateral and vertical displacements;
- Varying liquid holdup in the pipeline; and
- Extension to three-phase flow (gas, oil and water).

Most of the approaches considered in past studies implemented a control system that used the topside choke valve to keep the pressure at the riser base at or above the peak pressure in the riser slug cycle, thus preventing liquid accumulation in the bottom of the riser. The strategies effectively removed riser slugging in the system, but they did this by automating the old choking strategy rather than affecting the stability of the flow regimes in the pipeline. Consequently, an extra pressure drop was introduced in the system by the high setpoint for the pressure controller.

2.4 Slug Creation and Use of Experimental Results

Oil and gas operators rely on experimental measurements for analysis and design of anti-slug measures. Pedersen et al. (2016) documented a severe slug flow based on a series of experiments carried out in a lab-sized test facility (Biltoft et al., 2013). Their work focused on the physical parameters for emulating the slugging regime in an open-loop analysis of

the flow regimes, where traditional flow and bifurcation maps were created. With the data obtained, they developed a flow map. The stable surface was mapped to indicate the switching between slugging and non-slugging flows.

2.5 Impact of Active Slug on Downstream Fluid Recovery

Pederson et al. (2018) studied the influence of riser-induced slug flow on gravity-based separation and processing installations. They also tested different flow conditions on various control scenarios (separator pressurization, water level control, and the hydro cyclone's pressure-drop-ratio) to assess the downstream separation process performance. The downstream separation consisted of a 3-phase gravity separator and a water-oil de-oiling hydro cyclone. It was concluded that the separation performance is sensitive to flow oscillations. Similar to the results presented by previous researchers (Løhndorf et al, 2018), they reported that the presence of severe slugs significantly challenges the PDR controller. Furthermore, they showed experimentally that by integrating the water level and PDR reference tracking with an anti-slug controller, the production rate and separation performance could be improved significantly.

Previous studies (e.g., Luo et al., 2014; Xiaoming et al., 2011) evaluated the use of level controllers and separator pressure to mitigate the impact of slugging on downstream separation. Using the level controller installed in the separator, they simulated the liquid level and pressure under severe slugging flow conditions. They reported that the level control alone does not have a significant impact on the upstream flow, but is beneficial for normal operation and pressure control of the separator. When the separator pressure was increased, the peak pressure in the riser slightly diminished. However, gas/liquid slip

intensified for fully developed slug flow. This led to a long gas plug to flow through the riser rapidly, and it then slowly changed to medium-sized gas bubbles. It was concluded that the separator pressure control has a strong effect on the superficial gas/liquid flow.

Recently, these control strategies have been applied in different offshore production platforms with goog success in fluid separation and stabilization. Courbot (1996) presented a control system to prevent riser slugging in the Dunbar pipeline. Henriot et al. (1999) also presented a simulation study for the Dunbar pipeline, where the setpoint for the riser base pressure was set considerably lower. They focused on stabilizing an unstable operating point rather than just keeping the process away from the riser slugging region. As a result, fluid separation capabilities and stabilization improved.

Campos et al. (2014) also documented field implementation of anti-slug methods in the Campos and Santos basins. They reported the development, implementation and results obtained from the control measures used on the three platforms at the Campos and Santos basins. The controllers were designed to achieve improvement in operational stability and safety, reduce unscheduled compressor shutdowns, as well as increase operational efficiency. The operational difficulties experienced in the operation of the platform were discussed in previous studies (Fard et al., 2006; Godhavn et al., 2005). Similar to the studies by Biltoft et al. (2013), the platform operations recorded a low production rate, periodic overloading of processing facilities, and many emergency shutdowns.

Dalsmo et al. (2005) presented results of stabilization studies for horizontal wells with both gas lift and active choking. They reported that dynamic feedback techniques using the production choke at the wellhead might be used to stabilize the system fluctuations and

improve separation efficiency. The primary input to the dynamic feedback controller was the measured downhole pressure.

Table 2.1. Field application of active choke slug control technique.

Field location	**Source**	**Fluid type**	**Major problems**	**Controller location**	**Controller variable**	**Success**
East Malaysia	Yaw et al., 2014	Condensate	Slugging, High water cut, Pipeline vibrations	Topside choking	Flowrate	Extended field life by 20 months
Gulf of Mexico	Fong et al., 2013	Oil	Slugging	Topside choking	Pressure	10% (1400 bpd) increase
Offshore Nigeria	Lacy et al., 2014	Oil	Ineffective gas lift control, constrained gas supply	Topside choking	Pressure	
Valhall, North Sea	Calvert and Davis, 2013	Oil	Slugging, shut down due to low reservoir pressures, failed start-up attempts		Upstream pressure	Yes, 3500 bpa increase (10%)
ETAP, Norway	Calvert and Davis, 2010	Oil	Slugging, high water cut, 55% increase phase invasion in separating unit, high BS&W over 16% increase	Choke valve	Flowrate	Yes, 800 bpd increase
Otter and Eider fields, North Cormorant	Kovalev et al., 2003	Oil	Slugging high fluctuations in the separator	SSS controller	Flowrate	Yes, +/-5% average pressure level and +/-5% average flowrate

The field results were obtained from the Brage field operated by Norsk Hydro in the North Sea. Brage's oil productions began in 1993, and the field began to decline from its plateau in 1998. As the production decreased, the problems related to unstable production from some of the wells increased. The results from the initial field control tests on the Brage wells confirmed that the control method can help stabilize the flow. Both the pressure and flow variations reduced dramatically, enabling fluid production from wells with a lower downhole pressure and an increased flow separation efficiency.

Cheng et al. (2002) evaluated the performance of an anti-slug model application in different oilfields, and its pros and cons. They reviewed some field anti-slug control applications. Three severe slugging control methods were examined: GLCC separation, auto choking, and gas lift. GLCC combined with the original slug catcher solved the slug problem of the QK17-2 Oilfield, while online monitoring and an auto choking system was successfully installed and applied in the WC Oilfield. The researchers reported that the field operation is greatly improved, and higher production rates and stable fluid transport were recorded. Table 2.1 provides a summary of major field implementation outcomes of slug control measures.

2.6 Review of Actuators Used in Slug Control, Flow Stabilization, and Separation in Subsea Pipelines

Gas-lifting, choking, and a combination of choking and gas-lifting have been used over the years to mitigate slugging. In the following section, a critical review is conducted on specific topics related to well-known methods, as well as the current opportunities for advancing these techniques.

As discussed earlier, three common methods for slug elimination include choking, by reducing the opening of the fluid outlet on the topside of the riser (Schmidt et al., 1979); gas lifting (Hill, 1990; Hill and Wood, 1994; Pots et al., 1987), which involves injecting gas at the bottom of the riser where the liquid loading tendency is most anticipated; and the simultaneous application of gas-lifting and choking schemes. Gas lifting as an artificial fluid lifting process is widely used in the petroleum industry, mostly for increased oil recovery and production optimization. The challenges of gas lifting include high operating costs, gas handling problems, and overall safety, especially in offshore oil recovery, where a smaller footprint and compact design are required. Therefore, manual choking of the topside valve is often preferred to suppress slugging in offshore fields. Choking also lowers production significantly and may impose severe back pressures in the pipeline system, resulting in repeated shutdowns and production losses. Recently, in some oilfields, both gas-lifting and choking have been applied simultaneously.

Past studies (e.g., Di Meglio et al., 2009; Di Meglio et al., 2010a; Jahanshahi and Skogestad, 2014, 2015; Jahanshahi et al., 2012; Skogestad and Postlethwaite, 2005) have investigated various methods of topside choking to eliminate slugging. Analyses of choke behaviour and controllability have been presented in past literature (Jahanshahi and Skogestad, 2014; Jahanshahi et al., 2012; Pedersen et al., 2017). Some other methods of choking, such as feedback control with a topside choke valve as the control variable, and combined choking and gas-lifting, have also been examined as potential solutions to slugging in offshore fluid processes. These advanced forms of slug control techniques have received attention from field operators as viable alternatives to manual choking of the topside valve and the gas lift method (Ogazi, 2011). A combined scheme or controllers

could enable stabilized flows at a larger valve opening. In the traditional manual choking method, the slugging well is permanently choked, eliminating the slugs. However, this has negative operational impacts such as back pressure accumulation, leading to lower production rates (Di Meglio et al., 2009; Di Meglio et al., 2010a; Di Meglio et al., 2010b; Taitel, 1986; Taitel and Dukler, 1976; Yocum, 1973). With feedback control, the actuators can be controlled based on feedback signals from pressure, flow, or temperature transmitters when implemented in a feedback loop (Di Meglio et al., 2009; Jahanshahi and Skogestad, 2014; Jahanshahi et al., 2012.; Pedersen et al., 2017). However, the current methods of feedback control are limited with respect to robustness over a range of operating conditions (such as varying inflow, water cut, and GVF). An increased production rate reduced operational downtime, reduced costs, and improved safety are potential benefits of improving the feedback control method.

The slug phenomena are difficult to accurately predict due to their chaotic nature. For example, a Hopf bifurcation occurs at surface boundaries where the bifurcation point divides the slug/non-slug region. As a result of these complexities, predictive models often do not accurately represent a real system (Di Meglio et al., 2012). Therefore, the robustness of existing models for assessment and design of slug control approaches for real systems should be further examined. Many of the existing models have been used to gain insight into slug attenuation mechanisms. However, there are few investigations that present empirical models for evaluating the slugging phenomena and control devices for subsea pipeline flow situations. Also, mechanistic models have limitations that are often based on mass balance assumptions.

2.6.1 Formulation of Slug Flow in Pipelines

Past available empirical models combine the features of current designs of slug mitigation measures for offshore applications, including combined choking and gas-lift methods. This thesis focuses on developing new non-dimensional correlations for key operational variables in evaluating, designing, and implementing slug control. The models will provide useful tools for controller design and system analysis. The control techniques will be tested and compared. More accurate prediction of slug flow characteristics during fluid transport in pipeline-riser systems is crucial for proper design and safe operation of fluid transport and separation systems. Such designs require a better understanding and more robust description of the behavior of slugs in both upstream transport and downstream separation facilities. Hence, more reliable techniques are required for predicting gas-liquid slug flow characteristics in flowline risers. Currently, there are relatively few predictive models that are industry-relevant given the current trends in offshore field productions.

New predictive correlations are required for evaluating slug performance of different control schemes. New correlations for the system analysis and controller design will be presented in this thesis. Results for the various techniques for slugging control will be presented and discussed.

Nicklin et al. (1962) presented an empirical relationship for slug bubbles in horizontal pipes, in terms of the fluid velocity, as follows:

$$u_{sb} = C_0 u_{Ls} + C_1 (gD)^{\frac{1}{2}} \tag{2.5}$$

where C_0 is a weighted velocity distribution parameter; u_{sb} is the weighted mean velocity of the gas phase relative to the liquid phase; and C_1 is a constant of proportionality.

Weber (1981) reported that the slug bubble relative velocity in a vertical and/or horizontal pipe can be expressed by the following relationship:

$$u_{sb} = 0.35\sqrt{gD} \tag{2.6}$$

Naterer (2018) reported that the slug rise velocity can be calculated from a similar expression, as given below:

$$u_s = 0.345\sqrt{gD} \tag{2.7}$$

The relationship was used for horizontal pipes with low viscosity fluids.

Duckler and Hubbard (1965) developed a velocity profile of slug flow and expressed the translational velocity of the slug by the following equation:

$$u_t = (1 + C)U_M \tag{2.8}$$

where C is defined as follows:

$$C = -0.021\ln(Re_s) + 0.022 \tag{2.9}$$

in which, Re_s refers to the Reynolds number of the slug mixture

Majeed et al. (1989) presented an empirical correlation for slug liquid holdup based on 435 experimental data points collected from past literature. They noticed that the effects of pipe diameter and surface tension on the liquid slug holdup were relatively small. A correlation for the slug liquid holdup was developed, which is dependent on the fluid viscosity, mixture velocity, and angle of inclination, as shown below:

$$\alpha_{Ls} = (1.009 - C_m U_M)(1 - \sin\beta) \tag{2.10}$$

where

$$C_m = 0.006 + 1.3377x \tag{2.11}$$

where α_{Ls} refers to the slug liquid holdup; β represents the inclination angle; x introduces the ratio of the gas to liquid viscosities, and U_M is the mixture velocity.

Other researchers (Gregory and Scott, 1969; Weber, 1981) developed empirical correlations for slug flow in horizontal and vertical pipes. Marcano et al. (1998) presented a correlation that predicts the slug body holdup based on experimental data obtained from a 420 m pipeline flow loop, under varying gas and liquid flow rates. They expressed the liquid slug holdup as a function of the mixture flow velocity as follows:

$$\frac{1}{\alpha_{ls}} = 1.001 + 0.0179U_M + 0.001{U_M}^2 \tag{2.12}$$

Gomez et al. (2002) reported slug flow results in pipelines of varying diameters (51 mm to 203 mm), inclination angle between 0 and 90^0, and operating pressures between 1.5 and 20 bar. It was found that the slug holdup depends on the inclination angle and Reynolds number of the slug. They formulated a correlation as follows:

$$\alpha_{ls} = e^{-(0.45\theta + CRe)} \ , \theta \leq \theta_R \leq \frac{\theta}{2} \tag{2.13}$$

where θ introduces the angle of inclination and C is a coefficient, equal to 2.48×10^{-6}. Also, Re is the slug Reynolds number, as expressed below:

$$Re = \frac{\rho_L U_M D}{\mu_L} \tag{2.14}$$

where ρ_L and μ_L denote the liquid density and viscosity, respectively.

Taitel and Dukler (1977) also reported that the slug period (T) can be correlated as a function of the mixture velocity under a constant inflow superficial liquid velocity as follows:

$$T = e^x {U_m}^{-y} \tag{2.15}$$

where

$$x = 0.415 \ln(U_{sL}) + 5.339 \quad (2.16)$$

$$y = 0.072 \ln(U_{sL}) + 1.390 \quad (2.17)$$

The parameters x and y were determined by the superficial liquid velocity. Schmidt et al. (1979) also presented an empirical correlation of the slug period as a function of the flow rate as follows:

$$T = aU_m{}^b \quad (2.18)$$

where a and b are independent of the gas and the liquid flow rates. The period is $T\left(T = \frac{1}{f_s}\right)$ and f_s is the slug frequency. The researchers investigated various slugging types (SS1 and SS2) and they showed that the slug period correlates linearly with the mixture flowrate (Taitel and Dukler, 1977). They found that the correlation's accuracy lies within ±30%, which is in relatively good agreement with the experimental data. The exponent of U_m in Equation (2.9.14) is b = -1, therefore,

$$f_s = \text{a } U_m^{-1} \quad (2.19)$$

Hill and Wood (1994) also proposed a correlation for the slug frequency as follows:

$$f_s D = 0.27510^{2.68H_L} U_m \quad (2.20)$$

The mixture velocity is given by w_{mix}/A, where w_{mix} represents the mixture flow rate of the gas and liquid phases; and A is the cross-sectional area of the pipeline.

2.7 Review of Two-Phase Slug Flow Correlations

The general goal of the oil recovery process is to maximize the hydrocarbon extraction at the lowest cost per barrel at the same time, comply with safety and environmental

regulations. In the following section, a review of state-of-the-art on specific topics related to slug flow correlations is conducted.

In riser slugging, flowrate and pressure generally oscillate in an irregular manner. The irregular flow oscillations contribute to the lack of system stability. Slugging, when transporting fluid from the wellhead to the surface processing facilities, jeopardizes the economic and safe operation of the oil recovery processes (Pedersen et al., 2017; Taitel and Dukler, 1976)

Several slugging experiments and numerical investigations have focused on further understanding of flow characteristics, and modelling of fluid flow processes to improve process efficiency in offshore flow separation. However, poor design of two-phase process facilities aggravates slugging potential and prohibits anti-slug control measures. Slug frequency is crucial in topside process facilities design and it is required as an input parameter for mechanistic models. Therefore, a proper prediction of slug frequency is central for accurate flow characterization, and selection and design of appropriate mitigation methods. Although there are several research studies about normal slug frequency in both horizontal and inclined pipelines, a few studies have been performed to predict severe slugging frequency, related to flow assurance challenges in offshore petroleum production. In this thesis, an experimental investigation will be carried out, using air-water two-phase flow, in a pipeline-riser set-up, to develop a new slug frequency model with better accuracy and reliability for offshore applications.

Wang et al. (2010) performed a comprehensive investigation of air-water and air-oil two-phase slug flow in horizontal pipes and analyzed the effects of flow parameters such as flow rates, slug frequency, and Taylor bubble length on heat transfer coefficient.

According to past studies reported in the literature (Hill, 1990; Hill and Wood, 1994), eight parameters that affect the slugging frequency are the gas and liquid flow rates, liquid viscosity, liquid density, gas density, acceleration due to gravity, inclination angle, and diameter. Based on their experimental investigations, it was found that for the different gas and liquid flow rates, the depth of the liquids film or liquid level (liquid holdup) and slip velocity have predominant influences on the slug frequency in the testing rig. Early models for prediction of slug frequency were obtained by solving the unsteady mass and momentum balance equations (Gregory and Scott, 1969; Greskovich and Shrier, 1972; Heywood and Richardson, 1979; Zabaras, 1999). One of the early relationships was suggested by Gregory and Scot (1969), based on the experimental data where 19 mm and 35 mm pipes with water and CO_2 systems were used. Their correlation is expressed as follows:

$$f_s = 0.0026 \left\{\frac{U_{sL}}{gD}\left(\frac{19.75}{U_m} + U_m\right)\right\}^{1.2} \tag{2.21}$$

In Equation (2.21), f_s stands for the slug frequency; U_{sL} and U_m are the superficial velocities of the liquid phase and the mixture, respectively; D designates the pipe diameter; and g is the acceleration due to gravity. Although these correlations based on solving unsteady state equations can provide a good estimation of the slugging frequency, a solution of the two PDEs is challenging, sensitive to inclination angle, and fluid viscosities (Schulkes, 2011). Since the early 1980s, a different approach was used so that the liquid holdup equations were solved to obtain a steady-state liquid level (Hill, 1990; Hill and Wood, 1994; Trononi, 1990). Also, empirical models were developed based on slug

frequency data for fully developed slug flow tests (Al-Safran, 2008; Gokcal et al., 2010; Hill and Wood, 1994; Kjeldby et al., 2013; Kristiansen, 2004; Manolis et al., 1995; Shea et al., 2004; Zhou et al., 2018).

Schulkes (2011) analyzed 1,200 data points covering the main parameters for slug flow in pipeline risers and presented a new correlation for the prediction of slug frequencies. Introducing five dimensionless groups, namely the Froude number, Reynolds number, inclination angle, liquid fraction, and density ratio, they proposed the following correlation to calculate the dimensionless slug frequency:

$$\mathcal{F} = \Psi(\alpha) + 12.1\mathrm{R_e}^{-0.37} \times \Theta(\theta, \mathrm{F_r}) \tag{2.22}$$

In Equation (2.22), $\mathcal{F}$ stands for the dimensionless frequency; Re is the Reynolds number; Θ is a parameter which is a function of the Froude number (Fr) and inclination angle, while $\Psi(\alpha) = 0.016\alpha\,(2 + 3\alpha)$. Also α is the input liquid fraction. The analysis showed that the Froude number has a limited effect on slug frequency especially for the low-pressure flow cases, which characterize the slug flow regime. It did not produce a significant effect on the final correlation.

Similar methods have been used by previous studies to develop two-phase slug flow correlations for process design, analysis, operation, and optimization. Nada (2017) developed a two-phase correlation for slug flow in a horizontal and upward inclined pipeline as follows:

$$\frac{Nu_{2\varphi}}{Nu_{1\varphi}} = 1 - 0.2314{R_f}^{-0.77}(10^{-5}\,{Re_g}^2 - Re_g) \tag{2.23}$$

In Equation (2.23), Nu stands for the Nusselt number and the subscripts, 2φ and 1φ, denote two phase and single phase respectively; R_f is the mixture Reynolds number; and R_{eg} represents the Reynolds number of the gas phase. Their analysis was based on an air-water two-phase flow experiment in a tube at a constant temperature at 20°C. They reported that Equation (2.23) can be used to estimate the heat transfer coefficient for slug flow in the pipeline system with an upward inclination.

Elamvaluthi and Srinivas (1984) also proposed a two-phase correlation for upward slug flow in a vertical pipe as follows:

$$Nu = 0.5\left(\frac{\mu_g}{\mu_f}\right)^{0.25} {R_{em}}^{0.7} {P_{r_f}}^{\frac{1}{3}} \left(\frac{\mu_B}{\mu_w}\right)^{0.14} \tag{2.24}$$

In Equation (2.24), Nu stands for the Nusselt number; μ_g and μ_f denote the gas and mixture viscosities respectively; R_{em} is the mixture Reynolds number; P_{rf} is the Prandtl number; μ_B is the liquid viscosity; and μ_w refers to the water viscosity. This correlation used the mixture Reynolds number in terms of a sum of the liquid and gas velocities. The authors compared the calculated and measured heat transfer coefficients, concluding their correlation can predict 90% of the data within $\pm 25\%$.

Hill and Woods (1994) modified their previous correlation (Hill, 1990), for prediction of the slug frequency in which they showed the slug frequency dependency on the equilibrium film depth. They stated that the equilibrium film depth can be calculated using the procedure of Taitel-Dukler (1976). In their modification, they examined large gas and liquid superficial velocities, taken from a test rig and an oil field. It was found that time

would be required for the film depth to build back up to its equilibrium level, which decreases with a higher liquid inflow rate, and increases with a larger gas flow rate.

Gokcal et al. (2010) reported that the slug frequency increases at a higher liquid viscosity, based on their experiments with air and mineral oil where the viscosities varied between 0. 181 Pa.s and 0.589 Pa.s. Their findings were not valid for low-viscosity fluid cases (e.g., 0. 001Pa.s) such as kerosene and water. It was concluded that the slug frequency correlation deviates from the experimental data at high Reynolds number conditions. According to their results, the slug frequency increases with higher superficial liquid velocities and that the gas velocity increases first, and then starts to decrease.

Table 2.2 summarizes the important observed information about past correlations on slug frequency, based on the literature review.

Table 2.2. Overview of past slug frequency correlations

Source	**Fluid**	**Correlated variables**	**Pipe ID mm**	**Inclination degree**	**Viscosity, Pa.s**
Zhuo et al., 2018	Air-water	Pipe length, period, pressure, and flow rates of liquid	50	-5	0181-0.589
Shulkes, 2011	Air-water	Velocity and density of liquid and gas, inclination angle, gravity acceleration, diameter, temperature, and pressure	19-100	1-80	0.001-0.589
Gokcal et al., 2009	Air-mineral oil	Period, liquid viscosity, and flow rate of gas and liquid	50.8	-	high
Kjeldby, 2009	Oil-gas	Velocity and density of liquid and gas,	78	-	0.033-0.165

		inclination angle, and diameter			
Al-Safran, 2009	Air-mineral oil	Period, flow rate, pressure, and liquid holdup		-	
Wiken and Thomas, 2008	Air-water	Period, pressure, and velocity and density of gas and liquid	52		
Shea et al., 2004	Air-water	Period, pipe length, and gas and liquid flow rates		-	0.001
Kristiansen, 2004	SF6 + air-Exxsol	Liquid holdup, diameter, and flowrate	69	-1, 1	0.002
Zabaras, 2000	Air-water	Liquid holdup, diameter, gravity acceleration, slip velocity, and inclination angle	19	-	0.001
Manolis, 1995	Air-water	Liquid and gas velocities, gravity acceleration, diameter, and pressure	78	-	0.001-0.05
Hill and Wood, 1994	Air-water	Diameter, mixture velocity, and period	152		0.001
Hill and Wood, 1990	Air-water	Liquid holdup, diameter, gravity acceleration, and slip velocity	152		0.001
Tronconi, 1990	Air-water	Superficial gas and liquid velocities, density, period, and diameter			0.001
Heywood and Richardson, 1979	Air-water	Mixture velocity, Froude number, and no-slip liquid holdup	42	-	0.001
Gregory and Scot, 1969	CO_2 -water	Liquid holdup, diameter, gravity acceleration, and slip velocity	19.05	-	low

3 METHODOLOGY

In this section, the approaches used to conduct the research methodology will be described in detail. The first section of this chapter outlines the design of experiment and materials used to compare the performance of various actuators to suppress slugging during transport of multiphase fluids in pipeline-riser systems. The second section outlines the sets of equations and physical description of the problem, which is focused on improving existing anti-slug models. The third research methodology describes the analytical and experimental steps in addressing the third research objective, which involves non-dimensional correlations, such as slug frequency and slug velocity for the evaluation, design, and implementation of slug control.

3.1 Experimental Studies for Actuator Suppression of Slugging in Subsea Pipelines with Multiphase Separation

The purpose of the experiment was primarily to compare the various slugging suppression techniques and to develop criteria and guidelines for applying any chosen method. The experimental studies were also focused on evaluating the various actuators applied to suppress slugging in the pipeline-riser. It will also examine how the actuators can impact the transport and separation of multiphase flows in subsea pipelines. Two well-known approaches as well as a combined scheme will be considered.

The experiments were conducted in a multiphase flow facility of the Offshore Energy Laboratory at Aalborg University, Denmark (see Figure 3.1). The author travelled for an

extended period to Denmark for collaborative studies with researchers at the Offshore Energy Laboratory.

3.1.1 Experimental facility description

The experimental setup consists of several pipeline and riser sections. The internal pipeline diameter is 0.054 m, with a total length of 42 m, including a 12 m inclined section. The internal riser diameter is 0.054 m with a total length of 6.1 m. The setup also includes a 1.2 m topside section and a 3-phase gravity separator.

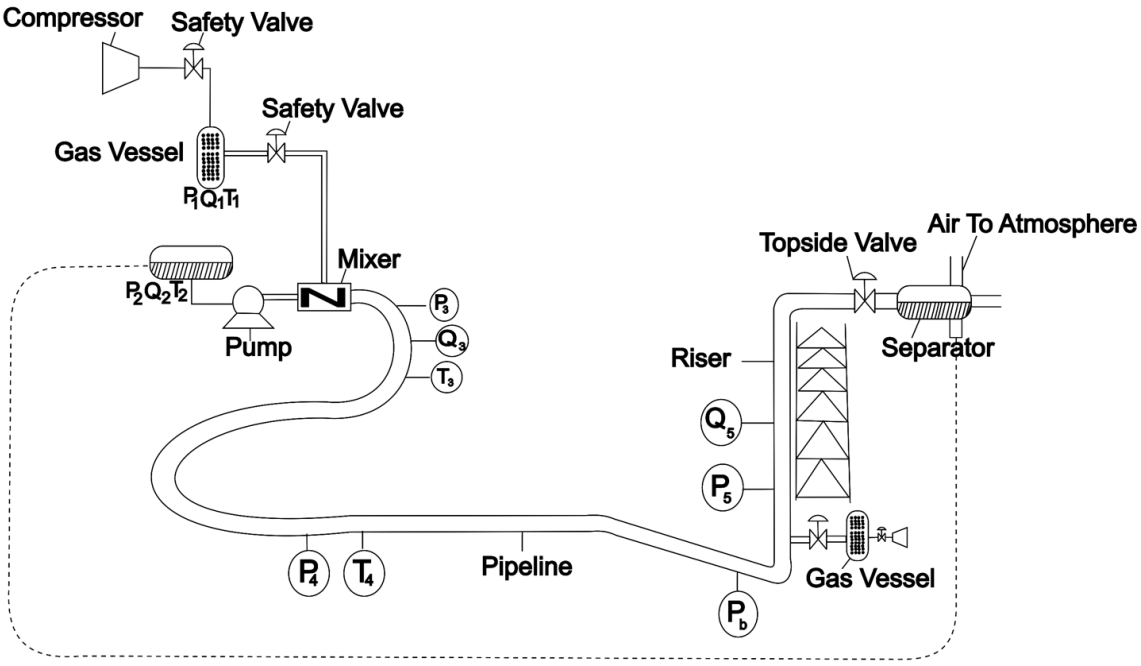

Figure 3.1. Experimental facility to study slugging suppression (P: pressure; Q: flowrate; T: temperature).

The experimental apparatus has transparent PVC pipes to enable visual observation of flow patterns in the piping. A liquid phase (mixture of water and mineral oil) is supplied into the

system from buffer tanks by centrifugal pumps. A centrifugal water feed pump with an operating range of 1 L/s at 162.7 m and a maximum pressure of 25 bar is used for supplying water into the system. A mechanically actuated diaphragm oil feed pump with an operating range of 1.94×10^{-7} to 0.0022 g/s, and maximum pressure of 16 bar, is used for supplying oil into the system. The water and oil flow into a mixer (N) with a venturi-based design. Each supply pipe is equipped with control safety valves to prevent back-flows. The multiphase mixture is supplied into the pipeline-riser test system after it has been thoroughly mixed. The outflow is received into a separator downstream where it is separated into component phases. The liquid phase in the underflow of the separator vessel is passed through the hydro-cyclone before it is subsequently returned into the buffer tank whereas the air is released into the atmosphere.

The pipeline-riser-separator system comprises a complete flow-loop. Each subsystem of the complete test loop can be studied separately. Transmitters and actuators are installed in the system for control and monitoring of the inflow and outflow, whereas the temperature, pressure, and flow rate are measured by sensors. The flow measurements were collected using a single-phase Coriolis flow transmitter with an operating range of 1.389×10^{-5} to 0.0033 L/s. Pressure is measured using transmitters installed along the pipeline-riser-system loop for the pipeline (P1 and P2), riser (P3 and P4), and the inlet of the separator (Ps). The pressure transmitter has operational range of 0 - 16 bar and a piezo-resistive measuring cell with a ceramic diaphragm. The pressure transmitter is noted for its fast-step response time of fewer than 5 m/s (Løhndorf et al., 2018). Gas inflow and gas lifting are regulated by control valves on the compressor outlet line. The riser topside choke valve

and outlet valves on the gravity separator's three outlets regulate flows through the choke and separator, respectively. The gravity separator is located downstream of the choke valve to avoid the siphoning effect of the vacuum pipeline. The test equipment and operating ranges are listed in Table 3.1.

Table 3.1. Experimental parameters and model input data.

Name	**Type**	**Description**	**Range/Size**
Water Pump	Grundfos CRNE 3	Centrifugal water feed pump	1 L/s at 162.7 m, maximum 25 bar
Oil pump	Grundfos DDA	Mechanically actuated diaphragm oil feed pump	(1.94×10−7 − 0.0022) g/s, maximum 16 bar
Pressure transmitters	Siemens Sitrans P200	Piezo-resistive pressure measuring cell	(0–16) bar
Flow transmitters	Rosemount 8732	Electromagnetic flow transmitter	DN50 (0–25.966) L/s @ 12 m/s
Flow transmitters	Bailey-Fischer-Porter 10DX4311C	Electromagnetic flow transmitter	DN15 (0–1.64034) L/s
Flow Transmitter	Micro-Motion Coriolis Elite	Coriolis flow transmitter	N10 (1.389× 10−5 − 0.0033) L/s
Mixer	In-house-designed Turner-	Venturi based mixer	D DN50
Valve	Bürkert 2301 + 8696	Globe valve	Vo = 3 mm , Vu = 15 mm

3.1.2 Data Acquisition

Similar to past studies (Durdevic et al., 2015; Durdevic et al., 2016; Pedersen, 2016; Pedersen et al., 2016; Pedersen et al., 2017), all data acquisition and controls are performed using Simulink Real-time models for real-time simulations. The transmitters and actuators are linked to the data acquisition system. Riser-induced and casing-heading slugs in the test rig's pipeline-riser section were documented by Pedersen et al. (2016) and Pedersen et

al. (2017). The multiphase flow in the system consists of gas and liquid phases. The liquid consists of oil and water in equal proportions. A Coriolis flowmeter is used. The liquid phase was kept at room temperature (20°C) and transported through the pipeline-riser to the separator in a closed flow loop. Compressed air is injected simultaneously into the pipeline and at the bottom of the riser for gas-lift processes. A topside choke valve was mounted on top of the riser between the two pressure sensors to control the flow regimes.

For each experiment, measurements were taken of the pressures, flow rates, temperatures, and densities in the pipeline-riser system. The liquid level in the separator, pump pressures, and gas injection rates at the inlet of the pipeline and bottom of the riser were also recorded. The main inputs were the choke valve opening, separator pressure, and gas lift. Gas and liquid inflow conditions were controlled by means of pumps and a constant gas volume fraction (GVF). For each test, measurements were taken with the aforementioned instrumentation at different locations in the flow loop. The sampling frequency was 100 Hz points per second for all experiments, each lasting about one and a half hours with approximately 520,000 measurements per test. Each new experiment was repeated to ensure reproducibility of the tests. The separator pressure was kept at the atmospheric condition. The temperature was relatively constant at 20°C, with an accuracy of $\pm 0.01\ ^{\circ}\mathrm{C}$. Further analysis of the measurement errors and experimental uncertainties are presented in Appendix A. In a typical petroleum fluid production system, the wellhead pressure (which in our case, the pump pressure) is maintained at a constant value. This is essential to achieve a constant volumetric flowrate at the wellhead. By maintaining a relatively constant pressure drop between the reservoir and the well top, an almost constant

volumetric rate is achieved. Similarly, the separator pressure is generally constant as the surface separation equipment are designed based on the constant separator pressure. We also maintain a relatively constant temperature since subsea temperature variation is not significant in real-life applications.

3.1.3 Operating conditions for the choking experiments

To study the impact of choking on the slugging, the gas injection was zero at all times. The separator pressure was nearly constant.

Table 3.2. System parameters and operating conditions for the choking experiment.

Experiment parameters	**Values**	**Comments**
Pump pressure	1.8 bar	The pressure fluctuates between 1.78 and 1.84 bar, an average of 1.8 bar was obtained
Separator pressure	1.0 bar	Atmospheric conditions, no pressurization
Choke openings	100%, 90%, 80%, 70%, 60%, 50%, 40%, 30%, 20%, 10%.	
No of tests	10	
Inlet liquid flowrate	0.4 kg/s	
Inlet gas flow rate	4.88×10^{-4} kg/s	
Liquid level in the separator	0 meters	The liquid level will be controlled by the underflow valve
Inlet gas viscosity	0.000181 Pa.s	
Inlet liquid viscosity	0.090445 Pa.s	
Inlet gas density	1.988×10^{-5} kg/m^3	
Liquid density	900 kg/m^3	
Pipe diameter	0.054 m	
Riser diameter	0.054 m	

The degree of choke opening is stepped down by 10% after a set period. First, a slug was created during the first 50 seconds and allowed for 700 seconds for the 100%-degree choke

opening. During the subsequent openings (90%, 80%, 70%, 60%, 50%, 40%, 30%, 20%, and 10%), the durations were 300 s for each degree opening tested. Table 3.2 describes the experimental design parameters and operating for the choking experiment.

3.1.4 Operating conditions for the gas lifting experiment.

For the gas-lift experiment, the choke valve was fully open. Gas was injected at the bottom of the riser where the liquid is accumulated. The aim of the gas injection at the bottom of the riser is to ensure continuous gas penetration into the riser, and to reduce the hydrostatic head imposed by the long liquid slug in the riser column, hence decreasing the pressure in the pipeline. The injected gas also helps to carry the liquid to the surface receiving facilities. When the gas volume in the system is sufficient to ensure continuous fluid lifting, a stabilised flow may be achieved. The detailed operating conditions and system parameters for the experiment are given in Table 3.3.

Table 3.3. System parameters and operating conditions for the gas lift experiment.

Experiment parameters	**Values**	**Comments**
Pump pressure	1.8 bar	The pressure fluctuates between 1.78 and 1.84 bar, an average of 1.8 bar was obtained
Separator pressure	1.0 bar	Atmospheric conditions, no pressurization
Inlet liquid flowrate	0.4 kg/s	
Inlet gas flow rate	4.88×10^{-4} kg/s	
Liquid level in the separator	0 meters	The liquid level will be controlled by the underflow valve
Choke openings	100%	Constant choke opening
Riser based gas injection	0.625 nm^3/hr	0.625 nm^3/hr increments every 300 seconds.
No of tests	7	
Inlet gas viscosity	0.000181 Pa.s	

Inlet liquid viscosity	0.090445 Pa.s	
Inlet gas density	1.988×10^{-5} kg/m^3	
Liquid density	900 kg/m^3	
Pipe diameter	0.054 m	
Riser diameter	0.054 m	

3.1.5 Operating conditions for the combined (choking and gas lifting) experiment.

The combined scheme involves simultaneous riser base gas-lift and topside choking. This was conducted to demonstrate slug control mitigation in some offshore applications, especially in production systems where the upstream pressure is largely depleted and insufficient to lift the reservoir productions. Compressed nitrogen gas was injected at the point where the elongated bubbles are formed at the bottom of the riser. At the same time, the choke opening was stepped down from 100% to 10%. The detailed operating conditions and system parameters for the experiment are given in Table 3.4.

Table 3.4. System parameters and operating conditions for the combined (choking and gas lift) experiment.

Experiment parameters	**Values**	**Comments**
Pump pressure	1.8 bar	The pressure fluctuates between 1.78 and 1.84 bar, an average of 1.8 bar was obtained
Separator pressure	1.0 bar	Atmospheric conditions, no pressurization
Inlet liquid flowrate	0.4 kg/s	
Inlet gas flow rate	4.88×10^{-4} kg/s	
Liquid level in the separator	0 meters	The liquid level will be controlled by the underflow valve
Choke openings	100% to 10%	Stepped down by 10%
Riser based gas injection	0.625 nm^3/hr	0.625 nm^3/hr increments every 300 seconds.

No of tests	5	
Inlet gas viscosity	0.000181 Pa.s	
Inlet liquid viscosity	0.090445 Pa.s	
Inlet gas density	1.988×10^{-5} kg/m^3	
Liquid density	900 kg/m^3	
Pipe diameter	0.054 m	
Riser diameter	0.054 m	

The test conditions were designed based on similar tests conducted by other researchers (Durdevic et al., 2015; Durdevic et al., 2016; Pedersen et al., 2016; Pedersen et al., 2017). Slug flow was characterized by pressure and flow rate oscillations in the pipeline. Under stable flow conditions, there was no liquid blockage at the bottom of the riser. The flow was steady with bubble or small slug pockets. The slug flow rate was maintained within the slug regime throughout each experiment. For each slug elimination scheme considered, a slugging flow regime was created in the pipeline system until a fully developed slug occurred. Flow regime maps were plotted using experiment data based on the Boe (1981) and Jansen (1996) criteria. The data points fall within the severe slugging region corresponding to $U_{sl} = 0.01 - 1\mathrm{m/s}$ (see Appendix B)

Figure 3.2 shows the configuration of a fully developed mechanism of severe slugging. Slugs were created with constant liquid and gas flow rates of 0.4 kg/s and 0.000484 kg/s, respectively. A constant air injection rate was maintained into the system through the inlet of the pipeline at a constant pump pressure of approximately 1.8 bar. A constant inlet pressure was achieved by maintaining a constant pump speed with a proportional-integral controller. The gas controller was used to maintain a constant gas flow rate through a GVF. For the case of gas-lift, an additional 0.625 nm^3/hr of air was injected into the flow system every 5 minutes through the riser base until a maximum capacity of 5 m^3 was reached.

The reservoir section accommodates the inflow supply equipment including the mixing of the water, oil, and gas at the pipeline inlet. The outlet fluid moves into the 3-phase separator (see Figure 3.1). Steady-state operating conditions are attained for each valve opening. The valve openings are in the range of 10% and 100%, which covers the majority of actual operating conditions for fluid recovery in offshore oil and gas processing applications.

3.2 Modelling of Severe Slugging in Offshore Fluid Transport

In the following section, the methods and procedures involved in the model development are described.

3.2.1 Model description

The model considers four state equations given by the mass balance equations in Equations (3.1a) through (3.1d). The multiphase flow through the riser-pipeline system is at isothermal conditions with an average temperature of 20℃. The simplified model is used to reproduce severe slugging phenomena in riser systems and can be applied for systems in which additional mass is introduced for flow assurance enhancement such as gas injected into the riser. It considers the riser, consisting of different segments. The segments are local positions expressed by the coordinates of points belonging to the riser which are not spatially separated from each other. The segments are identified with their distinct volumes and geometry. The model is based on extensions of past models of Stokaas (2005), Jehanshahi and Stokass (2012), and Balino (2010). The model is developed to improve the robustness of these past models by including the riser geometry to capture the features in catenary and flexible riser systems, which are commonly installed in offshore fluid transport systems (see Figure 1.1).

3.2.2 Flowline Riser System

Figures 3.2 (a) and (b) illustrate a simplified configuration of the pipeline-riser system. The pipeline-riser system is used to describe the multiphase transport of oil well productions. The system of piping consists of a section of downward inclination angle (end of pipeline), followed by a section of upward inclination angle (riser), as shown in Figure 3. The pipeline component is made of horizontal and inclined segments. Based on Figure 3.2 (a), there is a continuous gas penetration into the riser. Thus, there is no liquid accumulation at the bottom of the riser and the mass flow rate of gas is not equal to zero. The liquid level in the pipelines is less than the pipeline diameter. As seen in Figure 3.2 (b), the liquid phase blocks the pipe entrance and prohibits gas penetration into the riser. The liquid height is greater than the pipeline diameter.

3.2.3 Governing Equations

The state equations for the segments are given by the conservation of mass as follows:

$$\dot{m}_{Gp} = w_{G,in} - w_{G,lp} \tag{3.1a}$$

$$\dot{m}_{Lp} = w_{L,in} - w_{L,lp} \tag{3.1b}$$

The mass conservation equations are similarly used to describe the riser system as follows:

$$\dot{m}_{Gr} = w_{G,lp} + w_{gn} - w_{Gr,out} \tag{3.1c}$$

$$\dot{m}_{Lr} = w_{L,lp} - w_{Lr,out} \tag{3.1d}$$

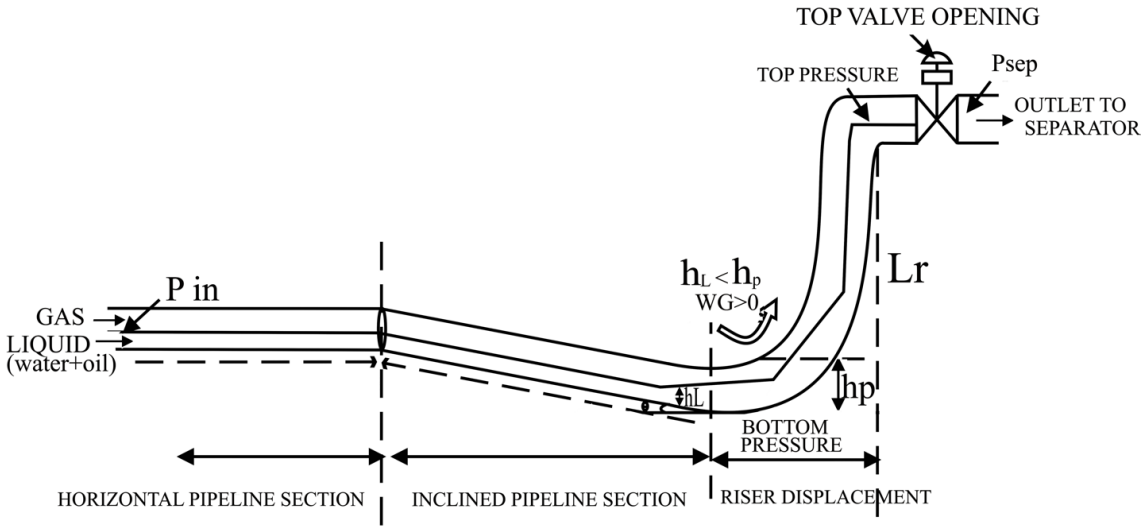

(a)

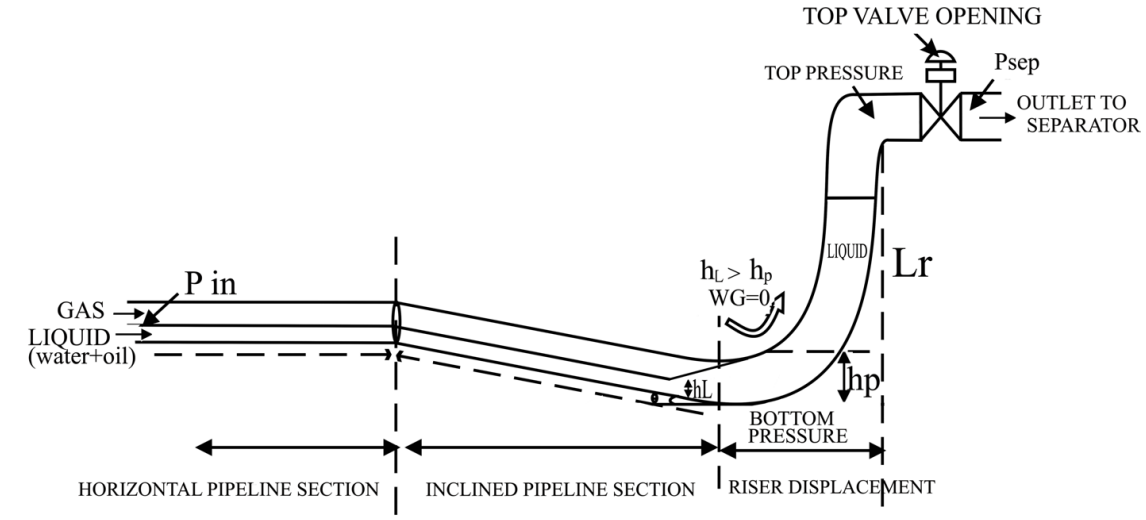

(b)

Figure 3.2. Flowline-catenary riser configuration for (a) non-slugging and (b) slugging flow regimes.

In the above equations, $w_{G,in}$ and $w_{L,in}$ are the inlet mass flow rates of the phases (correspondingly gas and liquid); and $w_{G,out}$ and $w_{L,out}$ designate the outlet mass flow rates for the gas and liquid, respectively. The subscripts lp and r represent the low point in the pipeline section and the risers, respectively. Also w_{gn} is a parameter that describes an additional mass input (such as gas-injection to boost the pressure, and injection of scavengers).

3.2.4 Model Assumptions

The assumptions considered in the model development are listed below.

(a) Constant mass flow rates are assumed at the inlet. The outlet mass flow rate is determined from an orifice equation.

(b) The two phases are well mixed and in equilibrium.

(c) No slippage occurs between the phases and the liquid fraction is determined based on the mass flow rates.

(d) The fluid properties are determined based on the ideal gas laws.

(e) The liquid phase is considered incompressible, while the gas phase is compressible.

(f) The liquid fraction in the riser is assumed to be the arithmetic average of the liquid fraction at the bottom of the riser and the top of the riser.

(g) Both the gravitational and frictional pressure drops are considered, while the dynamic pressure drop is neglected both in the riser and the pipeline.

3.2.5 Riser Model

Most offshore platforms use flexible pipes for the riser systems especially in deepwater environments. Flexible risers can adapt to the dynamic positioning systems in offshore

vessels, such as floating production, storage and offloading systems (FPSOs), and submersible production platforms. This model includes a geometry for the riser model to integrate this feature.

A catenary riser is considered for two-phase isothermal flow (see Figures 3.2 a-b). A simplified equation for gas and liquid phases flowing together is the governing equation for the riser section. A no-slip model is assumed, implying that the in-situ holdup is the no-slip liquid holdup. The second assumption is that the values of the velocity and temperature of the gas and liquid phases are identical. The liquid phase (oil and water) is assumed to be homogeneous; thus it is treated as a bulk liquid phase. As stated, ideal gas is assumed at isothermal conditions. In general, most of the gases deviate from ideal when the pressure is over 5 bar. However, air or air components (N_2 and O_2) still behave like an ideal gas even at pressures up to 50 bar (Smith et al., 2001).

Riser Geometry. The riser system can be represented by a function which describes the

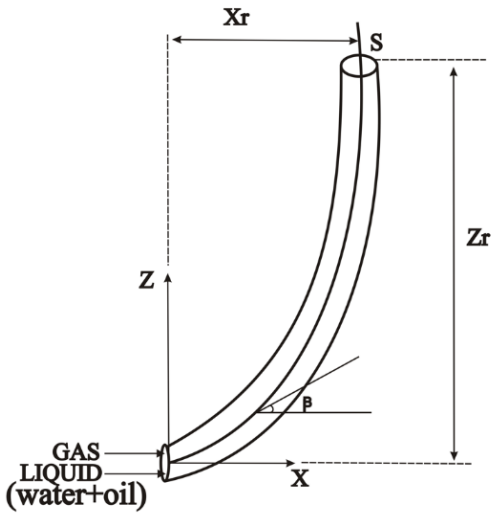

Figure 3.3. Geometry of the riser displacement.

system coordinates for all points where the riser extends, as shown in Figure 3.3 (Nemato, 2012).

The local height for each location can then be calculated from the following transcendental equation (Nemato, 2012):

$$Z_r = A\left[\cosh\left(\frac{X_r}{A}\right) - 1\right] \tag{3.2}$$

where Z_r and X_r characterize the coordinate points. The parameter A is obtained by solving Equation (3.2) through an iterative process until convergence is achieved. The total length of the riser can be calculated by substituting A into Equation (3.3) and using the following equations:

$$L_r = A\sinh\left(\frac{X_r}{A}\right) \tag{3.3}$$

$$L_i = L_{i-1} + \Delta L = (i-1)\Delta L = \left(\frac{i-1}{N-1}\right) L_r \tag{3.4}$$

$$\beta_i = \tan^{-1}\left(\frac{L_i}{A}\right) = \tan^{-1}\left[\left(\frac{i-1}{N-1}\right)\left(\frac{L_i}{A}\right)\right] \tag{3.5}$$

The local height for each segment and its corresponding inclination (β_i, L_i) can be determined from Equations (3.4) and (3.5), respectively. In Equation (3.5), β is the inclination of the riser displacement and L_i refers to the local length for a riser segment, while N is the total number of nodes.

Pressure Drop in Riser. Both the frictional pressure loss and hydrostatic pressure difference are considered for the riser section. The pressure drop associated with flow acceleration is neglected. The volume fractions and in-situ gas-liquid mixture density for the flow regime are determined to obtain the hydrostatic differential pressure. The friction

factor is then evaluated using the inflow boundary condition as follows (Pinder and William, 2008):

$$\frac{dP}{dL} = \bar{\rho}_L . g \sin\theta + \frac{\lambda_r \bar{\rho}_{mi} \bar{U}_{mi}}{4 r_i} \tag{3.6}$$

where θ is the inclination angle; $\bar{U}_{mi}$ represents the average mixture velocity; and λ_r is the friction factor for the riser segment. The pressure drop for each segment is calculated as follows:

$$\Delta P_i = \left(\frac{dP}{dL}\right)_i \Delta L \tag{3.7}$$

where ΔP_i stands for the total pressure drop of segment i; and $\bar{\rho}_L$ is the average liquid density. The friction factor of the mixture in segment i is obtained by the following relationship (Skogestad, 2010):

$$\lambda_r = 0.0056 + 0.5\, {R_{emi}}^{-0.32} \tag{3.8}$$

$$R_{emi} = \frac{\lambda_r \bar{\rho}_{mi} \bar{U}_{mi}\, r_i}{\mu_{mi}} \tag{3.9}$$

where R_{emi} is the Reynolds number of the mixture and μ_{mi} designates the mixture density. When the liquid level in the inclined pipeline section is above the critical level ($h_L > h_p$), the liquid level blocks the low point (base of the riser) and the gas flow rate; hence, $W_{G,lp}$ at the low point is zero.

3.2.6 Boundary Conditions

The inlet mass flow rates of the phases ($W_{G,in}$ and $W_{L,in}$) are measured at the pipeline entry point and are constant. The mass fractions of the phases can be expressed in terms of their respective volume fractions by dividing by their respective densities, as given below (Jahanshahi, 2011):

$$\alpha_L = \frac{\alpha_{Lm}/\rho_L}{\frac{\alpha_{Lm}}{\rho_L}+(1-\alpha_{Lm})/\rho_G} \tag{3.10}$$

where α_L is the liquid volume fraction. The average liquid mass fraction can be approximated using the inflow boundary condition as follows:

$$\bar{\alpha}_{Lm} = \frac{W_{L,in}}{W_{G,in}+W_{L,in}} \tag{3.11}$$

Combining the above two equations gives the average liquid volume fraction.

$$\bar{\alpha}_{Lm} = \frac{\bar{\rho}_G.W_{L,in}}{\bar{\rho}_G.W_{L,in}+\rho_L W_{G,in}} \tag{3.12}$$

The gas density ($\bar{\rho}_G$) can be calculated based on the nominal pressure (steady state) of the horizontal pipeline, as given below. Ideal gas phase is assumed:

$$\bar{\rho}_G = \frac{P_G \,.\, M_G}{RT_p} \tag{3.13}$$

where R is the gas constant; and T_p is the temperature in the pipeline segement.

3.2.7 Pipeline Model

A steady-state condition is assumed for the inflow and the gas and liquid phases are distributed homogenously along the pipeline.

Along the pipeline, the mass of liquid is given by $\bar{m}_{Lp} = \rho_L V_p \bar{\alpha}_{Lp}$. If the liquid contact of the pipeline increases by $\Delta\bar{m}_L$, it starts to fill up the pipeline from the low point. A length of pipeline equal to ΔL will be occupied by $\Delta h_L = \Delta L \sin\theta$.

$$\Delta m_L = \Delta L \pi {r_p}^2 (1-\bar{\alpha}_L)\rho_L \tag{3.14}$$

$$h_p = \bar{h}_p + \Delta L \sin\theta = \bar{h}_p + \frac{\Delta m_L}{\pi {r_p}^2 (1-\bar{\alpha}_L)\rho_L}\sin\theta \tag{3.15}$$

where θ $(0 \le \theta \le 90)$ is the pipeline inclination angle. The phase level is therefore approximated to the following equation (Jahanshahi, 2011):

$$\bar{h}_p = k_h h_L \bar{\alpha}_L \tag{3.16}$$

where h_L represents the liquid level in the pipeline before the fluid accumulation and k_h is an empirical parameter. Therefore, the level of liquid in the inclined section of the pipeline (h_p) can be written as follows (Jahanshahi, 2011):

$$h_p = \bar{h}_p + \left[\frac{m_L - \rho_L(V_p \bar{\alpha}_p)}{\pi {r_p}^2 (1-\bar{\alpha}_p)\rho_L}\right] \sin\theta \tag{3.17}$$

in which m_L refers to the liquid mass flow rate in pipeline. The other parameters in Equation (3.17) are constants and averaged values.

Volume occupied by gas in the pipeline. The volume of the pipeline occupied by the gas phase, $(V_g)_p$, is determined as follows:

$$(V_g)_p = V_p - {m_L}/{\rho_L} \tag{3.18}$$

The gas density in the pipeline is defined as follows:

$$\rho_{G_p} = \frac{m_G}{V_G} \tag{3.19}$$

The inlet pressure in the pipeline is calculated from the following equation:

$$P_p = \frac{\rho_{G_p} Z_p R T_p}{M_G} \tag{3.20}$$

It should be noted that the inlet pressure in the pipeline is approximately equal to the wellhead pressure, and the inlet temperature, T_p, is equal to the wellhead temperature and $Z_p = 1$.

Pressure drop in the pipeline. The total pressure loss in the pipeline is a summation of pressure drops due to friction and hydrostatic effects in the liquid phase. The frictional factor component of the pressure losses along the pipeline (under steady-state conditions) is calculated for the liquid phase by the correlation of Beggs and Brill (1973), as per below:

$$\Delta P_{f,p} = \frac{\bar{\alpha}_{Lp}\ \lambda_p\ \rho_L\ \bar{U}_{SL,in}{}^2\ L_p}{4r_p} \tag{3.21}$$

The no-slip friction factor is calculated based on the following relationship of Beggs and Brill (1973):

$$\lambda_p = \frac{1}{\{2\log[N_{Re}/(4.5223\log N_{Re} - 3.8215)]\}^2} \tag{3.22}$$

The friction factor can also be determined from the smooth pipe curve of the Moody diagram (Beggs and Brill, 1978). The Beggs and Brill (1991) empirical models for multiphase flow are widely used in the petroleum industry for oil and gas fluid transport analysis. The Reynolds number is calculated as:

$$N_{Re_p} = \frac{2\rho_L \cdot \bar{U}_{SL,in}\, r_p}{\mu_L} \tag{3.23}$$

where μ_L is the viscosity of the liquid and $\bar{U}_{SL,in}$ denotes the superficial velocity of the liquid at the inlet, as defined below:

$$\bar{U}_{SL,in} = \frac{W_{L,in}}{\pi p^2 \rho_L} \tag{3.24}$$

The hydrostatic pressure drop due to the pipeline downward inclination is written as $\rho_L g \Delta L \sin\theta$. Hence, the total pressure drop in the pipeline is given as follows:

$$\Delta P_p = \Delta P_{f,p} + \rho_L g \Delta L \sin\theta \tag{3.25}$$

where $\Delta P_{f,p}$ is the pressure drop due to friction, L is the inclined pipe length and θ is the inclination angle of the pipeline with the horizontal plane.

3.2.8 Averaged Fluid Properties

A different flow regime may exist when gas, oil, and water from petroleum wells are transported through the pipelines. Slug flow may exist where the liquid phase (oil and water) either separates completely, partially mixes, or fully mixes along the flowline (Hall,

1992, 1993). The distribution of the liquid and gas phases in the system has a strong effect on the modelling of the transition to the slug flow regime. The constitutive equation for the gas phase is written as:

$$\rho_G = \frac{\gamma_g M_a}{RT}\frac{P}{Z} \tag{3.26}$$

where $\gamma_g = M_g/M_a$, is the gas specific gravity. Also $M_a(= 28.966\ g/gmol)$ and M_g are the molecular weights of air and gas respectively. The compressibility factor (Z) depends on the temperature and pressure, which equal 1 for ideal gases, and R ($8.314 m^2 s^{-1} K^{-1}$) is the universal gas constant.

Averaged mixture velocity. The average mixture velocity for each segment can be written as follows:

$$\overline{U}_{mi} = \overline{U}_{sLi} + \overline{U}_{sGi} \tag{3.27}$$

where U_{sGi} and U_{sLi} introduce the gas superficial velocity and liquid superficial velocity in the riser, respectively, as determined from the inflow conditions by the following equations:

$$\overline{U}_{sLi} = \frac{W_{Li}}{\pi {r_i}^2 \rho_L} \tag{3.28a}$$

$$\overline{U}_{sGi} = \frac{W_{Gi}}{\pi {r_i}^2 \rho_{Gi}} \tag{3.28b}$$

The phase volumetric flow rates are known from measurements obtained at the wellhead flowmeters. The local gas velocity is estimated from the drift flux model (Zuber and Findlay, 1965) as follows:

$$U_G = \frac{U_{sG}}{\alpha_G} = C_d U_m + U_d \tag{3.30}$$

Given that $U_m = U_{sG} + U_{sL}$, then:

$$U_{sL} = U_m - \alpha_G(C_d U_m + U_d) = U_m(1 - \alpha_G C_d) - \alpha_G U_d \quad (3.31a)$$

$$U_{sL1} = U_{m1}(1 - \alpha_{G1} C_{d1}) - \alpha_{G1} U_{d1} = U_{mi}(1 - \alpha_{Gi} C_{di}) - \alpha_{Gi} U_{di} \quad (3.31b)$$

$$U_{mi} = \frac{U_{mi-1}(1-\alpha_{Gi-1}C_{di-1})-\alpha_{Gi-1}U_{di-1}}{(1-\alpha_{Gi}C_{di})} \quad (3.32)$$

Assuming that the Froude number, which characterizes flow in the system, is lower than 3.5, the drift flux parameters can be written as follows:

For $F_{r_j} < 3.5$

$$\left\{\begin{matrix} C_{d_i} = 1.05 + 0.15 \sin\theta_i \\ U_{d_i} = (0.35 \sin\theta_i + 0.54 \cos\theta_i) x \sqrt{g D_1} \end{matrix}\right\} \ (D = 2r) \quad (3.33)$$

Average density of mixture. The average mixture density for each segment is calculated as follows:

$$\bar{\rho}_{mi} = \frac{m_{Gi} + m_{Li}}{V_i} \quad (3.34)$$

Volume fractions of phases. The volume fraction of the liquid phase is estimated based on the volumetric average of each phase.

3.2.9 Gas Flow at the Low Point

When the liquid level in the inclined pipeline section is above the critical level ($h_L > h_p$), the liquid level blocks the low point (base of the riser) and the gas flow rate, $W_{G,lp}$ at the low point is zero, as shown below:

$$W_{G,lp} = 0, \ h_L \geq h_p \quad (3.35)$$

When the liquid is not blocking at the low point ($h_L < h_p$), the gas will flow from volume V_G to V_{G1} with a mass flow rate of $W_{G,lp}$ $\left(\frac{kg}{s}\right)$. The key parameters that determine the gas flow rate are the pressure drop over the low point and the opening area (Jahanshahi, 2014).

This suggests that the gas transport can be described by an orifice equation where the gas flow is driven by the pressure drop across the orifice with an opening area, A_G (Stokaas and Skogestad, 2005). The gas flow rate is calculated by the following equation:

$$W_{G,lp} = k_G A_G \sqrt{\left(\rho_{G,B} \Delta P_G\right)} \qquad h_L < h_p \tag{3.36}$$

where

$$W_{G,lp} = k_G A_G \sqrt{\left(\rho_{G,B} \Delta P_G\right)} \qquad h_L < h_p \tag{3.37}$$

$$\Delta P_G = P_t + \sum_{i-1}^{N-1} \Delta P_i \tag{3.38}$$

The liquid mass flow rate at a low point can also be determined using the orifice equation given below (Stokaas and Stogestad, 2005):

$$W_{L,lp} = k_L A_L \sqrt{\left(\rho_{L,} \Delta P_{l,p}\right)} \tag{3.39}$$

where $\Delta P_{l,p} = \Delta P_L = \Delta P_{lG} = P_p - P_{r1}$

$\Delta P_{L,p} = P_t + \sum_{i-1}^{N-1} \Delta P_i$

In the above equations, k_L and k_g are the empirical parameters. The free area for gas flow is approximated using the quadratic relationship (Jahanshahi and Skogestad, 2011):

$$A_G = \pi r^2 \left(\frac{h_p - h_L}{h_p}\right)^2 \qquad h_L < h_p \tag{3.40}$$

$$A_L = \pi r^2 - A_G \tag{3.41}$$

3.2.10 Phase Distribution Model at the Outlet Choke Valve

To calculate the mass flow rate of the individual phases, the phase distribution of the two phases and the density of the two-phase mixture at the top of the riser are determined as follows:

$$\alpha_{Lm,t} = \frac{\alpha_{L,t}\ \rho_L}{\alpha_{L,t}\,\rho_{L,}+(1-\alpha_{L,t})\rho_{G,t}} \tag{3.42}$$

$$\rho_{m,t} = \ \alpha_{L,t}\,\rho_{L,} + (1-\alpha_{L,t})\rho_{G,t} \tag{3.43}$$

where $\alpha_{Lm,t}$ is the average mass fraction at the top of the riser; $\rho_{m,t}$ designates the average density at the top of the riser, and ρ_L and $\rho_{G,t}$ represent the densities of the liquid and gas, respectively, at the top of the riser.

3.2.11 Outlet Flow Conditions

The separator is considered the outlet boundary of the system. The separator pressure is assumed constant and the outflow of the fluid mixture is calculated using a choke valve equation as follows (Skogestad, 2005):

$$W_{mix,\ out} = C_v, f(z)\sqrt{\rho_r max(P_{n-1} - P_s)} \tag{3.44}$$

where $W_{mix,\ out} = W_{G,\ out} + W_{L,\ out}$ is the total mass flow rate of the mixture downstream of the choke; C_v resembles the choke valve coefficient; and $f(z)$ is the characteristic valve equation. A linear valve is desired, i.e., $f(z) = z$, $0 < z < 1$, which refers to the normalized valve opening. Also, P_{n-1} is the pressure at the top of the riser and P_s stands for the separator pressure.

The mass flow rates at the choke outlet are determined as follows:

$$W_{G,out} = \alpha_{Lmt}\, W_{mix,out} \tag{3.45}$$

$$W_{L,out} = (1-\alpha_{Lmt})\, W_{mix,out} \tag{3.46}$$

3.2.12 Model Validation

The experimental facility described in Figure 3.1 was used to validate the results obtained from the numerical models. The same fluid system and flow conditions were used for the

model predictions and experiments. However, the gas module was operated by an in-built controller that adjusts the valve to the desired location.

3.3 Two-Phase Correlations for Evaluation and Design of Slug Mitigation Measures

3.3.1 Experimental Facility Description

Figure 3.4 shows a detailed schematic of the experimental facility for slug mitigation testing at the Offshore Energy Laboratory of Aalborg University, Denmark. As mentioned earlier, the author travelled for an extended period to Denmark for collaborative studies with researchers at the Offshore Energy Laboratory of Aalborg university.

The experimental setup used for this study is an extension of the setup described previously in section 3.1. The extension included measurement of the phase flow rates at before mixing as shown in figure 3.4. Ten experiments were conducted for this test. For each experiment, the pressures, flow rates, temperatures, and densities along the pipeline-riser system were also measured.

Similarly, the slug flow rate was maintained within the slug regime throughout the experiment. During each experiment, the choke degree opening is lowered by 10% after a specific time period. First, the slug was created during the first 50-second period and allowed for 700 seconds for the 100%-degree choke opening. During the subsequent openings (90%, 80%, 70%, 60%, 50%, 40%, 30%, 20%, and 10%), the duration was 300 seconds for each degree opening. The experimental results were also presented on stability maps of the past studies (Boe, 1981; Jansen et al., 1996) by plotting their gas and liquid velocities (see Appendix B).

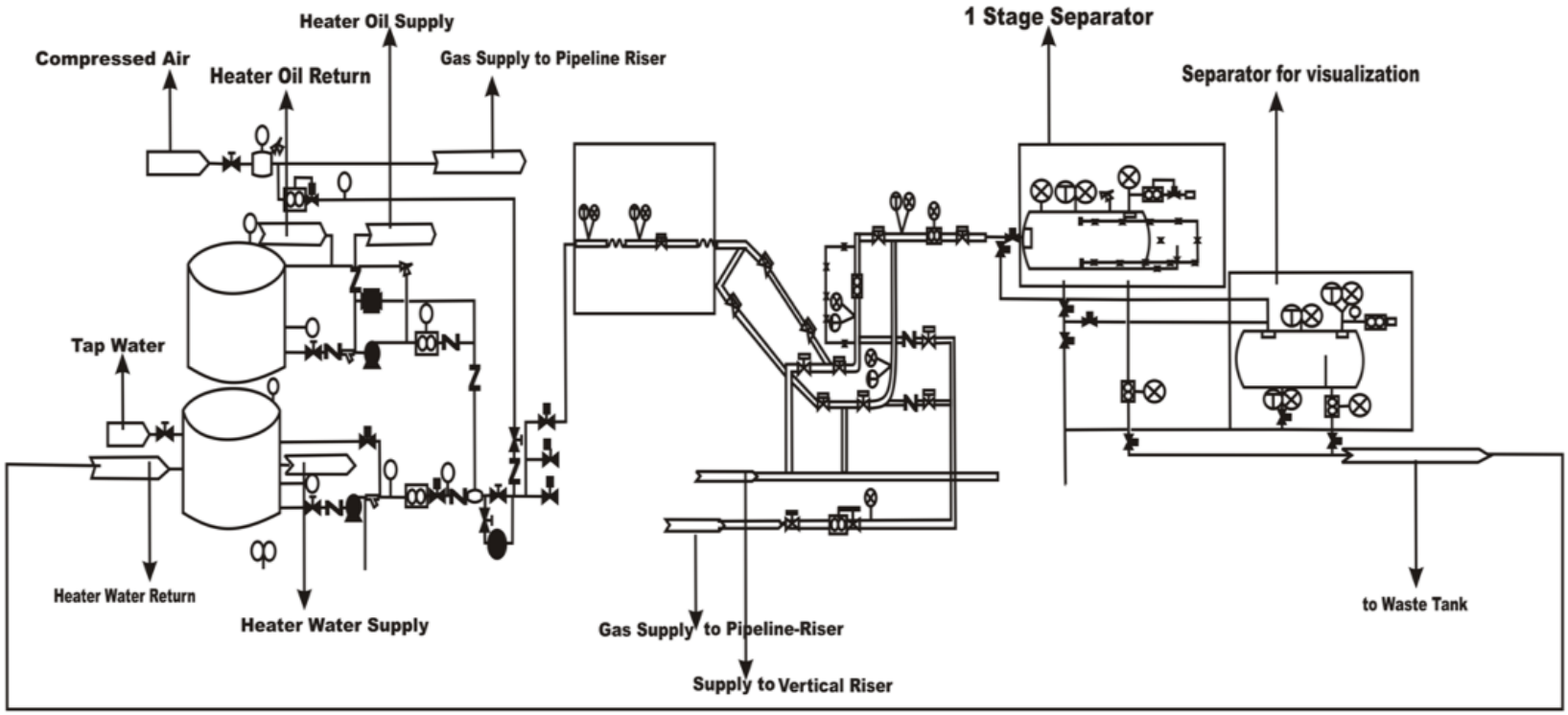

Figure 3.4. Experimental facility to conduct slug mitigation tests.

3.3.2 Model Formulation for Slug Frequency

A semi-analytical approach will be used to develop models of the slug frequency. The model development involves non-dimensional empirical correlations in terms of relevant dimensionless groups, which are obtained based on the design of the experiment. The dimensionless π terms are formed from the Buckingham π-theorem (Buckingham, 1914). First, the slug frequency is expressed as a function of the nine key parameters that describe slugging in pipeline-riser systems, as given below:

$$f_s = F[w_{li,}, w_{gi}, Z, \Delta P, \rho_{gi}, \rho_l, \mu_m, w_m, D] \quad (3.47)$$

In Equation (3.47), f_s refers to the slug frequency; $w_{li,}$ is the liquid flow rate into the pipeline; $w_{gi,}$ is the gas flow rate into the pipeline; Z is the choke opening; ΔP is the change in pressure; ρ_{gi} is the gas density at the pipe inlet; ρ_l is the liquid density; μ_m is the mixture viscosity; w_m represents the mixture flow rate at the choke outlet; and D is the pipe diameter. Based on the two-phase flow properties and system geometrical parameters, the identified variables/parameters are grouped into appropriate dimensionless terms (see Table 3.5).

According to the Buckingham π-theorem (Buckingham, 1914), Equation (3.47) can be rewritten in terms of the relevant dimensionless groups as follows:

$$\pi_0 = \phi(\pi_1, \pi_2, \pi_3, \pi_4, \pi_5) \quad (3.48)$$

The various dimensionless groups are obtained as functions of the parameters that influence slugging in a flow system.

Table 3.5. Summary of dimensionless groups describing slug frequency in pipeline-riser.

π Terms	**Dimensionless group**		**Description**
π_0	Keulega - Carpenter's number, Kc (Keulegan, 1958):	$\frac{v_m T^*}{D}$	A ratio of drag forces to the inertia for an oscillating fluid flow
π_1	Choke valve opening, Z	Z	Percentage of choke opening
π_2	Reynolds number for flow in pipeline, Re_p (Reynolds, 1883)	$\frac{\rho_{m,p} v_{m,p} D_p}{\mu_m}$	A ratio of inertia and viscous forces in the pipeline
π_3	Bejan number for flow in pipeline, Be_p (Bejan et al., 1997)	$\frac{\Delta P_p {L_p}^2}{\mu_{m,p} \epsilon_{m,p}}$	Dimensionless pressure drop along the pipeline
π_4	Maximum Bejan number for flow in riser, $Be_{r,max}$	$\frac{\Delta P_r {L_r}^2}{\mu_{m,r} \epsilon_{m,r}}$	Dimensionless pressure drop along the riser
π_5	Density ratio, D. R	$\frac{\rho_g}{\rho_l}$	A ratio of the gas density to the liquid density

The dimensionless groups are chosen based on a review of previous studies and key parameters identified in the experimental work:

$$\pi_0 = C \cdot \pi_1^{n_1} \pi_2^{n_2} \pi_3^{n_3} \pi_4^{n_4} \pi_5^{n_5} \tag{3.49}$$

$$Kc = C_0 \cdot Z^{n_1} \; Re_{m,i}{}^{n_2} \; Be_p{}^{n_3} \; Be_{r,max}{}^{n_4} \; \left(\frac{\rho_g}{\rho_l}\right)^{n_5} \tag{3.49}$$

$$Kc = C_1 \cdot Z^{n_1} \, Re_{m,i}{}^{n_2} \; Be_p{}^{n_3} \, Be_{r,max}{}^{n_4} \; \left(\frac{\rho_g}{\rho_l}\right)^{n_5} \tag{3.50}$$

where the constant is

$$C_1 = \; C_0 \lambda_2^{n_3} \lambda_3^{n_4} \tag{3.51}$$

The $\pi-$terms are used to define the dimensionless groups, while the exponents are parameters that should be determined from the coefficients of data curve fitting. The logarithmic expansion of Equation (3.50) is given below:

$$log\, Kc \; = \; log\, C_1 + n_1\, log\, Z + n_2\, log\, Re_{m,i} + n_3\, log\, Be_p +$$

$$n_4\, log\, Be_{r,max} + n_5\, log\left(\rho_g / \rho_L\right) \tag{3.52}$$

Using Equation (3.50), the slug frequency (f_s) can be calculated from the following relationship (Keulegan, 1958):

$$f_s \; = \frac{K_C \, \mathrm{D}}{\mathrm{V_m}} \tag{3.53}$$

According to Equation (3.53), the slug frequency is expressed in terms of the mixture velocity (V_m) as the slug front propagation velocity is proportional to the mixture velocity (Bendiksen, 1984). Also K_C is the Keulegan-carpenter number, which is the ratio of drag to inertia forces for oscillating fluid flow (Keulegan, 1958) as defined below:

$$K_C \; = \frac{V_m T}{D} \tag{3.54}$$

Here V_m refers to the interfacial flow velocity for oscillating fluid flow; T represents the period of the slug; and D is the diameter of the flow path. The mixture interfacial velocity is obtained as $v_m = \; v_L + v_G$. The mixture velocity can be expressed in terms of the fluid mass flow rate (w_l and w_g) and the area of the flow channel (A) as follows:

$$V_m = \frac{1}{A}\left(\frac{w_l}{\rho_l} + \frac{w_g}{\rho_g}\right) \tag{3.55}$$

where w and ρ refer to the mass flow rate and density, respectively. The subscripts, g and l, denote the gas and the liquid phases, respectively. The Keulegan-Carpenter number in Equation (3.54) can be written as a function of the experimental variables and slug frequency as follows:

$$Kc = \frac{4m_l}{\alpha_l \pi \rho_l D^2} \cdot \frac{1}{f_s D} \tag{3.56}$$

In the following section, a sensitivity analysis will be carried out. The first step in the analysis is to only consider the impact of the choke opening (Z) on the slug frequency correlation:

$$Kc = f(Z) \tag{3.57}$$

where Z is the choke opening. Including the effect of the inflow conditions in the form of the inflow mixture Reynolds number on the slug frequency is expressed below:

$$Kc = \mathrm{F}\,(Z, Re_{m,i}) \tag{3.58}$$

The inlet Reynolds number ($Re_{m,i}$), as a ratio of inertia to viscous forces, is given as follows:

$$Re_{m,i} = \frac{\rho_m v_m D_p}{\mu_m} = \frac{w_{m,i} D_p}{A_p \mu_{m,i}} \tag{3.59}$$

Here the mixture mass flow rate of the liquid and gas phases ($\mathrm{w_{m,i}}$) is obtained as follows:

$$w_{m,i} = w_{l,i} + w_{g,i} \tag{3.60}$$

Equation (3.59) is then rewritten in the following form:

$$Re_{m,i} = \frac{4\,(w_{l,i}+w_{g,i})}{\pi \mu_{m,i} D_p} \tag{3.61}$$

The dimensionless pressure drop in the pipeline-riser loop can be evaluated by the Bejan number (Be_p). Including the effect of the pressure drop, the following expression is obtained:

$$Kc = \mathrm{f}(Z, R_{em,i}, Be_p) \tag{3.62}$$

The Bejan number for flow in the pipeline segment of the flow system is a function of the pressure drop across the pipeline (ΔP_p), pipeline length (L_p), mixture viscosity ($\mu_{m,p}$), and diffusivity ($\epsilon_{m,p}$), as expressed below:

$$Be_p = \frac{\Delta p_p \, L_p^2}{\mu_{m,p} \, \epsilon_{m,p}} \tag{3.63}$$

The total pressure drop along the length of the pipeline section is the sum of the pressure drops due to gravity, friction, and acceleration. To simplify the model, the pressure drop contributions of the acceleration and frictional terms are included as the ratios of gravitational pressure drop, as shown below:

$$\Delta p_p = \Delta p_{gravity} + \Delta p_{friction} + \Delta p_{acceleraion} \tag{3.64}$$

Also,

$$\Delta p_p = \varphi_1 \Delta p_{gravity} = \varphi_1 \cdot \bar{\rho}_m g L_{p\theta} \sin\theta_p \tag{3.65}$$

where $\varphi_1 = (1 + \mathrm{m}_1 + \mathrm{m}_2)$; m_1 and m_2 represent the ratios of the pressure drops due to friction and acceleration, respectively, to the pressure drop due to gravity.

Substituting Equation (3.65) in Equation (3.63) leads to:

$$Be_p = \frac{\lambda_1 \bar{\rho}_m L_{p\theta} \sin\theta_p \, L_p^2}{\mu_{m,p} \, \epsilon_{m,p}} = \lambda_2 \cdot \frac{\rho_{m,i} L_{p\theta} L_p^2 \sin\theta_p}{\mu_{m,i} \, \epsilon_{m,i}} \tag{3.66}$$

A simplified equation for the mixture viscosity is used for the homogenous two-phase system where both phases flow together. As stated in section 3.2.4, the system is

isothermal, and the mass flow rates are constant at the inlet. The two phases are well mixed and in equilibrium. No slippage occurs between the phases, and the liquid fraction is determined based on the mass flow rates. A comprehensive review of viscosity models for two-phase flow is discussed in section 3.4.

The mixture viscosity at the pipeline inlet ($\mu_{m,i}$) is defined as follows (Ishii and Mishima 2008):

$$\mu_{m,i} = \mu_{l,i}\,\alpha_{l,i} + \mu_{g,i}\,(1-\alpha_{l,i}) \tag{3.67}$$

The mixture diffusivity at the pipeline inlet ($\epsilon_{m,i}$) is obtained by the following expression:

$$\epsilon_{m,i} = \epsilon_{l,i}\,\alpha_{l,i} + \epsilon_{g,i}\,(1-\alpha_{l,i}) \tag{3.68}$$

The liquid volume fraction at the inlet ($\alpha_{l,i}$) is also determined as follows (Pinder and Willian, 2008):

$$\alpha_{l,i} = \frac{\dot{Q}_{li}}{\dot{Q}_{li}+\dot{Q}_{gi}} = \left(1+\frac{w_{g,i}}{w_{l,i}}\cdot\frac{\rho_{g,i}}{\rho_{l,i}}\right)^{-1} \tag{3.69}$$

The adjustment factor, $\varphi_2 = \frac{\mu_{m,i}\,\epsilon_{m,i}/\rho_{m,i}}{\lambda_1\bar{\mu}_m\,\bar{\epsilon}_m/\bar{\rho}_m}$, is assumed to be constant in the correlation. Therefore, the Bejan number in the pipeline can be written as follows:

$$Be_p = \varphi_2\cdot\frac{\rho_{m,i}L_{p\theta}L_p^2\,sin\,\theta_p}{\mu_{m,i}\,\epsilon_{m,i}} = \varphi_2\cdot\ddot{Be}_p \tag{3.70}$$

The Bejan number for flow in the riser segment is expressed as a function of the maximum pressure drop in the riser (e.g., between the bottom of the riser and the separator downstream of the riser). In Equation (3.70), $\ddot{Be}_p$ is the adjusted Bejan number in the pipeline. The Bejan number for the riser is thus defined by the following equation:

$$Be_r = \frac{\Delta P_r\,{L_r}^2}{\mu_{m,r}\,\epsilon_{m,r}} \tag{3.71}$$

The total pressure drop across the riser is obtained as follows:

$$\Delta P_r = \left(P_i - \Delta p_p\right) - P_{sep.} = \left(P_i - P_{sep.}\right) - \varphi_1 \cdot \bar{\rho}_m L_{p\theta} \sin\theta_p \quad (3.72)$$

where P_i is the pressure at the inlet of the pipeline and P_{sep} refers to the separator pressure, topside of the riser. This pressure is equivalent to the pressure of the first stage separator for multi-stage separation installation.

Due to the complexity and difficulty in obtaining φ_1, the Bejan number is obtained instead as shown below:

$$Be_r = \frac{\Delta P_{r_{max}} {L_r}^2}{\mu_{m,r}\,\epsilon_{m,r}} = \varphi_3 \frac{\left(P_i - P_{sep.}\right){L_r}^2}{\mu_{m,i}\,\epsilon_{m,i}} = \varphi_3 \cdot \ddot{Be}_r \quad (3.73)$$

Similarly, the adjustment factor, $\varphi_3 = \frac{\mu_{m,i}\,\epsilon_{m,i}}{\bar{\mu}_m\,\bar{\epsilon}_m}$, is assumed to be constant.

In Equation (3.73), $\ddot{Be}_r$ is the adjusted Bejan number in the riser.

The effect of Bejan number in the riser on the slug frequency is considered in the correlation, as presented below:

$$Kc = F\,(Z, R_{em,i}, Be_p, Be_r) \quad (3.74)$$

Thus, the combined form of the dimensional group, $\frac{Kc}{Z^{n_1} Re_{m,i}^{n_2} Be_p^{n_3}}$ will be plotted against the Bejan number in the riser (Be_r).

In the last step of the analysis, the influence of the fluid densities is evaluated. The density ratio, $\frac{\rho_g}{\rho_l}$ (ratio of the gas density to the liquid density), at the system inlet, is given below:

$$DR = \frac{\rho_{g,i}}{\rho_{l,i}} \quad (3.75)$$

To assess the influence of the fluid densities on slug frequency, the combined dimensionless expression ($\frac{Kc}{Z^{n_1} Re_{m,i}^{n_2} Be_p^{n_3} Be_{r,max}^{n_4}}$) will be plotted against the density ratio

$\left(\frac{\rho_g}{\rho_l}\right)$. To obtain a more accurate correlation, the first step of the 2nd iteration evaluates the sensitivity of combined dimensionless term to Z where the term considers other dimensionless groups with their final coefficients, as expressed below:

$$\frac{Kc}{Re_{m,i}^{0.693} Be_{,p}^{5.955} Be_{m,r}^{-2.54}} \; vs \; Z \tag{3.76}$$

Obtaining a new coefficient for *Z*, other coefficients are updated, and the sensitivity analysis is conducted as follows:

$$Step\ 1\text{:}\ \frac{Kc}{Z^{-0.415} Be_{,p}^{5.955} Be_{m,r}^{-2.54}} \; vs \; R_{em,i} \tag{3.77}$$

$$Step\ 2\text{:}\ \frac{Kc}{Z^{-0.415} Re_{m,i}^{0.693} Be_{m,r}^{-2.54}} \; vs \; B_{e,p} \tag{3.78}$$

$$Step\ 3\text{:}\ \frac{Kc}{Z^{-0.415} Re_{m,i}^{0.693} Be_{,p}^{5.955}} \; vs \; B_{e,r} \tag{3.79}$$

$$Step\ 4\text{:}\ \frac{Kc}{Z^{-0.415} Re_{m,i}^{0.693} Be_{,p}^{5.955}} \; vs \; \frac{\rho_g}{\rho_l} \tag{3.80}$$

In the last step of the analysis, the influence of the fluid densities is evaluated by including the ratio of the gas to liquid densities. Individual sensitivity studies were carried out in Equations (3.76) through (3.80) by comparing the individual π_i groups on the combined groups.

Thus, the resulting model is obtained as follows:

$$Kc^* = 1.07 \cdot Z^{0.415} Re_{m,i}^{0.693} Be_{,p}^{-5.955} Be_{m,r}^{2.54} \tag{3.81}$$

After several iterations, the resulting final correlation is expressed as follows:

$$Kc^* = Z^{-0.660} Re_i^{0.744} Be_p^{8.932} Be_{max\,r}^{-2.914} \tag{3.82}$$

Results from this correlation will be presented and discussed in the next chapter.

3.3.3 Model Formulation for Two-Phase Slug Velocity Prediction

A dimensional analysis will also be performed to obtain the empirical form of an equation governing the slug flow velocity in a slug regime dominated flow. The dimensionless π terms are formed from the correlation variables based on the Buckingham π-theorem. The production is expressed as a function of the nine main parameters in describing slugging in pipeline-riser systems.

$$W_{mix} = f\left[w_{l,in}, w_{g,in}\, Z, P_{in}, P_{sep}, \rho_m\, , \mu_m, w_{Li,} D\right] \tag{3.83}$$

Based on the two-phase flow properties and the system geometrical parameters, the identified variables are grouped into appropriate dimensionless groups and shown in Table 3.6. The Buckingham π-theorem is used to determine the non-dimensional form of the correlation. Equation (3.83) can be written in terms of the relevant dimensionless groups as follows:

$$\pi_1 \; = f\left(\, \pi_1 \, , \pi_2 \, , \pi_3 \, \ldots \pi_i \, \right) \tag{3.84}$$

Table 3.6. Summary of dimensionless groups for slug velocity in the riser.

π term	**Dimensionless group**	**Expression**	**Description**
π_1	Mixture Reynolds number at the choke outlet	$\frac{\rho_{m,p} v_{m,p} D_p}{\mu_m}$	A ratio of inertia and viscous forces in the pipeline
π_2	Choke valve opening, Z	Z	Percentage of choke opening

π_3	Mixture Reynolds number for flow in pipeline inlet, $\mathrm{Re}_{m,i}$	$\frac{\rho_{m,p} v_{m,p} D_p}{\mu_m}$	A ratio of inertia and viscous forces in the pipeline
π_4	Bejan number for flow in the pipeline, Be_p	$\frac{\Delta P_p {L_p}^2}{\mu_{m,p} \epsilon_{m,p}}$	Dimensionless pressure drop along the pipeline
π_5	Bejan number for flow in riser, Be_r	$\frac{\Delta P_r {L_r}^2}{\mu_{m,r} \epsilon_{m,r}}$	Dimensionless pressure drop along the riser
π_6	Density ratio, D. R	$\frac{\rho_g}{\rho_l}$	A ratio of the gas density to the liquid density

The various dimensionless groups are obtained as functions of the parameters that influence slugging in flow systems. The six dimensionless groups were chosen based on past literature, system parameters, and flow variables identified during experiments involving slug creation.

$$\pi_0 = C \cdot \pi_1^{n_1} \pi_2^{n_2} \pi_3^{n_3} \pi_4^{n_4} \pi_5^{n_5} \pi_6^{n_6} \tag{3.85}$$

$$R_{em} = C_0 z^{n_1} \times {R_{em,i}}^{n_2} \times {B_{e,p}}^3 \times {B_{e,R}}^{n_4} \times {B_{e,}}^{n_5} \times {\rho_g}/{\rho_L}^{n_6} \tag{3.86}$$

$$R_{em} = C_1 \cdot Z^{n_1} \times {R_{em,i}}^{n_2} \times {B_{e,p}}^3 \times {B_{e,R}}^{n_4} \times {B_{e,}}^{n_5} \times \left(\frac{\rho_g}{\rho_l}\right)^{n_6} \tag{3.87}$$

where the constant is

$$C_1 = \frac{C_0}{\varphi_0} \tag{3.88}$$

Equations (3.84) to (3.87) are used for the correlation development. The π terms are used to define the dimensionless groups while the exponents are parameters determined from the coefficient of data fit. The logarithmic expansion of Equation (3.87) gives the following expression:

$$log\, R_{em,o} = log\, C_1 + n_1\, log\, z + n_2\, log\, R_{em,i} + n_3\, log\, B_{eL,p} + n_4\, log\, B_{e,R} +$$

$$n_5\, log\, B_e + n_6\, log\, {\rho_g}/{\rho_L} \tag{3.89}$$

In Equation (3.87), the mixture velocity can be calculated from the following relationship:

$$U_m{}^* = \frac{R_{em}\,\mu_{mi}}{\rho_m D} \tag{3.90}$$

where R_{em} is the mixture Reynolds number, which is the ratio of inertia to the viscous forces, for fluid flow, as defined below:

$$R_{em}{}^* = \frac{\rho_m U_m D}{\mu_{mi}} \tag{3.91}$$

Here U_m is the mixture interfacial velocity for an oscillating fluid flow; ρ_m is the density of the slug; and D is the diameter of the flow path. The mixture interfacial velocity is obtained as $U_m = v_L + v_G$; where v_L represents the liquid velocity and v_g is the gas velocity. The mixture velocity can also be written in terms of the fluid mass flow rate and the area of the flow channel as follows:

$$U_m = \frac{1}{A}\left(\frac{w_l}{\rho_l} + \frac{w_g}{\rho_g}\right) \tag{3.92}$$

The Reynolds number in Equation (3.91) can be expressed directly in terms of the variables of this experiment and the slug flow velocity as written below:

$$R_{em}{}^* = \frac{4U_m}{\alpha_l \pi \rho_l D} \times \frac{1}{\mu_m} \tag{3.93}$$

In the following section, a step-by-step analysis will be carried out to examine the relationship of the main parameters with the mixture slug velocity.

The first step in the analysis evaluates the choke opening. Equation 3.89 can be written as follows:

$$log\left(R_{em,o}{}^*\right) = log\, C_1 + n_1\, log(z) \tag{3.94}$$

where *z* is the choke opening.

$$\left(log\, R_{em,o}\right) = log\, C_0 + n_1 (log\, z) \tag{3.95}$$

Recall,

$$R_{em,o} = \varphi_0 \frac{w_m D_r}{\mu_{m,i}} \tag{3.96}$$

where φ_0 is obtained by assuming that the viscosity of the mixture at the outlet varies linearly with the viscosity of the mixture at the inlet as follows:

$$\mu_{m,o} = \mu_{m,i} \cdot {}^{1}/_{\varphi_0} \tag{3.97}$$

Recall from Equation (3.67) that the mixture viscosity at the inlet can be calculated as follows:

$$\mu_{m,i} = \mu_{L,i}\,\alpha_{L,i} + \mu_{g,i}\,(1 - \alpha_{L,i}) \tag{3.98}$$

where $\alpha_L = \frac{1}{1+\frac{w_g}{w_L}+\frac{\rho_L}{\rho_g}}$ (3.99)

It can be shown that $\alpha_L = \frac{\alpha_{Lm}\rho_g}{\rho_L\,(1-\alpha_{Lm})+\,\alpha_L\rho_g}$ (3.100)

where

$$\alpha_{Lm} = \frac{w_L}{w_L + w_g} \tag{3.101}$$

$$\alpha_{L,m} = \frac{\alpha_L\rho_L}{\alpha_L\rho_g+\rho_g\,(1-\alpha_L)} \tag{3.102}$$

Here $\alpha_{L,m}$ is the mass fraction of the liquid phase.

Expanding Equation (3.95) results in:

$$log\left(R_{em,o}{}^{*}\right) = [\,log\,C_0 - \,log\,\varphi_0] + n_1\,log(z)\,,\quad C_1 = \frac{C_0}{\varphi_0}$$

$$log\left(R_{em,o}{}^{*}\right) = \,log\,C_1 + n_1\,log(z) \tag{3.103}$$

Step 2 evaluates the influence of the inflow. Thus, Equation (3.95) can be written as:

$$log\left(\frac{R_{em}}{z^{\,n_1}}\right) = \quad log\,C_2 + n_2\,log\left(R_{em,i}\right) \tag{3.104}$$

The Reynolds number in the pipeline is determined based on the fluid flow into the system. The Reynolds number, as a ratio of inertial to viscous forces, is determined as follows:

$$Re_{m,i} = \frac{\rho_m \, v_m \, D_p}{\mu_m} = \frac{w_{m,i} \, D_p}{A_p \mu_{m,i}} \tag{3.105}$$

Here the mixture mass flow rate of the liquid and gas phases ($w_{m,i}$) is obtained as $w_{m,i} = w_{l,i} + w_{g,i}$.

Hence, the inlet Reynolds number is expressed as follows:

$$Re_{m,i} = \frac{4\,(w_{l,i}+w_{g,i})}{\pi \mu_{m,i} \, D_p} \tag{3.106}$$

The third step obtains the pressure drop in the pipeline. The dimensionless pressure drop in the pipeline-riser loop can be evaluated by the Bejan number. Equation (3.95) can be written as follows:

$$log\left(\frac{{R_{em,o}}^*}{z^{\,n_1} {R_e}_{m,i}^{\,n_2}}\right) = \quad log\, C_3 + n_3\, log\left(B_{e,p}\right) \tag{3.107}$$

The Bejan number for flow in the pipeline segment of the flow-system is calculated as a linear function of the total pressure drop across the pipeline section (ΔP_p) and an inverse function of the mixture viscosity ($\mu_{m,p}$) and diffusivity ($\epsilon_{m,p}$). The Bejan number is expressed mathematically as:

$$B_{e,p} = \frac{\Delta p_{p,} \times {L_p}^2}{\mu_m \, \epsilon_m} \tag{3.108}$$

Similarly, the total pressure drop across the pipeline section is determined from Equation (3.65). Hence, the Bejan number in the pipeline is given as follows:

$$B_{e,p} = \quad \varphi_1 \varphi_2 \frac{\rho_{m,i} g {L_{pi}}^2 sin\theta_p}{\mu_{m,i} \, \epsilon_{m,i}} \tag{3.109}$$

where $L_{p,i}$ is the length of the inclined section of the pipeline.

$$\varphi_2 = \frac{\mu_{m,i}\,\epsilon_{m,i}/\rho_{m,i}}{\bar{\mu}_m\,\bar{\epsilon}_m/\bar{\rho}_m} \tag{3.110}$$

$$B_{e,p} = \varphi_3 \frac{\rho_{m,i} g {L_{pi}}^2 sin\theta_p}{\mu_{m,i}\,\epsilon_{m,i}};\quad (\varphi_3 = \varphi_1\varphi_2) \tag{3.111}$$

The adjustment factor $\varphi_2 = \frac{\mu_{m,i}\,\epsilon_{m,i}/\rho_{m,i}}{\bar{\mu}_m\,\bar{\epsilon}_m/\bar{\rho}_m}$ is assumed to be constant. Therefore, the Bejan number in the pipeline can be written as:

$$B_{e,p} = \varphi_3 {B_{e,p}}^*;\ \left({B_{e,p}}^* = \frac{\rho_{m,i} g {L_{pi}}^2 sin\theta_p}{\mu_{m,i}\,\epsilon_{m,i}}\right) \tag{3.112}$$

The log-log relationship is given below:

$$log\left(\frac{{R_{em,o}}^*}{z\ {n_1 R_e}_{m,i}^{n_2}}\right) = \ log\,{C_3}^+ + n_3\,log\left({B_{e,p}}^*\right) \tag{3.113}$$

where ${C_3}^+ = C_3\varphi_3\ ^{n_3}$.

In the 4th step, the Bejan number for flow in the riser segment is expressed as a function of the maximum pressure drop in the riser (pressure drop between the bottom of the riser and the separator downstream of the riser). The Bejan number corresponding to this flow is obtained as follows:

$$Be_r = \frac{\Delta P_r\,{L_r}^2}{\mu_{m,r}\,\epsilon_{m,r}} \tag{3.114}$$

Due to the complexity in approximating φ_1, the Bejan number is approximated as follows:

$$Be_r = \frac{\Delta {P_r}_{max}\,{L_r}^2}{\mu_{m,r}\,\epsilon_{m,r}} = \varphi_3 \frac{(P_i - P_{sep.})\,{L_r}^2}{\mu_{m,i}\,\epsilon_{m,i}} = \varphi_3 \cdot \ddot{Be}_r \tag{3.115}$$

Assuming $\bar{\mu}_{mr}$ is proportional directly to μ_{mi},

$$\bar{\mu}_{mR} = \varphi_4\,\mu_{mi} \tag{3.116}$$

Similarly,

$$\bar{\epsilon}_{mr} = \varphi_5 \epsilon_{m,i} \tag{3.117}$$

The pressure drop in the riser is taken for the entire riser length, as expressed below:

$$(\Delta p)_r = \left(p_{in} - p_{sep}\right) - p_p \cong \left(p_{in} - p_{sep}\right) - \rho_{m,i} l_{pi} sin\theta_p \quad (3.118)$$

The total pressure drop across the riser is obtained as:

$$\Delta P_r = \left(P_i - \Delta p_p\right) - P_{sep.} = \left(P_i - P_{sep.}\right) - \varphi_1 \cdot \bar{\rho}_m L_{p\theta} \sin\theta_p \quad (3.119)$$

where P_i is the pressure at the inlet of the pipeline and P_{sep} is the separator pressure, topside of the riser. This pressure is equivalent to the first stage separator pressure for multi-stage separation installation.

$$B_{e,r} = \frac{1}{\varphi_4 \varphi_5} B_{e,r}{}^* = \frac{1}{\varphi_6} B_{e,r}{}^*, (\varphi_6 = \varphi_4 \varphi_5) \quad (3.120)$$

where

$$B_{e,p}{}^* = \frac{L_r{}^2}{\mu_{mi} \epsilon_{m,i}} \left[\left(p_{in} - p_{sep}\right) - \rho_{m,i} l_{pi} sin\theta_p\right] \quad (3.121)$$

where p_{in} is the pressure at the inlet of the pipeline and p_{sep} is the separator pressure, topside of the riser. This pressure is equivalent to the first stage separator pressure for multi-stage separation installation.

The log-log relationship is given as follows:

$$log\left(\frac{R_{em,o}{}^*}{z\ n_1 R_e{}^{n_2}_{m,i} B_e{}^{n_3}_{m,p}}\right) = log\ C_4 + n_4\ log\left(B_{e,r}\right) \quad (3.122)$$

$$log\left(\frac{R_{em,o}{}^*}{z\ n_1 R_e{}^{n_2}_{m,i} B_e{}^{n_3}_{m,p}}\right) = log\ C_4{}^+ + n_4\ log\left(B_{e,r}{}^*\right) \quad (3.123)$$

where $C_4{}^+ = C_4 \frac{1}{\varphi_6{}^{n_4}}$ (3.124)

The fifth step calculates the total pressure in the system.

Recall:

$$B_{e,R} = \frac{\Delta p_{t,} L_t{}^2}{\bar{\mu}_m \bar{\epsilon}_m} \quad (3.125)$$

where Δp_t stands for the total pressure drop in the flow system (pipeline + riser):

$$\Delta p_t = p_{in} - p_{sep} \tag{3.126}$$

$$L_t = L_p + L_r \tag{3.127}$$

Assuming $\bar{\mu}_m \bar{\epsilon}_m \cong \varphi_7 \mu_{mi} \epsilon_{m,i}$, then

$$B_{e,R} == \frac{1}{\varphi_7} B_{e,r}{}^* \tag{3.128}$$

where

$$B_e{}^* = \frac{(p_{in} - p_{sep})(L_p + L_r)^2}{\mu_m \epsilon_m} \tag{3.129}$$

The log-log relationship is the given as follows:

$$log\left(\frac{R_{em,o}{}^*}{z\ {n_1}{R_e}_{m,i}^{n_2}{B_e}_{m,p}^{n_3}}\right) = \ log\ C_5 + n_5\ log(B_e) \tag{3.130}$$

$$log\left(\frac{R_{em,o}{}^*}{z\ {n_1}{R_e}_{m,i}^{n_2}{B_e}_{m,p}^{n_3}}\right) = \ log\ C_5 + n_5\ log(B_e{}^*) \tag{3.131}$$

where $C_5{}^+ = C_5 \frac{1}{\varphi_7\ n_5}$ (3.132)

The last step evaluates the phase densities. The density ratio, $\frac{\rho_g}{\rho_l}$, is obtained at the inlet as the ratio of the gas density to the liquid density.

$$DR = \frac{\rho_{g,i}}{\rho_{l,i}} \tag{3.133}$$

The log-log relationship can be written as follows:

$$log\left(\frac{R_{em,o}{}^*}{z\ {n_1}{R_e}_{m,i}^{n_2}{B_e}_{m,p}^{n_3}{B_e}_{m,r}^{n_4}{B_e}^{n_5}}\right) = \ log\ C_6 + n_6\ log\left({\rho_g}/{\rho_L}\right) \tag{3.134}$$

Recall:

$$R_{em,o}{}^* = C_6\ {\pi_1}^{n_1}{\pi_2}^{n_2}\ {\pi_3}^{n_3}\ \ldots\ {\pi_6}^{n_6} \tag{3.135}$$

Substituting appropriate values, the preliminary equation is obtained as follows:

$(\mathrm{n}_1 = -0.076,\ \mathrm{n}_2 = -0.061,\ \mathrm{n}_3 = 0,\ \mathrm{n}_4 = 0.02497,\ \mathrm{n}_5 = 0,\ \mathrm{n}_6 = 0)$

$$R_{em,o}{}^{*} = 10^{0.235} z^{-0.076} R_{em,i}{}^{-0.061} B_{e,r}{}^{0.249} \tag{3.136}$$

$$R_{em,o}{}^{*} = 0.934 z^{-0.076} R_{em,i}{}^{-0.061} B_{e,r}{}^{0.249} \tag{3.137}$$

Further iterations are performed on the preliminary correlation to improve the coefficients. A stepwise analysis is carried out as given in Equations (3.138) through (3.143).

Iteration 2 Step 1:

$$\frac{\mathrm{R_{em,o}}^{*}}{0.934\mathrm{R_{em,i}}^{-0.061}\mathrm{B_{e,r}}^{0.249}} \text{ vs } \mathrm{z} \tag{3.138}$$

Iteration 2 Step 2:

$$\frac{\mathrm{R_{em,o}}^{*}}{0.934\mathrm{z}^{-0.076}\mathrm{B_{e,r}}^{0.249}} \text{ vs } \mathrm{R_{em,i}} \tag{3.139}$$

Iteration 3 Step 3:

$$\frac{\mathrm{R_{em,o}}^{*}}{0.934\mathrm{z}^{-0.076}\mathrm{R_{em,i}}^{-0.061}\mathrm{B_{e,r}}^{0.249}} \text{ vs } \mathrm{B_{e,p}} \tag{3.140}$$

Iteration 2 Step 4:

$$\frac{\mathrm{R_{em,o}}^{*}}{0.934\mathrm{z}^{-0.076}\mathrm{R_{em,i}}^{-0.061}} \text{ vs } \mathrm{B_{e,r}} \tag{3.141}$$

Iteration 2 Step 5:

$$\frac{\mathrm{R_{em,o}}^{*}}{0.934\mathrm{z}^{-0.076}\mathrm{R_{em,i}}^{-0.061}} \text{ vs } \mathrm{B_{e,max}} \tag{3.142}$$

Iteration 2 Step 6:

$$\frac{\mathrm{R_{em,o}}^{*}}{0.934\mathrm{z}^{-0.076}\mathrm{R_{em,i}}^{-0.061}\mathrm{B_{e,r}}^{0.249}} \text{ vs } \frac{\rho_g}{\rho_l} \tag{3.143}$$

Following these successive improvements of the model empirical parameters from the repeated iterations, the final correlation is given below:

$$R_{em,o}{}^{*} = 0.528\, z^{-0.0431} R_{em,i}{}^{-0.056} B_{e,r}{}^{0.276} \tag{3.144}$$

Results based on this correlation will be presented and discussed in the next chapter.

3.4 Two-Phase viscosity model

Mixture viscosity is an important parameter in multi-phase flow modelling due to its influence in pressure drop calculations. This brief review examines existing mixture viscosity models for their suitability in modelling two-phase flows. Two-phase modelling and simulation require accurate and fast algorithms for fluid property calculations. In research studies and industrial applications, two-phase simulations are carried out for a wide range of flow systems, such as in nuclear, refrigeration, automotive, air-conditioning, and pipeline systems. A review of the literature shows that most of the mixture viscosity models are developed for homogeneous fluid modelling. Further, differences exist for some mixture viscosity models developed for conventional pipes, mini channels, and microchannels.

3.4.1 Homogeneous two-phase viscosity model

The homogeneous flow model is commonly used for analyzing two-phase flow. The model assumes that both the liquid and gas phases move at the same velocity. Hence, the multi-phases may be treated as a single-phase, and the slip ratio equals 1. The homogeneous two-phase flow model considers average fluid properties and is basically expressed as a function of their mass fractions. The void fraction for the homogeneous model may be expressed as follows:

$$\alpha_g = \frac{q_g}{q_g + q_l} \tag{3.145}$$

where α and q are the void fraction and flowrate, respectively. The subscripts, $g\ and\ l$, denote the gas and liquid phases, respectively. The void fraction may be expressed in terms of mass quality as follows:

$$\alpha_g = \frac{1}{1+\left(\frac{1-x}{x}\right)+\left(\frac{\rho g}{\rho_l}\right)} \tag{3.146}$$

The Reynolds number based on the homogenous model may be defined as

$$Re = \frac{\rho_m v_m D}{\mu_m} \tag{3.147}$$

where v_m ($v_m = v_g + v_l$) is the mixture velocity, and ρ_m ($= \rho_g + \rho_l$) is the mixture velocity.

The isothermal frictional pressure drops can be readily determined from the values of the Reynold number obtained from Equation (A.50); μ_m represents the mixture velocity.

The viscosity of fluid containing N components may be expressed as a function of pressure, temperature and pressure, as follows:

$$\mu_f = \mu(P, T, \alpha^i)\ i = 1, \ldots, N-1. \tag{3.148}$$

Past studies (Pinder and William, 2009; Ishii and Mishima 2008; Ishii and Hibiki, 2011) have shown that the influence of pressure on viscosity can be neglected except for very high pressures. For isothermal conditions, the fluid viscosity may be written in terms of

their mass fractions. Pinder and William (2009) defined the viscosity of multicomponent fluid mixture under isothermal conditions as follows:

$$d\mu_f = \sum_{i=1}^{N-1} \frac{\partial \mu}{\partial \alpha^i}\, d\alpha^i, i = 1, \ldots, N-1 \tag{3.149}$$

Ishii and Hibiki (2008) showed that the mixture velocity of a multi-phase flow system may be determined by the following equation if the effect of relative velocities of the component phases is negiligible.

$$\mu_m = \sum_{k=1}^{2} \alpha_k\, \mu_k \tag{3.150}$$

They expressed the mixture velocity for two-phase flow as follows:

$$\mu_m = \alpha_g\, \mu_g + \alpha_l\, \mu_l \tag{3.151}$$

Beggs and Brill (1973) defined the two-phase mixture viscosity as follows:

$$\mu_m = \alpha_g\, \mu_g + (1 - \alpha_l)\, \mu_l \tag{3.152}$$

They developed correlations based on experiments conducted on an air-water fluid system in a 25.4 mm and 38.1 mm pipes at different angles of inclination. The authors correlated the liquid fraction to pipe inclination for different flow patterns, including intermittent, segregated and distributive flow patterns. They developed a correlation for frictional pressure drop calculation; the no-slip friction factor may be read from the Moody chart as a function of the no-slip Reynolds number.

There are significant differences in flow behaviour for capillary tubes, and micro and mini channels compared to a conventional pipe when calculating pressure drop (Inaska et al., 1989; Lin et al., 1991; Fouran and Borie, 1995; Serizawa et al., 2001; Chen et al., 2001;

Siansorn, 2006; Wongwises, 2008) and two-phase flow patterns (Suo and Grifith, 1964; Barnea et al., 1983;1989; Fukano and Kerayasaki, 1993; Triplett 1999; Cavallini, 2009). Mini channels are characterized as capillary tubes or multi-port extruded aluminium tubes with internal diameters between $200\mu m - 3mm$, while the range of hydraulic diameters for microchannels is between $10\mu m - 200\mu m$ (Cavallini et al., 2001; 2009). Some researchers found that the dominating flow driving force can significantly affect flow characteristics of multi-phase systems. This review identifies that the flow patterns in convectional sized pipes are dominated by gravity, whereas for mini and micro-sized tubes, the flow is dominated by surface tension, viscous, and inertia forces. Also, Barnea (1983) argued that the widely used Kelvin-Helmholtz type instability criterion of Taitel and Dukler (1976) is not suitable for micro and mini channels, due to the dominance of surface tension effects over gravitational force.

Many researchers have also proposed a different mixture of viscosity correlations in the past, especially in modelling pressure drop in mini channels and microchannels. Table 3.7 outlines the common mixture viscosity models proposed by various studies mostly conducted for mini channels and microchannels.

McAdams (1942) proposed a model for calculating two-phase viscosity as follows:

$$\mu_m = \frac{1}{\mu_g} + \frac{(1-x)}{\mu_l} \tag{3.153}$$

They expressed the mixture viscosity as a function of the reciprocals of averaged flow quality. The authors suggested the use of fanning friction factor to calculate the frictional pressure drop. They suggested a fanning friction factor ($f_f = 16/Re_f$) for Reynolds

numbers less than or equal to 2000 and a fanning friction factor ($f_f = 0.046/Re_f^{0.2}$) for Reynolds numbers greater than 2000.

Davidson et al. (1943) proposed a correlation for mixture viscosity calculations based on their experiment conducted for the steam-water fluid system as follows:

$$\mu_m = \mu_l \left[1 - x\left(\frac{\rho_l}{\rho_g} - 1\right)\right] \tag{3.154}$$

Their experiment was conducted under high pressures between 3600 Pa and 23900Pa. The authors showed that the steam-water two-phase mixture compared reasonably with the Blasius equation for single-phase pressure drop calculation. Their correlation, however, fails when the flow quality approaches 1.

Cicchitti et al. (1960) examined the frictional pressure drop for different flow regimes including dispersed flow for both adiabatic and non -adiabatic conditions, and proposed a homogenous correlation for mixture viscosity calculation as follows:

$$\mu_m = x\,\mu_g + (1 - x)\,\mu_l \tag{3.155}$$

They showed that the homogenous model can predict pressure drop with good accuracy and suggested that they could be effectively used for pressure drop calculation in mini and microchannels.

Owen (1964) defined the mixture viscosity for two-phase flow based on the liquid viscosity as follows:

$$\mu_m = \mu_l \tag{3.156}$$

The author explained that the viscosity of the liquid phase is dominant in two-phase flows.

Table 3.7. Summary of common mixture viscosity models in the literature

Author	Year	Model
McAdams et al.	1942	$\mu_m = \frac{1}{\mu_g} + \frac{(1-x)}{\mu_l}$
Davidson et al.	1943	$\mu_m = \mu_l \left[1 - x\left(\frac{\rho_l}{\rho_g} - 1\right)\right]$
Cicchitti et al.	1960	$\mu_m = x\,\mu_g + (1-x)\,\mu_l$
Owen et al.	1964	$\mu_m = \mu_l$
Dukler et al.	1964	$\mu_m = \alpha_g\, v_g + \ (1-\alpha_l)\, v_l$
Beatie and Whalley	1982	$\mu_m = \beta_g\, \mu_g + \ (1-\beta_g)\,(1+2.5\beta_g)\,\mu_l$
Lin et al.	1991	$\mu_m = \frac{\mu_g \mu_l}{\mu_g + x^{1.4}\,(\mu_l - \mu_g)}$
Fourar and Borie	1995	$\mu_m = \rho_m \langle \sqrt{x v_g} + \sqrt{(1-x)\, v_l} \rangle$
Garcia et al.	2003	$\mu_m = \mu_l \left(\frac{\rho_m}{\rho_l}\right)$
Bozorgzadeh and Gringarten	2006	$\mu_m = S_g\,\mu_g + S_o\,\mu_o$

The models of Owen et al. (1964), Davidson et al. (1943) and Garcia et al. (2003) are largely dependent on the liquid viscosity, and they are based on the assumptions that the liquid phase is dominant and essentially contribute to the pressure drop due to flow resistance. However, when the flow mixture composition is such that the mass quality approaches 1, these models have been reported to fail (Siasorn, 2006; Awad and Muzychka, 2008) for example in gas dominated flows. Generally, for high liquid content fluid mixture, the impact of gas viscosity will be insignificant. Hence these model types may be sufficient both for air-gas and liquid-liquid flows. Many past researchers (Triplett, 1999; Aung, 2012) has shown that that the Owens model fairly predict the mixture viscosity for most fluid flows in pipes.

The models of Cicchitti et al. (1960), Duckler et al. (1964), Bozorgzadeh and Gringarten (2006), Beattie and Whalley (1982) and Fourar and Borie (1995) are simplified homogenous models based on mass averaged values similar to equations 3.149 – 3.152. These models are based on the assumption that the fluid components are uniformly mixed, and the relative motion between the phases is negligible. These models are reported to perform well for larger diameter pipes for both air-liquid and liquid-liquid systems but overpredict the mixture viscosity for mini channels and microchannels (Triplett, 1998; Kawahara, 2002; Saisorn et al., 2006; Aung et al., 2012).

Other definitions of mixture viscosity have been proposed by other authors such as the McAdams et al. (1942), Lin et al. (1991). The model of McAdams et al. (1942) is based on the reciprocals of the averaged mass fractions and is widely used for viscosity calculations in mini and microchannels. However, both the models of McAdams et al. (1942) and Lin

et al. (1991) are reported to underpredict mixture viscosity for larger hydraulic diameters (Kawahara et al., 2002; Aung et al., 2012). Chen et al. (2001) concluded that these models' predictive abilities are inadequate for tube diameters above 3mm and for high mass flux in pipes between 3mm and 5mm, compared to the homogenous models of Cicchitti et al. (1960) and Beatie and Whalley (1982).

Saisorn and Wongwises (2008) examined the suitability of six widely used two-phase viscosity models for frictional pressure drop calculations in microchannels. The authors used the experimental data from the air-water fluid mixture flown through a microchannel of 0.53mm diameter. For a given mass quality, they showed that the McAdams et al.'s model (1942) performed fairly good when compared to Beattie and Whaley (1995) and Cicchitta et al.'s (1960) models.

Awad and Muzuchka (2008) compared the root mean square errors existing for various mixture viscosity models developed for mini and microchannels when used in predicting pressure drop for refrigeration systems. They used data obtained for refrigerant fluids (R12, R22, R740, R717, R134a, R410A and R290) in mini and microchannel experiments. The authors then proposed a new mixture viscosity model using an analogy between the thermal conductivity of porous media and two-phase viscosity. They showed that even for nearly equal phase densities ($\frac{\rho_g}{\rho_l} = 1$), their model is able to predict pressure drop with good accuracy. They reported that their proposed model, like the type of McAdams et al., performs well for systems where $\mu_m = \mu_g,\ x = 1$. This condition suggests that this type

of model is not typical for an elongated bubble, slugs and churn flow compositions, but maybe more accurate for a dispersed bubble, mist or annular flow systems.

The authors also compared their model's performance with other models for frictional pressure drop prediction in circular pipes. The results showed that the Cicchitti et al. model (1960) performed best in circular pipes.

Typically, for very narrow channels, it is almost impractical to observe stratified patterns and slug flow may not develop. This thesis uses the viscosity model type of equations 3.149-3.152, Cicchitti et al. (1960), Dukler et al. (1964), Beggs and Brill (1973), and Bozorgzadeh and Gringarten (2006), typical for conventional pipes, and considering that the fluid mixture is uniformly mixed together. Also, the effect of surface tension is considered insignificant since the flow is dominated by gravity. As described above, the fluid viscosity is virtually constant under the isothermal conditions, and since there were minor flow variations, the void fraction is essentially linear.

Review studies conducted by past authors (Siansorn et al., 2006; Triplett, 1998) reported that many models of bubbly flow to slug flow transition and slug flow to churn flow transitions were developed based on the models of Ishii et al. (2008; 2011). A CFD multi-phase simulation studies conducted by Ragan (2008) using equation 3.151 for the mixture viscosity reported that the model is suitable for stratified and slug flows since both fluids share same velocity, pressure and temperature field. Over the years, several authors (Jansen, 1999; Skogestad, 2005; Balino, 2010; Azevado, 2014; Jahanshahi, 2011; 2012;

Pedersen, 2016) have used these equations (3.149 – 3.152) to model two-phase slug flows in pipeline systems.

A number of studies have also shown that many viscosity models developed for microchannels and capillaries underestimates the pressure drop for larger sized tubes (Triplett, 1999, Aung et al., 2012; Kawahara, 2002). Analysis conducted for nine viscosity models in Table A.6 using experimental data obtained from 10.7mm and 12mm pipes in a vapour-liquid mixture flow loop (Kattan, 1996) showed that the models which are based on the liquid viscosity (such as Owen et al., 1964), performs better when compared to models precisely fitting for microchannels, such as the models of McAdams et al. (1942).

3.4.2 Comparison of two-phase viscosity models with experimental data

Experimental data obtained for this study for the choking and gas lift experiments were compared for the various two-phase viscosity correlations. Experimental data of Jansen et al. (1990) and Wordsworth et al. (1998) were also compared.

Figures 3.5 and 3.6 show the comparison of five well-known viscosity models in the literature for the choking and gas lift experiments, respectively. Models of Lin et al. (1991), Beatie and Whalley (1982), Beggs and Brill (1973), Dukler et al. (1964) and McAdams et al. (1943) were compared against the experimental results. The results represent data collected for a regular-sized pipe of 50 mm in internal diameter, and air-water flows.

Details of the experiment are previously described and reported in the thesis

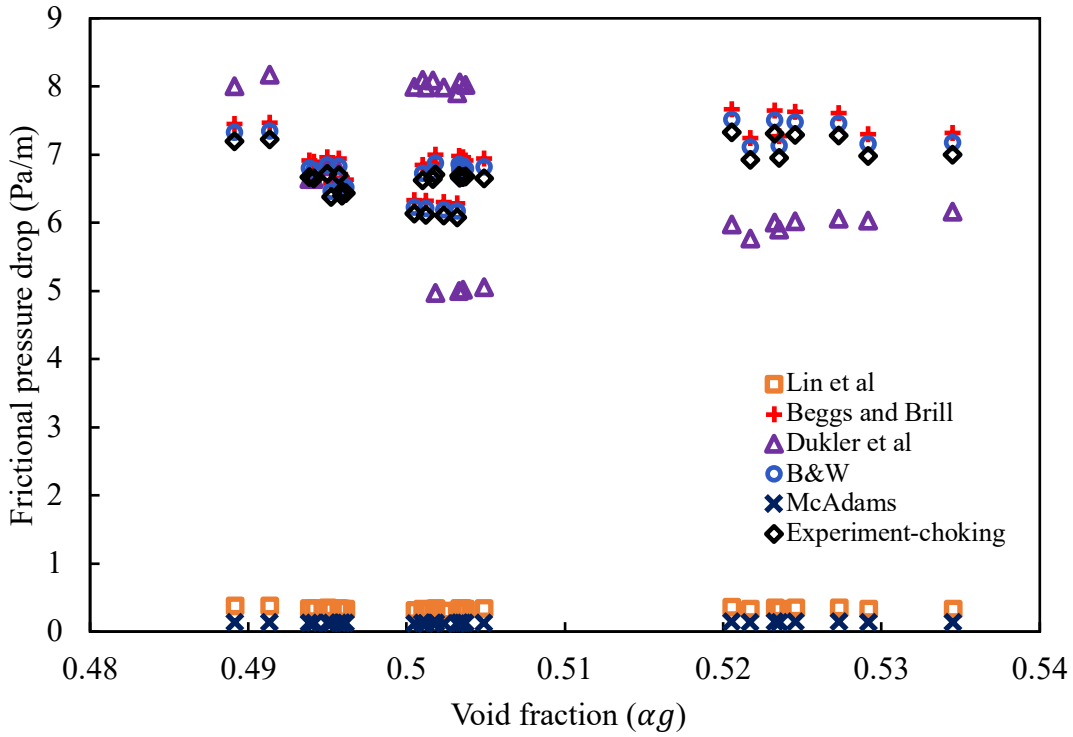

Figure 3.5. Mixture viscosity comparison of different models for the choke experiment

For the given range of mass fractions, it can be seen in Figure 3.5 that models of Beggs and Brill (1973), Beatie and Whalley (1982) and Dukler et al. (1964) estimates the frictional pressure drop in the pipeline with reasonable accuracy. Models of Lin et al. (1991) and McAdams (1943) can be clearly seen to underpredict the pressure drop. Past researchers (Tripett, 1991; Chen et al., 2001) concluded that McAdams model underpredicts the frictional pressure drop for regular-sized pipes. This evaluation shows that while it is convenient to use any of the three previous models, the models of McAdams (1964) and Line et al. (1991) are not suitable for these flow parameters.

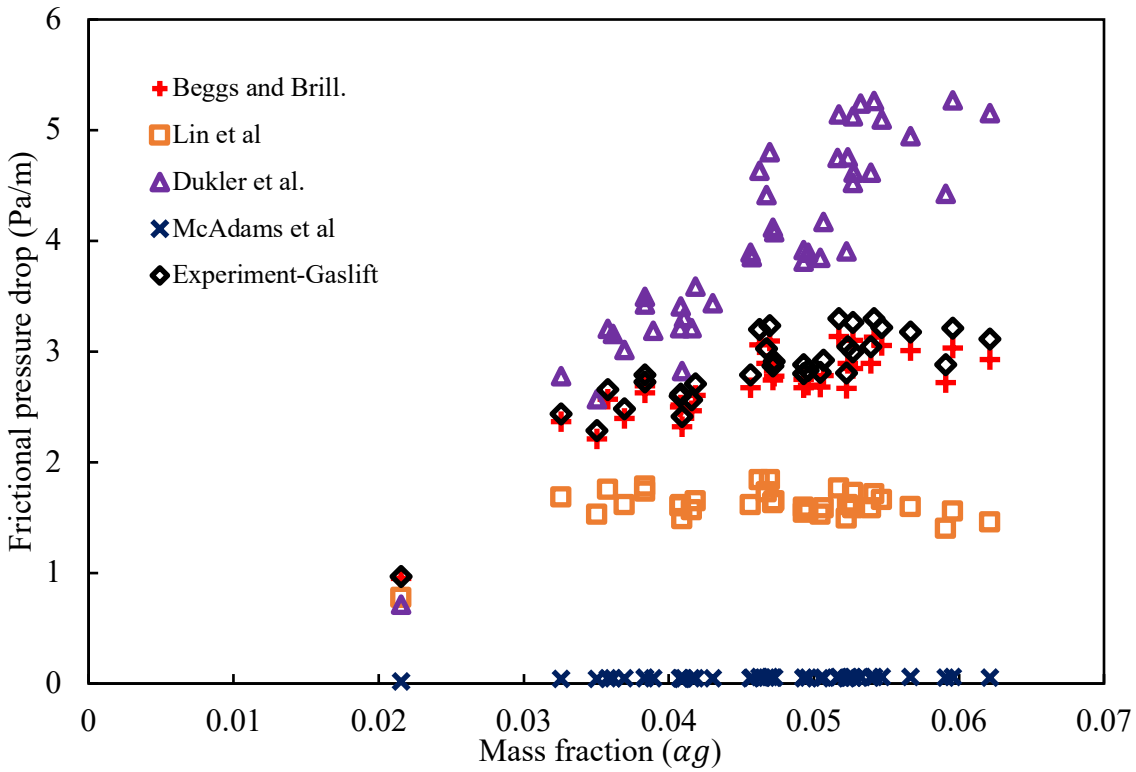

Figure 3.6. Mixture viscosity comparison of different models for the choke experiment

Similarly, the predictions of Beggs and Brill (1973) and Dukler et al. (1964) models in Figure A.45 are in good agreement with the experimental data. However, Dukler et al.'s model showed overestimations when the void fraction increased considerably. This behaviour may be attributed to the variation of mixture density with pressure.

Because the Dukler's type model is influenced by the phase densities, the mixture viscosity calculation is affected by the pressure changes along the pipe length, even though flow viscosities are not influenced by pressure changes except in elevated pressure conditions. With decreasing pressure in the vertical pipe section, the gas phase is even more distributed in the pipe, resulting in an increase gas fraction and decrease in mixture viscosity. The flow

region with this behaviour is mostly characterized by a uniformly dispersed gas phase with relatively small-sized liquid bubbles.

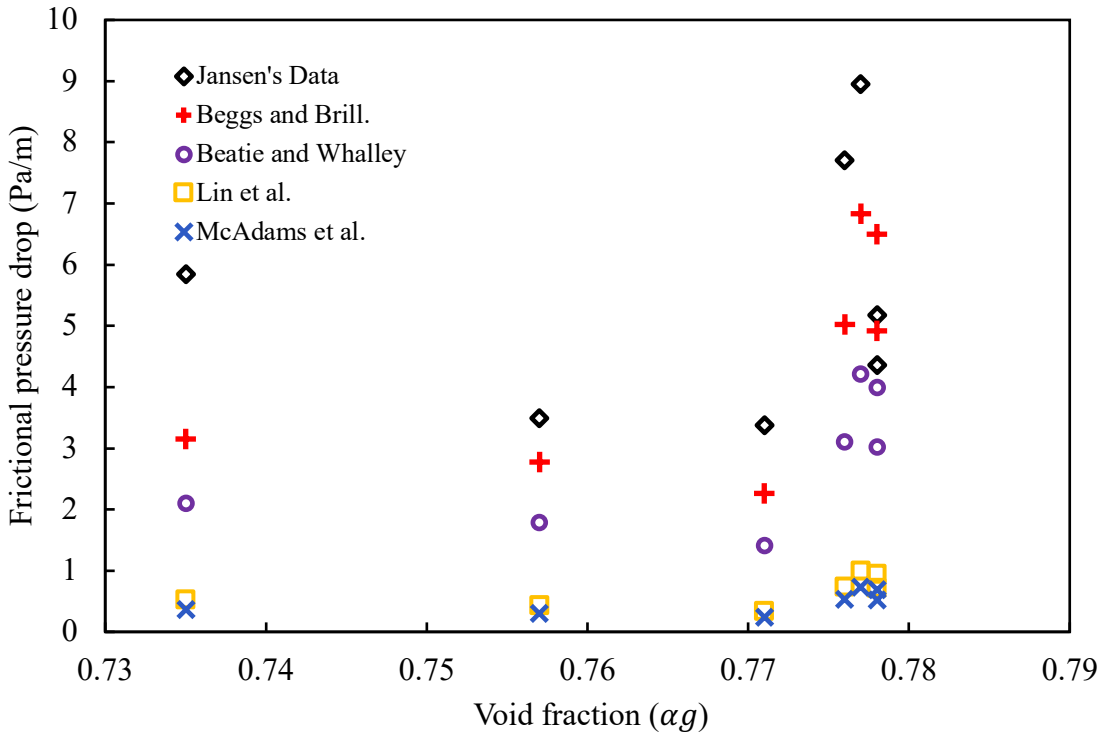

Figure 3.7. Mixture viscosity comparison of different models for Wordsworth experiment

This flow regime is often observed in stratified, or slugs flow systems, which may be sustained for a short period before the flow transits to annular flow regime. The Dukler's model (1964) uses averaged mass values of fluid kinematic viscosity and may not be suitable in slug or churn flows, or systems with high void fraction variations. The performance of the Lin et al.'s (1991) model also improved for the gas lift experiment. However, both Lin et al.'s (1991) and McAdams et al.'s (1942) models underestimated the two-phase viscosity. Figure 3.7 shows the comparison of Jansen's (1990) experimental data obtained for the air-water flow system in a 25.4 mm internal diameter pipeline. The data was evaluated over four mixture viscosity correlations (see Figure 3.7).

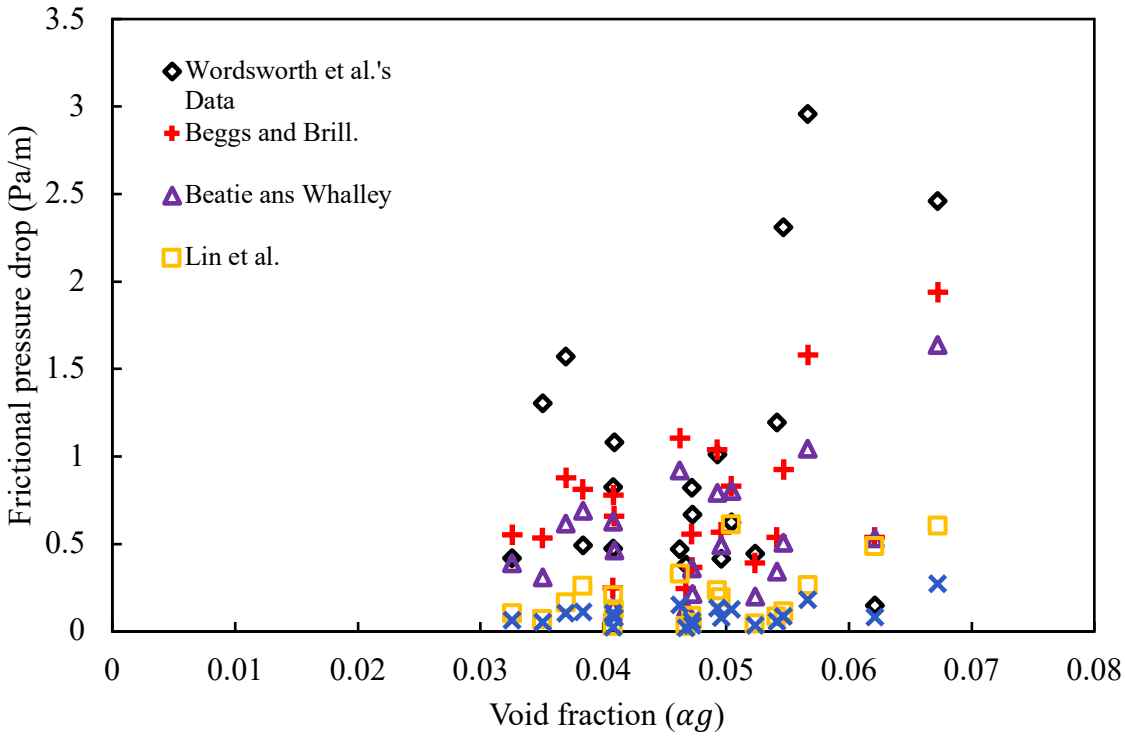

Figure 3.8. Mixture viscosity comparison of different models for Wordsworth et al. (1998) experiment

In Figure 3.8, the data for Wordsworth et al. (1998) experiment for an air-water system in a 50.8 mm pipe was also compared. It is clear that Beggs and Brill (1973) and Beatie and Whalley (1982) models accurately estimate both experimental data. Models of Lin et al. (1991) and McAdams et al. (1942) underpredicted the frictional pressure drop for both cases. This study shows that these model types are not suitable for frictional pressure drop calculations in regular-sized pipes even though they appear to be effective in mini channels and microchannels (Siasorn et al. 2008; Awad and Muzychka, 2008).

3.4.3 Summary of review on two-phase viscosity models

Several models reviewed have been previously studied and applied for regular-sized pipes, mini channels and microchannel. Examination of the literature shows that viscosity models developed for mini and microchannels are not suitable for use in regular sized tubes. However, viscosity models for regular-sized pipes may be effectively used as approximate models for mini and microchannels, especially for fluid systems with low flow quality. Widely used two-phase viscosity models have been reviewed in this study. It is concluded that mixture viscosity models which assume an equivalent liquid viscosity such as Owen's model are convenient for high liquid content flows. However, these models give over predictions when the gas fraction is significant.

The model types of Equation (3.149) through (3.152) are widely used for modelling intermittent and segregated flows in regular-sized pipes for decades. These fundamental equations have been used to develop flow regime maps and frictional pressure loss equations for pipeline systems. Past studies, such as the Cicchitti et al. (1964) model, have also shown that the equation form may be used to predict pressure drop in mini and microchannels with reasonable accuracy. The model types based on the reciprocal of averaged mass fractions such as the McAdams et al. (1942) model underpredict pressure drop for regular-sized pipes. A reliable model is crucial for accurate predictions and proper design of flow systems where frictional pressure drop can affect operational efficiency. Under estimations can result in frequent system shutdown due to insufficient input power, whereas overestimates can result in increased operating and maintenance costs. Further studies are recommended for a wider variation in pipe diameters and fluid compositions.

4 RESULTS AND DISCUSSION

4.1 Topside Choking and Gas Lift

The first objective of this research aims to find how various actuators can suppress slugging in the transport and separation of multiphase flows in subsea pipelines. These actuators (choke and riser base gas-lift) have been investigated, and the results are presented in the following section. It investigates their potential to control and stabilize an undesired and unstable flow regime, optimize flow production, reduce operating costs, and improve overall safety requirements for operating offshore installations. It also discusses the flow changes caused by choking, energy costs of gas lifting, and the impact of each technique on the other when applied co-currently. In the following section, the results obtained for this first research objective are presented and discussed in detail.

4.1.1 Correlations of Slugging Frequency and Flow Rates

The experiments focused on two different actuators for anti-slug control in fully developed flow conditions. Measurements were taken for pressures at the entrance and throughout the pipeline, bottom and top of the riser, separator pressure, fluid densities, temperature, and flow rates at the inlet and outlet of the setup, for different gas injections and choke openings. The scaled laboratory results were used in this section to develop non-dimensional correlations and design for scaled pilot and field applications. A summary of the correlation parameters are presented in Table 4.1. System parameters and flow conditions are highlighted in Tables 4.2 – 4.4.

A plot of the dimensionless production rate, $w_m/w_{m,max}$, against the percentage choke opening, for a range of decreasing choke openings (100% down to 10%, in 10% decrements) is shown in Figure 4.1. It should be noted that w_m is the individual production rate and $w_{m,max}$ stands for the maximum production rate value. The asterisk (*) in the plots is used to denote the dimensionless forms of the variables.

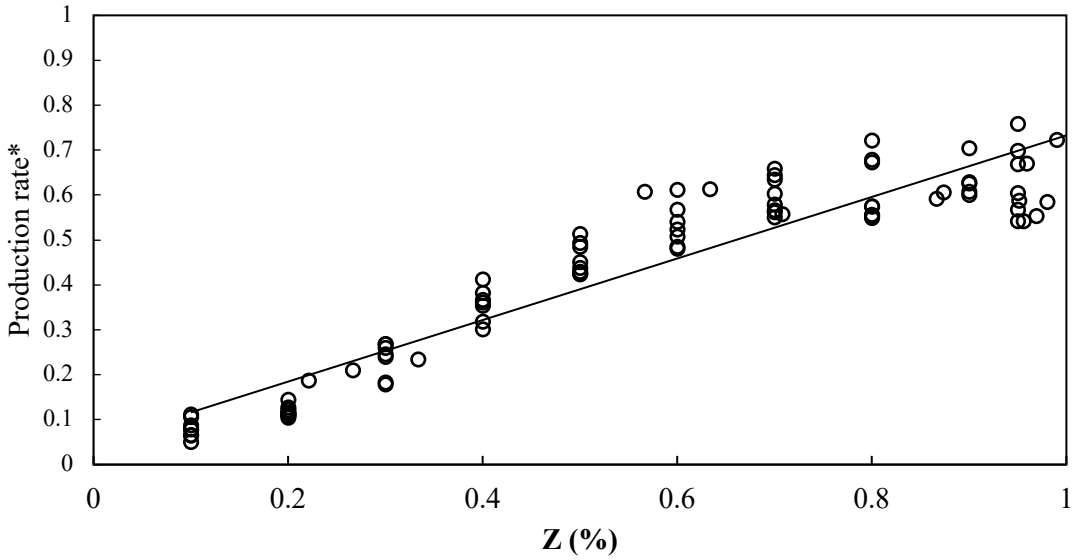

Figure 4.1. Measured dimensionless average production rate at the choke outlet for various choke percentage openings over an average test period of 4,300 seconds (a = 0.705, b = 0, and $R^2 = 0.88$).

Based on the previous studies, the general functional form of the slug flow rate can be expressed in a linear form of ax + b. From Figure 4.1, it can be seen that a nearly linear relationship exists between the flow velocity and the choke opening. A coefficient of variation (R^2) and gradient of 0.88 and 0.705 were obtained, respectively. It can be observed that for low choke openings, the system is more stable, which is depicted in the

distribution of the data signatures. The data cluster for high choke sizes (choke openings above 42%) indicates repeated oscillations at high amplitudes. While for the choke openings below 42%, the data signatures are seen to be better distributed (see Figure 4.1) The correlation is similar to the previous forms of correlations presented by Nicklin (1962). The system variation in the amplitudes for the stable region below the bifurcation choke opening may be attributed to the valve dynamics, which are crucial for effective control implementation. The valve dynamics refer to the adjustment (opening and sealing) of the cross-sectional area of the pipe open to flow. This adjustment in a timely and effective manner may vary for various valve configurations. A static valve was used in the study. The static valve was observed to produce faster bandwidth compared to the flow dynamics. A valve with a more dynamic feature which did not exist in our case may respond more quickly to instantaneous flow changes or opening size, leading to better system control.

The correlation developed here is a function of the choke size opening, which has a linear relationship with the slug production at the outlet. The production rate varies linearly with the choke opening. The flow through the choke is maximum for a 100% opening, and lowest for the 10% opening. The R^2 of 0.88 indicates that the mixture flow out of the choke is well correlated to the percentage choke opening. From the experimental data, the mixture produced from the choke outlet can be correlated as a function of the percentage choke opening as $u_{mix} = 0.567D^2z$, where u_{sl} is the slug mixture velocity topside of the choke valve, D is the pipe internal diameter, while z is the choke opening percentage.

The slug frequency is the average number of slugs per unit time, as recorded by a stationary observer (Gregory and Scott, 1969; Hubbard, 1966). Frequency data in the analysis was obtained from measurements taken over 500 seconds at a sampling rate of 100 Hz. The sampling rate is essentially oversampling as the riser-induced slugs have low frequencies. However, it is used in order that all dynamics are captured such as trends during the slug. Figure 4.2 shows the normalized frequency plotted against the choke opening. It is found that a logarithmic relationship exists between the slug frequency and choke opening.

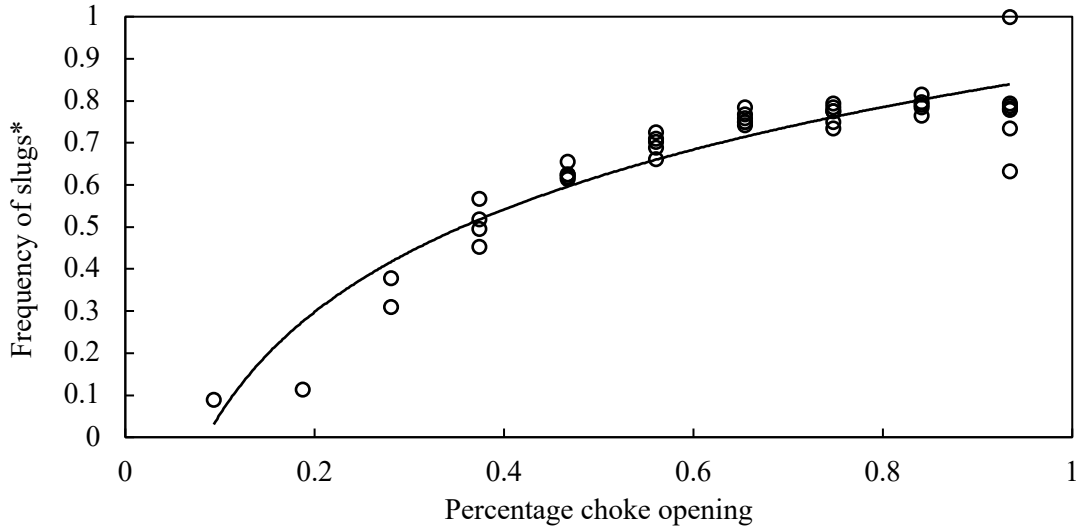

Figure 4.2. Normalized average frequency of slug as a function of the percentage choke opening at choke sizes between 100% and 10% (a = 0.352, b = 0.864, and $R^2 = 0.87$).

A logarithmic regression analysis was used to obtain R^2, a, and b, as 0.87, 0.35, and 0.864, respectively. The slug period is the length of time for one full slug cycle and is recorded from the oscillating flow responses and then used to estimate the slug frequency. The frequency of slugs is the number of slugs units passing through a particular cross-sectional opening in a given time. Slug velocity is the rate of slug unit production over a cross-

sectional area. The slugging frequency can provide key information in the design of the appropriate controller bandwidth based on the flow conditions since the slugging frequency is an important input for the design of actuators in active slug control.

The final form of the correlation for the estimation of the slug frequency is given in a logarithmic form based on previous studies. The slug frequency is a modified form of the correlation of Schmidt et al. (1979). The final correlation for estimating the frequency of slugging is expressed as a function of the choke opening as $f_{slug} = 0.864 + 0.351 \ln(z)$, where f_{slug} is the slug frequency.

According to Figure 4.2, the frequency of slugs decreases as the choke opening decreases, although the slug frequency is relatively constant for choke openings between 100% and 60%. The frequency declines for smaller choke openings until the slugging is eliminated for choke openings of about 24%. This phenomenon indicates that the gas and liquid velocities become higher when more liquid slugs are produced (frequency of slug production).

A plot of the dimensionless pressure at the bottom ($p_b/p_{b,max}$) and top ($p_t/p_{t,max}$) of the riser against the choke opening is presented in Figure 4.3. The correlations were based on 5,000 data points of the experiments. The general form of the correlation for the pressure is ax^b, for the bottom pressure, and $a \ln(x) + b$, for the top pressure. After a regression analysis, the values of R^2, a, and b obtained were 0.496, 0.865, and -0.009, respectively, for the bottom pressure, and 0.386, 0.0049 and 0.862, respectively, for the pressure at the top of the riser.

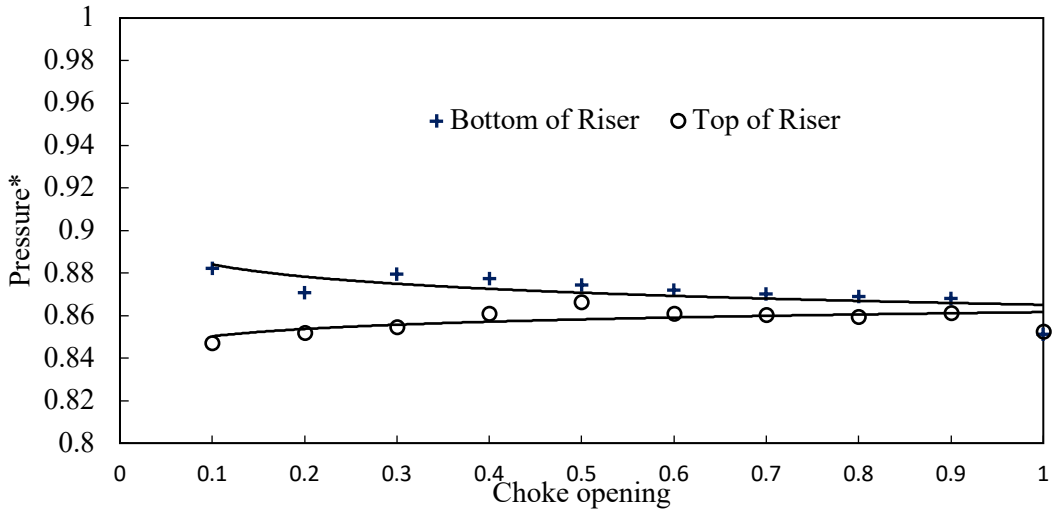

Figure 4.3. Dimensionless average pressure measured at the bottom of the riser (a = 0.865, b = 0, and R^2 = 0.5) and top of the riser vs. percentage choke opening (a= 0.005, b=0.4, and R^2 = 0.5).

The gas injection rate is an input parameter in the gas lift design and compression power requirements. The gas injection ratio was obtained from the ratio of the inlet gas and total system gas flow rates.

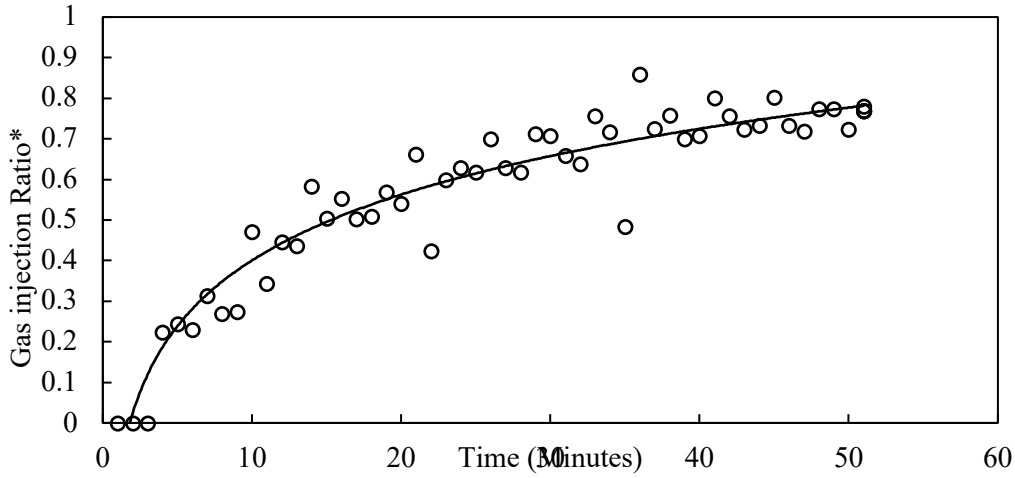

Figure 4.4. Dimensionless gas injection requirement for slug elimination vs. time the gas lift application (a = 0.234, b = 0.138, and R^2 = 0.91).

A plot of the ratio is illustrated in Figure 4.4, which represents the volume of gas injection requirements as a function of time. The data indicates that the gas injection should be maintained to continue liquid production and prevent slug development. Although the gas lifting method increased fluid production (Figure 4.5), minimal stability was reached before large volumes of gas were injected. This behaviour affects operating costs and increases gas handling problems. A larger separator is required to accommodate large gas volumes and unstable slug production.

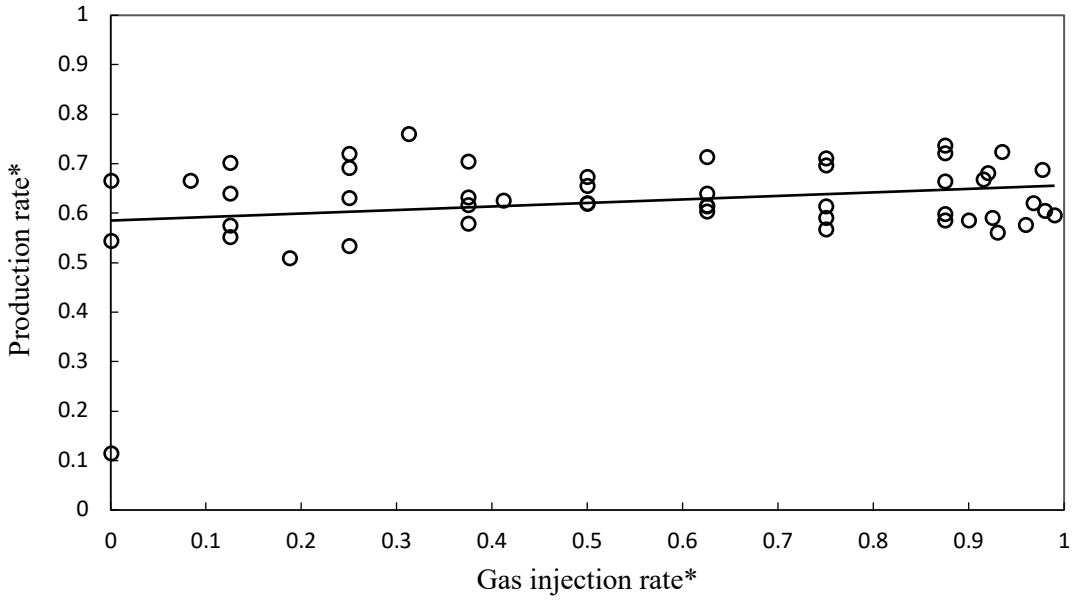

Figure 4.5. Dimensionless production rate versus gas injection ratio (a = 0.531, b = 0.209, and $R^2 = 0.1$).

From the analysis of the gas-lift data, a general form of the gas requirement parameter is derived in the form of $a \ln(x) + b$. The coefficient of variation, a and b, are obtained for the dimensionless gas injection as 0.913, 0.234, and -0.138, respectively. The regression shows that the functional variables are linearly correlated to the injection rates. The final

correlation to estimate the volume of gas required to maintain a slug free flow system is given by the following relationship, $w_{Ginj} = (0.0239 \ln(t) - 0.01382)\alpha w_L$, where w_{Ginj} is the gas injection rate required to keep the system in a non-slugging region, α is the void fraction, and w_L represents the liquid flow rate into the pipeline, which is equivalent to the liquid production rate at the wellhead of a production platform.

A correlation for the production rate with gas lifting is primarily used for anti-slug control. After a linear regression analysis, 0.069, 0.577, and 0.047, respectively, were obtained for a, b, and R^2. The general form of the correlation is ax + b. Figure 4.5 depicts the dimensionless fluid production, $w_m/w_{m,max}$, at the choke outlet, correlated as a function of time for the gas injection method. The results indicate that fluid recovery increases as the injected gas volume rises. Based on Figure 4.5, the production rate continues to increase until saturation is reached, called the optimal operating condition. Beyond this value, an average constant fluid production rate is obtained at the receiving facility. Any further increase in the gas injection rate beyond the optimal operating condition increases the gas volume fraction, without a fluid recovery increment. As seen in Figure 4.5, the production rate decreases slightly and becomes constant. The gas injection can result in a negative impact on fluid production when the optimal gas volume is exceeded for a given choke opening. The regression analysis reveals that the fluid recovery is not well correlated to the gas injection rate.

It can be observed in Figure 4.6 that gas injection boosts the production until an optimal value of about 0.6 kg/m^3 is reached.

This occurs at an average choke opening of 53%, even though the gas injection rate increased over time, as shown in Figure 4.7. However, the increased gas injection rate did not impact the recovery as shown in Figure 4.6.

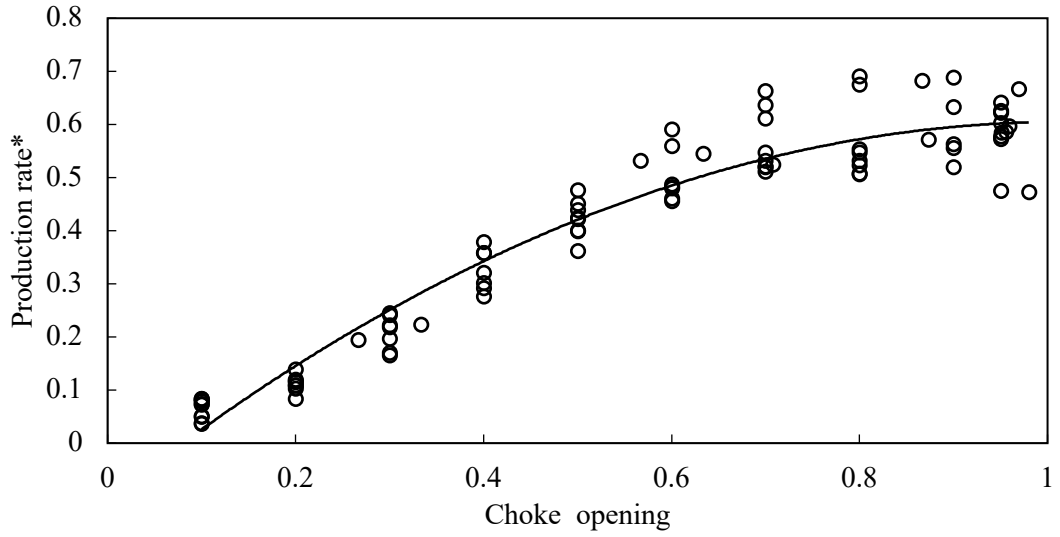

Figure 4.6. Dimensionless measured production rate at the choke outlet at varying choke openings (a = 0.84, b = 0.126, and $R^2 = 0.84$).

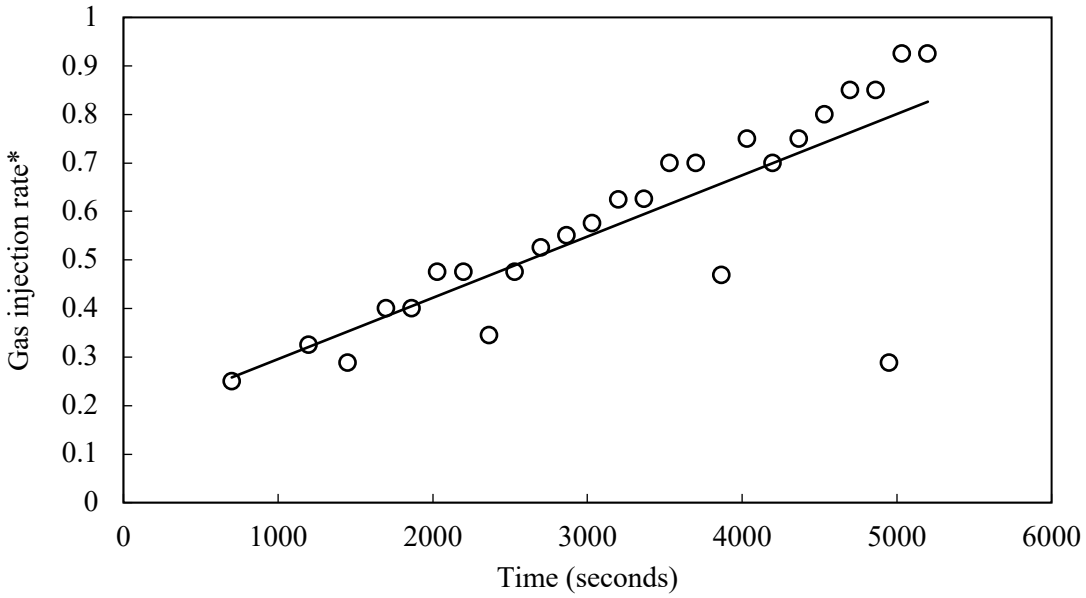

Figure 4.7. Dimensionless measured gas injection rate over time (a = 0.001, b = 0.170, and $R^2 = 0.64$).

Further gas injection beyond that operating point can negatively affect liquid recovery and increase the operational costs without commensurate returns. An optimal volume of injection can, therefore, be selected for a given choke opening. Figures 4.7 and 4.8 describe how the gas volume fraction is affected by the gas injection rate and the choke opening. According to Figure 4.7, the injection rate is increased over time for the combined gas injection and choking case. Figure 4.8 shows that the GVF decreases as the choke opening is reduced. In contrast, the average GVF increases over time for a given choke opening due to the incremental gas volume in the system by the riser base gas-lift. The GVF is lowest for small choke opening even at high gas injection rate conditions.

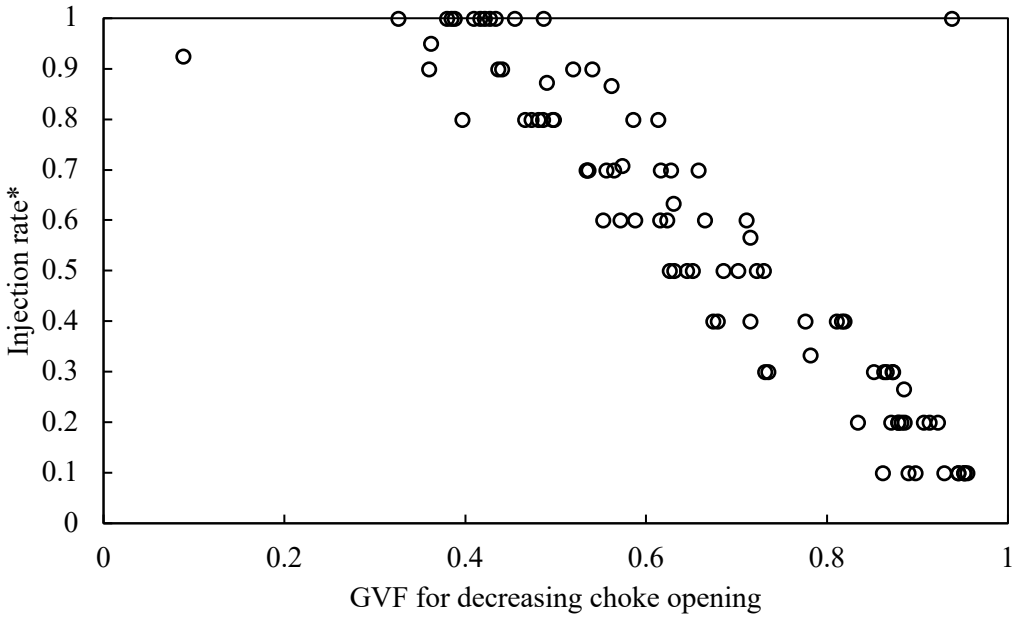

Figure 4.8. Dimensionless gas volume response for gas lifting as the choke valve choke openings decreases.

Table 4.1. Coefficient of correlation based on the experimental data.

Relationship	Correlation	R^2	a	b
Production rate vs. choke opening	$ax + b$	0.7419	0.7216	0
Bottom pressure vs. choke opening	ax^b	0.500	0.8651	-0.009
Slug frequency vs. choke opening	$a \ln(x) + b$	0.8704	0.3514	0.8635
Gas injection required over time	$a \ln(x) + b$	0.9132	0.2339	-0.1382

In the following sections, the experimental results for three different slug elimination schemes are presented: (1) slugging elimination by topside choking; (2) gas lifting at the bottom of the riser, and (3) combined choking and gas lifting. The experimental results for the various scenarios are compared to evaluate their effectiveness and robustness for control procedures. The criteria for the comparative studies are based on the production rate, gas volume fraction, performance of each control technique, in terms of frequency, flow stability, and the slug amplitude.

4.1.2 Case 1 - Active Choking at the Top of the Riser

The open-loop stepwise choking of the topside valve is illustrated in Figure 4.9. In order to study the impact of choking on the slugging and overall fluid recovery, the choke valve opening was stepped down by 10% for each test, from fully open (100%), and continued until 10% open. This lower limit is below the bifurcation point, or the choke opening in which the system shifts from slugging to non-slugging. The separator pressure can increase the pipeline operating pressure and act as an anti-slug control mechanism. Increasing the pipeline pressure decreases the volume of gas in the pipeline and causes an increase in the pipeline liquid holdup (Sarica and Tengesdal, 2000). As a result, the separator pressure is maintained at the atmospheric condition (e.g., 1 bar) without pressurization of any point

throughout the test. This ensures that the measurements were solely affected by topside choking. Severe slugging exists for low liquid and gas flow rates, mostly for mature oilfields, where the reservoir is primarily sustained by secondary or tertiary processes. Thus, they require a sustained low inflow condition.

Constant liquid and gas flow rates of 0.4 kg/s and 0.00048 kg/s, respectively, were maintained in the system through a 0.054 m inlet pipeline. The fluid densities and viscosities were 900 kg/m^3 and 0.090445 Pa.s for the liquid phase and 1.988×10^{-5} kg/m^3 and 0.000181Pa.s for the gas phase, respectively. Constant inflow rates were maintained at a constant average pump pressure of 1.8 bar. Minor fluctuations in pressure were observed as a result of the back pressures introduced when the valve openings were reduced. The liquid and gas injected into the pipeline are related to the mixture production at the outlet to the separator, which is controlled by the topside choke valve. If the inflow conditions, liquid and gas injection rates, outflow condition, and separator pressure, are kept constant, the system flow responses for various choke openings can be evaluated. A slug regime was created at about 45 seconds after the injection was started. The experimental results are illustrated in Figures 4.9 – 4.13. These results show the input/output relationships and how they affect the system operating conditions.

The gas injection was zero at all times. The separator pressure was nearly constant. Figure 4.9 demonstrates that the separator pressure is maintained at the atmospheric condition, while the riser base injection nozzle was shut-off, and then, the choke valve was stepped down from fully open (100%) to 10% (see Figure. 4.9).

In Figure 4.10, a GVF fluctuation occurs due to slugging. The fluctuation amplitude is higher in the slugging region, while it is lower in the non-slug region.

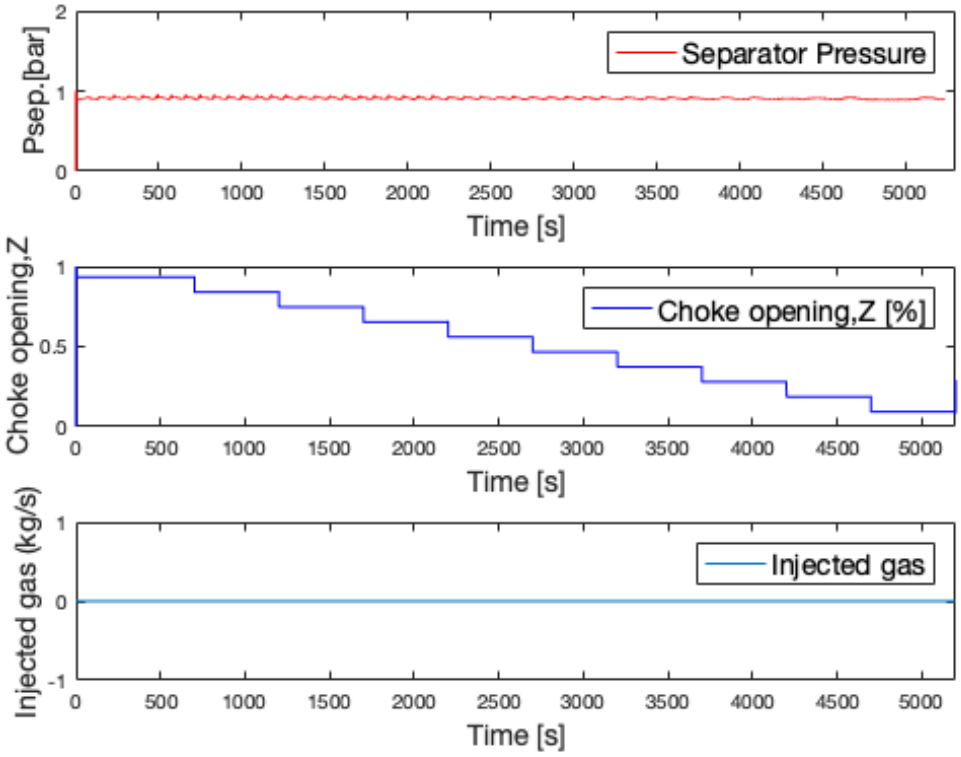

Figure 4.9. Scenario 1 - System inputs showing no gas support and constant separator pressure (atmospheric) while the choke valve is stepped down from 100% to 10% opening.

The fluctuations challenge the controller because the actuator's time constant is much shorter than that for the pump or the influence caused by slugging. It reacts rapidly to any disturbance; however, this is not valid for the pump since the pump dynamics are much slower, compared to the compressor dynamics. However, the gas controller manages to keep the resulting oscillations at the minimum level so that the GVF remains almost constant (Figures 4.9 and 4.10).

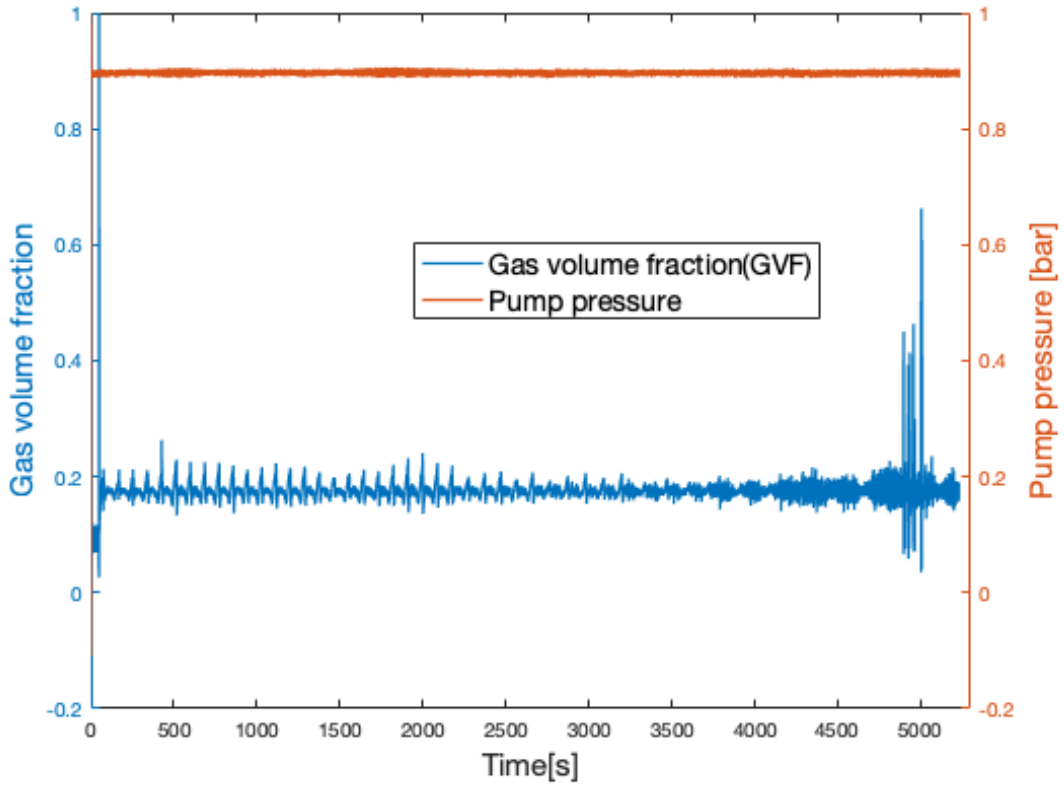

Figure 4.10. Scenario 1 - Measured flow controller responses as a function of time.

The pump pressure in Figure. 4.10 is more steady because the induced backpressure added from the topside choking is minor compared to the pump controlling the pressure. It also is stepped over long periods, which gives the pump time to stabilize.

Figure 4.11 depicts the measured average gas inflow and liquid inflow rates. The inflow rates show the flow responses based on the system flow condition.

Due to the oscillating system pressures and mass flow rates, the inflow performance varied, particularly for larger choke openings, where the fluctuations are highest. At lower choke openings, the inflow variables are observed to be nearly constant, since the system tends toward a stable flow regime. Flow stabilization in the non-slug region impacts both the

liquid and gas mass flowrates (Figure. 4.11). The pressure and flowrates stabilize after 4,000 s.

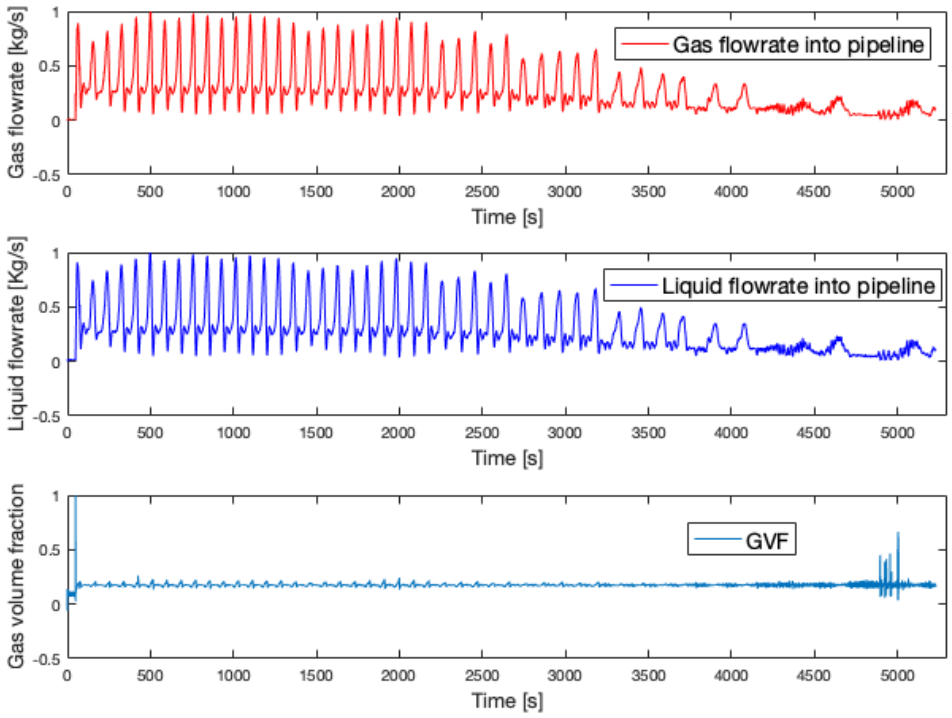

Figure 4.11. Scenario 1 - Measured average inflow performance at the pipeline inlet against time.

In Figures. 4.11 and 4.12, the slug is eliminated at about 4,000 s. Table 4.2 shows the production at each step size of the choking. Table 4.2 also compares the impact of slugging on fluid recovery at the process facility outlet of the choke valve.

At larger openings, the production rates are higher than smaller choke openings. However, the slugging frequency is more intense, compared to lower choke openings. In our study, choking is recommended for slug mitigation; but where the production rate is significantly

uneconomical, a combined scheme may be used. Minor slugs may also be acceptable to increase the production where a robust separation capability is feasible.

According to Figure 4.13, fluid recovery at the choke valve decreases close to the stabilization point when the choke opening decreases.

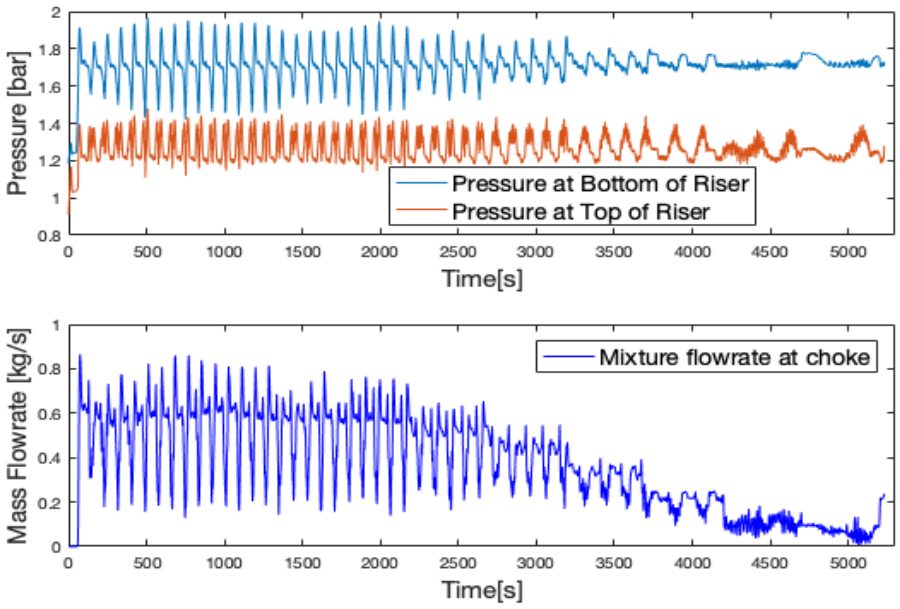

Figure 4.12. Scenario 1 - Measured output variables for the choke test over the period of the experiments.

This production loss is shown in Table 4.2. Acceptable production rates may not be reached for particular choke openings when the system stabilizes in a real application. Generally, acceptable production rates depend on the operator's objectives, a life of the well, and economic parameters. Hence, choking may not be most beneficial for situations where high production rates are most desired and when other mitigated approached are feasible.

Therefore, other techniques, such as robust feedback control, can be used to improve the production rate.

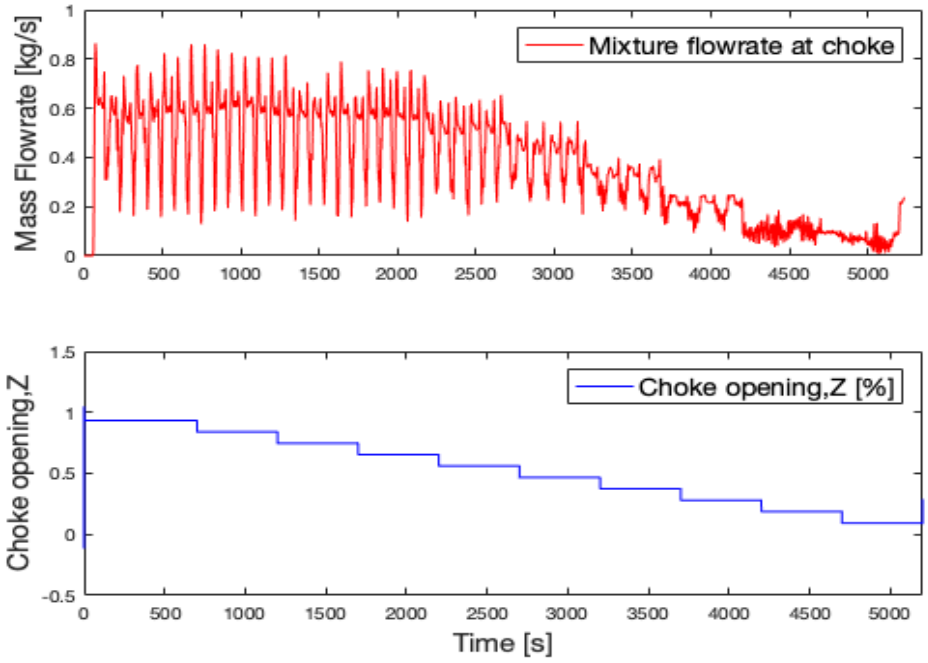

Figure 4.13. Scenario 1 - Production performance for stepped choke valve testing.

In the active choking technique, the choke valve is manipulated to add back pressure in order to modify the gas volume fraction (GVF). When the choke is sufficiently decreased, the slug flow turns into bubble flow, in which bubbles flow along with the continuous liquid phase in the riser. The choking technique controls the slug flow by suppressing the development and/or growth of liquid slugs at the base of the riser. During the initial slug formation, when the liquid blocking starts, the volume flow rate and the pressure in the riser decrease. This differential pressure actuates the valve to maintain a set volumetric flowrate. Consequently, the pressure downstream of the slug formation location decreases

and the liquid slugs are pushed upward by the pipeline pressure. Topside choking is effective as a practical approach to eliminate slug flow in subsea pipelines.

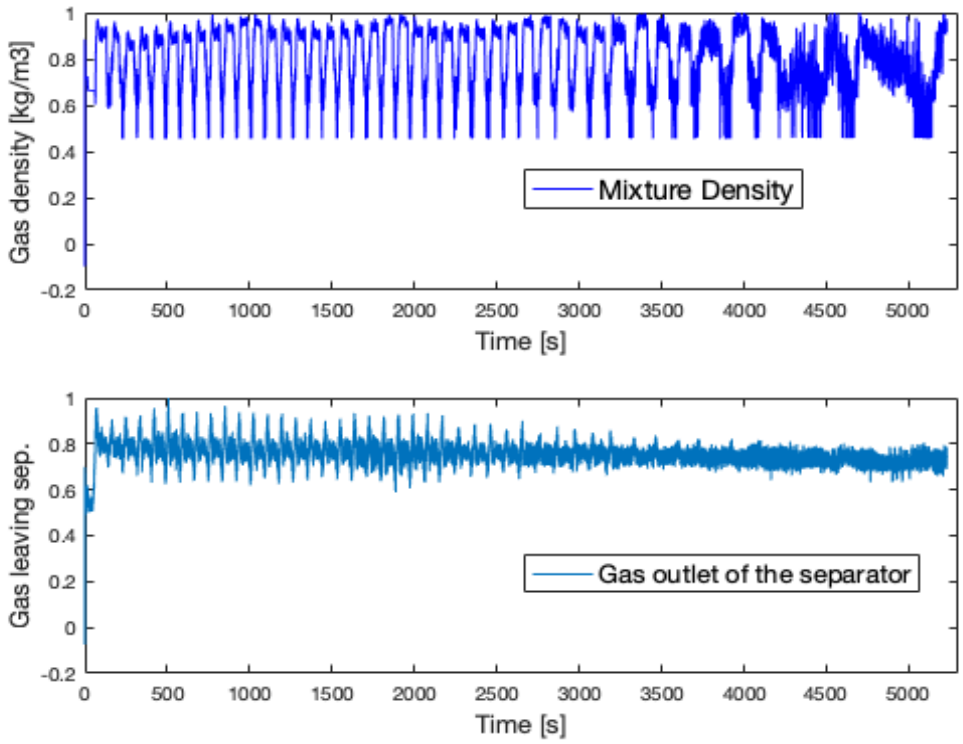

Figure 4.14. Scenario 1 - Fluid densities for stepped choke valve testing.

Table 4.2 also compares the impact of slugging on the flow conditions. A sharp change is noticed between the slugging and non-slugging choke openings. Each slug cycle has an average of 87 seconds for choke amounts between 100% and 70%. The period doubles between 40% and 30% openings. In the non-slugging flow (<20%), the period is infinite, and the back pressures also increase at a smaller choke opening when the system stabilizes.

Table 4.2. Impact of various choke openings on slugging.

Choke Opening	Production Rate (kg/s)	Slug Period (s)	Slug
100%	0.500	87.134	Yes
90%	0.535	85.46	Yes
80%	0.517	87.833	Yes
70%	0.514	89	Yes
60%	0.459	96.8	Yes
50%	0.384	107.6	Yes
40%	0.298	133.5	Yes
30%	0.187	217	Yes
20%	0.099	infinite	No
10%	0.056	infinite	No

Figure 4.14 shows that the density fluctuates overtime during the slugging. The slug frequency, however, significantly decreases as the system stabilizes. The decreases in the flow, pressure, and density variations under non-slug gas flow are also an indication that the gas bursts out from each slug until it is eliminated.

4.1.3 Case 2 - Gas Injection Scheme

The setup for the gas lifting experiment is depicted in Figure 3.1. In the second scenario, the choke valve is fully open. Similar to the previous case, constant liquid and gas flow rates of 0.4 kg/s and 0.00048 kg/s, respectively, were maintained into the system through the 0.054 m inlet pipeline, while increasing the gas injection rate at the bottom of the riser. The fluid density and viscosity for the experiment were 900 kg/m^3 and 0.090445 $kg/m/s^2$, respectively, for the liquid phase and 1.988×10^{-5} kg/m^3 and 0. 000181Pa.s, respectively, for the gas phase. The constant inflow rates were maintained with an average pump

pressure of 1.8 bar. Minor fluctuations in pressure were observed as a result of the back pressures introduced when the valve openings were reduced. Gas was injected at the bottom of the riser where the liquid was accumulated to ensure continuous gas penetration into the riser.

Gas was injected at 0.625 nm^3/hr increments every 300 seconds until the maximum capacity of 5 nm^3/hr was reached. The additional gas injection into the riser base increased the total volume of gas into the system, resulting in higher flow velocities. The results obtained from the gas-lift experiments are shown in Figures 4.15 – 4.18.

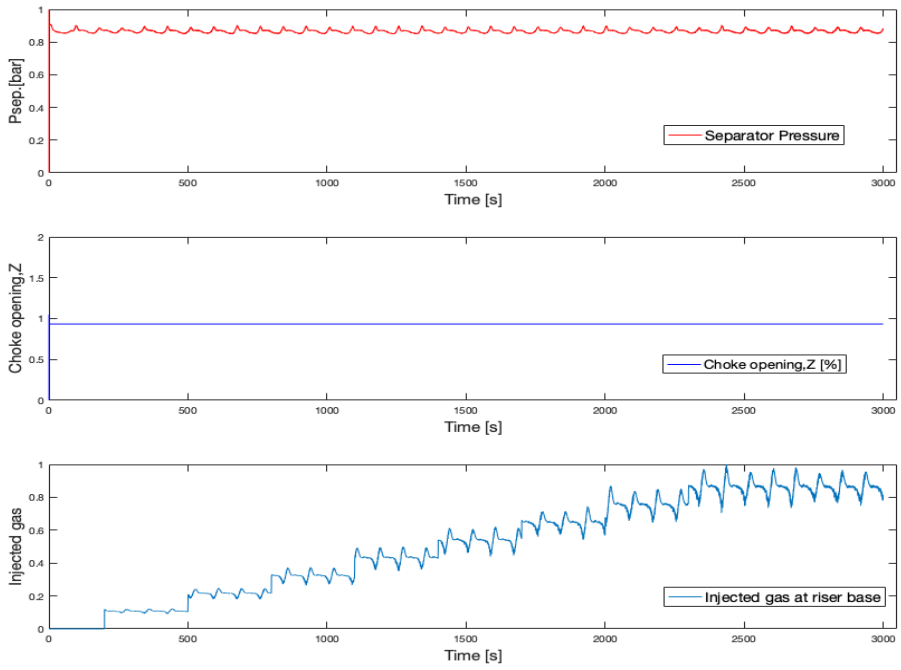

Figure 4.15. Scenario 2 - Measured system inputs when the choke is fully open and the air-water mixture is separated by a gravity separator under atmospheric conditions.

The results were generated from normalized data points during the period of 3,000 seconds for the experiments. In the results for this gas injection scenario, the gas lift impacts the pressure at the bottom of the riser, top pressure, production rates, and the frequency of the slugs. Based on the experimental results, the improvement in the system stability is relatively small before large volumes of gas were injected. Before stability is achieved for the gas lifting technique, the system flow changes into an annular flow regime. The gas lift potential to obtain system stability is observed in Figures. 4.15 – 4.17. The fluctuations produced by the system are depicted in both high frequencies and high amplitudes. This variation in amplitudes are observed in Figures 4.15 through 4.18. As more gas is injected in the system and produced at the separator, this causes a slight pressure reduction at the separator as seen in Figure 4.15.

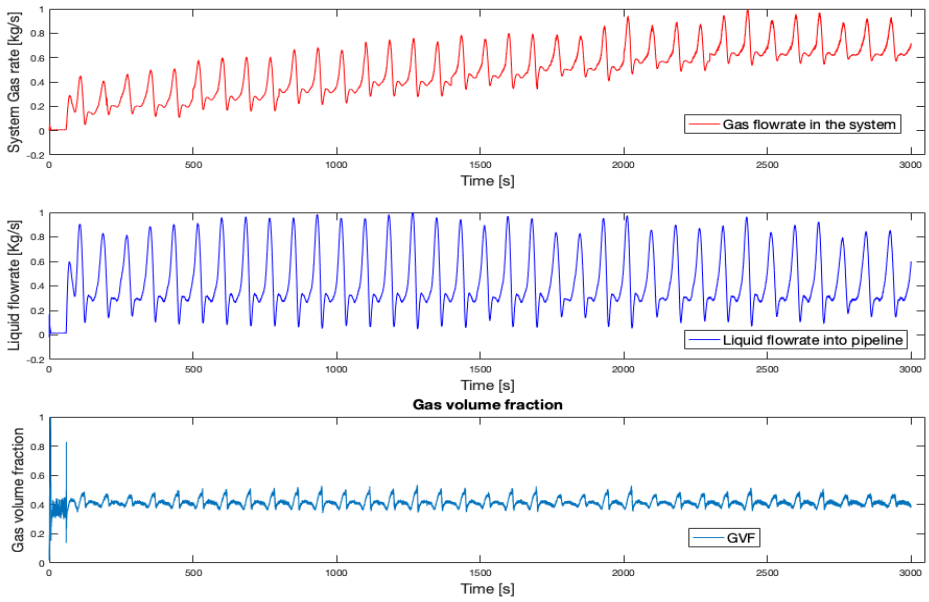

Figure 4.16. Scenario 2 - Average system flow conditions for the gas injection case.

The separator pressure is slightly smaller than the state value. Although small reductions in the amplitude were briefly observed around 2,500 seconds, the oscillations were not significantly reduced when the maximum injection capacity was reached. Similar to previous studies (Hill, 1990; Hill and Wood, 1994; Pots et al., 1987), this study confirms that large volumes of gas are required to reduce the severity of slugging.

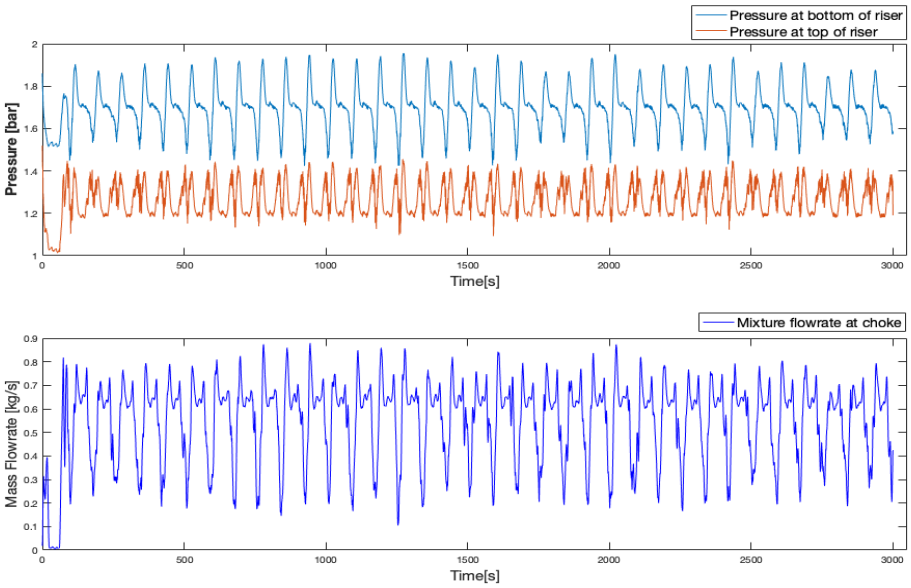

Figure 4.17. Scenario 2 - Measured average pressure at the top of the riser and the measured average riser-base pressure with time.

A large separator or slug catcher is required to accommodate both the large gas volumes and unstable slug productions. The riser-based gas-lift method can reduce system instability and increase production (see Figure. 4.17). However, this is not suitable for offshore applications due to cost, space, and weight constraints. Gas lift mainly increases the fluid velocity in the riser and the gas flow eventually dominates the riser flow as gas injection continues, before stability is achieved.

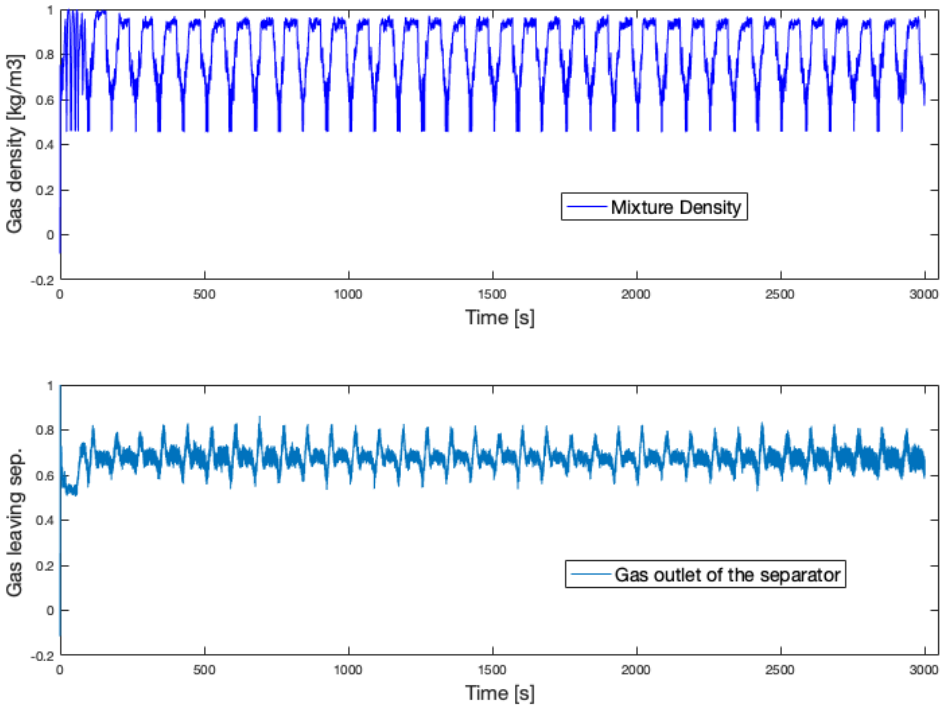

Figure 4.18. Scenario 2 - Average density measurements at the outlet of the choke valve.

The significant positive impact on the system includes the reduction of system pressure and slugging frequency. The gas lift also reduced the severity of blowout of liquid in the pipeline and allowed a continuous steady fluid flow in the flowline and riser. This is because the injection gas aerates the hydrostatic column, thereby reducing the force required to push the fluid to the surface, allowing for smoother fluid recovery downstream. In a blowout (sudden and uncontrolled flows) situation, there are uncontrolled fluid productions downstream, which strain the fluid processing equipment to limit and impair the fluid handling capabilities of downstream devices. Some of the problems associated with gas-lifting, such as operational costs and gas handling with regard to compression or pressurization were also discussed in Schmidt et al. (1979, 1980, 1985). Additional

problems can include the Joule-Thompson effect, which could aggravate the flow conditions by making the transported gas susceptible to wax precipitation and hydrate formation (Johal & Cousins, 2001).

The data also shows that the volume of gas required for injection to eliminate slugging is higher than the flow rate of gas in the pipeline. Gas injection reduces the pipeline pressure and can boost production. It is also beneficial for well and riser unloading to enhance start-ups, rate improvement or injection to aid production stability. However, high compression requirements and injection capabilities in offshore environments prohibit the wider application of gas injection. A riser-based, gas-lift method can reduce system instability and increase production. However, gas-lift is not recommended for offshore applications due to cost, and footprint implications. This study also shows that no substantial improvement in stability is attained when large volumes of gas are injected, while considerable amount of energy is consumed.

Table 4.3. Production performance for the gas lift scenario.

Gas Injection (kg/s)	**Production Rate (kg/s)**	**Slug Period (s)**	**Slugging**
1.25×10^{-6}	0.449	78.5	Yes
0.125	0.635	83.6	Yes
0.249	0.629	84.1	Yes
0.375	0.639	86	Yes
0.499	0.662	83	Yes
0.625	0.638	82	Yes
0.750	0.637	84	Yes
0.875	0.629	83	Yes
0.999	0.628	86	Yes

In gas lift applications, the gas injected at the bottom of the riser reduces the hydrostatic head imposed by a long liquid slug in the riser column. Hence, the pressure of the pipeline decreases (Jansen & Shoham, 1994; Jansen et al., 1996; Minami & Shoham, 1994). Gas lifting increases the velocity and reduces the liquid holdup in the riser (Balino, 2010; Jansen, 1996). The injected gas also helps to carry the liquid to the surface receiving facilities. When the gas volume in the system is sufficient to ensure continuous fluid lifting, a stabilized flow can be achieved. Large volumes of gas are required to achieve stability and eliminate slugging. This also increases the potential for gas handling challenges at the surface processing facility, as well as energy costs (Hill, 1990). Insufficient injection gas volumes and associated multiphase flows processes have also been reported to increase slugging frequency (Enilari and Kara, 2015). Compressor requirements and costs are also challenging in the application of gas lift as a slug elimination technique, especially for offshore environments. The installation and operation of the compressor also increase safety operational concerns and costs.

4.1.4 Case 3 - Combination of Active Choking and Gas Injection

In some subsea operations, installations use both topside choking and gas-lifting to eliminate slugging flow problems. This slug elimination technique involves 1) the injection of compressed gas, at the bottom of the riser, at the point where the elongated bubbles are formed, and 2) choking the topside choke valve, simultaneously. In this section, combined active gas injection and topside choking are examined. The system performance is assessed based on how slugs, productivity, and system stability, are affected.

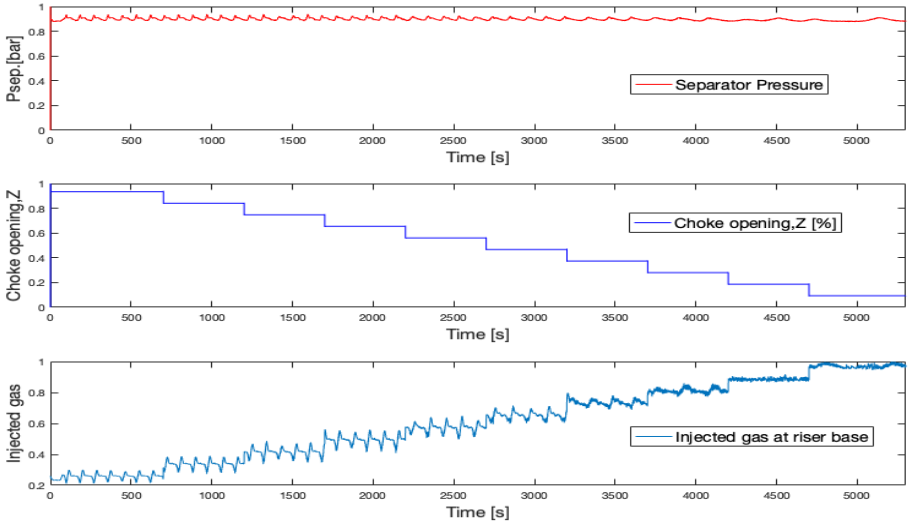

Figure 4.19. Scenario 3 - Inlet pipeline gas injection rate with varied choke valve opening and separator pressure.

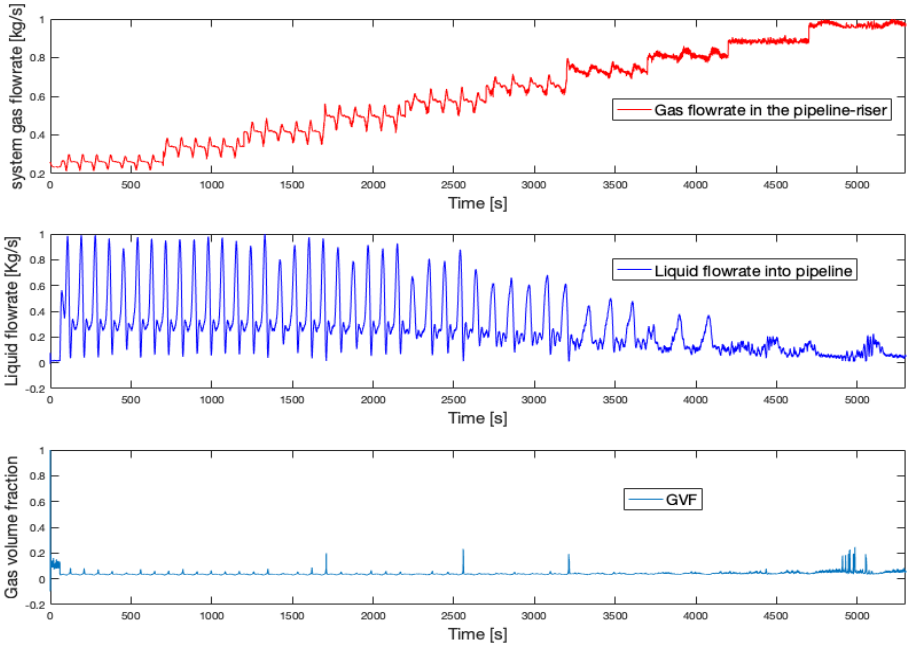

Figure 4.20. Scenario 3 - Inflow conditions (liquid and gas flowrates) along the flowline.

Figure 4.21 demonstrates that the GVF continues to fluctuate and produce high peaks under this scenario, indicating that the system did not stabilize. The GVF fluctuation occurs due to slugging. The fluctuations challenge the actuator, but the gas controller cannot manage the high oscillations from the slugging regime due to the high gas production. On the other hand, pressure measurements are steadier, as shown in Figure. 4.21. This occurs because the induced back pressure from the choke and impact from the slugs are small compared to the pump pressure. It is also stepped over long periods thereby giving the pump time to stabilize.

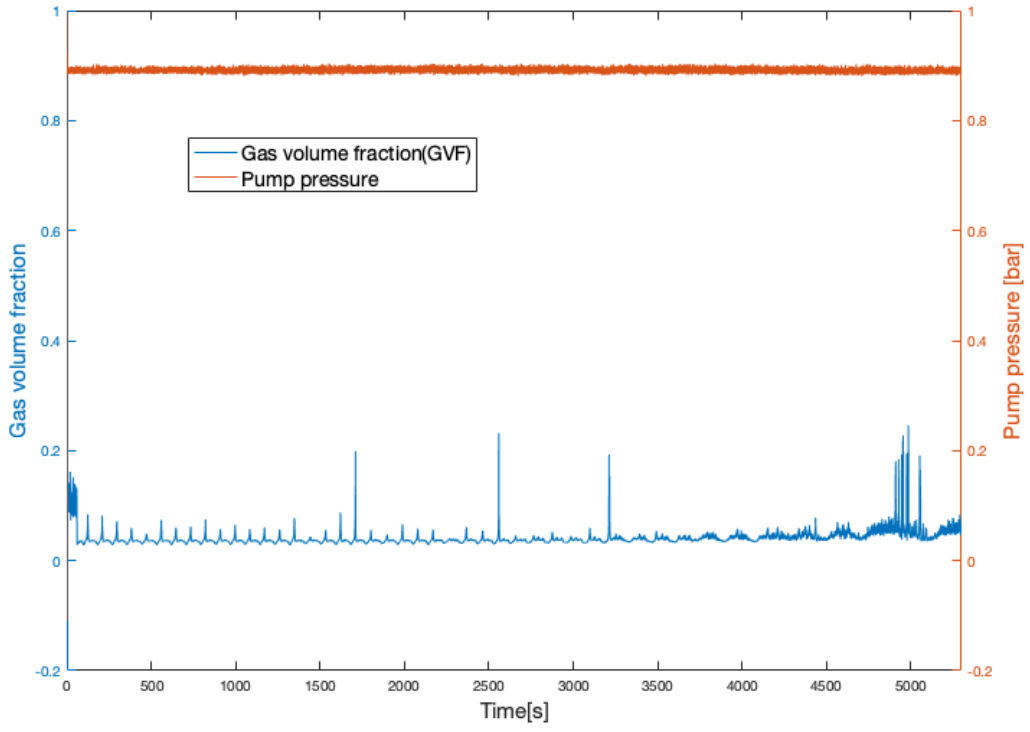

Figure 4.21. Scenario 3 - Measured flow controller responses as a function of time.

Figure 4.22 shows that gas injection increases the fluid recovery at the receiving downstream facility. However, a continuous increment in production was not achieved

over time, even though the riser-base gas injection was continued (see Figures 4.6 and 4.7). Since gas injection should be maintained to keep the high liquid production, compression and gas handling costs may significantly impact the operating costs. This is an important consideration and a limiting factor for the application of this combined scheme. A trade-off can be made between production rates and operating costs by selecting an optimal operating conditions (smaller gas injection and an optimal choke size) based on the outcomes such as Figures 4.6 and 4.7. A coordinated multiple-input and multiple-output (MIMO) control may give optimal solution when considered as one solution since choke decreases GVF, whereas gas-lift increases GVF. However, gas lifting and choking can work against each other if not effectively controlled, which is often the case when decentralized control is used.

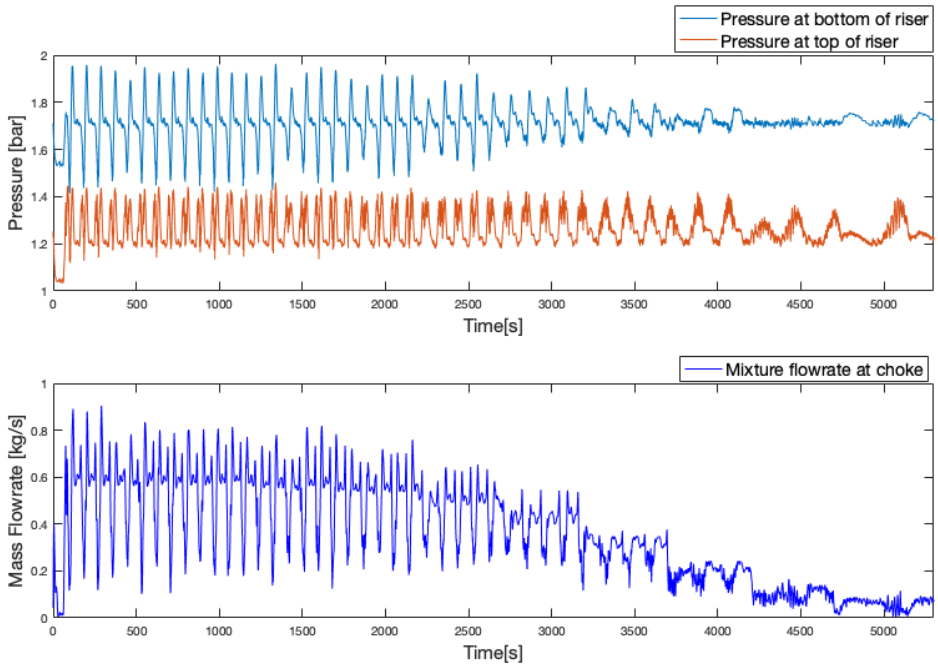

Figure 4.22. Scenario 3 - System output measurements at the choke outlet.

In Figure 4.6, the volume of gas required for injection to eliminate slugging is higher than the flow rate of gas in the pipeline. Gas injection reduces the pipeline pressure and boosts production. Continuous fluctuations in the inflow conditions and high peaks are observed for the GVF, indicating that the system did not stabilize. It can also be observed (Figure 4.5) that gas injection increases fluid recovery at the receiving downstream facility. However, the increased gas injection does not cause the resultant production to increase over time. Optimal operating conditions may be deduced and implemented for improved productions.

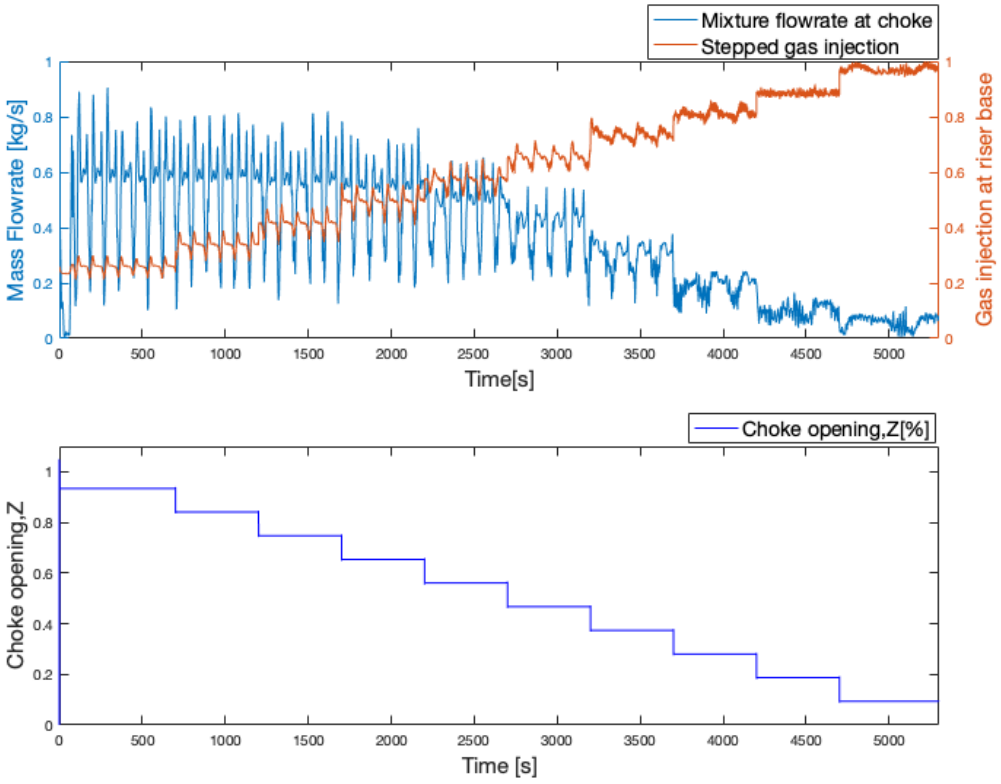

Figure 4.23. Scenario 3 - Impact of the gas injection on the production rate at the choke valve outlet.

Figure 4.22 shows that slugs are not eliminated. However, the slug frequency and amplitude decreased, although the burst time is still relatively long. This suggests that the same amount of liquid is blown out for 100% and 10%, although it takes longer in each slug cycle for the 10% opening case. From Figures 4.22 and 4.23, slugging is damped in terms of amplitude, but the negative consequences are still present. The riser-based gas lift still propagates the unsteady flow regime at low frequencies (otherwise called casing heading). The low frequencies indicate a shift from the slug to annular flow regime.

Table 4.4. Combined gas injection and choking for slug elimination.

Choke Opening (%)	**Gas Injection Rate (kg/s)**	**Production Rate (kg/s)**	**Slug**
100%	0.25	0.500	Yes
90%	0.325	0.535	Yes
80%	0.4	0.517	Yes
70%	0.475	0.514	Yes
60%	0.55	0.459	Yes
50%	0.625	0.384	Yes
40%	0.7	0.298	Yes
30%	0.775	0.187	Yes
20%	0.85	0.099	Yes
10%	0.925	0.056	Yes

The results indicate that the combined scheme can yield higher production for certain conditions. However, gas lift and choking can work against each other if not effectively controlled while decentralized. A significant pressure fluctuation can be observed at the

topside pressure in Figure 4.22 for almost a stable flow at the riser base, which is the injection point, as demonstrated in the pressures for the bottom riser (Figure 4.22). The riser induced slugs are propagated to the topside pressure. The continued gas injection can lead to large slugs which are sufficient to trip inlet vessels. In cases where the risers are stacked together, the combined contributions from the different risers can trip downstream equipment. Hydrodynamic slugs can be substantial in deep offshore operations with larger diameter pipelines (8" to 10"). Therefore, this problem can be exacerbated for coupled systems (Carroll et al., 2005). This has been reported in field applications where riser base gas lift was used including the Kepler field, GOM (Hudson et al., 2002) and Ariel fields (Lawson, 2002).

4.2 Numerical Simulations

The model developed in the previous chapter will be tested and compared with experimental data in this section for catenary risers. The model equations will be used to simulate a catenary riser system susceptible to vertical and lateral displacement. This geometrical property is captured by a transcendental equation as presented in a past study (Balino, 2010) for catenary risers. The following section describes the results obtained in the experiments, as well as modeling and simulation results.

4.2.1 Numerical Implementation and Preliminary Simulation Results

The system of mass balance and algebraic equations was solved in MATLAB software using the ODE15s solver. A constant liquid fraction was assumed in the pipeline section.

In the riser section, the liquid fraction was obtained as the average between the riser top and bottom values. Table 4.5 summarizes the input data in the simulation studies.

The simulation results are illustrated for the pressure at the bottom and top of the riser (Figure 4.24) and the mass flow rate at the choke outlet (Figure 4.25). From Figure 4.24, the simulation results emulate the slugging characteristics without active choking for the catenary riser in Figure 3.1.

Table 4.5. Input data for simulations.

Symbol	**Variable Description**	**Values**	**Units**
ρ_w	Water density	1,000	kg/m^3
ρ_o	Oil density	800	kg/m^3
ρ_G	Air (gas) density	1.649	kg/m^3
WOR	Water oil ratio	0.5	
Z_t	Riser vertical displacement	6.1	m
X_t	Riser lateral displacement	0.5	m
T_p	Pipeline temperature	293.15	$^{\circ}K$
T_r	Riser temperature	293.15	$^{\circ}K$
ε	Pipe roughness	1.5×10^{-6}	m
L_0	Horizontal pipeline length	30.1	m
L_p	Inclined pipeline length	12.2	m
D_r	Riser diameter	0.25	m
D_p	Pipeline diameter	0.25	m
μ_L	Liquid viscosity	8.9	kg/m^3
μ_g	Gas viscosity	8.9×10^{-4}	kg/m^3
g	Gravitational constant	9.8	m/s^2
R	Gas universal constant	8314	$J/(kmol \times K)$

In Figure 4.25, the flow rate is stabilized at about 700 seconds for a 24% choke opening. The oscillation at the beginning is attributed to instabilities associated with system initialization such as the start-up operation (opening an oil well for production). This is also valid for field start-up when the pressure at the sand face continues to change and affect the entire production system until the system becomes stable. Referring to Figure 4.26, results are shown for simulations at a 60% choke opening. It is found that the slug flow continues to produce high peaks in the riser. The slugging frequency is reduced but the effect of slugging is still significant. The repeated high peaks in the pressure response occurs because the pressure upstream of the riser bottom counters the backpressure induced by choking.

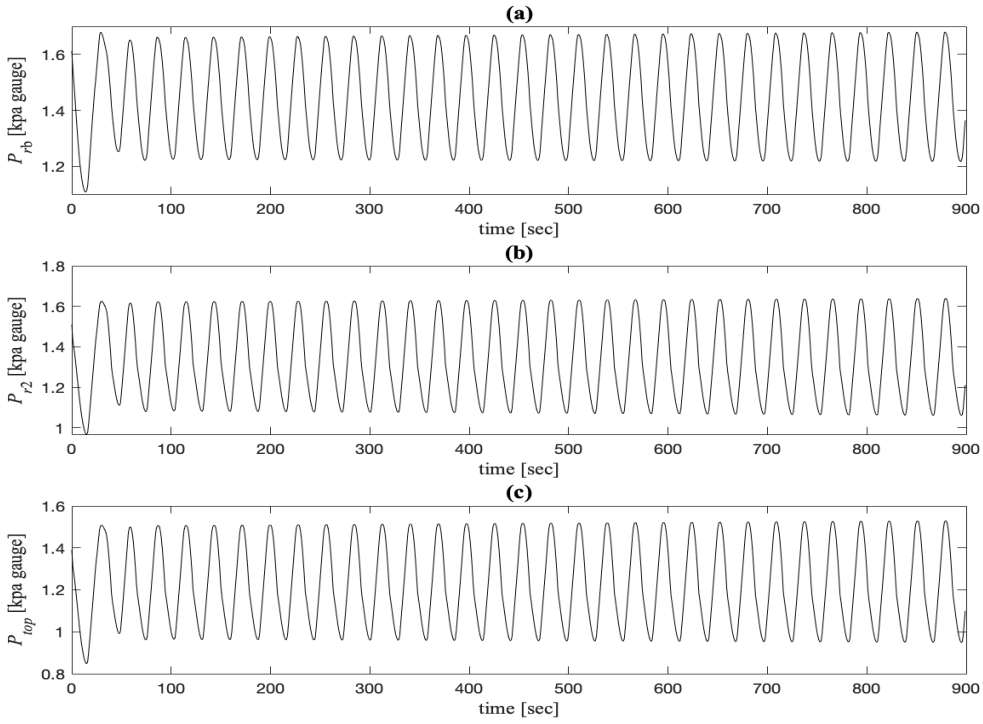

Figure 4.24. Simulation results showing (a) pressure at the bottom of the riser; (b) pressure along the riser; and (c) pressure at the top of the riser.

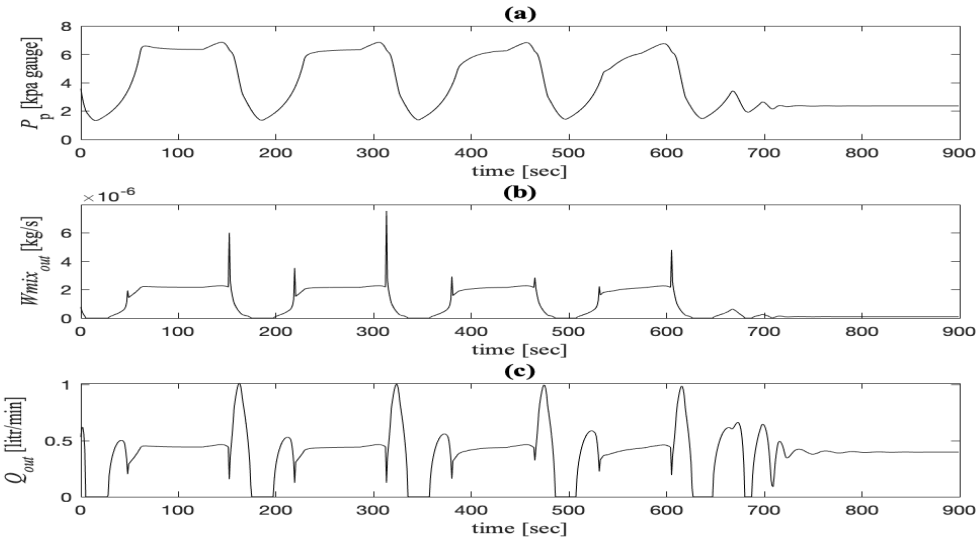

Figure 4.25. Simulation results to show (a) pressure at the top of the riser; (b) mass flow rate out of the choke; and (c) volume flow rate out of the choke versus time.

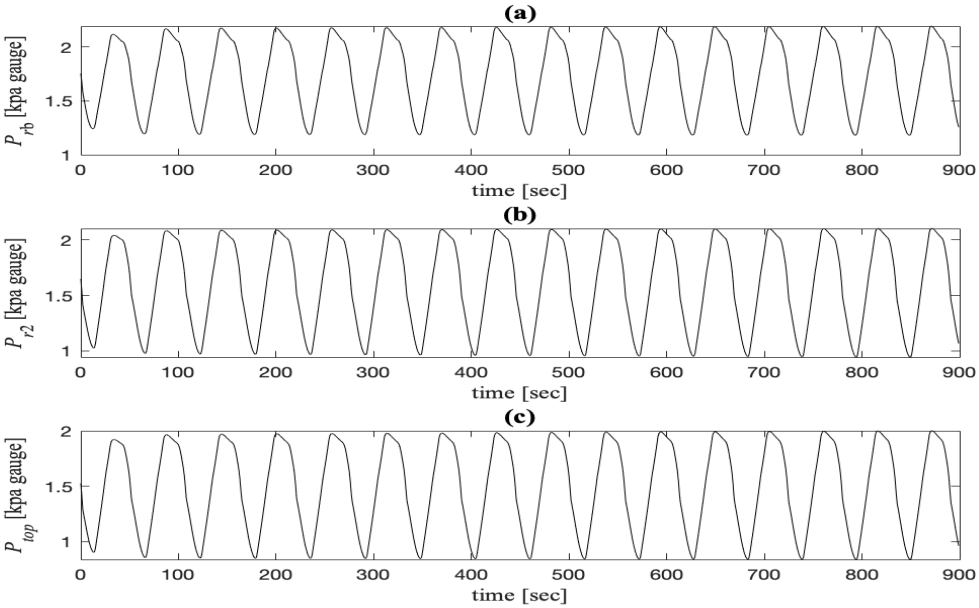

Figure 4.26. Simulation results showing the slugging characteristics for 60% choke opening, for a catenary riser, where the system slug frequency is reduced for (a) pressure at the bottom of the riser; (b) pressure at second segment; and (c) pressure at the top of the riser.

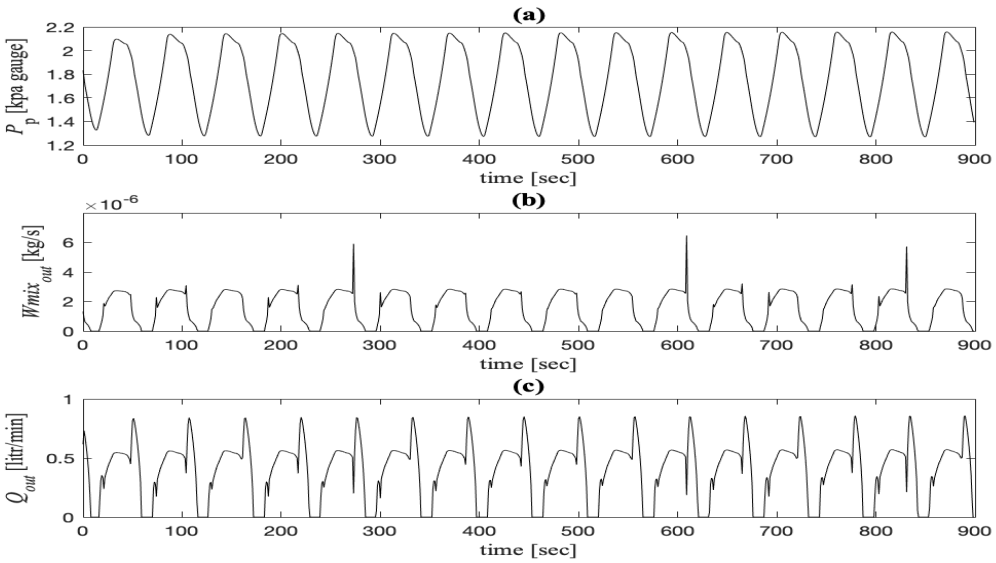

Figure 4.27. Simulation results for 60% opening: (a) pressure at the top of the riser; (b) mass flow rate out of the choke; and (c) volume flow rate out of the choke as a function of time.

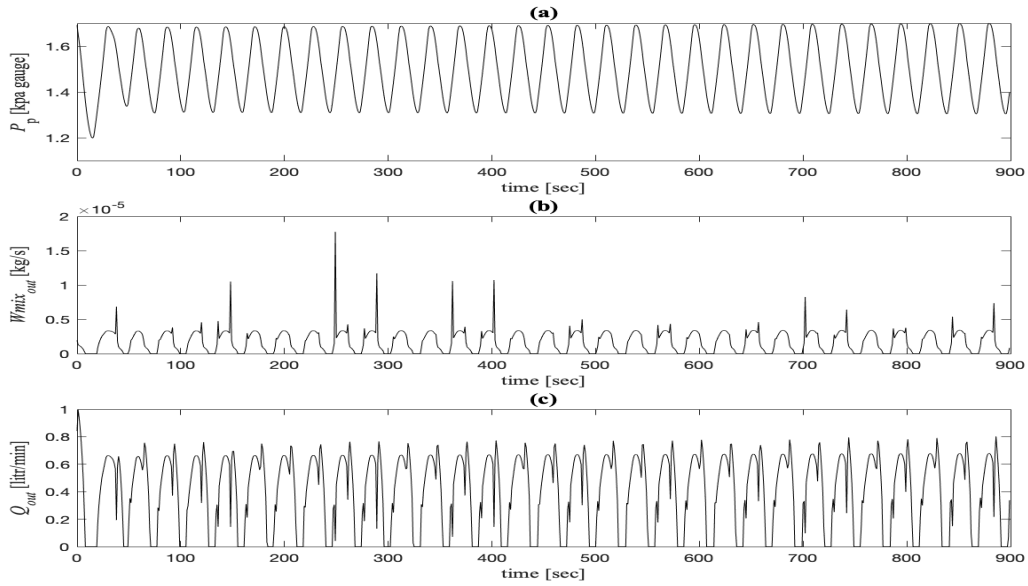

Figure 4.28. Modeling results demonstrating the slugging characteristics for a fully open catenary riser (without active choking) where the system oscillating performance is infinite for (a) pressure at the top of the riser; and (b) mass flow rate out of the choke.

4.2.2 System Identification and Validation

The experimental facility described in section 3.2 was used to validate the predicted results. A reasonable match between the model results and the experimental data was observed.

An error propagation model will also be presented for the analysis of measurement uncertainties under different flow conditions and control methods. The parameters are determined by a gradient descent-based algorithm. A system parameter is evaluated by measurements obtained from the flowline-riser experimental setup. A model parameter is obtained by minimizing the error between the model results and system identification data from an experiment. The identification can be formulated as a minimization problem using a least squares mean error function as follows:

$$Error = \sum_{k=1}^{N} \left\{ \left(\phi_1 \frac{P_{b,model} - P_{b,exp}}{\bar{P}_{b,model}} \right)^2 + \left(\phi_2 \frac{P_{t,model} - P_{t,exp}}{\bar{P}_{tmodel}} \right) + \left(\phi_3 \frac{P_{in,model} - P_{in,exp}}{\bar{P}_{in,model}} \right) + \left(\phi_4 \frac{w_{mix,model} - w_{mix,exp}}{\bar{w}_{mix,model}} \right) \right\} \quad (4.1)$$

where P_b denotes the bottom pressure; P_t is the top pressure; P_{in} is the inlet pressure; and w_{mix} represents the mixture flowrate at the choke valve. The subscripts $model$ and exp denote the model and measured outputs respectively, while ϕ_i $(i = 1,2,3,4)$ refers to the weight factors assigned to variables; and N is the number of grid points in the experimental data. The equation weighs the output error as a relative deviation rather than an absolute deviation. The relative deviations are chosen to prevent the pressure errors from having higher numerical significance than flow errors. The experiments provide measurements of P_{in}, P_{ipe}, P_{base}, P_{top}, w_{Lin}, w_{Gin}, w_{mix_out} and P_{sep}, which are used for parameter identification.

The maximum absolute error between the model and experimental data are within a range of 5% and 13%, with the riser base pressure being the maximum.

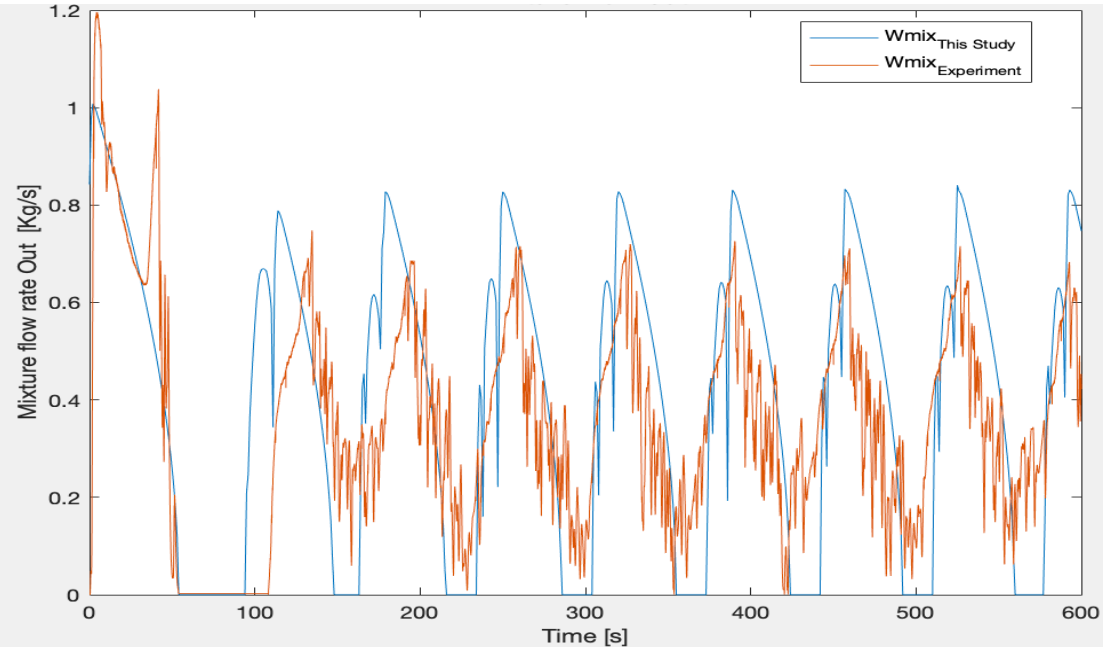

Figure 4.29. Mass flow rate of the fluid mixture at the topside choke where the predicted flow rates are compared with the experimental mass flow rates at the top of the catenary riser for 100% valve opening.

Figure 4.29 compares the calculated mixture flow rates at the choke outlet with the measured mass flow rates. The data shows a chaotic behaviour for both the model outputs and the experimental results. Storkaas (2003) suggested the use of outlet flow measurement as a variable to suppress anti-slug applications especially for high-frequency slugs. This sugesstes that an accurate prediction of flowrate at the outlet is important for effective control applications where the mass flow rate is utilized as a control variable.

Model results are seen to slightly vary from the experimental data in phases and amplitudes. This is most predominant for the pressure results (Figures 4.30 - 4.32). Considering that pressure measurements were taken at different locations along the riser, this may account for the differences in amplitude between the experiment and model results.

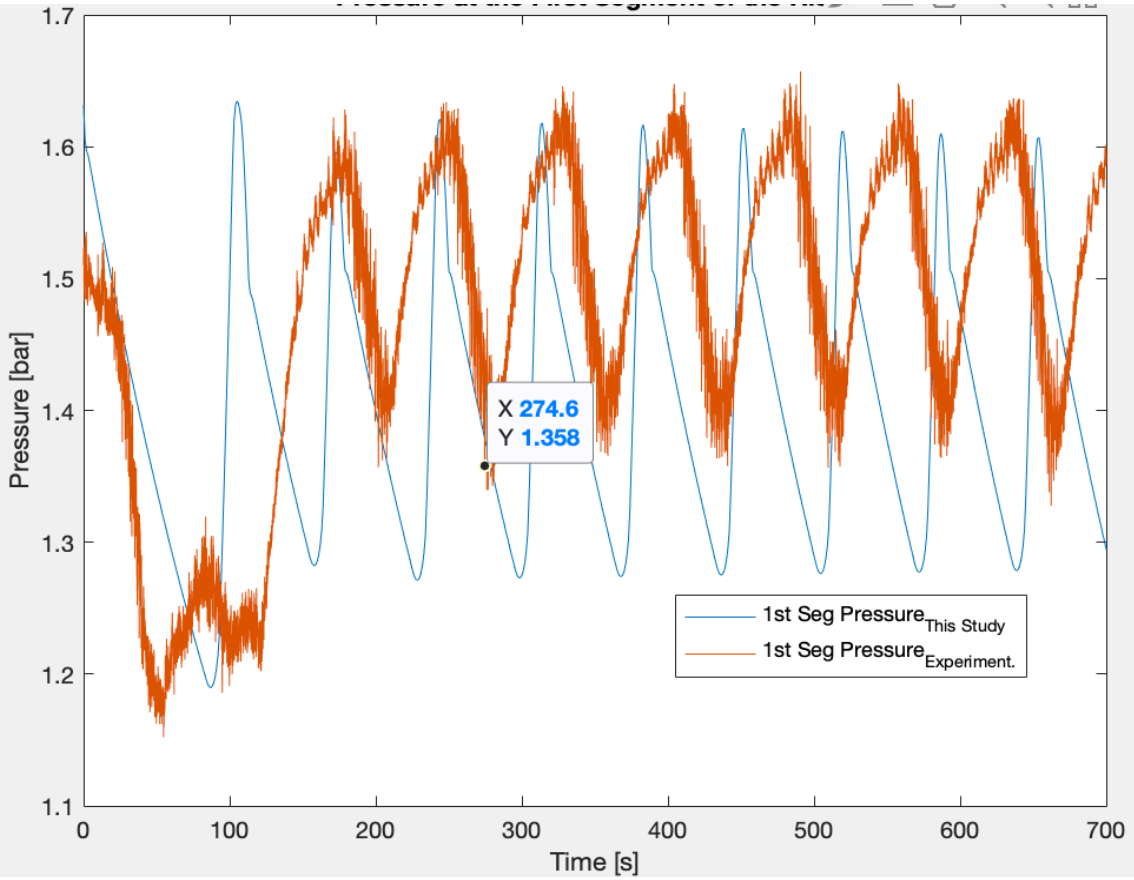

Figure 4.30. Comparison of model results with the experimental data where the predicted pressure in the first riser segment is compared with the experimental pressure at the first segment of the catenary riser for 100% valve opening.

The model results show good agreement with the flow measurements. Other studies (Jahanshahi, 2012, Storkaas, 2007) have also proposed to combine the upstream pressure measurement (pipleine or riser bottom) with the outlet mixture flowrate to achieve system stability in MIMO or SIMO configurations. The new model matches the mixture flow rate closely, hence, it can be applied for control studies. We have demonstrated that our models match the experimental data with good accuracy. This validates these models for application in designing and simulating slug behaviours in pipeline-risers. These models can also be used for control analysis, such as evaluating the most crucial system properties and locations that would be most suitable for installation and implementation of slug control. Both the mixture flow rate at the choke outlet and the pressure at the top of the riser are recommended for control analysis. Where possibil, the riser base is recommended for installation of control devices; otherwise the riser top may be used.

Figures 4.30 and 4.31 compare the calculated topside and bottom pressures, respectively, with the experimental results. Both the model and experimental results show high oscillation peaks. The model pressure amplitudes are slightly higher than the experiments, though the model still matches fairly well with the experiments. The flow dynamics may be attributed to the minor variations in phase behaviour observed since a static valve was used. The static valve produced faster bandwidth compared to the flow dynamics.

Our study shows that mass flow rate at the topside and pressure at the top of the riser is more suitable for control strategy using our models. The choice of the control strategy is significantly impacted by economics and data availability. Although the current technologies enable downhole measurements to be deployed subsea where the wellheads

are located for upstream data acquisition, the operation can have negative economic and safety implications.

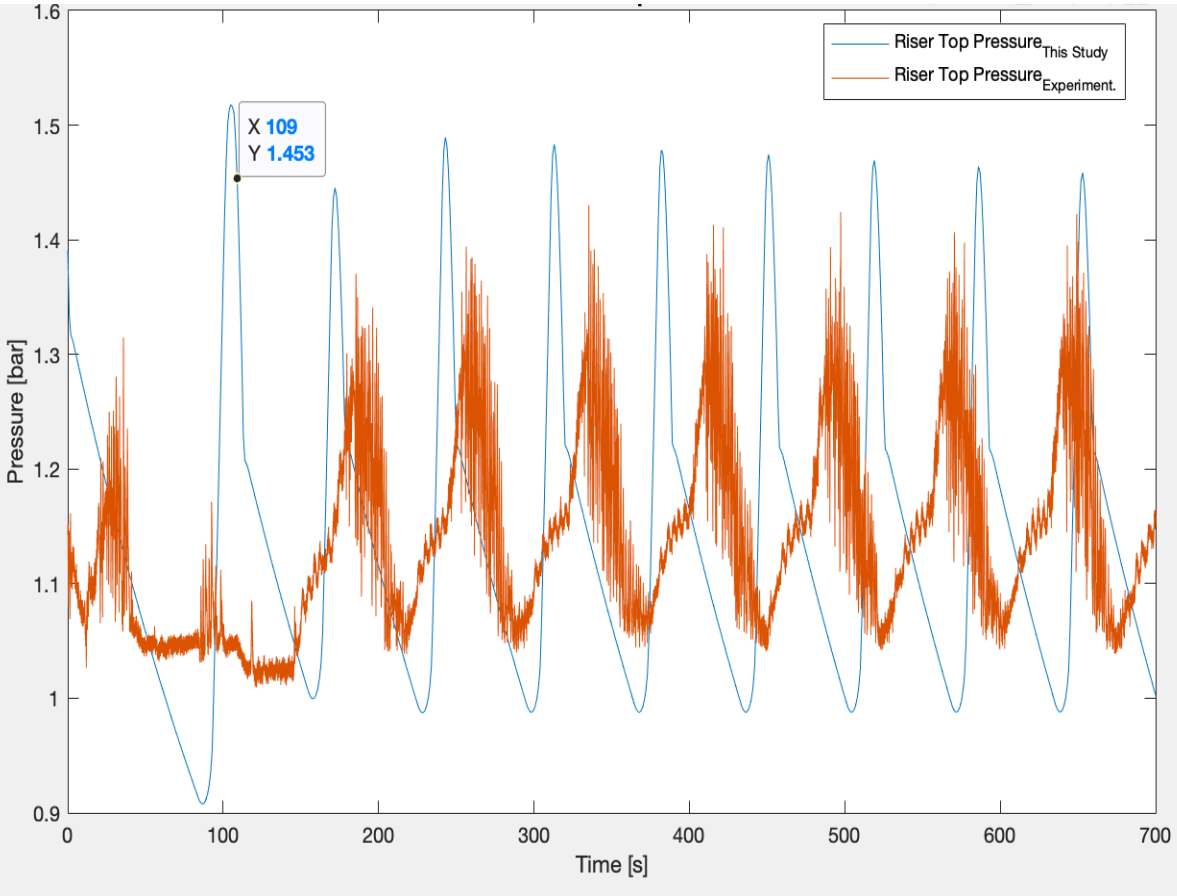

Figure 4.31. Pressure versus time where the predicted pressure at the top of the riser segment is compared with the experimental pressure at the top of the catenary riser.

In situations where no upstream data is unavailable, it has been shown (Siverstsen et al., 2010) that topside pressure measurements and topside flow rates are sufficient to control variables to stabilize the system. Hence, cost and ease of implementation using topside measurements are favoured for offshore applications.

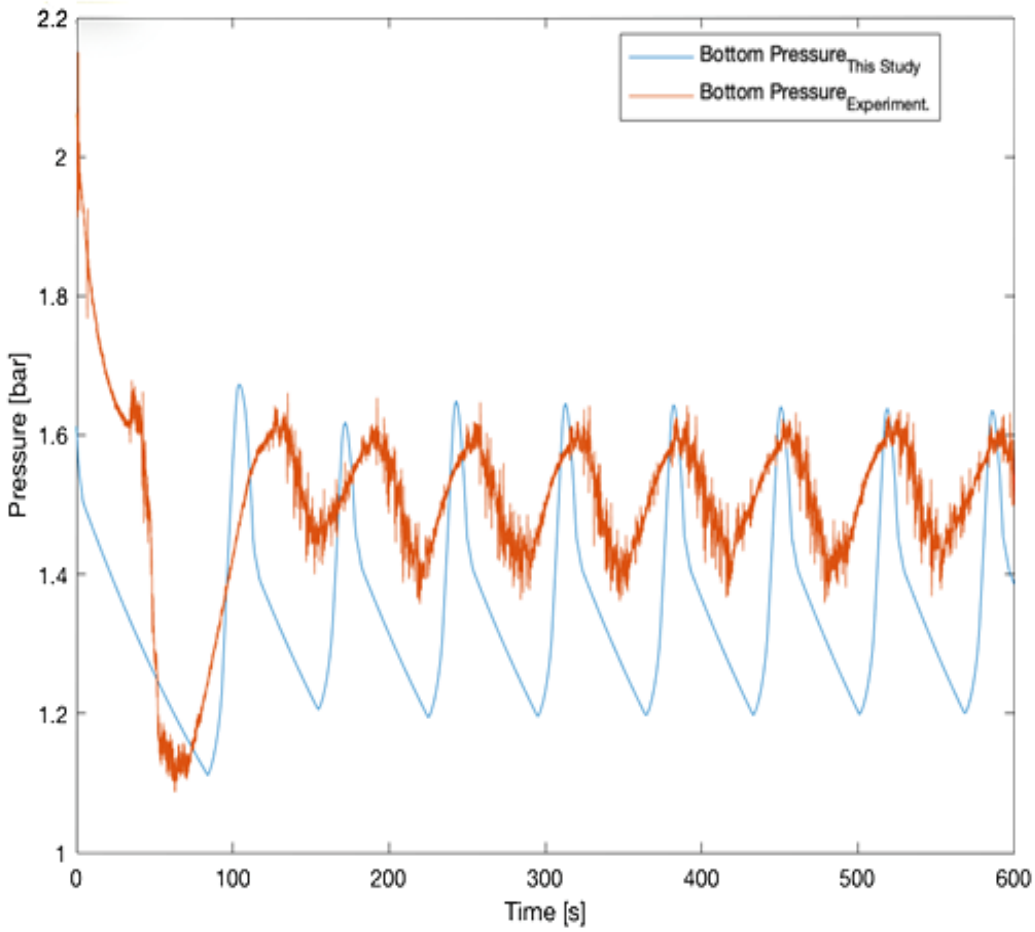

Figure 4.32. Experimental and predicted pressure at the bottom of the riser for 100% valve opening versus time.

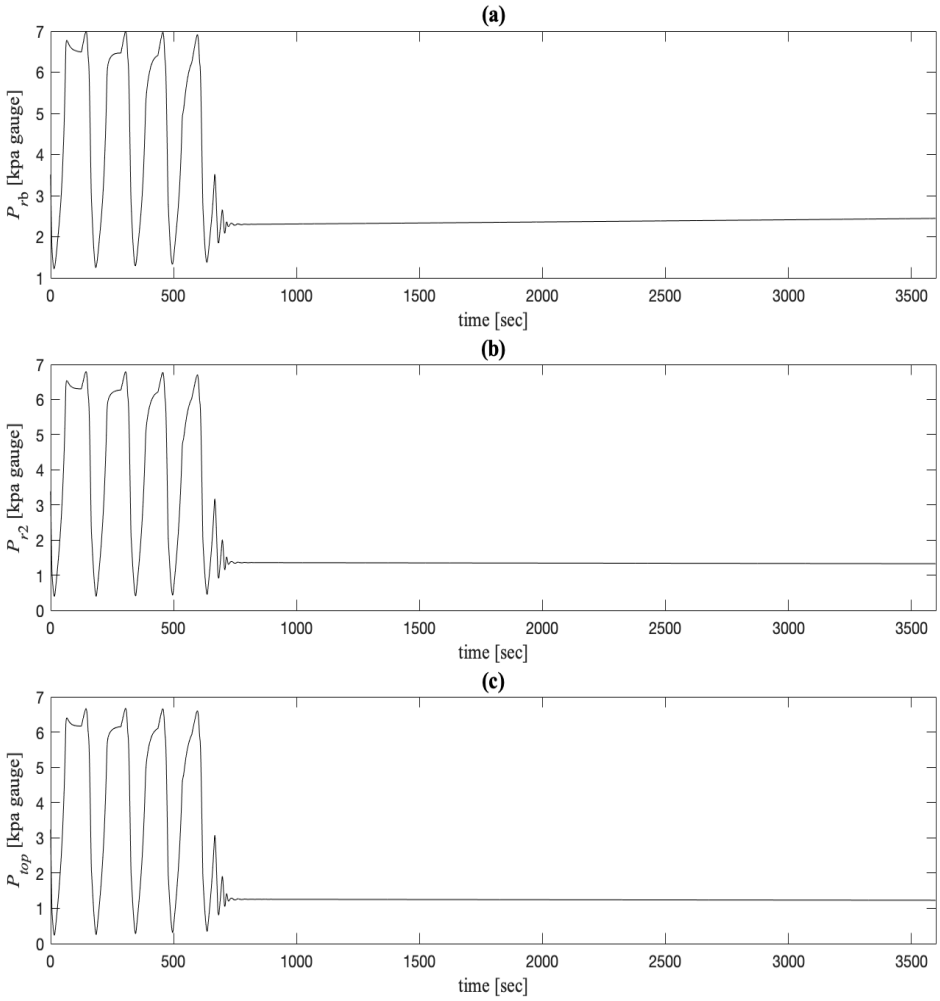

Figure 4.33. Model predictions for longer period of simulation below the bifurcation where the system becomes relatively stable at about 700 seconds and is maintained for the period of the simulation: (a) pressure at the bottom of the riser; (b) pressure at second segment; and (c) pressure at the top of the riser.

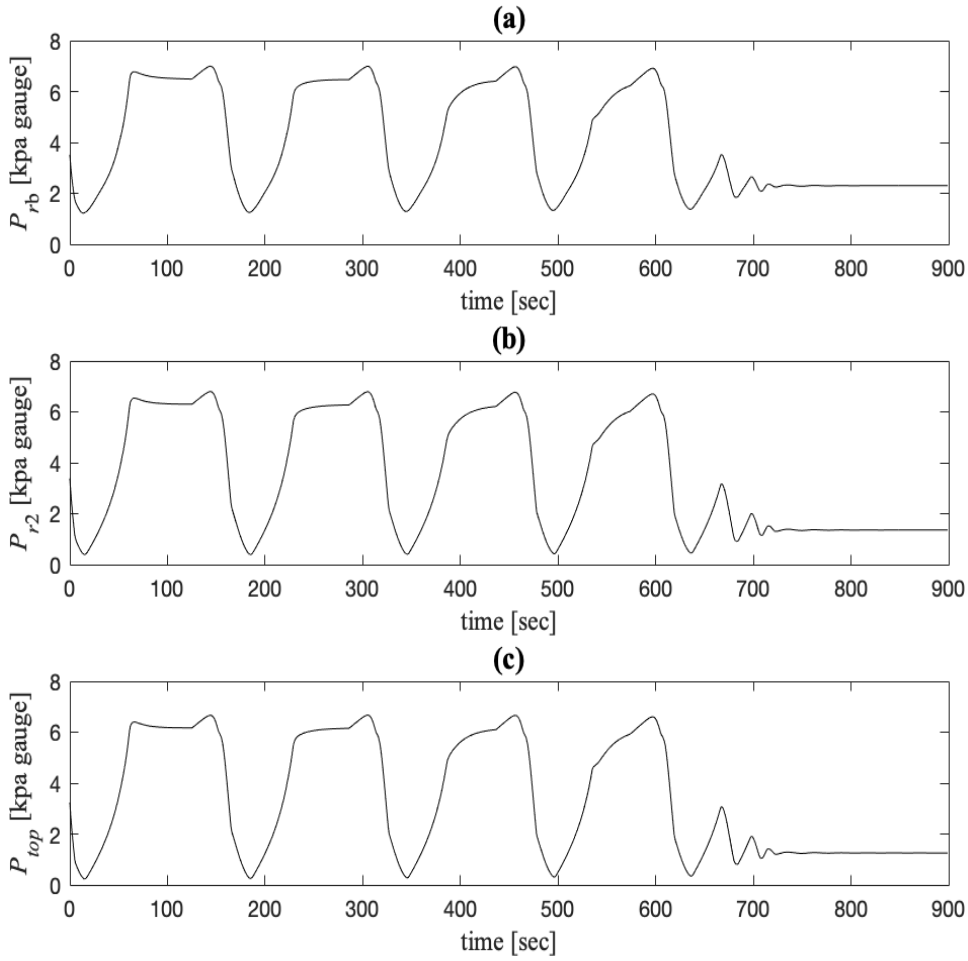

Figure 4.34. Model results for short period of simulation below the bifurcation where the system becomes relatively stable at about 700 seconds: (a) pressure at the bottom of the riser; (b) pressure along the riser; and (c) pressure at the top of the riser versus time.

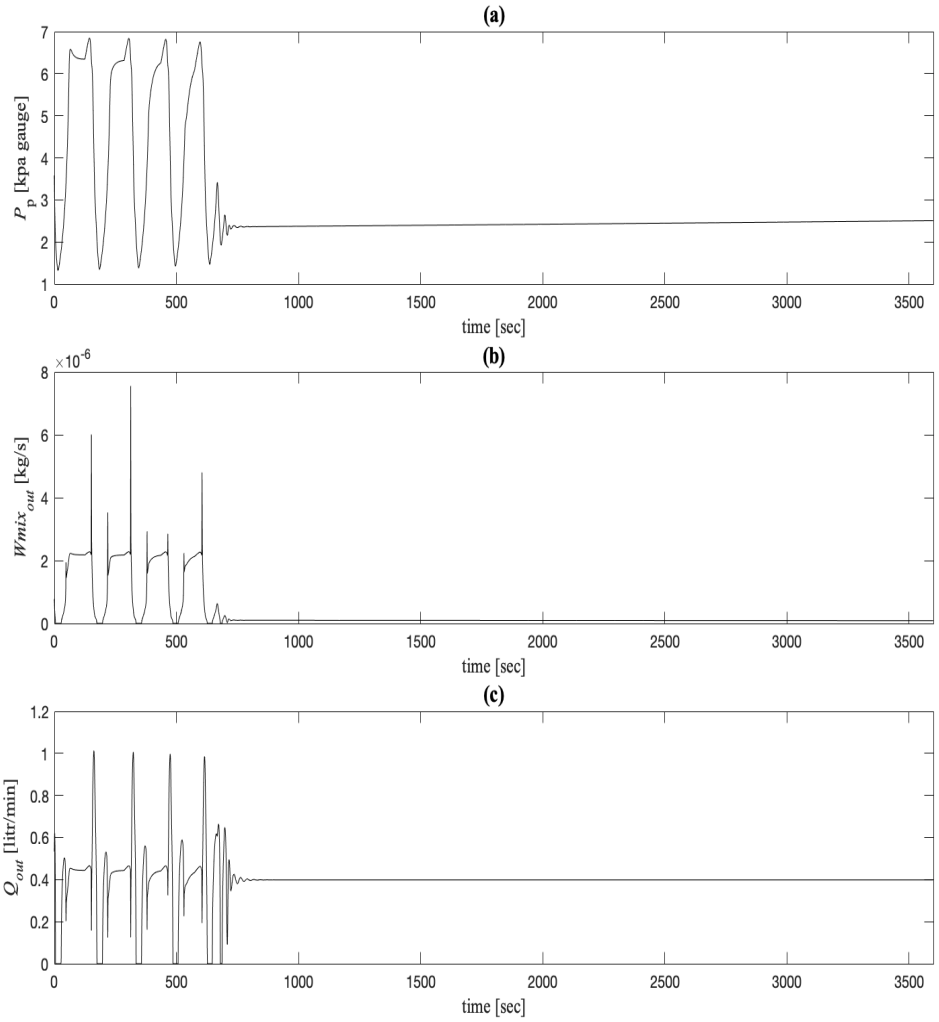

Figure 4.35. Model outputs for longer period of simulation below the bifurcation where the system becomes relatively stable at about 700 seconds and is maintained for the entire period of the simulation: (a) pressure at the top of the riser; (b) mass flow rate at the choke outlet; and (c) volumetric flowrate at the choke outlet.

4.3 Correlations of Slugging Variables

In the previous chapter, Equation (3.47) identified parameters affecting the slug frequency and a correlation in terms of dimensionless groups. As reported earlier, both fluid and

geometrical parameters have significant effects in the flow behaviour of a slugging regime in the pipeline-riser system. The experimental data showed significant peaks in amplitude within the slug flow regime. Average values were obtained, which also account for the variations. Dimensional analysis was implemented to obtain dimensionless groups used for the model development through a combination of problem variables. Table 3.3 provided a summary of the dimensionless groups that affect the slugging phenomenon.

To determine the coefficients and exponents in the general predictive expression, manual iterations were performed, using the experimental data. Scatter plots were drawn and evaluated using linear regression on a log-log scale. An iterative technique was employed to obtain the final empirical correlation. The iterative procedure was performed using individual dimensionless numbers and a combination of dimensionless groups. The results from each iteration process were the input into the subsequent iterative steps, leading to the final model.

The slopes of the fitted curve/line on the scatter plots give the coefficients (n_k) of the combined group. The coefficient of determination (goodness-of-fit measure) is then used to assess how well the model fits the data. Generally, R-squared (R^2) values lie between 0 and 1, representing no relationship and perfect fitness, respectively. The R^2 value of the relationship is calculated for every step in the iteration. A minimum of 15% R-squared value is assumed as an acceptable criterion. Thus, each dimensionless group should meet this criterion before it is considered for further iterations. Generally, a procedure in dimensionless analysis involves starting up with lower criteria (such as15% in our case), which allows for more system variables to be included at the initial stage, and then eliminating the variables with lesser impact to the overall correlation through sensitivity

studies. However, the low R-squared criteria are not used for deciding on acceptance of final correlation. The correlation parameters should be improved through sensitivity studies and several iterations.

The slope, a, in Equation (3.50) is the index of a given dimensionless group, n_k, value, in the correlation. The slope, intercept, and R^2 of each step are also provided in Tables 4.5 and 4.6 for the first and second iterations, respectively.

The first step in the analysis evaluates the impact of the choke opening (Z) on the slug frequency by plotting Kc versus Z. The scatter plot gives R^2 of 0.16 and the gradient of the linear regression line is obtained as -0.415. Thus, 0.415 is taken as the initial coefficient of the choke opening. Figure 4.35 is presented to demonstrate the best relationship after several iterations. It shows the relationship between the slug frequency and choke opening. The result agrees with previous studies (Schulkes,2000; Zabaras,1999) wherein the frequency of slugs decreases as the choke size decreases. This occurs particularly for choke openings below 60%, where an increase in the gas and liquid velocities occurs as more liquid slugs are produced at the choke outlet.

The second step includes the effect of the inflow conditions on the empirical model by plotting $\frac{Kc}{Z^{n_1}}$ versus $R_{em,i}$ (see Figure 4.36). The scatter plot has an R^2 of 0.54 and a slope of 0.69. It should be noted that the Reynolds number in the pipeline is determined at the inlet of the pipeline section using flowrate measurements at the point of fluid entry into the pipeline section. The Reynolds number in the riser section did not have a significant R^2; hence, it was neglected in further iterations. The Bejan number is used to examine the influence of the pressure drop on the slug frequency correlation, for both the pipeline and

riser sections. Similar to the Reynolds number in the pipeline, the Bejan number in the riser did not have a considerable contribution. Thus it was not considered in further iterations. The dimensionless pressure drop in the riser section gave R^2 of 0.34 and a slope of 0.254. The last step of the analysis evaluates the influence of the fluid densities. Again, the results of the density ratio exhibited a small R^2 and zero gradient; thus, it was neglected.

At this stage, the approximate coefficients are obtained. Further iterations are performed until the coefficients converge and do not improve the coefficients subsequently. This step also compares the individual π_i groups on the combined groups as shown in Equations (3.76) through (3.80). The iteration assists to investigate the impact of the various groups on the overall π group combinations, since sensitivity analysis of each π group is carried out while all other numbers are present. Hence, the order in which the π groups are combined does not affect the results of the final empirical model.

Table 4.6. Correlation coefficients for the first iteration.

Dimensionless group	**R^2**	**a**	**b**
Kc vs Z	0.163	-0.415	9.04
$\frac{Kc}{Z^{n_1}}$ vs $R_{em,i}$	0.537	0.693	5.54
$\frac{Kc}{z^{n_1}{R_{em,i}}^{n_2}}$ vs $B_{e,p}$	0.159	5.955	43.95
$\frac{Kc}{z^{n_1}{R_{em,i}}^{n_2}{B_{e,p}}^{n_3}}$ vs $B_{e,r}$	0.335	-2.540	18.97
Final model prediction $f_{s,model}$ vs $f_{s,actual}$	0.847	1.070	0

Additionally, the key flow characteristics influence the integrated process performance. To further improve the model in terms of accuracy, the frequency is calculated for each of the

steps and compared with the actual frequency using a scatter plot. An ideal case would give a slope of unity and an R-squared value of unity. The relationships with very small R-squared values, as neglected during the 1st iteration, are not included in the combined group for the 2nd iteration.

The general form of the linear regression obtained for each of the iterative step demonstrated in Figures 4.35 through 4.38 is given as $y = ax + b$.

Equation (3.82) is the two-phase correlation for predicting severe slugging frequency in offshore pipeline-riser systems. The slug frequency can be determined from the Keulegan-Carpenter expression, $f_s = \frac{v_m}{D \cdot Kc}$, where v_m is the mixture velocity and D is the pipeline diameter. In a practical offshore application where the velocity measurement is not available, flowrate data obtained at the wellhead can be used to calculate the mixture velocity through the relationship between the volumetric flow rate and flow cross section area (or pipe diameter).

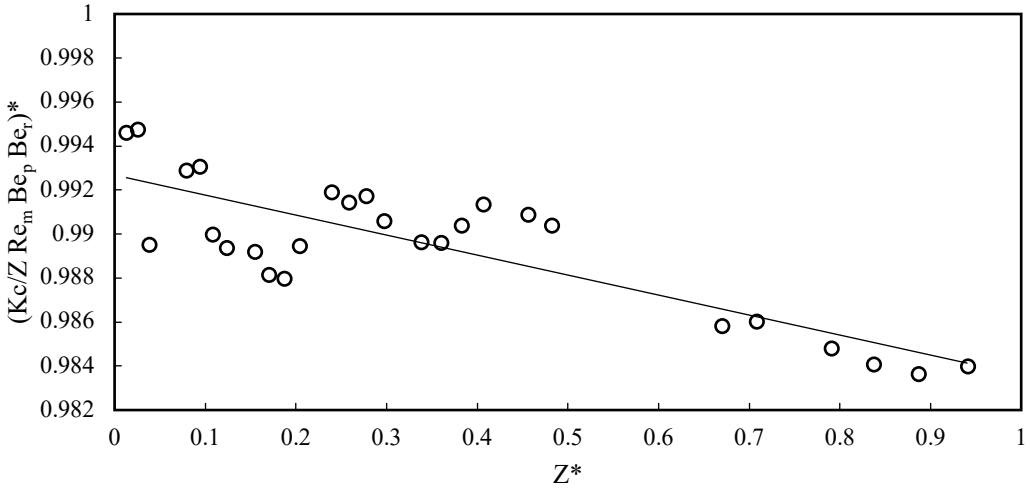

Figure 4.36. Combined dimensionless group versus choke opening (a = -0.009, b = 0.99, $R^2 = 0.68$).

In Figure 4.35, the relationship between the combined Kc and the choke opening number (Z) is shown. The slope, intercept, and R-squared values are listed in Table 4.6.

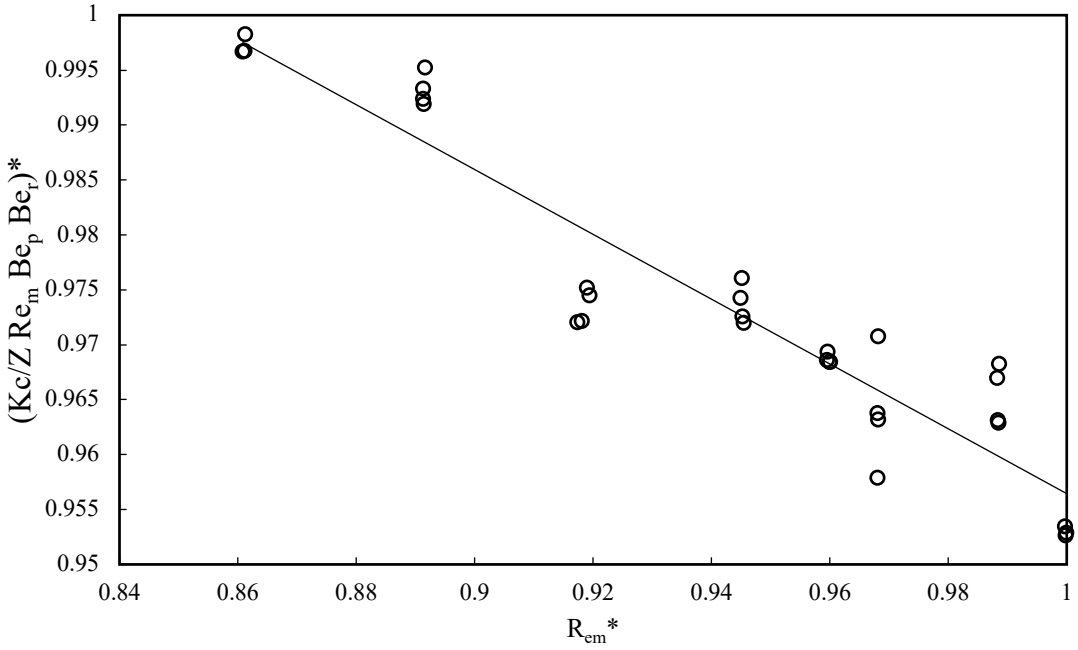

Figure 4.37. Combined dimensionless group as a function of Reynolds number in the pipeline (a = -0.29, b = 1.25, $R^2 = 0.89$).

In Figure 4.36, the slope of the linear regression provides the coefficient for the Reynolds number where the relationship between the combined Kc and the choke opening with the Reynolds number ($R_{em,i}$) for flow in the pipeline is demonstrated. In other words, the curve fit for the plot of $\log\left(\frac{\mathrm{Kc}}{\mathrm{Z}^{\,n_1}}\right) = \log \mathrm{C}_2 + \mathrm{n}_2 \log\left(\mathrm{R}_{\mathrm{em},\mathrm{i}}\right)$ is shown. The slope, intercept, and R-squared values of this step are also listed in Table 4.6

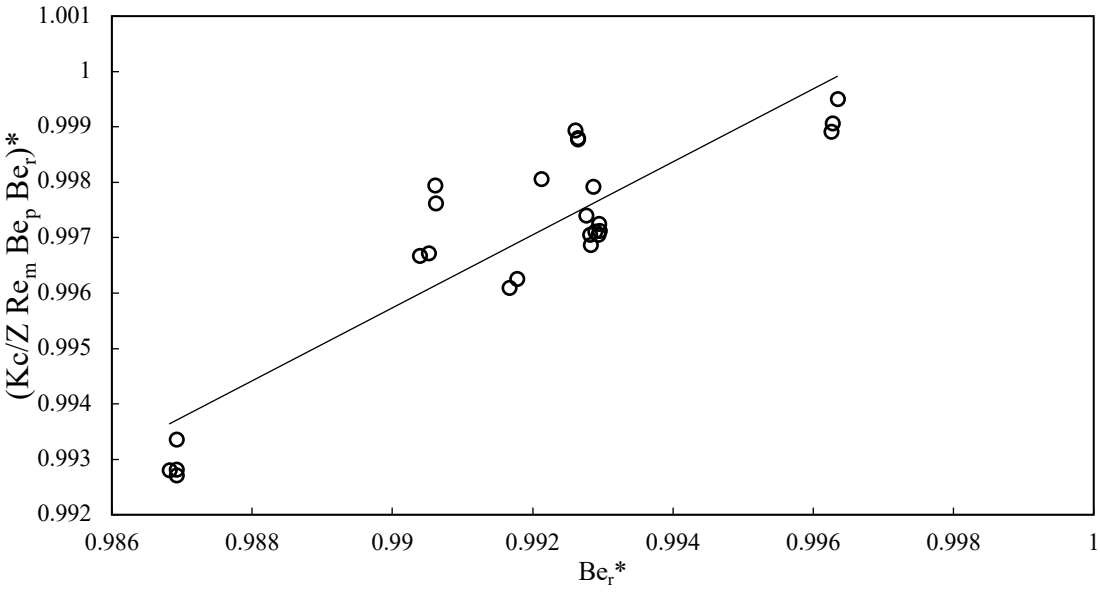

Figure 4.38. Combined dimensionless group versus Bejan number in the riser (a = 0.66, b = 0.3, $R^2 = 0.789$).

Table 4.7. Correlation coefficients and gradients for the second iteration.

Dimensionless group	**R^2**	**a**	**b**
$\frac{Kc}{Re_{m,i}^{0.693} Be_{,p}^{5.955} Be_{m,r}^{-2.54}}$ vs Z	0.7223	-0.66	19.06
$\frac{Kc}{Z^{-0.415} Be_{,p}^{5.955} Be_{m,r}^{-2.54}}$ vs $Re_{m,i}$	0.777	0.75	19.32
$\frac{Kc}{Z^{-0.415} Re_{m,i}^{0.693} Be_{m,r}^{-2.54}}$ vs $Be_{,p}$	0.50	8.93	44.06
$\frac{Kc}{Z^{-0.415} Re_{m,i}^{0.693} Be_{,p}^{5.955}}$ vs $Be_{,r}$	0.51	-2.91	40.37
Final model prediction $f_{s,model}$ vs $f_{s,actual}$	0.89	1.07	0

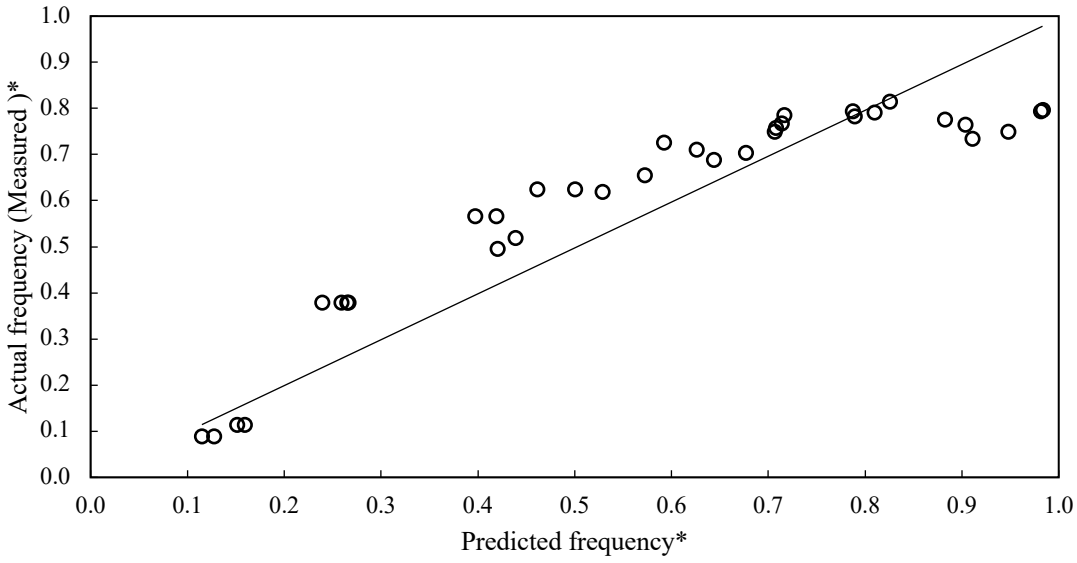

Figure 4.39. Comparison of the slug frequency measurements and model predictions (a = 0.995, b = 0, R^2 = 0.766).

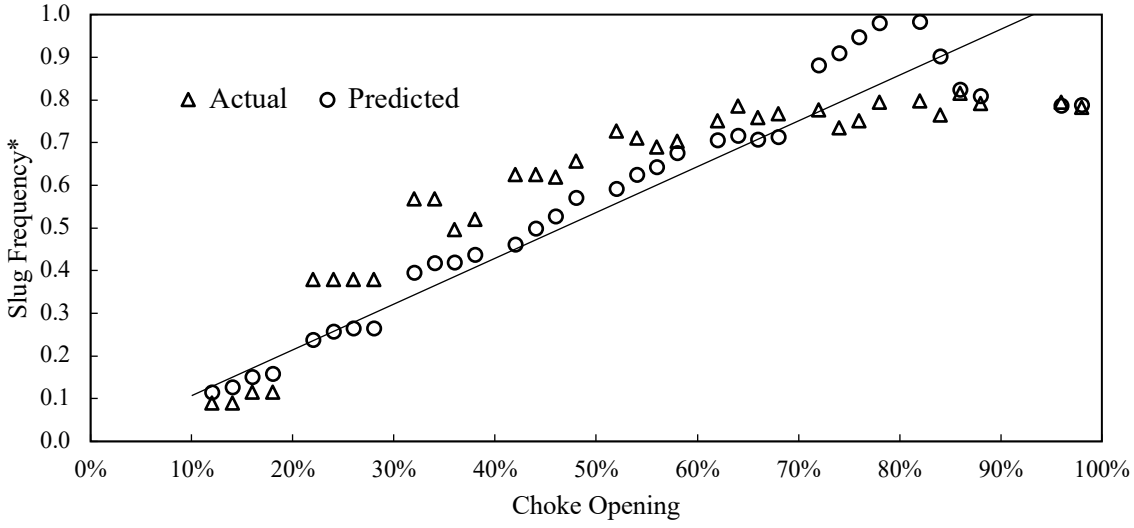

Figure 4.40. Comparison of the calculated slug frequency from the new correlation with the frequency measurements (a = 1.07, b = 0, R^2 = 0.89).

There is a good match between the predicted values and experimental results as shown in Figure 4.39. An absolute mean error is estimated to be 10%. The predictions in Figure 4.39 are compared with the slug frequency data obtained from the experiments for various choke sizes (see Figure 4.40). It can be seen from Figure 4.40 that the model reasonably estimates the slug frequency for different choke sizes. An R-squared value of 0.89 was obtained. According to statistical evaluation of the model for the various choke openings, a maximum absolute error of 18.3% was obtained when the choke opening was 20%, as presented in Table 4.7. However, for the most critical (high) peaks, which lie between fully open (100%) to 40%, the absolute error lies between 0.53% and 11.1%. Further analysis is shown for selected choke sizes in Appendix C.

Table 4.8. Measured data, predictions, and error percentage.

Percentage choke opening	100	90	80	70	60	50	40	30	20	10
Average measured frequency	0.489	0.547	0.529	0.515	0.469	0.399	0.304	0.203	0.104	0.071
Average predicted frequency	0.474	0.602	0.547	0.480	0.418	0.363	0.302	0.221	0.123	0.067
Absolute error	3.1%	10%	3.4%	6.8%	10.9%	9.0%	0.66%	8.8%	18.3%	5.6%

The correlation predicts 92.3% of the measurements lie within ±8% absolute error and the mean absolute deviation of the correlation is about 6.13%. The newly developed correlation can be applied for flow rates between 0.1 kg/s and 0.6 kg/s and for choke openings between 10-98%.

4.4 Two-Phase Slug Velocity Correlation

In this section, the results for the two-phase slug velocity correlation are presented. The equation formulation, methods and stepwise analysis were previously reported in section 3.3.2 of chapter 3.

Using the dimensionless analysis technique, the parameters and variables that describe the process are combined to obtain the dimensionless groups for the model development. Through an iterative process, the final empirical correlation is determined. The coefficients and exponents in the general correlation relationships were determined by performing iterations on the experimental data. Scatter plots were created and evaluated using linear regression on a log-log scale. The iterative procedure was also performed on a combination of the various dimensionless groups for the analysis, which included the process variables that affect the slug flow regime.

The slopes of the curve fit on the scatter plots provided the coefficients for the general correlation. Again, a minimum of a 15% R-squared value is taken as the acceptance criterion, before it is considered for further iterations. The graphs (Figures 4.41 to 4.45) presented below were obtained through a stepwise iteration conducted on the dimensionless groups.

The first step in the analysis was to include the influence of the choke opening on the slug velocity. A plot of $\log\left(R_{em,o}{}^{*}\right)$ vs $\log(z)$ verifies their relationship.

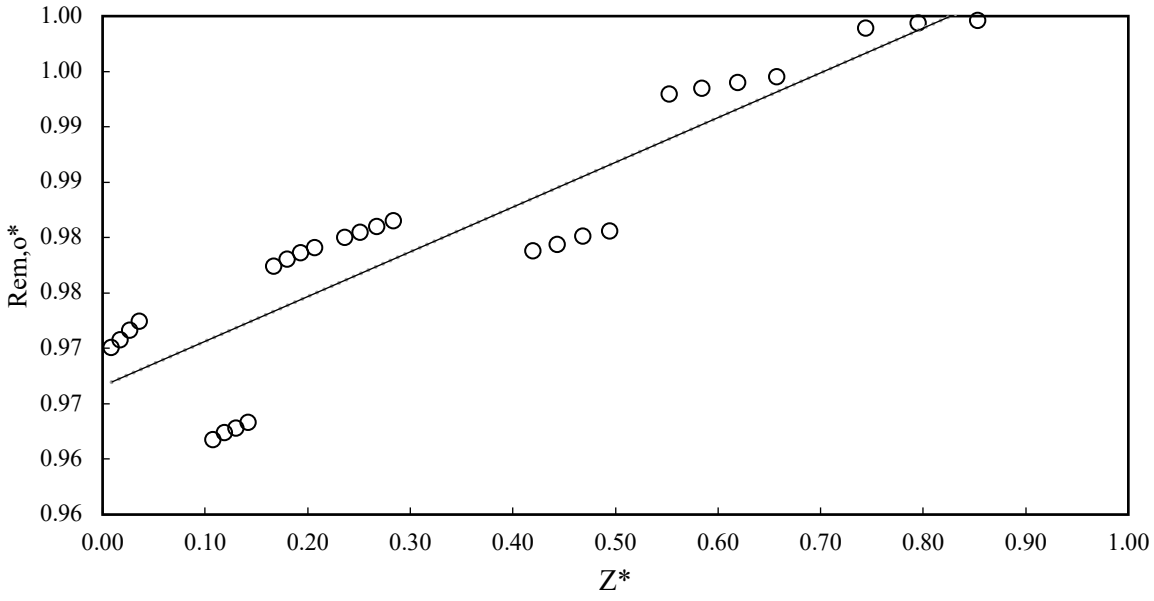

Figure 4.41. First iteration - Mixture Reynolds number versus choke opening (a = -0.08, b = -2.32, R^2 = 0.485)

From Figure 4.41, it can be seen that the Reynolds number increases linearly with the choke opening. An R^2 value of 0.49 suggests that a strong relationship exists between them. A previous study has shown that the gas and liquid velocities increase as the choke opening increases. This result supports the previous study. The second step of the analysis evaluates the influence of the inflow conditions on the slug velocity. At this stage, the effects of the choke opening and the Reynolds number in the pipeline are included in the combined correlation.

The mixture Reynolds number in the pipeline is examined in the second step by plotting $\frac{R_{em}}{Z^{n_1}}$ vs $R_{em,i}$. The Reynolds number in the pipeline is determined at the pipe inlet.

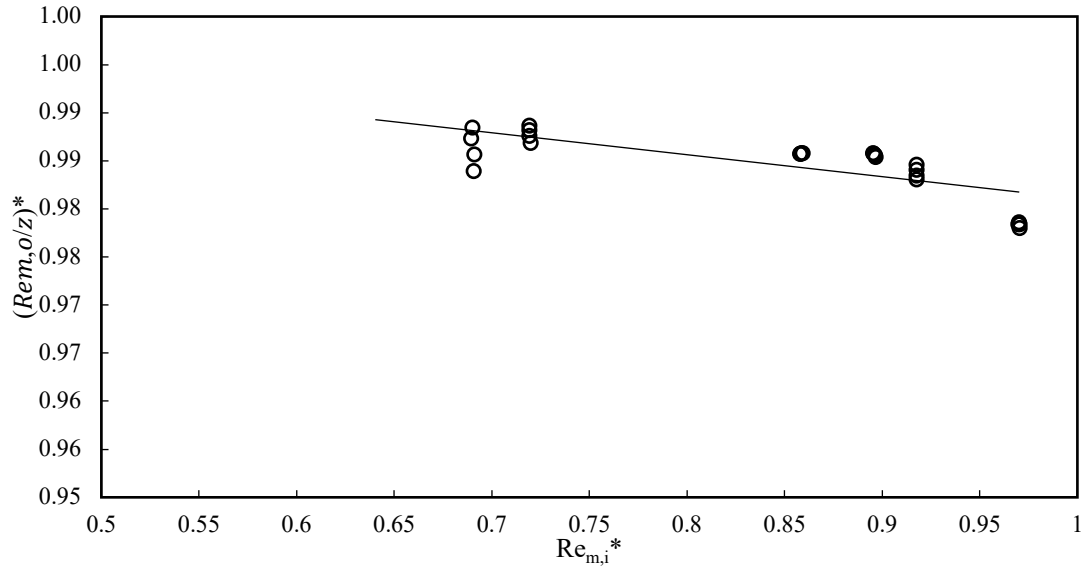

Figure 4.42. First iteration –Reynolds number based on slug mixture flow rate over choke opening (Re_m/Z) versus Reynolds number at pipeline inlet (a = -0.06, b = 2.4, R^2 = 0.6).

In oilfield practice, the flowrate measurements are readily obtained at the subsea wellheads, which define the point of fluid entry into the pipeline section. Again, the coefficients of the dimensionless groups are determined from the gradient of the graph. A curve fit for the plot of $\frac{R_{em,o}}{z^{n_1}}$ vs $R_{em,i}$ provided a slope and R^2 values of 2.4 and 0.6, respectively.

The analysis of the pressure drop in the pipeline section is included by the Bejan number. The effect of the parameters in the earlier steps is included at this stage. The effect of the Bejan number in the pipeline was insignificant so that it was neglected.

A curve fit for the plot of $\frac{R_{em,o}{}^{*}}{z^{n_1} R_{e\,m,i}^{n_2}}$ vs $B_{e,p}{}^{*}$ is obtained for the relationship as given in Table 4.8. The obtained value of R^2 is very small, thereby indicating a weak correlation. Therefore, $n_3 = 0$.

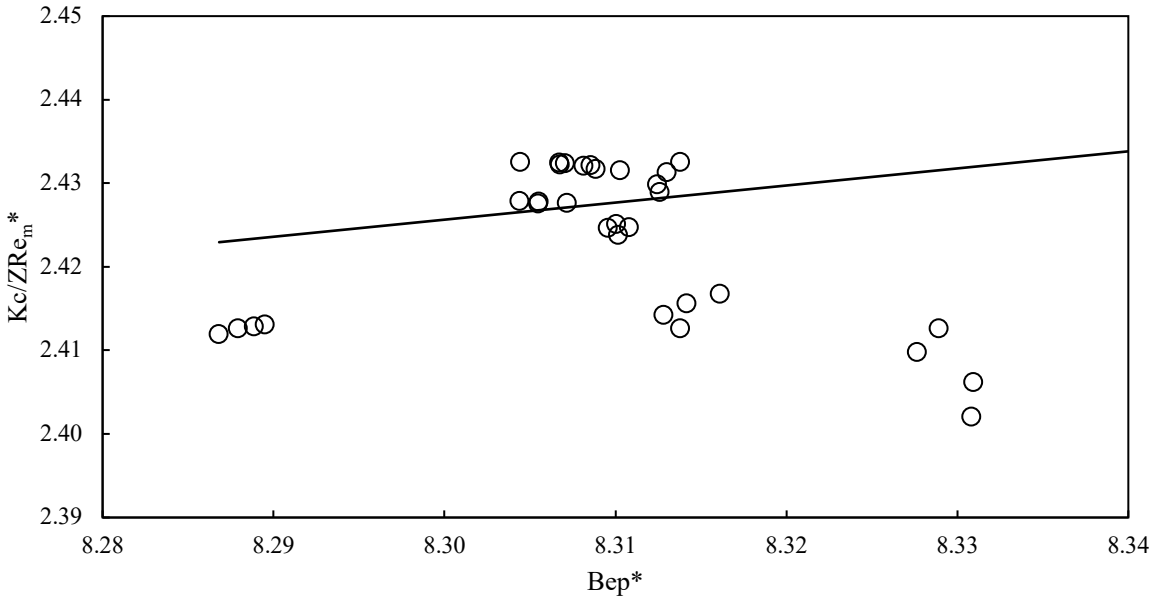

Figure 4.43. Combined dimensionless group ($Kc/Z\ Re_m$) versus Bejan number in the pipeline (a = -0.125, b = 1.3, $R^2 = 0.0118$).

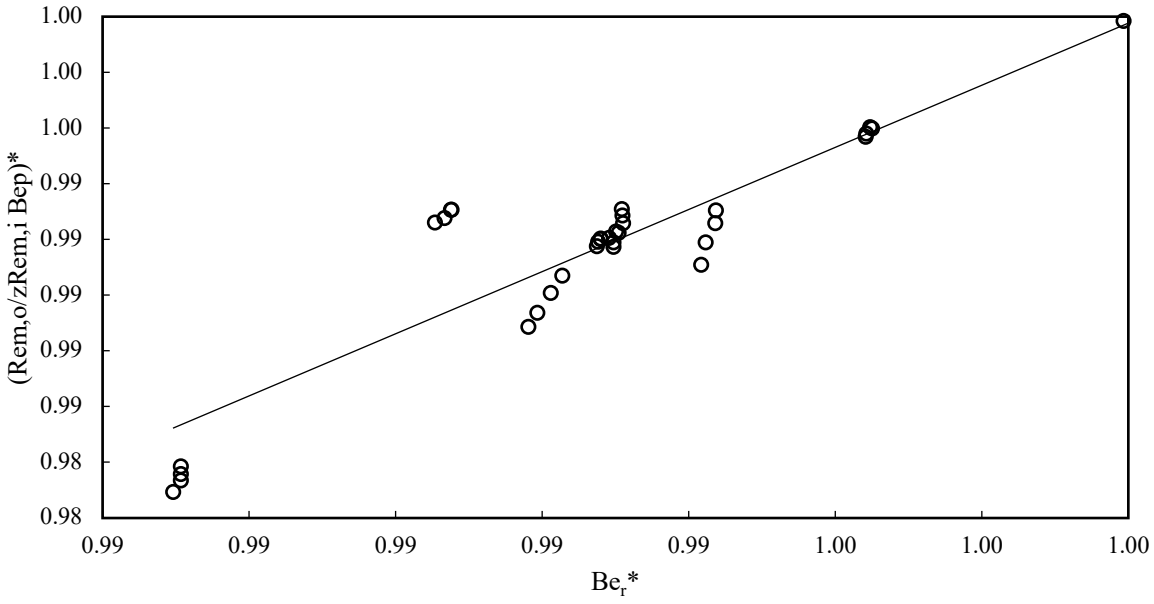

Figure 4.44. First iteration – Combined dimensionless group versus Bejan number in the riser (a = 0.25, b = -0.029, $R^2 = 0.455$).

For the pressure drop in the riser, the maximum Bejan number is used. It is calculated based on the pressure difference between the riser base and the downstream separator. Again, the previous parameters are included. A curve fit for the plot of $\frac{R_{em,o}{}^{*}}{z^{n_1} R_{e\,m,i}^{n_2} B_{emp}}$ vs $B_{e,r}{}^{*}$ led to an R^2 value of 0.455.

In the final step, $\frac{R_{em,o}{}^{*}}{z^{n_1} R_{e\,m,i}^{n_2} B_{emp}\, B_{e,r}{}^{*}}$ is plotted against the density ratio, $\left(\frac{\rho_g}{\rho_l}\right)$. A curve fit gave an R^2 value of 0.003.

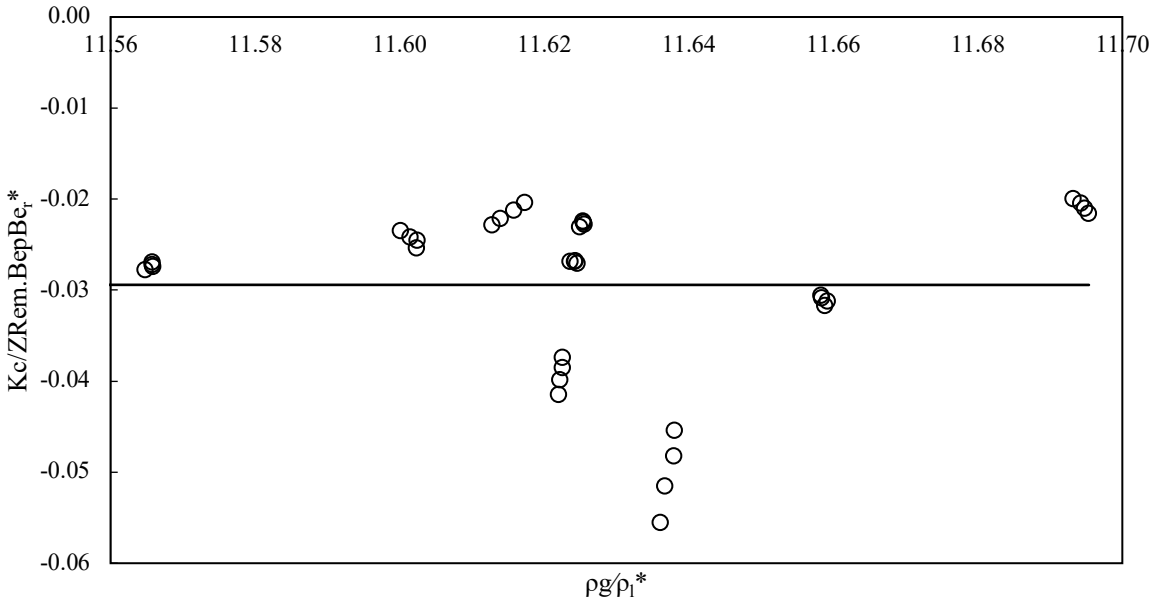

Figure 4.45. Combined dimensionless group versus density ratio ($a = -7\times10^{-5}$, $b = -0.029$, $R^2 = 0.6\times10^{-7}$).

.

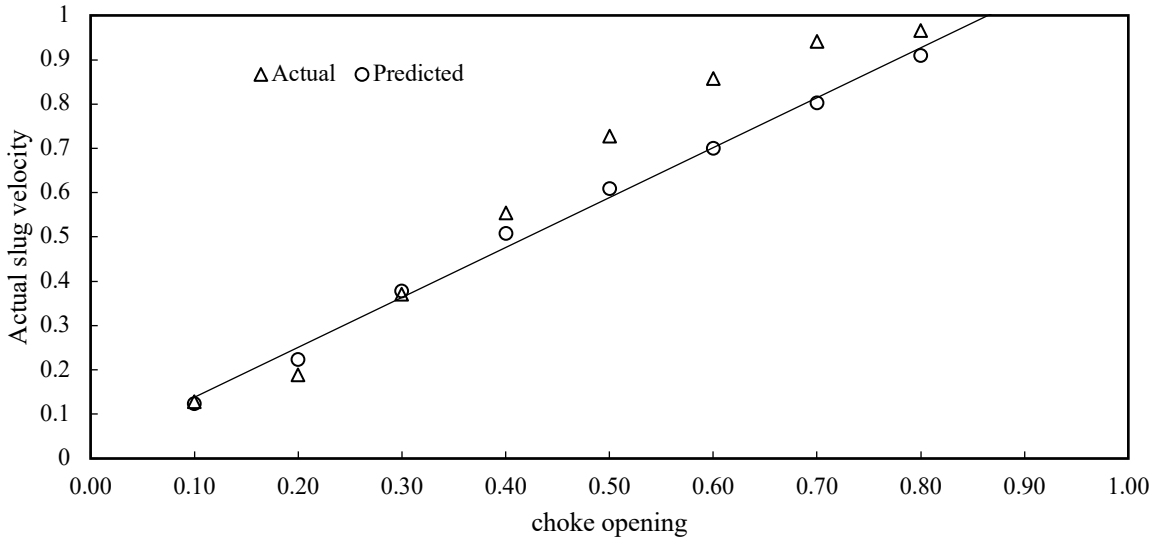

Figure 4.46. Correlation comparison.

A summary of the coefficient obtained from the curve fit for the first iterations is presented in Table 4.9.

Table 4.9. Correlation coefficients for the first iteration.

Dimensionless group	**R^2**	**a**	**B**
$R_{em,o}{}^{*}$ vs Z	0.486	-0.076	2.320
$\frac{R_{em,o}{}^{*}}{Z^{n_1}}$ vs $R_{em,i}$	0.601	-0.061	2.426
$\frac{R_{em,o}{}^{*}}{z^{n_1}R_{em,i}{}^{n_2}}$ vs $B_{e,p}$	0.012	-0.125	1.386
$\frac{R_{em,o}{}^{*}}{z^{n_1}R_{em,i}{}^{n_2}B_{e,p}{}^{n_3}}$ vs $B_{e,r}$	0.455	0.250	-0.029
$\frac{R_{em,o}{}^{*}}{z^{n_1}R_{em,i}{}^{n_2}B_{e,p}{}^{n_3}}$ vs ρ_g/ρ_L	0.003	0.035	0.235

The second phase of the data analysis is conducted to improve the empirical parameters for the model. Figure 4.46 depicts the match obtained for the preliminary correlation after the first iteration, which is compared with the choke openings of the experiment. Further iterations are performed on the preliminary model to obtain more accurate coefficients. The first step of the second iteration involves a sensitivity study on the percentage choke opening. The general correlation, which combines the other dimensionless groups with their coefficients is utilized to conduct the sensitivity analysis.

The general form of the equation relating the flow velocity to the opening of the choke valve is linear and given by: $y = b + ax$. Therefore, the plot is shown as $\log(R_{em,o})$ vs $\log(Z)$.

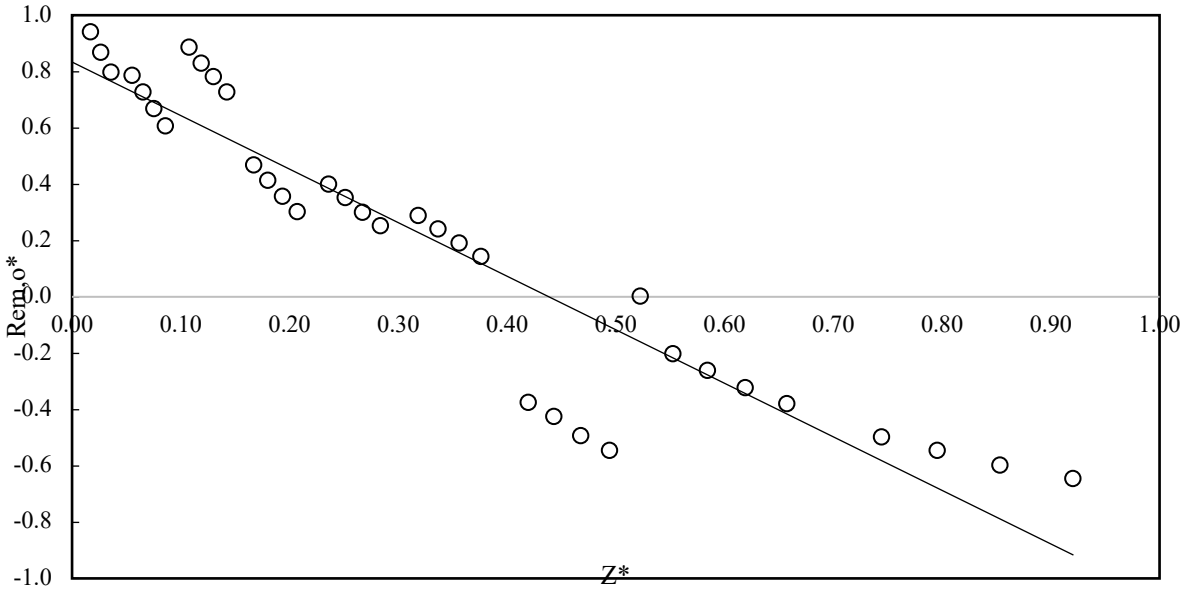

Figure 4.47. Combined dimensionless group versus choke opening (a = -0.076, b = 2.32, $R^2 = 0.486$)

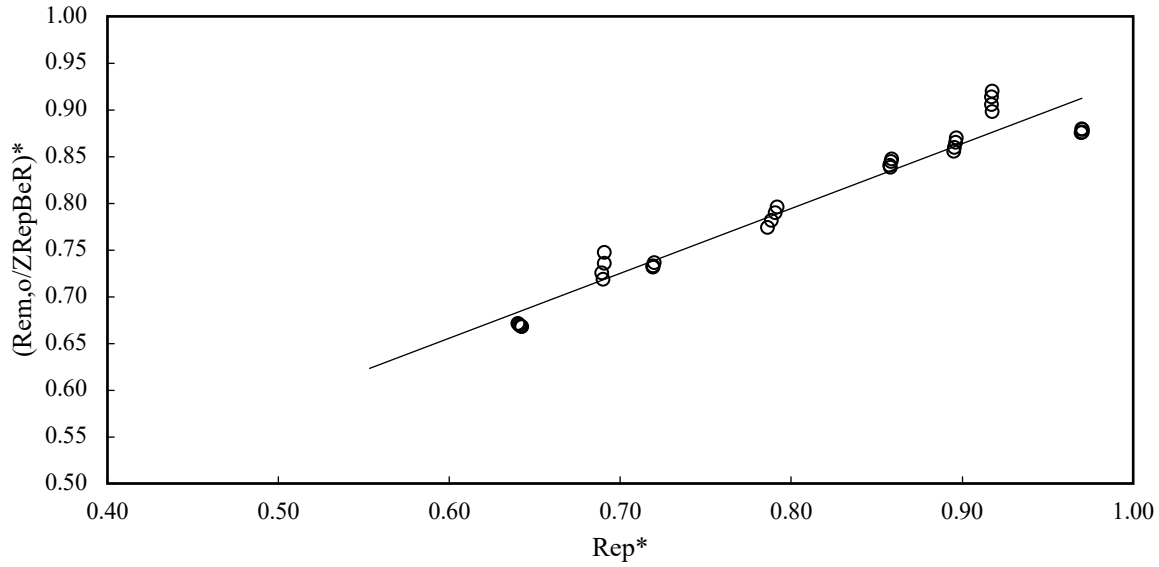

Figure 4.48. Combined dimensionless group versus Reynolds number in the pipeline (a = -0.056, b = -0.027, $R^2 = 0.933$).

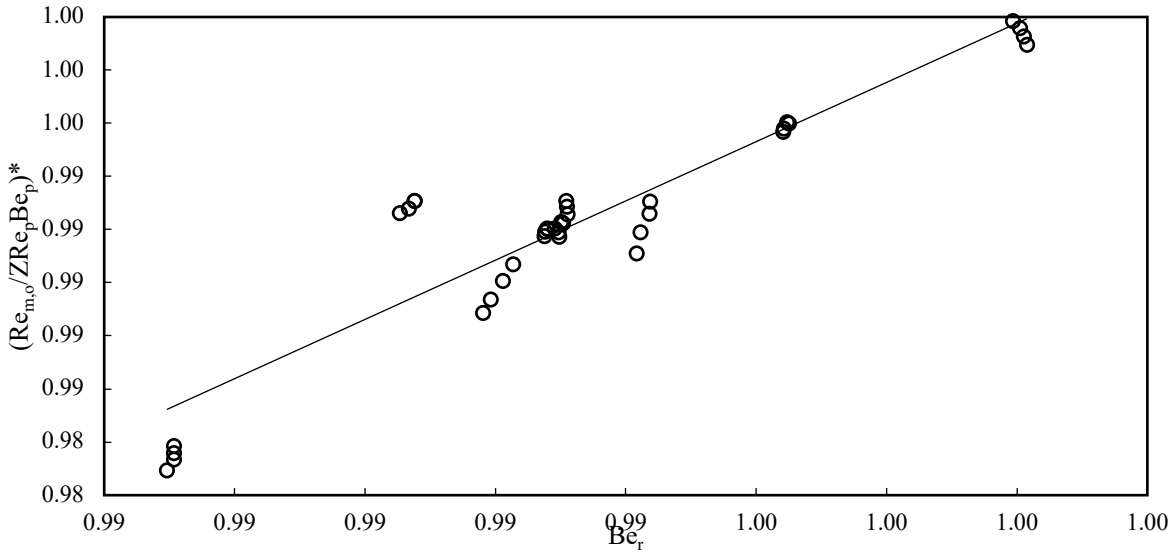

Figure 4.49. Combined dimensionless group against Bejan number in the riser (a = 0.275, b = -0.28, $R^2 = 0.865$).

Equations (3.138) to (3.143) show the sensitivity analysis conducted for each dimensionless group, which was compared with the individual π_i groups in the final correlation.

The sensitivity analysis shows that the flow velocity and the pipeline diameter considerably affect the production of slugs at the choke outlet (see Figure 4.48). Plotting the preliminary correlation versus the Reynolds number in the pipeline leads to a straight line with a regression coefficient of 0.93. Similarly, the pressure drop in the riser influences the final slug velocity correlation, as demonstrated in Figure 4.49 so that the R-squared value is equal to 0.86. Essentially, high inflow rates will propagate higher velocity slugs in shorter time intervals, though the slug size may be relatively small.

Following the improvement of the model fitness through several iterations, the resulting final correlation was obtained as: $R_{em,o}{}^{*} = 0.528 \times z^{-0.0431} R_{em,i}{}^{-0.056} B_{e,r}{}^{0.276}$, as presented by Equation (3.144). After the calculated slug velocity is compared with the experimental data, the general form of correlation is: $y = ax + b$, where a is a coefficient. The slope (a) is the index of a given dimensionless group (n_k) value in the correlation. The slope, intercept and the R^2 value of each step as well as the general form of the correlations are provided in Tables 4.8 and 4.9 for the first and second iterations, respectively.

Equation (3.143) has a very small R^2 value, showing that there is little or no correlation between the combined terms and the density ratio. Thus, the density ratio was neglected in the preliminary correlation.

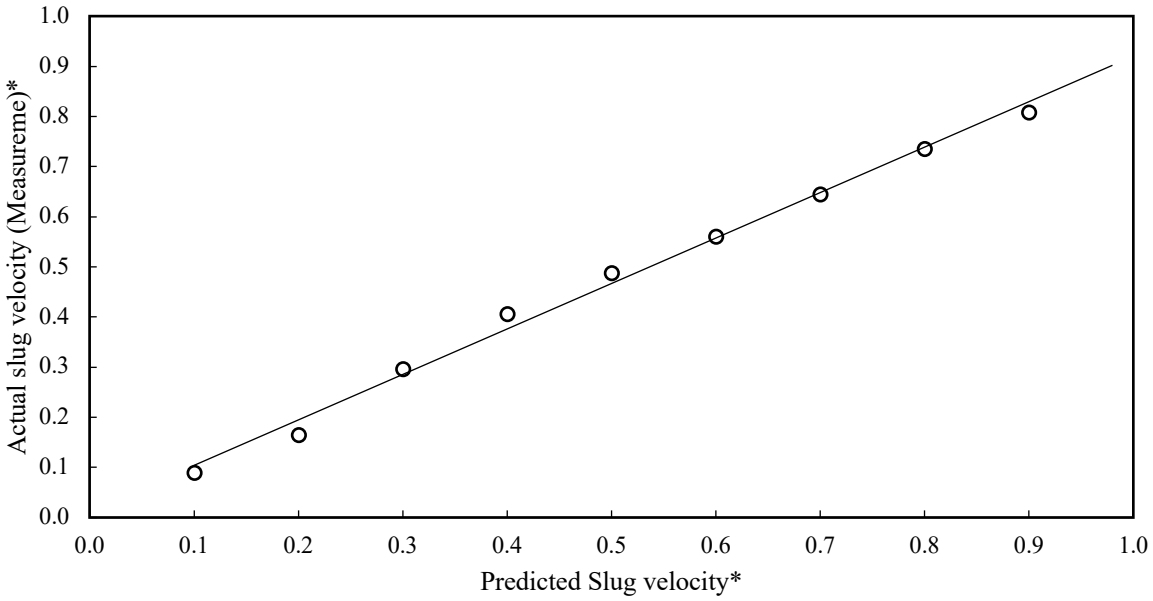

Figure 4.50. A comparison of the actual slug flow velocity measurements and the predictions calculated from the new model (a = 0.995, b = 0, R^2 = 0.766).

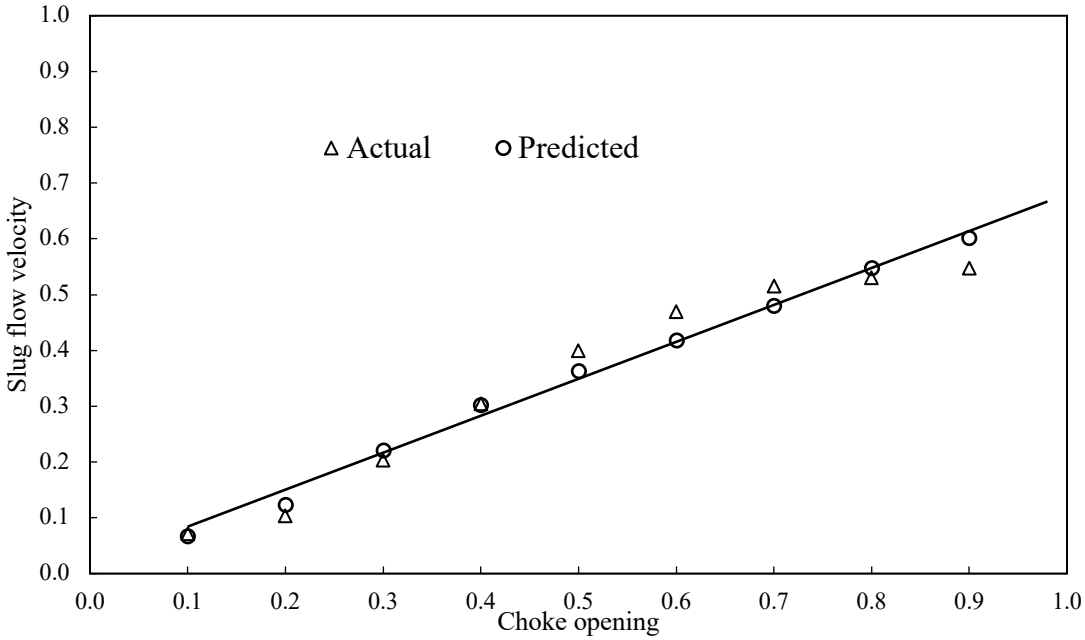

Figure 4.51. Comparison of the slug flow velocity obtained from the new correlation and the velocity measurements (a = 0.6, b = 0.6, R^2 = 0.87).

The empirical parameters are ($n_1 = -0.076,\ n_2 = -0.061,\ n_3 = 0,\ n_4 = 0.02497,\ n_5 = 0,\ n_6 = 0$). From the first iteration, the approximate coefficients were obtained. The second iteration steps involved a sensitivity analysis on each dimensionless group with the other dimensionless groups and coefficients. The final correlation was compared to experimental data of flow velocity measurements as given in figure 4.50. The results obtained from the final correlation were also compared to the experimental data at typical choke opening sizes in oil and gas production systems (see Figure 4.51). It was found that the correlation predicts the slug flow velocity with reasonable accuracy for the various choke sizes. The new correlation performs best for choke openings between 10% and 45%.

The second iteration determined the impact of the various dimensionless groups individually on the overall π group combinations, since each of the π group's sensitivity analysis is carried out while the other dimensionless numbers are present. Hence, the order in which the π groups are combined does not affect the results of the final empirical model. Equation (3.144) is the two-phase correlation for predicting the production rate in a slugging offshore pipeline-riser system. The rate term can be derived from the Reynolds number expressed as $w_m = \frac{R_{em,U_m,D}}{\rho_m}$, where w_m is the mixture flow rate and D is the pipeline diameter. In a practical offshore application where velocity measurements are not available, flowrate data obtained at the wellhead can readily be substituted into Equation 3.93 to determine the slug flow velocity.

Table 4.10. Correlation coefficients and gradient for the second iteration.

Dimensionless group	**R^2**	**a**	**b**
$\frac{R_{em,o}{}^*}{0.934 R_{em,i}{}^{-0.061} B_{e,r}{}^{0.249}}$ vs z	0.8823	-0.0188	-0.0431
$\frac{R_{em,o}{}^*}{0.934 z^{-0.076} B_{e,r}{}^{0.249}}$ vs $R_{em,i}$	0.9326	-0.0274	-0.0561
$\frac{R_{em,o}{}^*}{0.934 z^{-0.076} R_{em,i}{}^{-0.061} B_{e,r}{}^{0.249}}$ vs $B_{e,p}$	0.0382	0.0684	-0.5954
$\frac{R_{em,o}{}^*}{0.934 z^{-0.076} R_{em,i}{}^{-0.061}}$ vs $B_{e,r}$	0.8645	0.2756	-0.2825
Final model prediction $w_{m,model}$ vs $w_{m,actual}$	0.94	0.7	0.018

5 CONCLUSIONS AND RECOMMENDATIONS

Three techniques were examined to control slugging in subsea pipeline-riser installations. New correlations for the design, analysis, and control of slugging in multiphase flows were also developed. Dimensionless correlations were developed to estimate various design parameters in slugging mitigation operations. Results were presented for active choking of the topside valve, gas lifting, and the combined application of gas lifting and topside choking. The major conclusions are summarized as follows.

a) Unlike compact designs with an additional flowline to separate gas upstream, this study shows that an active topside choking can suppress slugs and stabilize the system flowrates and pressures without the requirement of such separation upstream of the topside valve.

   Choking is also appropriate within the compact and footprint constraints of offshore facilities.

b) Choking is shown to be cost-efficient. It stabilizes flow behavior by suppressing riser-induced slugs and effectively controlling the slugs propagated through the horizontal pipelines. This enables better fluid recovery optimization and extends the life of a producing field, particularly in brownfield applications where slugging is predominant.

c) A riser-based, gas-lift method can reduce system instability and increase production. However, sometimes it is not suitable for offshore applications due to cost, space, and weight aspects.

d) This study also shows that no substantial improvement in stability is attained when large volumes of gas are injected, while a lot of energy is consumed. The system shifts into an annular flow regime when the injection is further increased.

e) A large separator/slug facility is required to accommodate a significant gas volume, which further imposes higher demand on the downstream flaring process.

f) This thesis showed that combined gas lifting and choking can yield higher production rates. A coordinated multiple-input and multiple-output (MIMO) control can be the best solution when considered as one solution since choking decreases GVF whereas gas lifting increases GVF.

g) It is also shown that gas lifting and choking can work against each other if not effectively controlled, which is often the case when a decentralized control system is employed. Thus, they are not necessarily the best option in general for a combined control scheme.

h) New non-dimensional correlations, including slug control inputs in offshore installations such as choke openings, are developed based on new experimental data

New slug control models for simulating catenary riser systems were developed to address the challenges of riser geometry and the ability to handle flow variations. The thesis also developed new models that predicted phenomena of slugging behavior. The predictive models used curve fitting for control analysis in offshore flow separation.

The governing equations were formulated to capture the physical parameters of slugging characteristics with state equations. The resulting simplified models are suitable for control design and system analysis purposes. The new models also integrated the geometrical features of the riser to accommodate a representative offshore installation configuration,

enabling the relevant system parameters to be calculated locally. The local position of the riser at any point was determined through a transcendental equation, which includes the coordinate system points and the riser angular displacement, thereby increasing the model robustness.

Through systematic experimental tests, the model parameters were validated. The results demonstrated that the model is capable of predicting the slugging phenomenon with good accuracy. Also, the model can stabilize the system flow rates and pressures. The model is a useful tool for control and process optimization studies.

Also, detailed experimental analysis using the Buckingham pi-theorem was carried out in this thesis to investigate the frequency of slugs and slug velocity in a slugging regime dominated by two-phase flows. A unified correlation for slug frequency prediction was developed. From the results, the correlation can effectively simulate the experimental data. It is found that slug frequency is strongly influenced by the system differential pressure and mixture flowrate. The mixture flow rate in the pipeline has a larger impact on the slug frequency, compared to the pressure drop in the riser. However, there is no strong relationship between the pressure drop in the pipeline and slug frequency based on the experimental data and sensitivity analysis conducted on the dimensionless groups. Slugs are essentially formed at the end of the pipeline section where it connects to the bottom of the riser; they are then carried through the vertical section. The frequency of slug formation directly impacts the rate of their production and subsequent dumping at the receiving facility. The new correlation predicts 92.3% of the measurements within ±8% absolute error. The mean absolute deviation of the correlation is about 6.13%. The new correlation

can be applied for choke openings between 10 to 98%. The model is expected to perform well for pipeline systems with a downward inclination followed by an upward riser.

A new correlation for slug velocity estimation was also developed in this thesis. Through the results and analysis, it was demonstrated that the correlation performs well with a large set of experimental data. According to the results, the liquid and gas flow rates in the pipeline influence the velocity of the slug production at the downstream receiving facility. This is evident in the developed correlation where the Reynolds number in the pipeline inlet correlates with the flow slug velocity at the choke outlet. Similarly, the Bejan number correlated with the slug production demonstrates that the pressure drop and diameter of the flow path also have effects on the slug velocity. The dimensionless numbers to develop the relevant correlations clearly showed the dependence of the slug velocity on differential pressures, choke valve opening, and the mixture flowrate. The correlation predicts 90% of the measurements within a 10% maximum percentage error. The mean absolute deviation of the correlation is about 9%.

The model can also be applied to low flow rates typical of flow conditions in subsea pipelines, and choke openings between 10 - 98%. The correlation can predict slug velocity and production rates for vertical and catenary riser systems. The model is expected to result in acceptable performance for the pipeline system with downward inclination followed by an upward riser.

The following recommendations are proposed for further research:

a. The numerical simulations presented in this thesis are based on the mass balance and ideal gas laws assumptions. In high temperature and high pressure (HTHP) environments, it may be interesting to include thermodynamic features to the model

equations. Heat transfer properties could provide vital information on the flow properties and dynamics at elevated temperatures.

b. The model results presented also show a close match for key control variables, such as the pressure at the top of the riser, pressure at the bottom of the riser, and mass flow rate at the choke outlet. A controllability analysis studies may be used to evaluate the variables that would be most suitable for process control (the variable that produces greatest and fastest response).

c. For both the experimental and modelling investigations, a static valve was used. The valve dynamics are crucial for effective control implementation. It may be interesting to add more features to the valve to include more dynamics. The static valve was observed to produce faster bandwidth compared to the flow dynamics. However, in some offshore installations, the opening and closing of the valve can take a longer time.

d. A sensitivity study is also recommended for varied inclination angles to further evaluate the influence of riser inclination on the performance of the empirical parameters.

APPENDICES

The following appendices present the measurement uncertainties of the experimental setup, flow regime maps of the flow experiments and empirical correlations for select slug frequencies. The uncertainty analysis helps to quantify the precision and bias uncertainties of measurements. The experimental results are presented based on stability maps of past studies (Boe, 1981) by plotting the gas and liquid velocities. Some data corresponding to severe intermittence were observed to fall outside the unstable region predicted by these maps, demonstrating that even for simple geometries such as offshore risers, there is no satisfactory stability criterion.

Appendix A: Experimental Uncertainty Analysis

This appendix presents an analysis of experimental uncertainties based on the Kline and McClintock method (1953). The measurement errors in each experiment are classified as bias or precision errors. Bias errors were estimated from the calibration procedures based on curve fitting of calibrated data. The measured and manufacturer prescribed uncertainties are presented in Tables A.1 and A.2. The uncertainties in Table A. 1 include the variables determined from direct sensor measurements, which are largely dependent on the equipment accuracy. The uncertainties for the measurement equipment were obtained from the manufacturer's data sheets of the fixed error estimates for the flow rates, density, temperatures, and pressure sensors utilized for the experiment. While in Table A.2, the calculated uncertainties associated with other quantities, which were obtained by substituting average values of the measurements into the appropriate equations are given. For this analysis, it was necessary to use a large number of measurements. Hence,

observations were taken for at least 400 seconds for each test. Also, data was collected when the system had attained reasonable operating conditions in order to ensure that the observations measured by the transmitters were accurate representations of the process. This was necessary since the transient start-up was characterized by system fluctuations, so observations recorded during the first 108 seconds were neglected.

The procedure for reporting measurement uncertainties for single measurements, such as pressure and flow rate, were previously reported by Adeyinka and Naterer (2005), Kline and McClintock (1953), and Moffat (1988). Errors propagated in an individual measurement can be evaluated separately using sensitivity coefficients which involve the measured variables. The overall uncertainties for a single measurement can be determined by the following propagation equation (Kline and McClintock, 1953):

$$U_{0.95} = \left[\left(B_{x_i}\right)^2 + \left(S_{x_i}\right)^2\right]^{\frac{1}{2}} \tag{A.1}$$

where B is the bias. Since calibration is considered in the measurement, the fixed errors represent the bias, while the random errors due to measurement variations are determined by the precision limit calculations.

The precision errors are estimated from the unsteadiness in the measuring process. These measurement errors are affected by the measurement system and spatial variations in the measured variables. The precision limit of the individual measurement, x_i , which includes the pressures at different locations in the pipeline-riser, flowrates, and mixture density are calculated from the measured data based on the following equation Moffat (1988):

$$S_{x_i} = \frac{t\sigma}{N} \tag{A.2}$$

where S_{x_i} refers to the precision error; t is the confidence coefficient which equals 2 for an experiment within a 95% confidence level; and N is the number of measurement samples. Also, σ represents the standard deviation determined directly from the measured data as follows (Moffat, 1988):

$$\sigma = \left\{\frac{1}{N-1}\sum_{i=1}^{N}(X_i - \bar{X})^2\right\}^{\frac{1}{2}} \tag{A.3}$$

The precision limit of the mean measurement ($\bar{X}$) of the sample, N, used for this analysis is determined by (Kline and McClintock, 1953; Moffat,1988):

$$\bar{S}_{x_i} = \frac{1}{N}\left\{\sum_{i=1}^{N}\frac{X_i - \bar{X}}{N-1}\right\}^{\frac{1}{2}} \tag{A.4}$$

The total uncertainty (B + P) for single measurements such as $T, P_s, P_p, P_{in}, \ w_l, w_g$, and w_{mix} is obtained from the method of (Kline and McClintock, 1953):

$$\psi_{0.95} = \left\{\left(B_{x_i}\right)^2 + \left(2\sigma S_{x_i}\right)^2\right\}^{\frac{1}{2}} \tag{A.5}$$

Typical values of the standard deviation are estimated for the production rate, pipeline pressure, pressure at the bottom of the riser, and pressure at the top of the riser as 14.3%, 0.04%, 9%, and 0.4% respectively. The values gave precision limits of 0.4%, 0.002%, and 0.02% respectively.

The total uncertainty (B+S) of the pressure measurements along the pipeline-riser setup is calculated as follows (Moffat, 1988):

$$\psi_{P_i} = \sqrt{S_{P_i}^2 \pm B_{P_i}^2} \tag{A.6}$$

The total uncertainty of the flow rates and temperature are calculated in the same manner by replacing the pressure components with flow rates and temperatures, respectively. The pressures, temperatures, and the flowrates then become:

$$P_i = \overline{P_i} \pm \psi_{P_i} \tag{A.7}$$

$$T_i = \overline{T_i} \pm \psi_{T_i} \tag{A.8}$$

$$w_i = \overline{w_i} \pm \psi_{w_i} \tag{A.9}$$

Here, i is used to denote the position in which the measurements were taken, such as the top of the riser and the bottom. The mean variables $\overline{P_i}$, $\overline{T_i}$, and $\overline{w_i}$ are determined as follows:

$$\bar{X}_i = \frac{1}{N}\sum_{i=1}^{N} X_k \tag{A.10}$$

According to the method of Kline and McClintock (1953), when several variables are involved, the resultant uncertainty can be expressed as follows:

$$R = f\,(x_1, x_2, x_3., x_4 \ldots x_n), \tag{A.11}$$

The component terms can be combined using the root-sum-squared method as follows:

$$dR^2 = \left(\frac{\partial R}{\partial x_1}x_1\right)^2 + \left(\frac{\partial R}{\partial x_2}x_2\right)^2 + \left(\frac{\partial R}{\partial x_3}x_3\right)^2 + \left(\frac{\partial R}{\partial x_4}x_4\right)^2 \ldots + \left(\frac{\partial R}{\partial x_n}x_n\right)^2 \tag{A.12}$$

Gas volume fraction (GVF). The mass flow rates of gas and liquid phases are measured rather than their volumes. Hence, the gas volume fraction is expressed in terms of the mass flow rate as follows:

$$GVF = \frac{w_g}{w_t} \tag{A.13}$$

where w_t equals $w_g + w_l$. It is known that the gas volume fraction is a function of the gas flow rate, and the total flow rate. Thus, the uncertainty, ψ, in the gas volume fraction is calculated by the following expressions:

$$B_{GVF} = \left[\left(\frac{\partial GVF}{\partial w_g} B_g\right)^2 + \left(\frac{\partial GVF}{\partial w_t} B_{w_t}\right)^2\right]^{\frac{1}{2}} \tag{A.14}$$

$$S_{GVF} = \left[\left(\frac{\partial GVF}{\partial w_g} S_{w_g}\right)^2 + \left(\frac{\partial GVF}{\partial w_t} S_{w_t}\right)^2\right]^{\frac{1}{2}} \tag{A.15}$$

The uncertainty of the GVF is written in terms of a percentage by dividing the entire function by the gas volume fraction as follows:

$$B_{GVF} = \left[\left(\frac{1}{w_g} B_{w_g}\right)^2 + \left(\frac{1}{w_t} B_{w_t}\right)^2\right]^{\frac{1}{2}} \tag{A.16}$$

$$S_{GVF} = \left[\left(\frac{1}{w_g} S_{w_g}\right)^2 + \left(\frac{1}{w_t} S_{w_t}\right)^2\right]^{\frac{1}{2}} \tag{A.18}$$

The total uncertainty for the gas volume fraction becomes:

$$\psi_{GVF} = \left[\left(\frac{\partial GVF}{\partial w_g} B_g\right)^2 + \left(\frac{\partial GVF}{\partial w_t} B_{w_t}\right)^2 + \left(\frac{\partial GVF}{\partial w_g} S_g\right)^2 + \left(\frac{\partial GVF}{\partial w_t} S_{w_t}\right)^2\right]^{\frac{1}{2}} \tag{A.19}$$

or

$$\psi_{GVF} = \left[\left(\frac{1}{w_g} B_g\right)^2 + \left(\frac{1}{w_t} B_{w_t}\right)^2 + \left(\frac{1}{w_g} S_g\right)^2 + \left(\frac{1}{w_t} S_{w_t}\right)^2\right]^{\frac{1}{2}} \tag{A.20}$$

By substituting the corresponding values, the experimental uncertainty for the GVF is obtained. Table 6 shows the summarized estimates of the measured variables and their associated uncertainties.

Mixture velocity. The mixture velocity is calculated from the liquid and gas velocities, as determined from their respective flow rate as follows:

$$U_m = \frac{w_l + w_g}{\rho_m \pi D^2/4} \tag{A.21}$$

It can be seen that the mixture density is a function of the mass flow rate of the liquid, mass flow rate of gas, mixture density, and the internal diameter of the pipe. The uncertainty associated with the mixture velocity is calculated from the following relationships:

$$B_{U_m} = \left[\left(\frac{\partial U_m}{\partial w_l} B_{w_l}\right)^2 + \left(\frac{\partial U_m}{\partial w_g} B_{w_g}\right)^2 + \left(\frac{\partial U_m}{\partial \rho_m} B_{\rho_m}\right)^2 + \left(\frac{\partial U_m}{\partial D} B_D\right)^2\right]^{\frac{1}{2}} \quad \text{(A.22)}$$

$$S_{U_m} = \left[\left(\frac{\partial U_m}{\partial w_l} S_{w_l}\right)^2 + \left(\frac{\partial U_m}{\partial w_g} S_{w_g}\right)^2 + \left(\frac{\partial U_m}{\partial \rho_m} S_{\rho_m}\right)^2 + \left(\frac{\partial U_m}{\partial D} S_D\right)^2\right]^{\frac{1}{2}} \quad \text{(A.23)}$$

The entire function can be expressed in terms of a percentage error as follows:

$$\frac{B_{U_m}}{U_m} = \left[\left(\frac{1}{w_l} B_{w_l}\right)^2 + \left(\frac{1}{w_g} B_{w_g}\right)^2 + \left(\frac{1}{\rho_m} B_{\rho_m}\right)^2 + \left(\frac{2}{D} B_D\right)^2\right]^{\frac{1}{2}} \quad \text{(A.24)}$$

$$\frac{S_{U_m}}{U_m} = \left[\left(\frac{1}{w_l} S_{w_l}\right)^2 + \left(\frac{1}{w_g} S_{w_g}\right)^2 + \left(\frac{1}{\partial \rho_m} S_{\rho_m}\right)^2 + \left(\frac{2}{D} S_D\right)^2\right]^{\frac{1}{2}} \quad \text{(A.25)}$$

The associated uncertainty is given below:

$$\psi_{U_m} = \left[\left(\frac{1}{w_l} B_{w_l}\right)^2 + \left(\frac{1}{w_g} B_{w_g}\right)^2 + \left(\frac{1}{\rho_m} B_{\rho_m}\right)^2 + \left(\frac{2}{D} B_D\right)^2 + \left(\frac{1}{w_l} S_{w_l}\right)^2 + \left(\frac{1}{w_g} S_{w_g}\right)^2 + \left(\frac{1}{\partial \rho_m} S_{\rho_m}\right)^2 + \left(\frac{2}{D} S_D\right)^2\right]^{\frac{1}{2}} \quad \text{(A.26)}$$

The uncertainties of ρ_m and ρ_g are determined in the same manner. The final precision errors, bias, and associated uncertainties are provided in Table A.1.

The calculated uncertainties associated with the liquid and gas flow rates, and top and bottom pressures, are shown in Table A.2. When the appropriate values are substituted in the uncertainty equations for the variables, it was found that the uncertainties of the liquid pipeline pressure, and pressures at the top and bottom, remained relatively constant at

±0.01, or between ±1.78% of the liquid flow rate value; ±5.56 x 10^{-4} or ±8.34% of the gas flow rate value; ±0.01 or ±0.63% of the pipeline pressure value; ±0.01 or ±0.85% of the pressure at the top of the riser value, and ±0.01 or ±1.08% of the pressure at the bottom of the riser value.

The largest uncertainties are associated with the gas volume fraction measurements and may be attributed to the slugging behavior.

Table A.1. Bias, precision, and total uncertainties associated with experiments.

Variable	**Averaged value, $\bar{X}$**	**Bias (±)**	**Precision (±)**	**Uncertainty, $\psi_{0.95}$ (±)**	**Uncertainty (% value)**
w_l(kg/s)	0.607	5.56×10^{-4}	0.011	0.0108	1.779
w_g(kg/s)	$6.82\text{x}10^{-4}$	5.56×10^{-5}	1.20×10^{-5}	5.69×10^{-5}	8.34
P_{in}(bar)	1.761	0.01	2.37×10^{-3}	0.011	0.625
P_p(bar)	1.172	0.01	4.79×10^{-4}	0.010	0.853
P_b(bar)	1.707	0.01	3.01×10^{-3}	0.011	0.609
P_{top}(bar)	0.925	0.01	1.6×10^{-4}	0.010	1.081
P_s(bar)	1.03	0.01	3.7×10^{-4}	0.010	0.971
w_{mix}(kg/s)	0.529	5.56×10^{-4}	0.005	0.005	0.907
$T(K)$	293.36	0.01	4.51×10^{-5}	5.41×10^{-5}	1.84×10^{-5}
ρ_{mt} (kg/m^3)	0.866	0.0005	0.004	0.004	0.462

GVF	1.55×10^{-3}		9.35×10^{-4}	9.35×10^{-4}	39.78
ρ_g	2.09	7.27×10^{-5}	1.54×10^{-7}	7.28×10^{-5}	0.004
U_m	0.529	4.75×10^{-4}	9.26×10^{-4}	4.83×10^{-4}	0.091

The gas volume fraction continued to change throughout each test as a result of the various stages in the slugging process, which involved the cyclical gas accumulation, zero gas production, and uncontrolled gas blowout. Further calculations were performed to determine the uncertainties associated with the variables used in the dimensionless analysis. The propagation equation of (Kline and McClintock, 1953) is used as follows:

$$\mathrm{R} = \mathrm{f}\left(\mathrm{x}_1, \mathrm{x}_2, \mathrm{x}_3., \mathrm{x}_4 \ldots \mathrm{x}_\mathrm{n}\right), \tag{A.27}$$

The component terms can be combined using the root-sum-squared method as follows:

$$\mathrm{dR}^2 = \left(\frac{\partial \mathrm{R}}{\partial \mathrm{x}_1}\mathrm{x}_1\right)^2 + \left(\frac{\partial \mathrm{R}}{\partial \mathrm{x}_2}\mathrm{x}_2\right)^2 + \left(\frac{\partial \mathrm{R}}{\partial \mathrm{x}_3}\mathrm{x}_3\right)^2 + \left(\frac{\partial \mathrm{R}}{\partial \mathrm{x}_4}\mathrm{x}_4\right)^2 \ldots + \left(\frac{\partial \mathrm{R}}{\partial \mathrm{x}_\mathrm{n}}\mathrm{x}_\mathrm{n}\right)^2 \tag{A.28}$$

Reynolds number. The Reynolds number was primarily used as the basis for evaluating the multiphase flow velocity measurements in the pipeline-riser experimental set-up. The mixture Reynolds number is defined as follows:

$$\mathrm{R}_{\mathrm{em}} = \frac{\rho_\mathrm{m}\, \mathrm{v}_\mathrm{m}\, \mathrm{D}}{\mu_\mathrm{m}} \tag{A.29}$$

where v_m represents the mixture velocity. Based on Equation (A.30), it is necessary to develop the uncertainty for the mixture velocity. The mixture velocity is calculated from the liquid and gas velocities, as determined from their corresponding flow rate as follows:

$$\mathrm{v}_\mathrm{m} = \frac{\mathrm{w}_\mathrm{l} + \mathrm{w}_\mathrm{g}}{\rho_\mathrm{m} \pi \mathrm{D}^2/4} \tag{A.30}$$

The mixture velocity is a function of the mass flow rate of the liquid and gas, mixture density, and pipe internal diameter. The bias and precision limits associated with the mixture velocity are calculated from the following relationships (Moffat, 1988):

$$B_{v_m}{}^2 = \xi_{w_l}{}^2 B_{w_l}{}^2 + \xi_{w_g}{}^2 B_{w_g}{}^2 + \xi_{\rho_m}{}^2 B_{\rho_m}{}^2 + \xi_D{}^2 B_D{}^2 \quad \text{(A.31)}$$

$$S_{v_m}{}^2 = \beta_{w_l}{}^2 S_{w_l}{}^2 + \beta_{w_g}{}^2 S_{w_g}{}^2 + \beta_{\rho_m}{}^2 S_{\rho_m}{}^2 + \beta_D{}^2 S_D{}^2 \quad \text{(A.32)}$$

where ξ and β are the sensitivity coefficients for the bias and the precision limits and defined as $\xi = \frac{\partial v_m}{\partial \chi}$ and $\beta = \frac{\partial v_m}{\partial \chi}$, respectively. The term χ is used to denote the variables.

By combining the contributions of the various sources of uncertainties, the mixture velocity bias and the precision errors are estimated at 0.048% and 0.098%, respectively.

The bias and precision errors associated with the Reynolds number calculation are determined by the following equations:

$$B_{R_{em}}{}^2 = \left(\frac{\partial R_{em}}{\partial \rho_m}\right)^2 B_{\rho_m}{}^2 + \left(\frac{\partial R_{em}}{\partial \rho_m}\right)^2 B_{v_m}{}^2 + \left(\frac{\partial R_{em}}{\partial v_m}\right)^2 B_{v_m}{}^2 + \left(\frac{\partial R_{em}}{\partial D}\right)^2 B_D{}^2 + \left(\frac{\partial R_{em}}{\partial \mu_m}\right)^2 B_{\mu_m}{}^2 \quad \text{(A.33)}$$

$$S_{R_{em}}{}^2 = \left(\frac{\partial R_{em}}{\partial \rho_m}\right)^2 S_{\rho_m}{}^2 + \left(\frac{\partial R_{em}}{\partial \rho_m}\right)^2 S_{v_m}{}^2 + \left(\frac{\partial R_{em}}{\partial v_m}\right)^2 S_{v_m}{}^2 + \left(\frac{\partial R_{em}}{\partial D}\right)^2 S_D{}^2 + \left(\frac{\partial R_{em}}{\partial \mu_m}\right)^2 S_{\mu_m}{}^2 \quad \text{(A.34)}$$

$$\psi_{R_{em}} = \pm\sqrt{B_{R_{em}}{}^2 + S_{R_{em}}{}^2} \quad \text{(A.35)}$$

By substituting the corresponding values, the experimental uncertainty for the mixture and the Reynolds number is obtained. Table A.2 shows a summary of the measured variables and their associated uncertainties.

Bejan number. The Bejan number was primarily used for evaluating the pressure drops in the pipeline and the riser sections. In order to simplify calculations and present results, the uncertainty analysis is performed by utilizing the maximum pressure drop due to the liquid phase in the pipeline-riser system. The Bejan number is defined as follows:

$$B_e = \frac{\Delta P L^2}{\mu_L \alpha_L} \tag{A.36}$$

The system pressure drop is $\Delta P = P_{in} - P_s$; and P_{in} and P_s denote the inlet and separator pressures, respectively. The bias and precision limits associated with the pressure drops were calculated from the following relationships (Moffat, 1988):

$$B_{\Delta P}{}^2 = \xi_{P_{in}}{}^2 B_{P_{in}}{}^2 + \xi_{P_s}{}^2 B_{P_s}{}^2 \tag{A.37}$$

$$S_{\Delta P}{}^2 = \beta_{P_{in}}{}^2 S_{P_{in}}{}^2 + \beta_{P_s}{}^2 S_{P_s}{}^2 \tag{A.38}$$

Similarly, ξ and β are the sensitivity coefficients for the bias and the precision limits and defined as $\xi = \frac{\partial P_{in}}{\partial \chi}$ and $\beta = \frac{\partial P_s}{\partial \chi}$, respectively. The term χ represents the component variables. The ΔP bias and precision errors were estimated at 1.03% and 0.14%, respectively. In a similar manner, the bias and precision of the liquid fraction are estimated. The bias and precision errors associated with the Bejan number calculation are determined as follows:

$$B_{B_e}{}^2 = \left(\frac{\partial B_e}{\partial \Delta P}\right)^2 B_{\Delta P}{}^2 + \left(\frac{\partial B_e}{\partial L}\right)^2 B_L{}^2 + \left(\frac{\partial B_e}{\partial \mu_L}\right)^2 B_{\mu_L}{}^2 + \left(\frac{\partial B_e}{\partial \alpha_L}\right)^2 B_{\alpha_L}{}^2 \tag{A.39}$$

$$S_{B_e}{}^2 = \left(\frac{\partial B_e}{\partial \Delta P}\right)^2 S_{\Delta P}{}^2 + \left(\frac{\partial B_e}{\partial L}\right)^2 S_L{}^2 + \left(\frac{\partial B_e}{\partial \mu_L}\right)^2 S_{\mu_L}{}^2 + \left(\frac{\partial B_e}{\partial \alpha_L}\right)^2 S_{\alpha_L}{}^2 \tag{A.40}$$

$$\psi_{B_e} = \pm\sqrt{B_{B_e}{}^2 + S_{B_e}{}^2} \tag{A.41}$$

By substituting the corresponding values, the experimental uncertainty for the Bejan number is obtained.

Slug frequency. The Koulegan-Carpenter number was used in evaluating the frequency of slugs in the experiments. The slug frequency measurements were conducted at the downstream fluid recovery units. Hence, the mixture flow productions are utilized in calculating the measurement uncertainties. The Koulegan-Carpenter number is defined as follows:

$$Kc = \frac{4w_{mix}}{\rho_m \pi D^3 f_s} \tag{A.42}$$

The bias and precision errors associated with the Kc number calculation are given below:

$$B_{Kc}{}^2 = \left(\frac{\partial B_e}{\partial w_{mix}}\right)^2 B_{w_{mix}}{}^2 + \left(\frac{\partial B_e}{\partial L}\right)^2 B_{\rho_m}{}^2 + \left(\frac{\partial B_e}{\partial D}\right)^2 B_D{}^2 + \left(\frac{\partial B_e}{\partial f_s}\right)^2 B_{f_s}{}^2 \tag{A.43}$$

$$S_{Kc}{}^2 = \left(\frac{\partial B_e}{\partial w_{mix}}\right)^2 S_{w_{mix}}{}^2 + \left(\frac{\partial B_e}{\partial \rho_m}\right)^2 S_{\rho_m}{}^2 + \left(\frac{\partial B_e}{\partial D}\right)^2 S_D{}^2 + \left(\frac{\partial B_e}{\partial f_s}\right)^2 S_{f_s}{}^2 \tag{A.44}$$

or

$$B_{Kc} = \sqrt{\left(\frac{1}{w_{mix}}\right)^2 B_{w_{mix}}{}^2 + \left(\frac{1}{L}\right)^2 B_L{}^2 + \left(\frac{3}{D}\right)^2 B_D{}^2 + \left(\frac{1}{f_s}\right)^2 B_{f_s}{}^2} \tag{A.45}$$

and

$$S_{Kc} = \sqrt{\left(\frac{1}{w_{mix}}\right)^2 S_{w_{mix}}{}^2 + \left(\frac{1}{L}\right)^2 S_L{}^2 + \left(\frac{3}{D}\right)^2 S_D{}^2 + \left(\frac{1}{f_s}\right)^2 S_{f_s}{}^2} \tag{A.46}$$

$$\psi_{Kc} = \pm\sqrt{B_{Kc}{}^2 + S_{Kc}{}^2} \tag{A.47}$$

The uncertainties of the density ratio $\frac{\rho_g}{\rho_L}$and ρ_g are determined through the same method (see Table A.2). In Table A.2, the calculated uncertainties associated with the liquid and

gas flow rates, and inlet and separator pressures, are provided. When the appropriate values are substituted into the uncertainty equations for the variables, the uncertainties of the slug frequency and the pressure drop became $\pm 1.03\times10^{-2}$ and $\pm 1.04\times10^{-2}$, respectively. The worst-case uncertainties are associated with the Bejan number calculations. These may be ascribed to the variations in the hydrostatic head resulting from the liquid loading and sudden release of the slug to the downstream receiving equipment.

Table A.2. Bias, precision, and total uncertainties associated with the measurements.

Variable	**Mean value, $\bar{X}$**	**Bias error (±)**	**Precision error (±)**	**Uncertainty, $\psi_{0.95}$ (±)**	**Uncertainty (%)**
f_s (1/s)	0.6	1.41E-3	1.02E-2	1.03E-2	1.71
w_{mix}(kg/s)	0.529	5.56e-4	0.005	0.005	0.907
P_{in}(bar)	1.761	0.01	2.37E-3	0.011	0.625
P_b(bar)	1.707	0.01	3.01E-3	0.011	0.609
P_s(bar)	1.03	0.01	3.7E-4	0.010	0.971
R_{em}	187.8	2.17E-3	9.23E-3	9.49E-3	0.005
B_e	0.71	0.015	9.34E-3	0.018	2.53
α_L	0.998	1.53E-3	1.98E-2	1.99E-3	0.199
ΔP	0.62	1.02E-2	1.039E3	1.04E-2	1.68
Kc	0.3	1.49E-3	1.17E-3	2.26E-3	0.75
ρ_{mt} (kg/m^3)	0.866	0.0005	0.004	0.004	0.462
ρ_g	2.09	7.27E-5	1.54E-7	7.28E-5	0.004
U_m (m/s)	0.529	4.75E-4	9.26E-4	4.83E-4	0.091

Appendix B: Slugging Flow Maps

Stability flow maps are used to determine the boundary between stable (non-slugging) and unstable (severe slugging) regions. A choke valve at the riser topside, placed upstream of the separator inlet, was utilized in the experiments. During the tests, the choke valve was manipulated in an open loop manner. The data collected within the first 108 seconds were neglected for analysis since this allows enough time for the system to attain a fully developed slug flow regime. Figures A.34 to A.43 show the flow regime maps corresponding to the Boe (1981) and Jansen (1996) criteria. It is clear that the data points for the analysis fall within the severe slugging region corresponding to Usl=0.01 - 1m/s and $Usl = 0.01 - 1\mathrm{m/s}$. In Figure A.42, a transition can be seen from severe slugging to bubble flow due to the system transition from slugging to non-slugging.

It is worth noting that slug creation is essentially a trial and error procedure. Although slug flows in pipelines are generally characterized by low flow rates of two-phase fluid system, a certain gas - liquid ratio or mixture composition may lead to slugging in a particular pipe geometry. Thus, the same mixture composition may become non-slugging in another flow path configuration. Other factors that affect slugging development include pipe diameter, terrain, and length of pipe. Flow regime maps are mostly preferred procedures for validating the flow behaviours/observations.

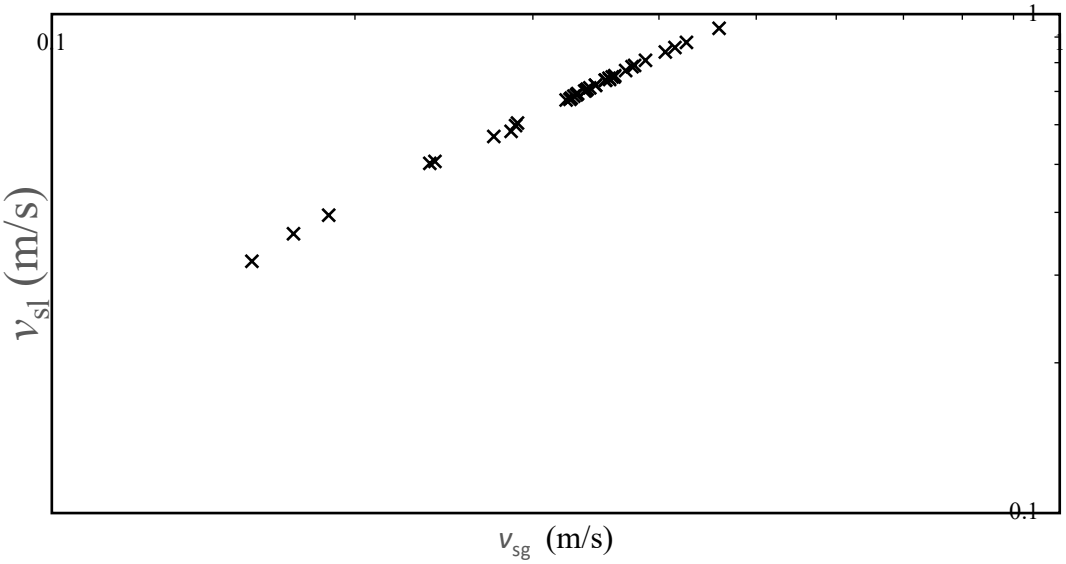

Figure A.1. Liquid superficial velocity versus gas superficial velocity data, showing the slugging regime for 100% choke opening.

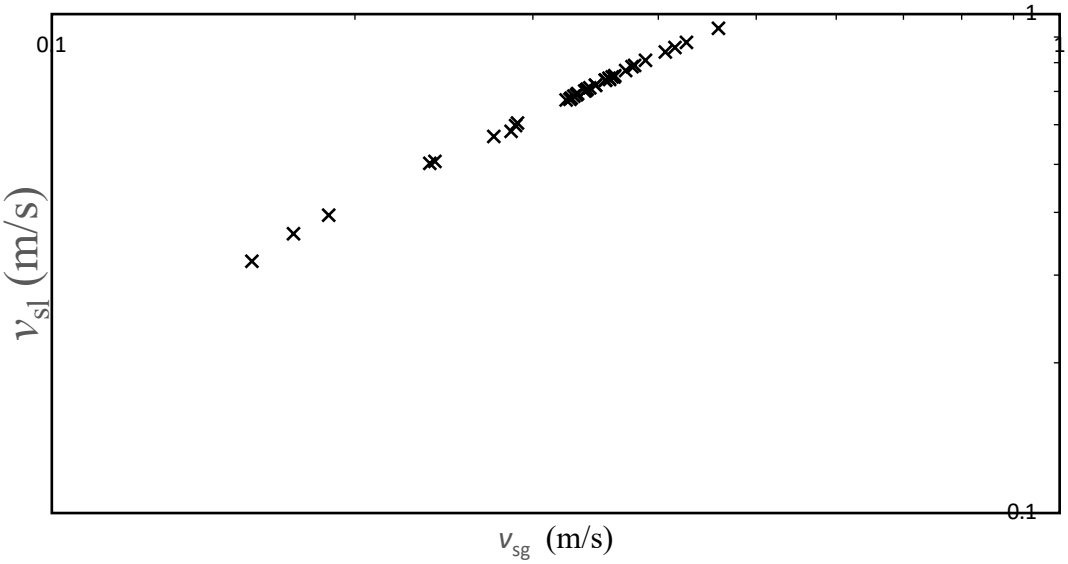

Figure A.2. Liquid superficial velocity versus gas superficial velocity data, showing the slugging regime for 90% choke opening.

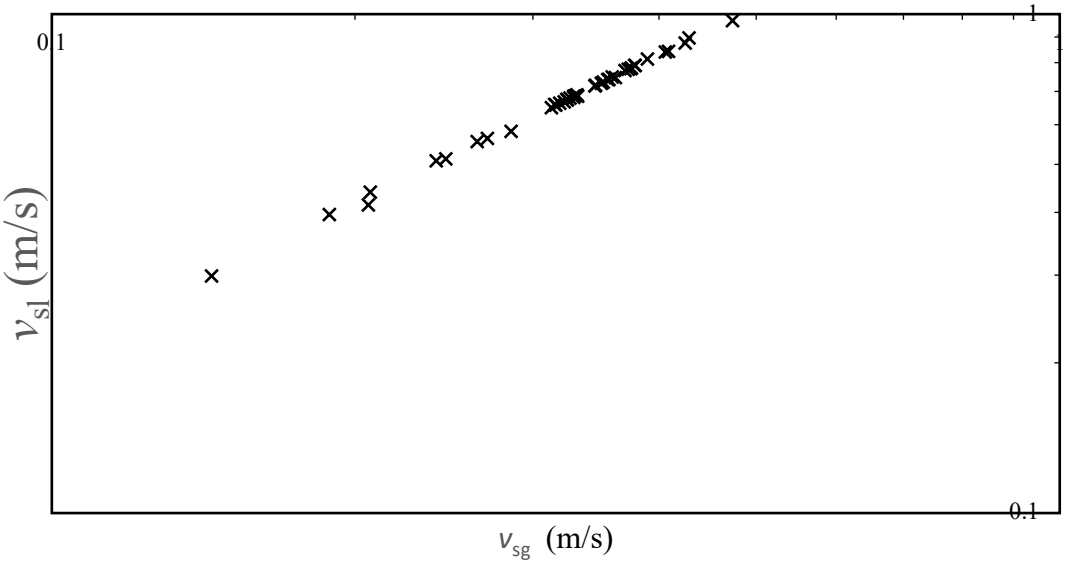

Figure A.3. Liquid superficial velocity versus gas superficial velocity data, showing the slugging regime for 80% choke opening.

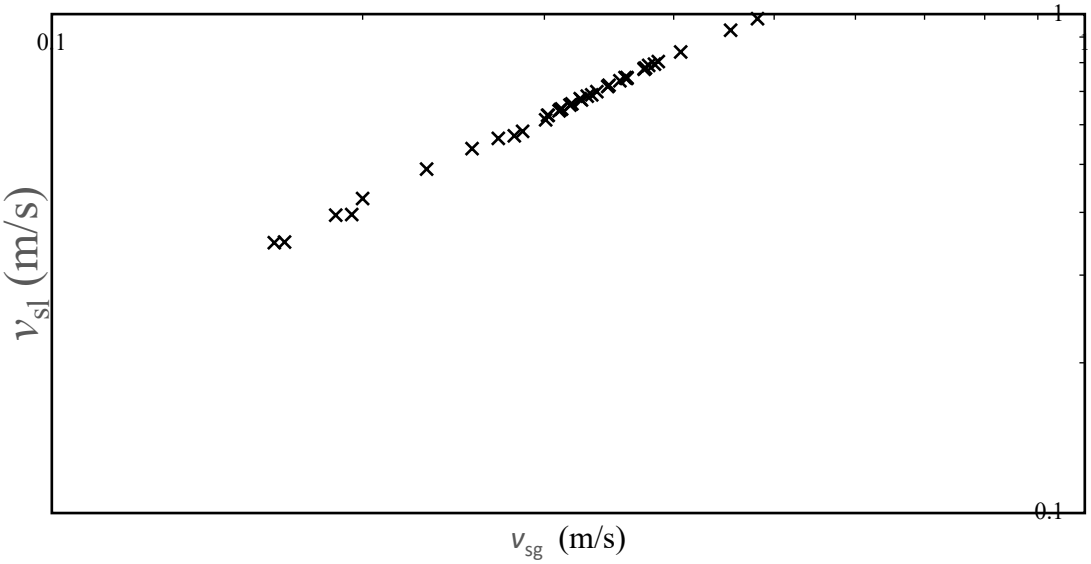

Figure A.4. Liquid superficial velocity versus gas superficial velocity data, showing the slugging regime for 70% choke opening.

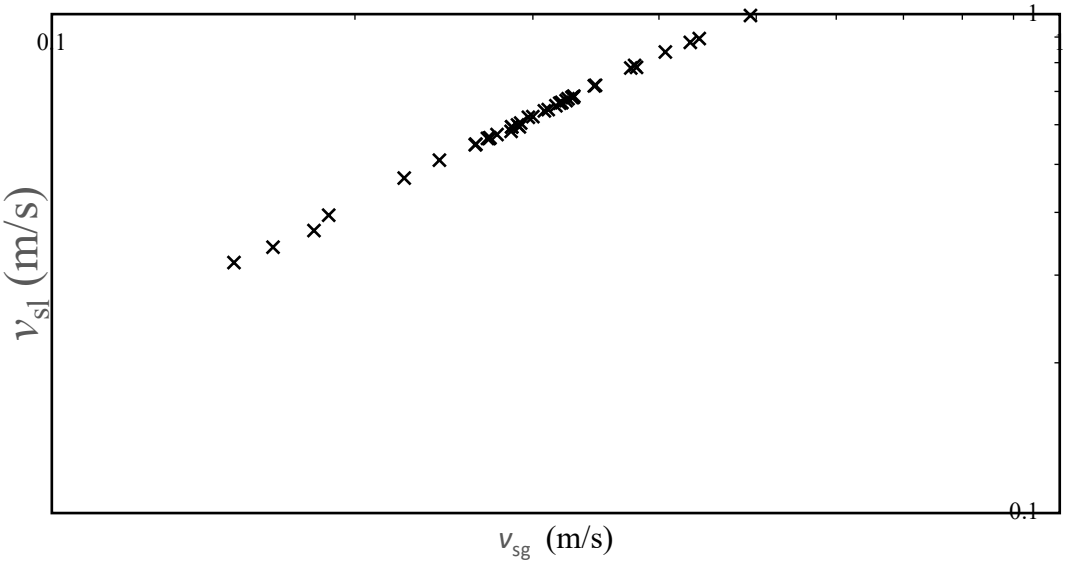

Figure A.5. Liquid superficial velocity versus gas superficial velocity data, showing the slugging regime for 60% choke opening.

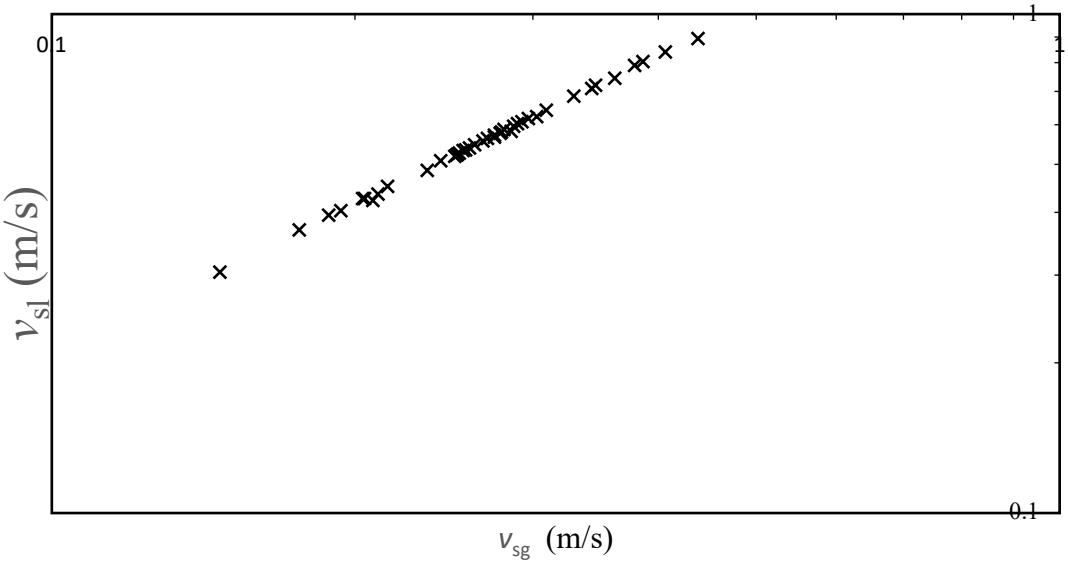

Figure A.6. Liquid superficial velocity versus gas superficial velocity data, showing the slugging regime for 50% choke opening.

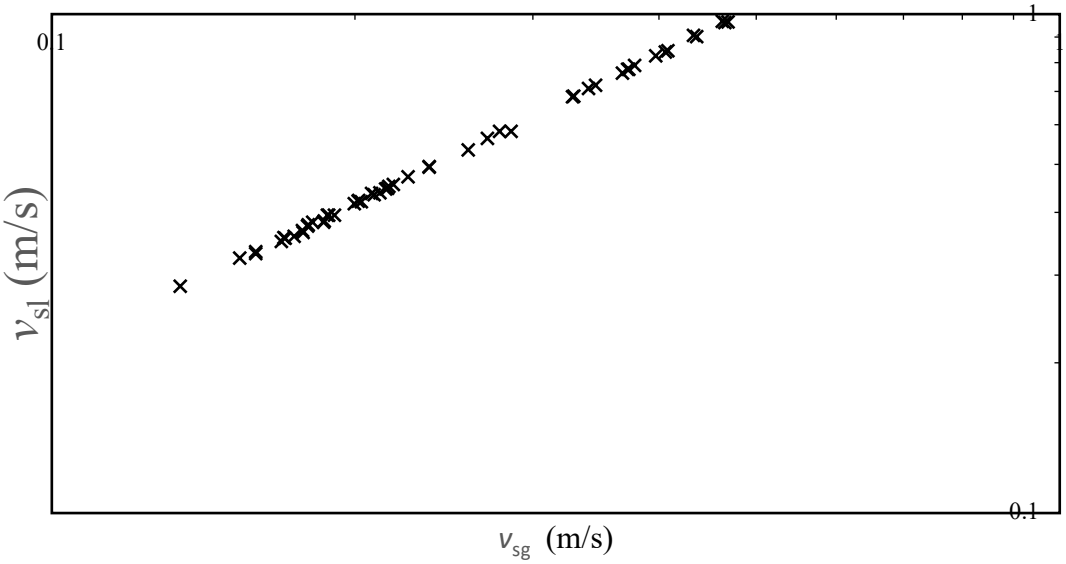

Figure A.7. Liquid superficial velocity versus gas superficial velocity data, showing the slugging regime for 40% choke opening.

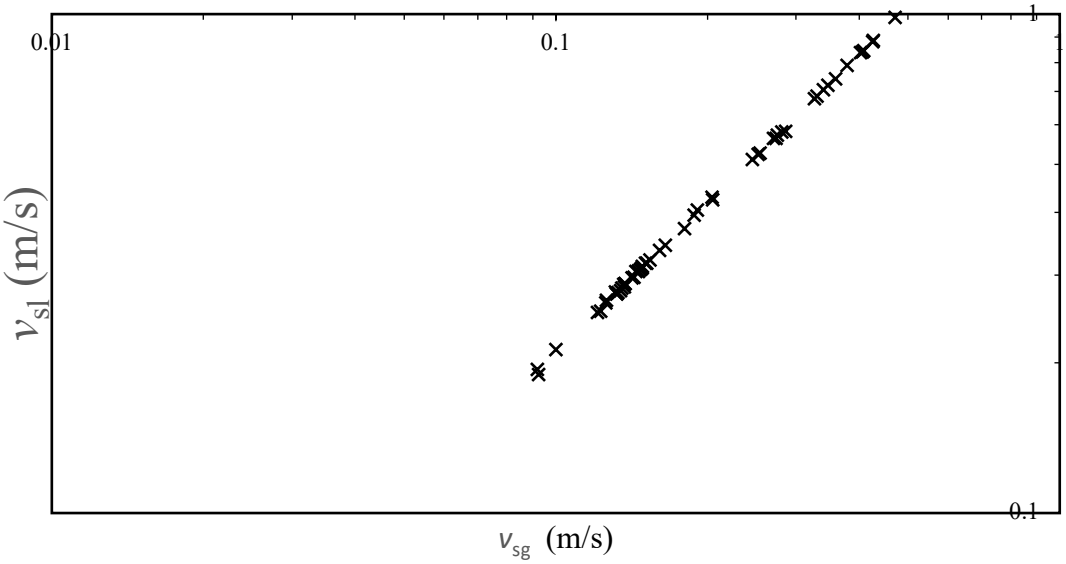

Figure A.8. Liquid superficial velocity versus gas superficial velocity data, showing the slugging regime for 30% choke opening.

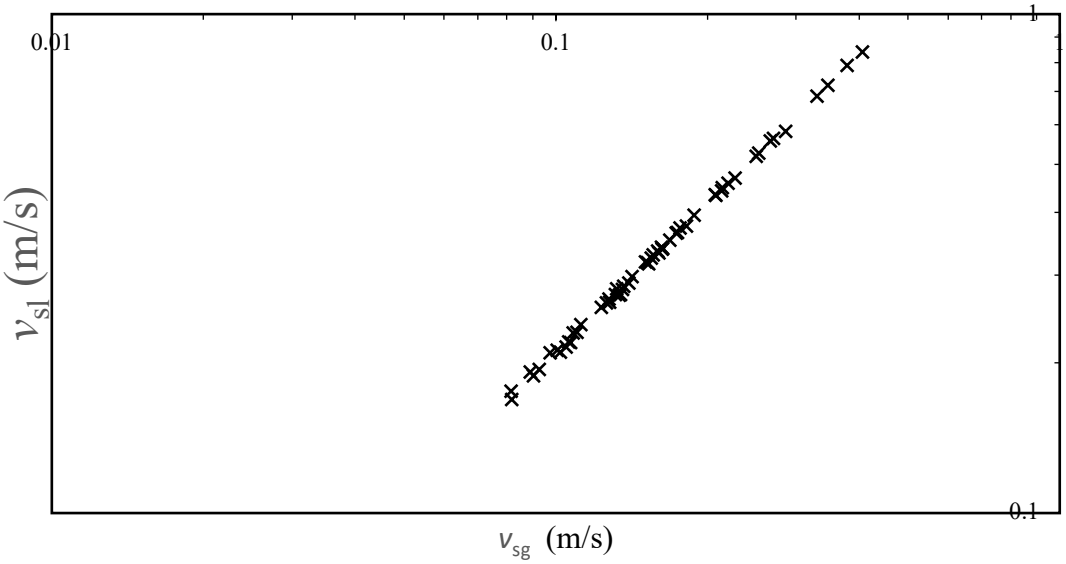

Figure A.9. Liquid superficial velocity versus gas superficial velocity data, showing the slugging regime for 20% choke opening.

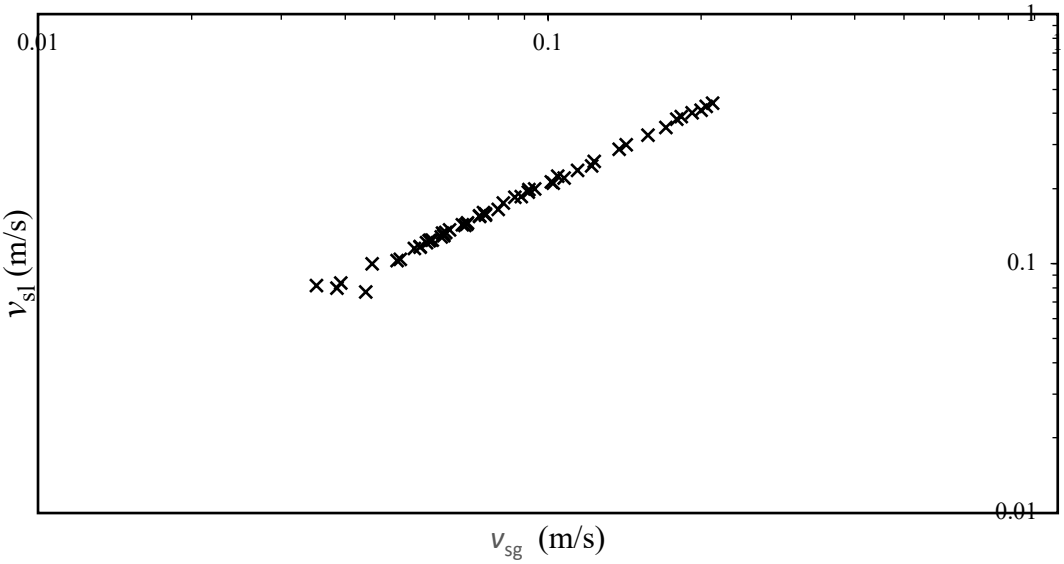

Figure A.10. Liquid superficial velocity versus gas superficial velocity data, showing the slugging regime for 10% choke opening.

Appendix C: Slug frequency Correlations for Selected Choke Openings

Similar to the method to obtain the slug frequency correlation for varied choke openings, selected choke sizes which represent the majority of offshore operating conditions are presented in this section.

C.1. Case 1 - 80% Choke Opening

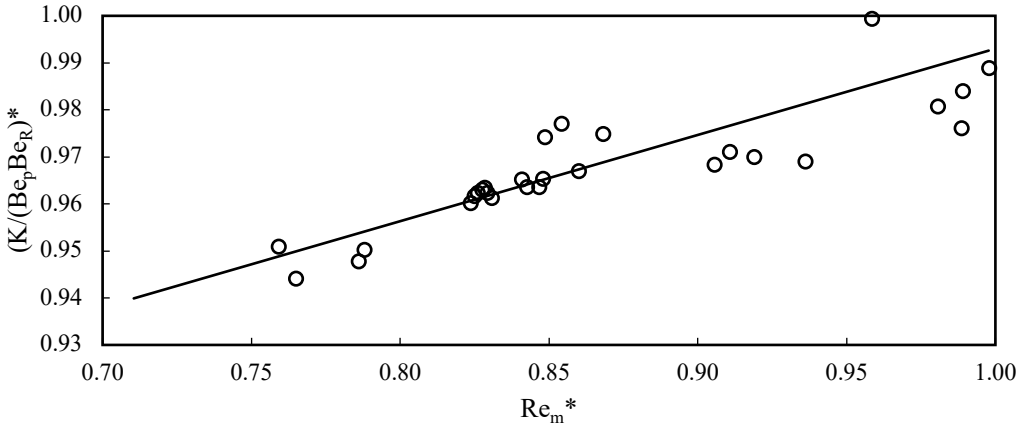

Figure A.11. Combined dimensionless group for Reynolds number in the pipeline for Case 1 (a = 0.18, b = 0.81, and R^2 = 0.78).

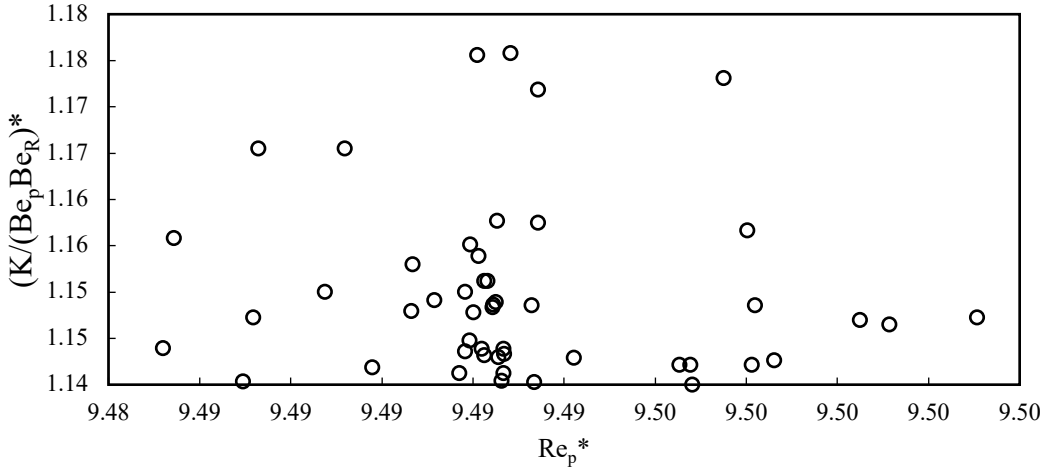

Figure A.12. Combined dimensionless group versus Bejan number in the pipeline for Case 1 (a= -0.39, b=4.89, and R^2=0.013).

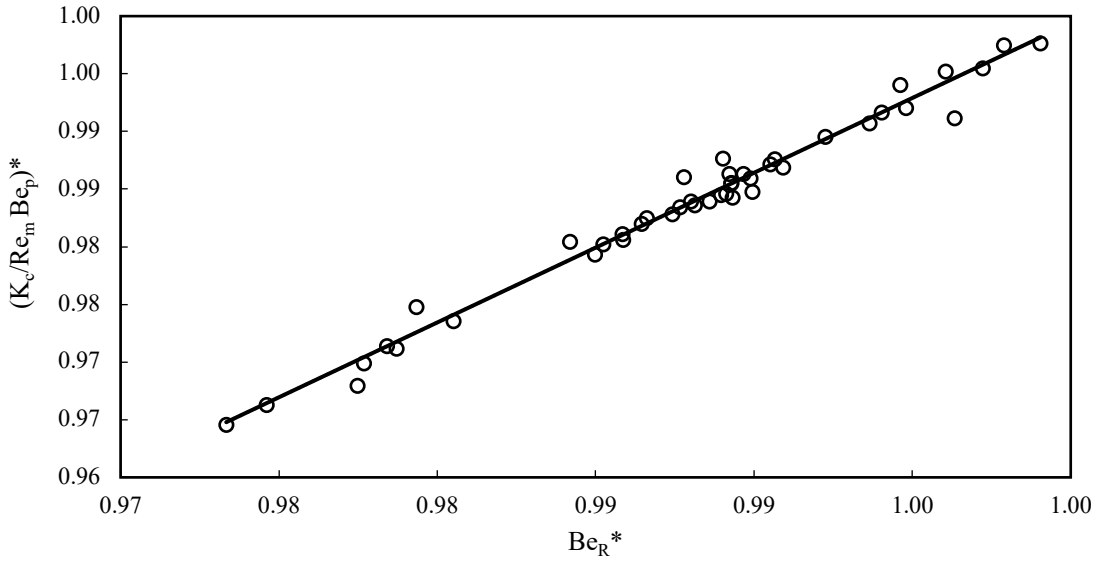

Figure A.13. Combined dimensionless group for Bejan number in the riser for Case 1 (a = 1.2, b = 0.29, and $R^2 = 0.98$)

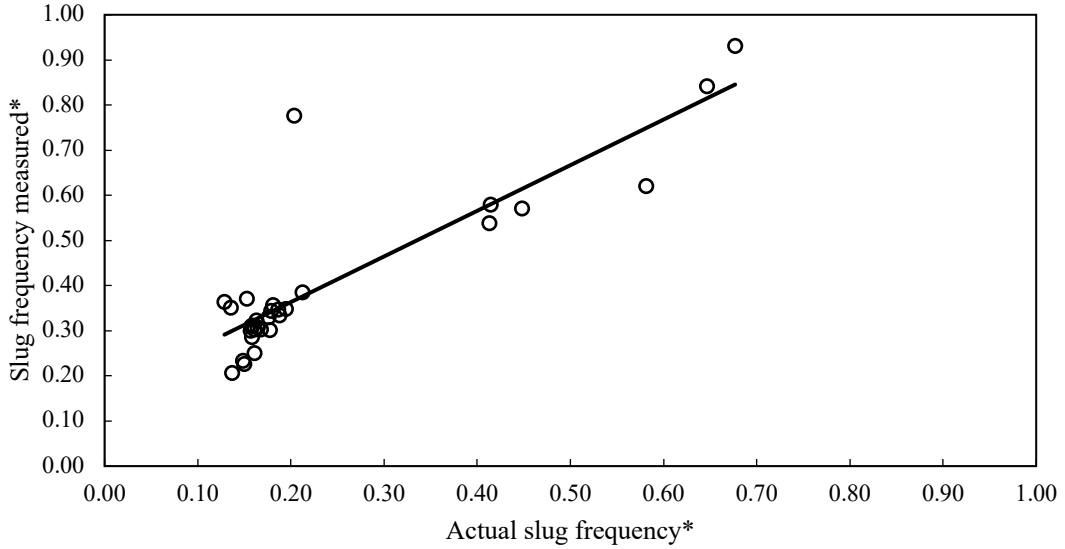

Figure A.14. Comparison of the actual slug frequency measurement with the predicted slug frequency calculated from the new model for Case 1 (a = 1.01, b = 0.16, and $R^2 = 0.753$).

The resulting correlation for a 80% choke opening is given as $Kc^* = Re_i^{0.184} Be_p^{-0.395} Be_r^{1.29}$.

C.2. Case 2 - 70% Choke Opening

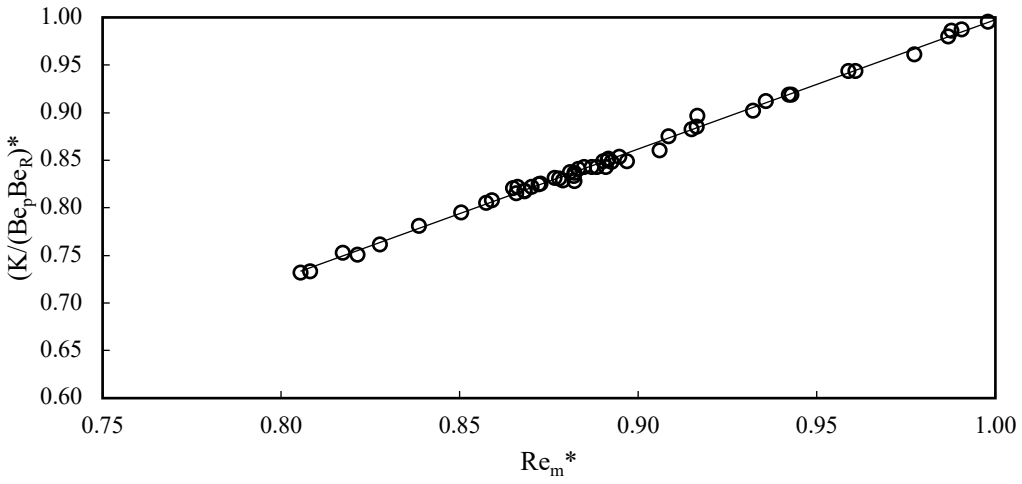

Figure A.15. Combined dimensionless group versus Reynolds number in the pipeline for Case 2 (a = 1.3, b = -0.36, and $R^2 = 0.996$).

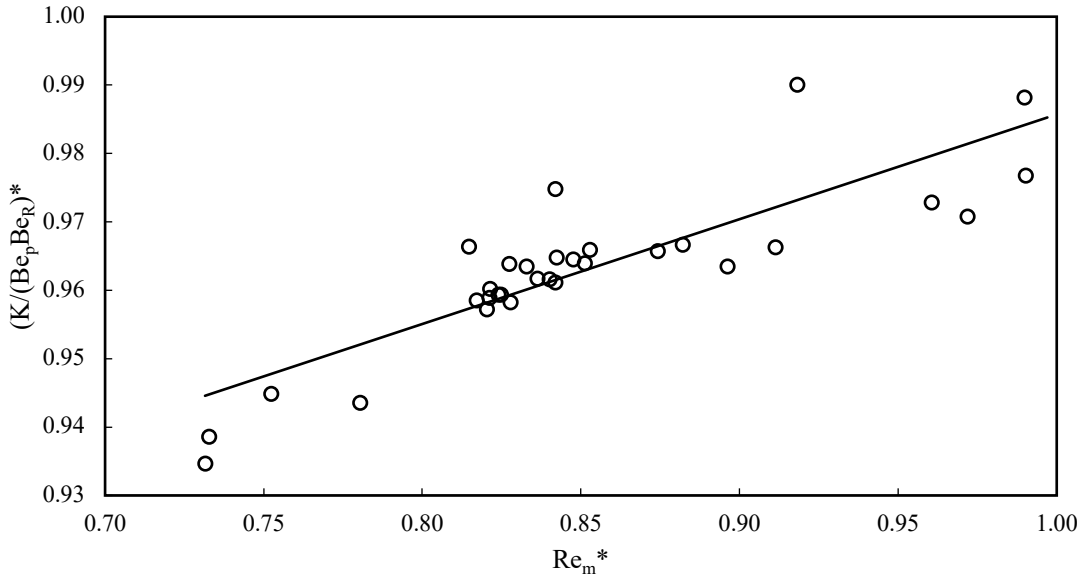

Figure A.16. Combined dimensionless group for Reynolds number in the pipeline for Case 2 (a = 0.15, b = 0.83, and $R^2 = 0.73$)

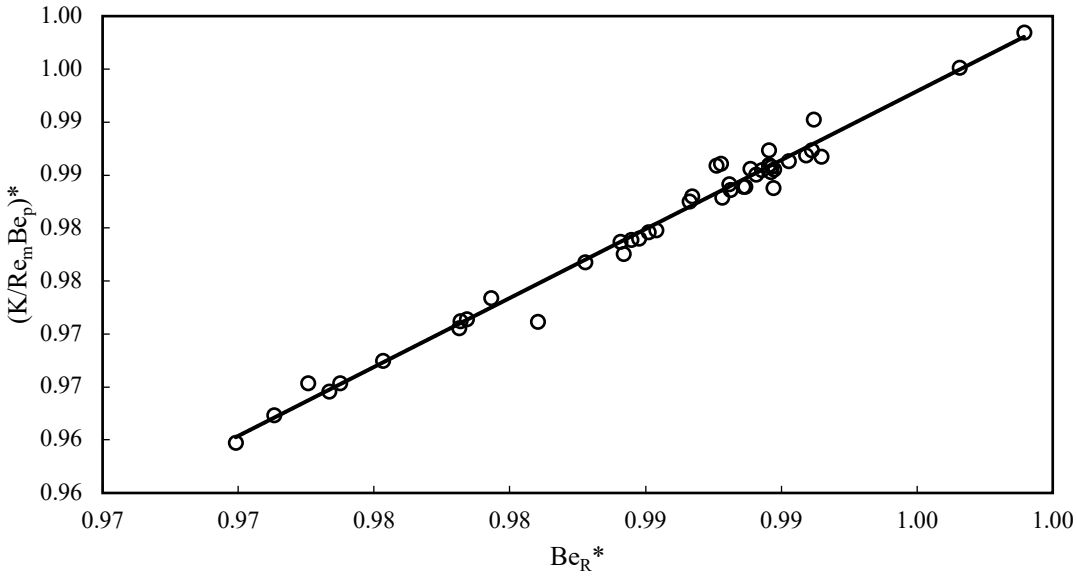

Figure A.17. Combined dimensionless group versus Bejan number in the riser for Case 2 (a = 1.3, b = -0.30, and $R^2 = 0.984$).

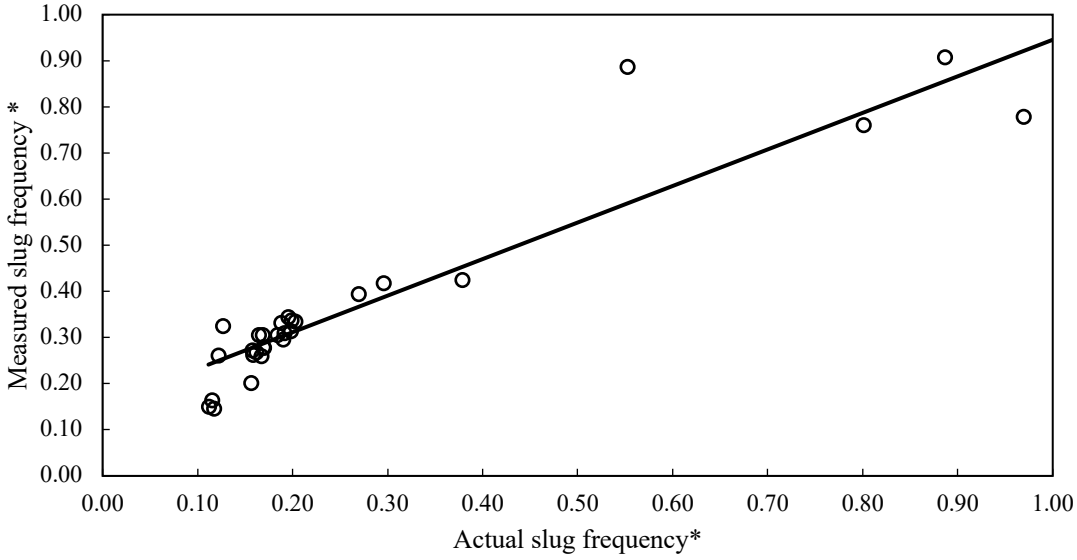

Figure A.18. Comparison of the actual slug frequency measurements and the predicted slug frequency calculated from the new model (a = 0.79, b = 0.153, and $R^2 = 0.89$).

The resulting correlation for a 70% choke opening is given as $Kc^* = Re_i^{0.153} Be_p^{0.34} Be_r^{1.3}$.

C.3. Case 3 - 60% Choke Opening

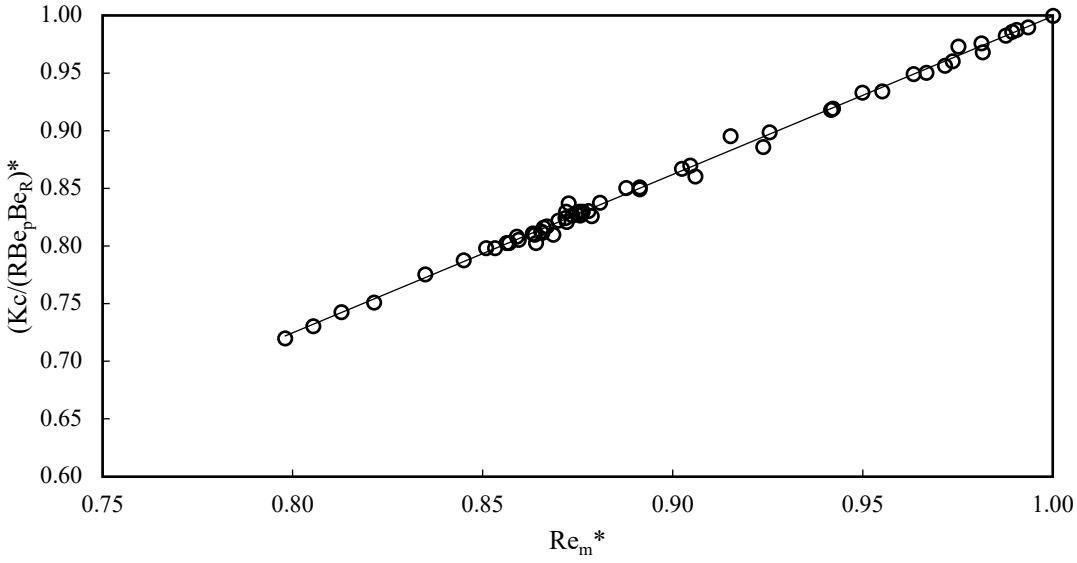

Figure A.19. Combined dimensionless group for Reynolds number in the pipeline for Case 3 (a = 1.3, b = -0.37, and $R^2 = 0.997$).

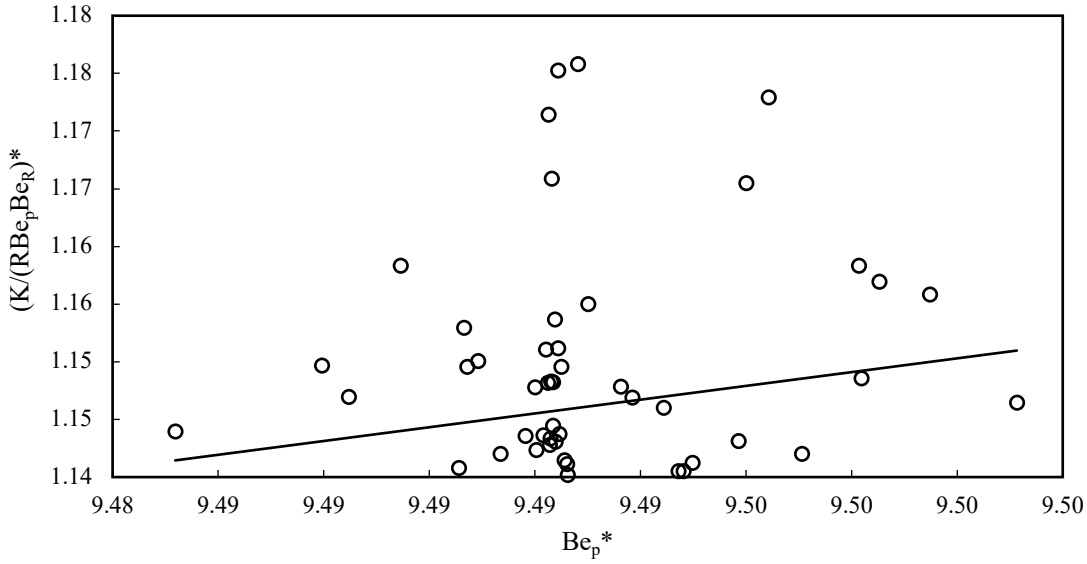

Figure A.20. Combined dimensionless group versus Bejan number in the pipeline for Case 3 (a = 0.597, b = -4.52, and $R^2 = 0.019$).

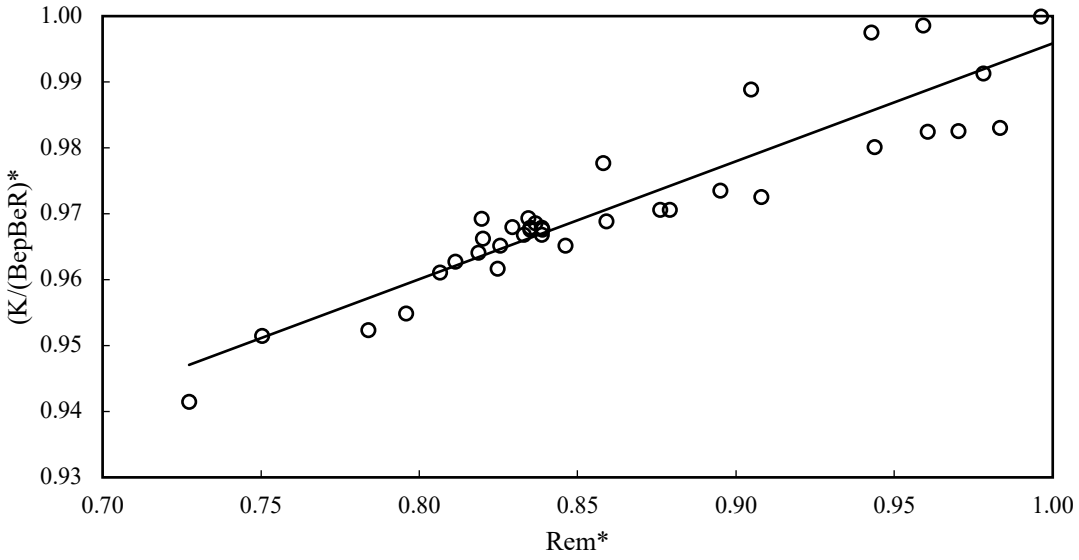

Figure A.21. Combined dimensionless group versus Reynolds number in the pipeline for Case 3 (a = 0.178, b = 0.81, and $R^2 = 0.85$).

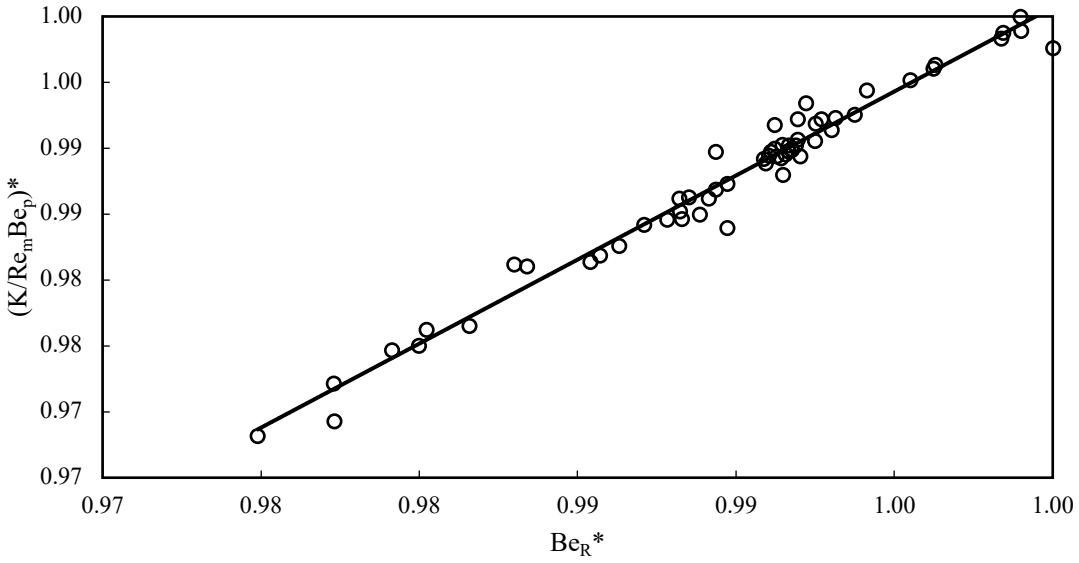

Figure A.22. Combined dimensionless group versus Bejan number in the riser for Case 3 (a = 1.23, b = -0.27, and $R^2 = 0.97$).

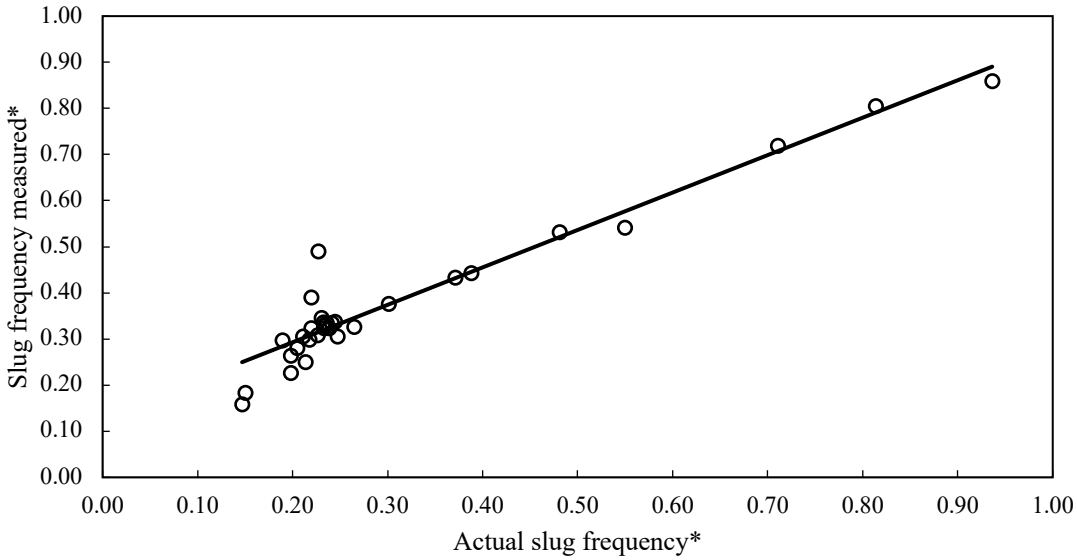

Figure A.23. Comparison of the actual slug frequency measurement with the slug frequency predicted from the new model for Case 3 (a = 0.81, b = 0.13, and $R^2 = 0.92$).

The resulting correlation for a 60% choke opening is given as $Kc^* = Re_i^{0.178} Be_p^{0.597} Be_r^{1.27}$

C.4. Case 4 - 50% Choke Opening

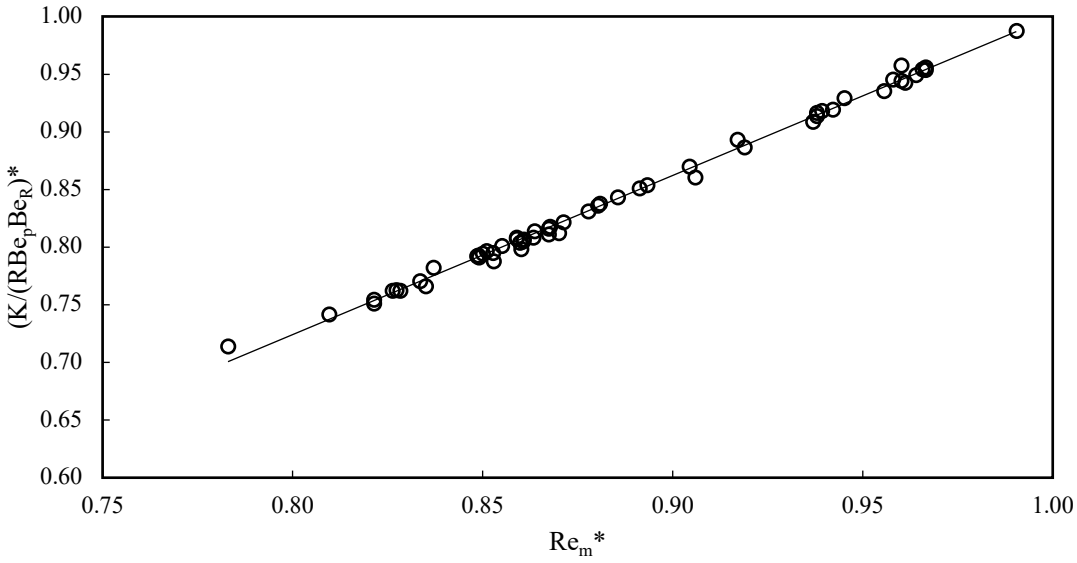

Figure A.24. Combined dimensionless group versus Reynolds number in the pipeline for Case 4 (a = 1.38, b = -0.38, and $R^2 = 0.99$).

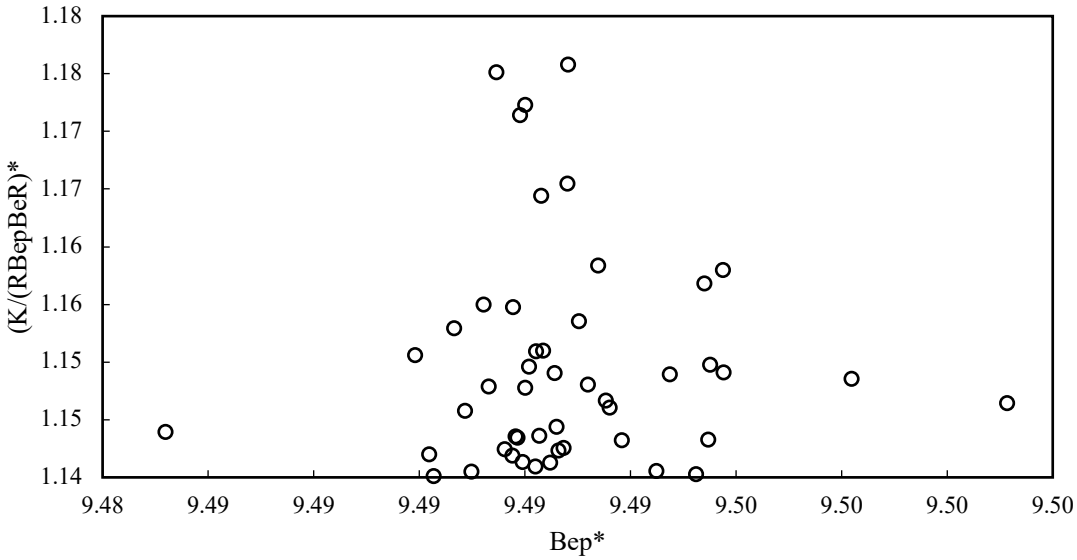

Figure A.25. Combined dimensionless group versus Bejan number in the pipeline for Case 4 (a = -0.028, b = 1.4, and $R^2 = 2\times10^{-5}$).

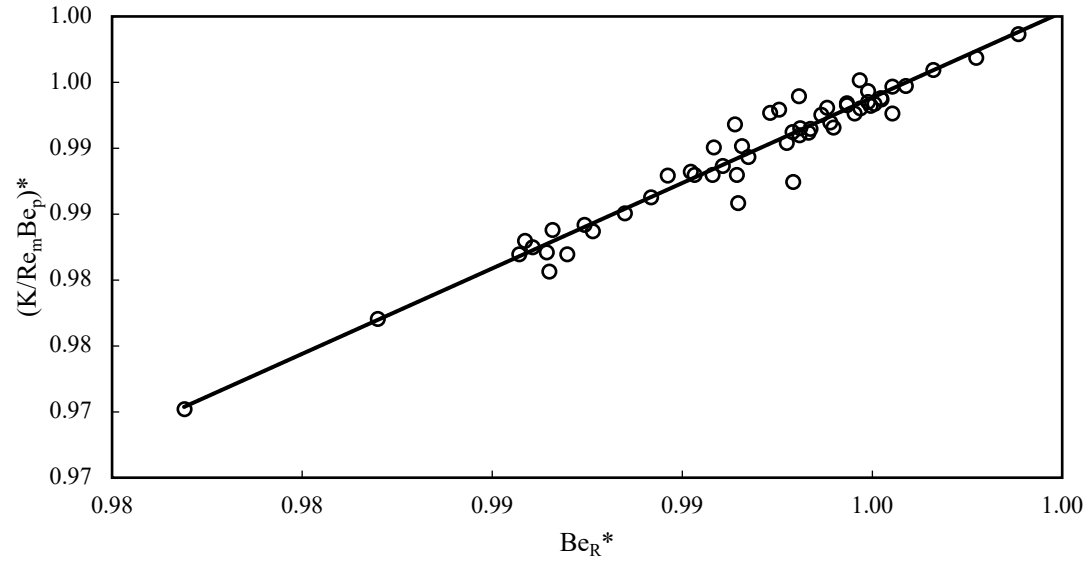

Figure A.26. Combined dimensionless group versus Bejan number in the riser for Case 4 (a = 1.29, b = -0.29, and $R^2 = 0.95$).

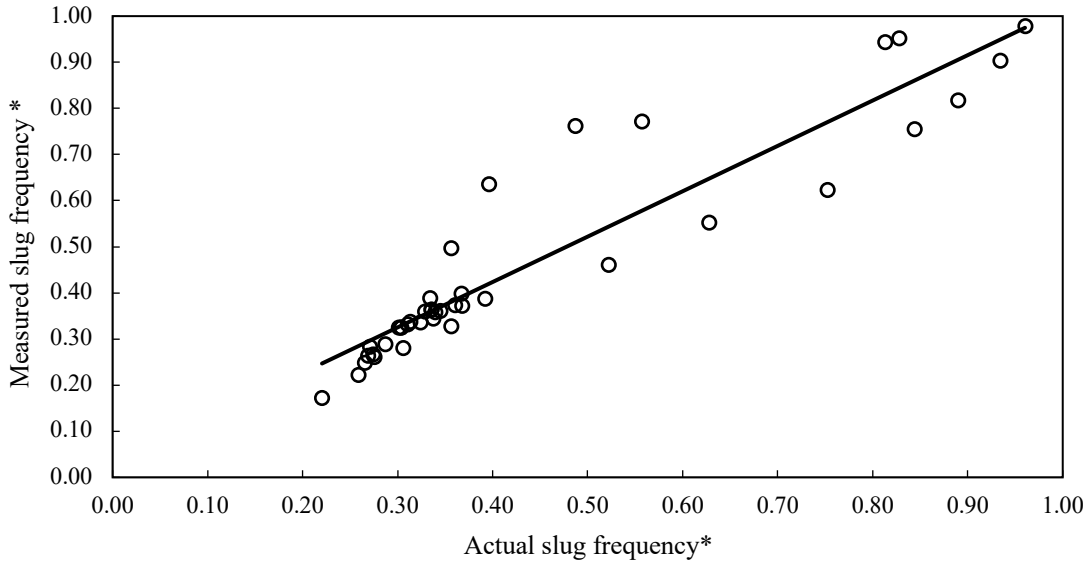

Figure A.27. Comparison of the actual slug frequency measurements and the slug frequency calculated from the new model for Case 4 (a = 0.98, b = 0.03, and $R^2 = 0.87$).

The resulting equation for a 50% choke opening is given as $Kc^* = Re_i^{1.35} Be_p^{-0.027} Be_r^{1.29}$.

C.5. Case 5 - 40% Choke Opening

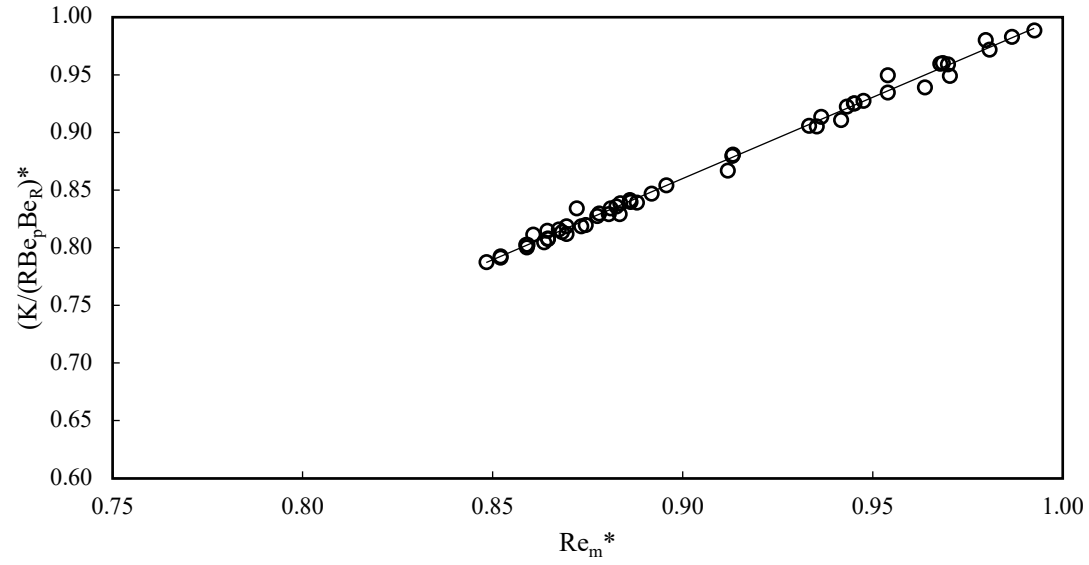

Figure A.28. Combined dimensionless group versus Reynolds number in the pipeline for Case 5 (a = 1.4, b = -0.41, and $R^2 = 0.99$).

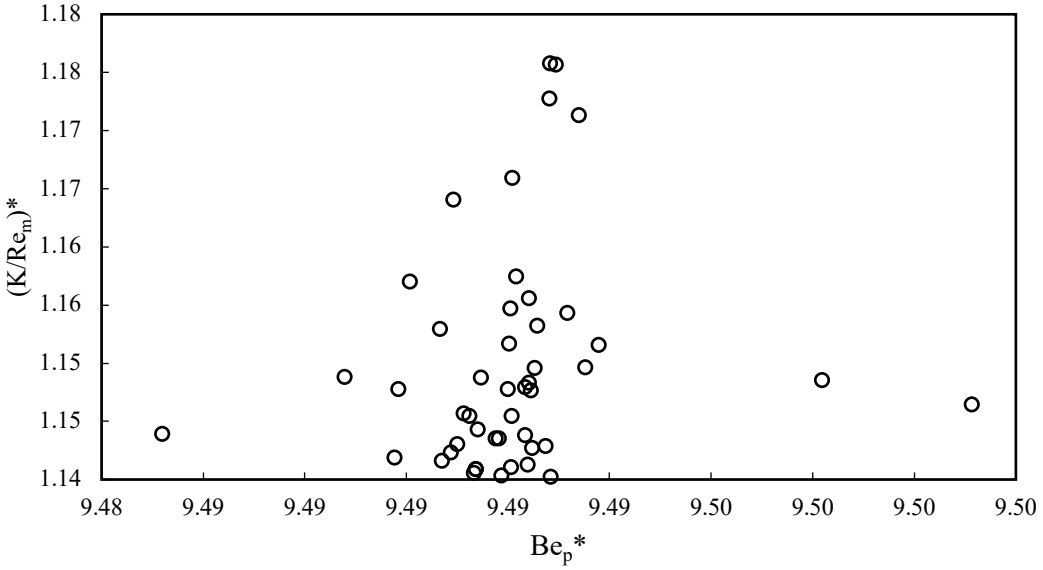

Figure A.29. Combined dimensionless group versus Bejan number in the pipeline for Case 5 (a = 0.7, b = -5.65, and $R^2 = 0.013$).

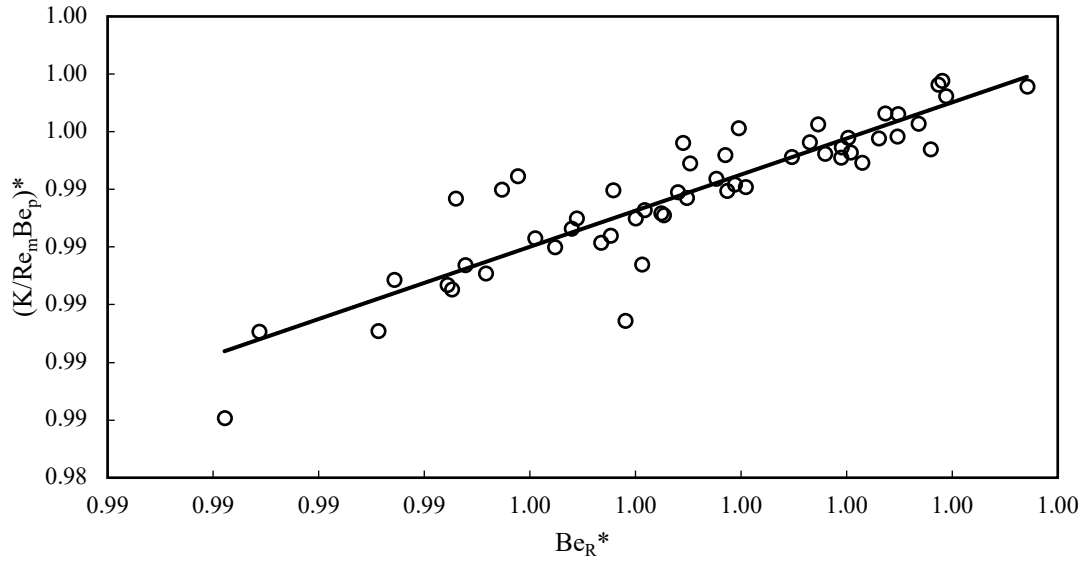

Figure A.30. Combined dimensionless group versus Bejan number in the riser for Case 5 (a = 1.25, b = -0.25, and $R^2 = 0.8$).

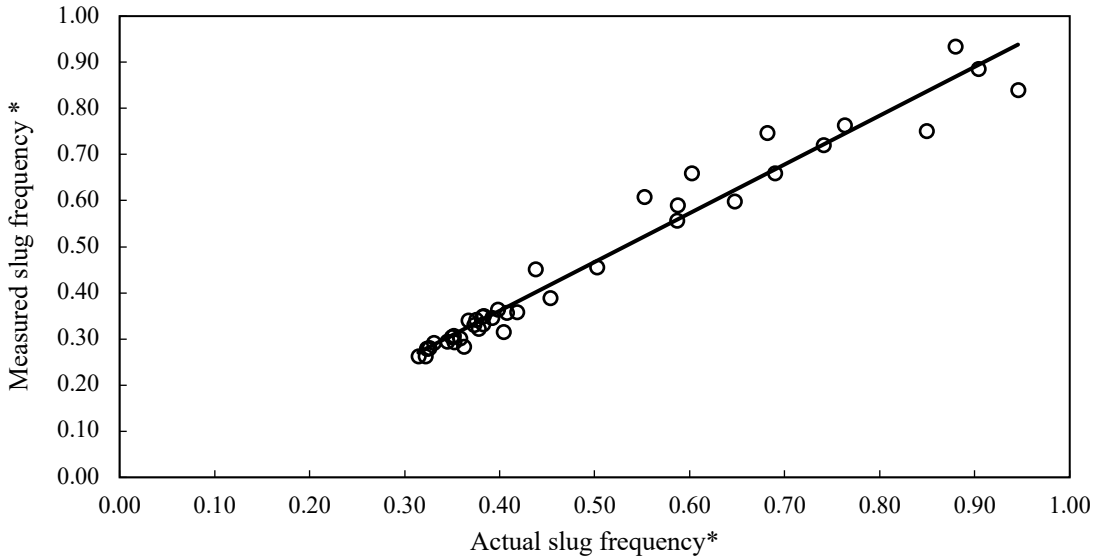

Figure A.31. Comparison of the actual slug frequency measurements with the slug frequency calculated from the new model for Case 5 (a = 1.01, b = -0.06, and $R^2 = 0.96$).

The resulting correlation for a 40% choke opening is given as $Kc^* = Re_i^{1.4} Be_p^{0.7} Be_r^{1.25}$.

C.6. Case 6 - 30% Choke Opening

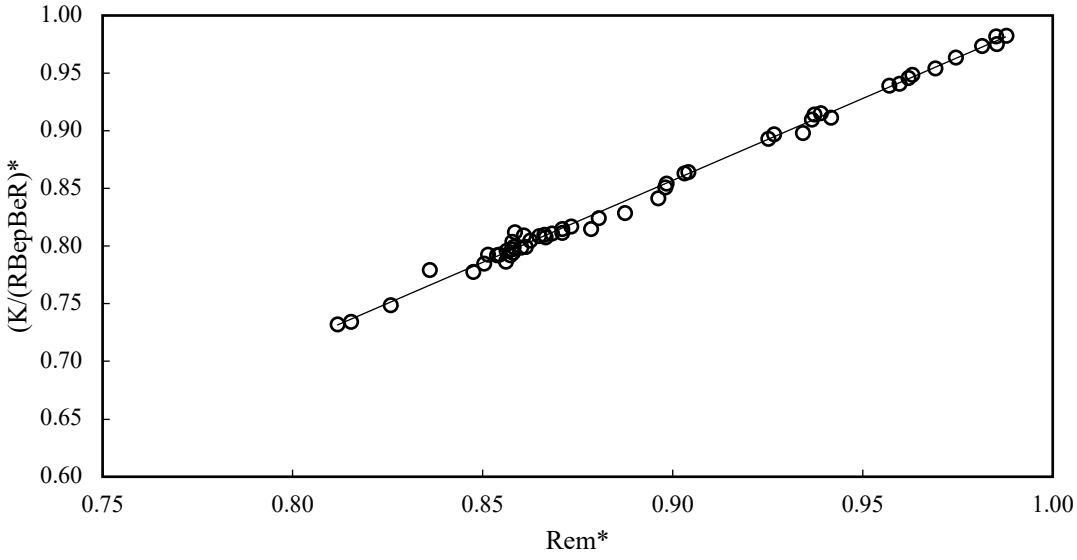

Figure A.32. Combined dimensionless group for Reynolds number in the pipeline for Case 6 (a = 1.42, b = 0.42, $R^2 = 0.99$).

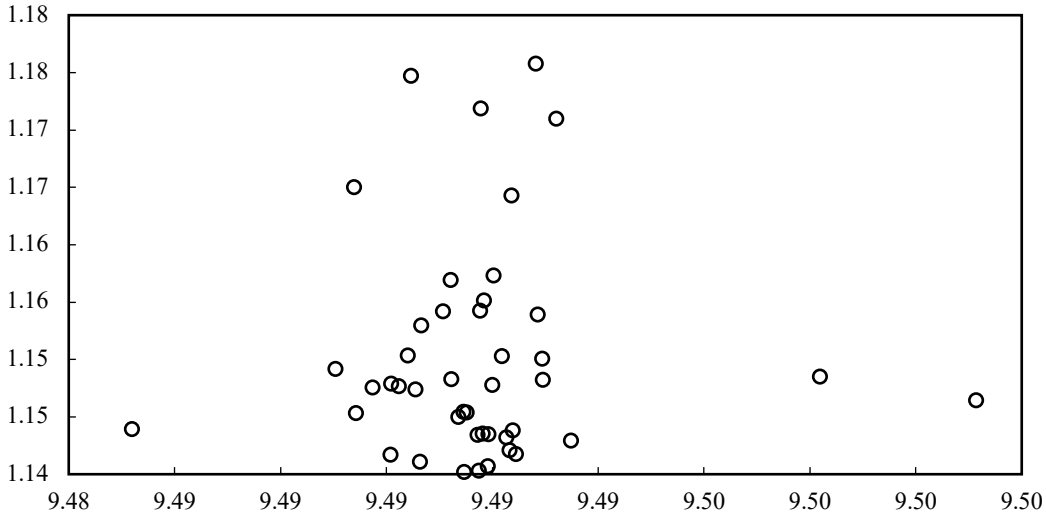

Figure A.33. Combined dimensionless group versus Bejan number in the pipeline for Case 6 (a = -0.072, b = 1.89, R^2 = 1E-4).

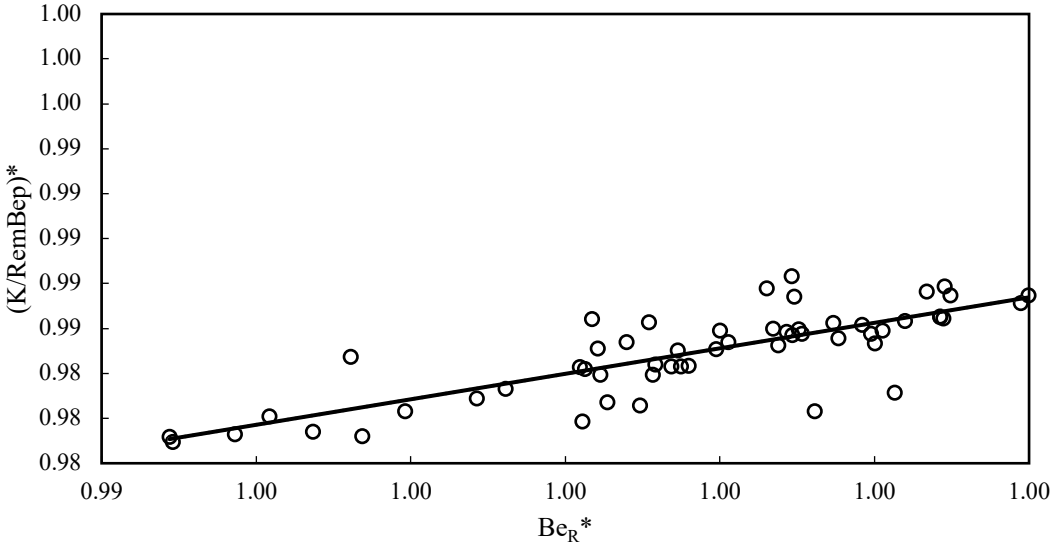

Figure A.34. Combined dimensionless group versus Bejan number in the riser for case 6 (a = 1.14, b = -0.15, R^2 = 0.64).

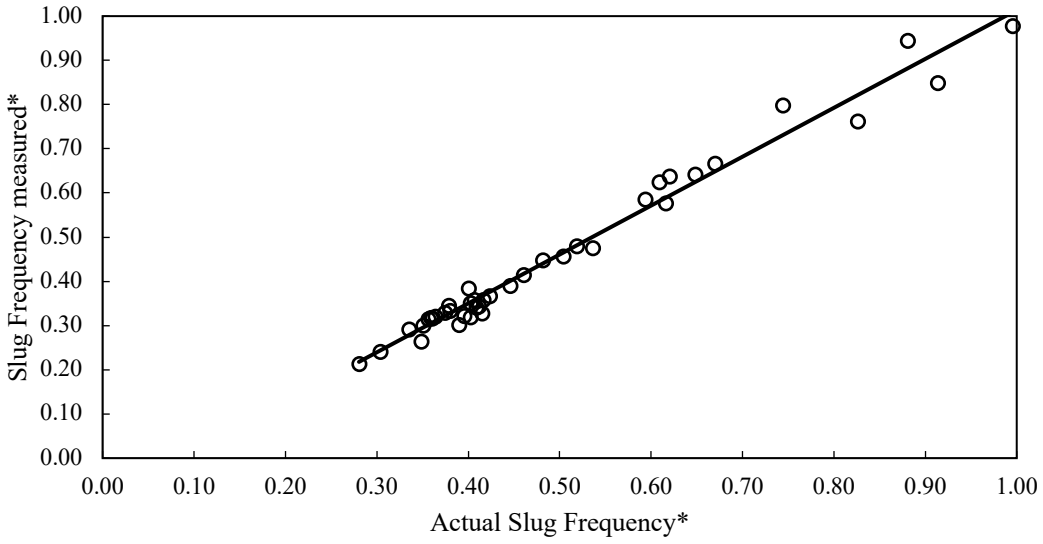

Figure A.35. Comparison of the actual slug frequency measurement with the predicted slug frequency calculated from the new model for Case 6 (a = 1.1, b = -0.09, $R^2 = 0.98$).

The resulting correlation for a 30% choke opening is given as $Kc^* = Re_i^{1.41} Be_p^{-0.07} Be_r^{1.14}$.

C.7. Case 7 - 20% Choke Opening

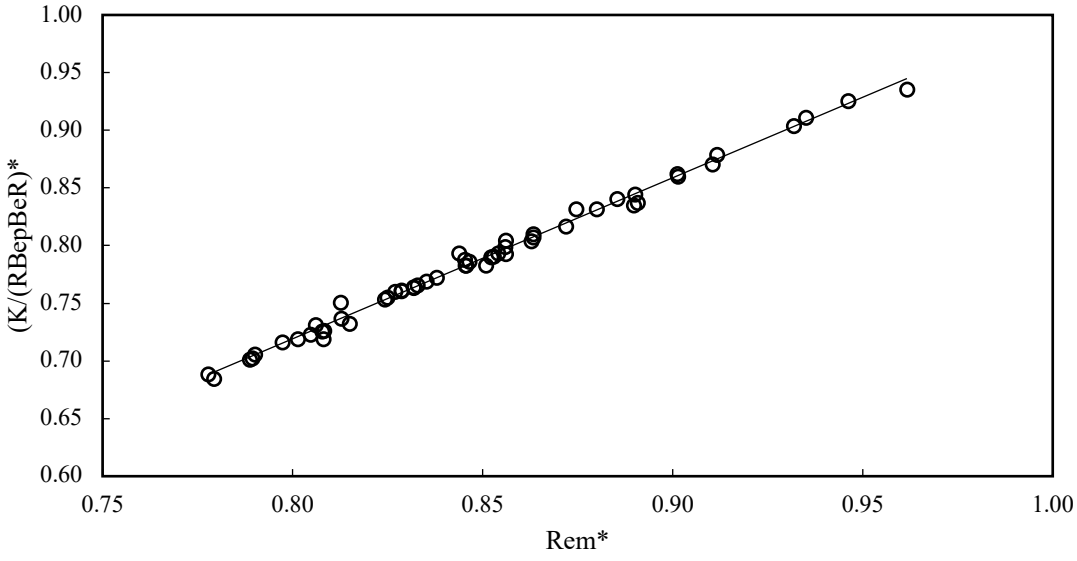

Figure A.36. Combined dimensionless group versus Reynolds number in the pipeline for Case 7 (a = 1.39, b = -0.39, $R^2 = 0.99$).

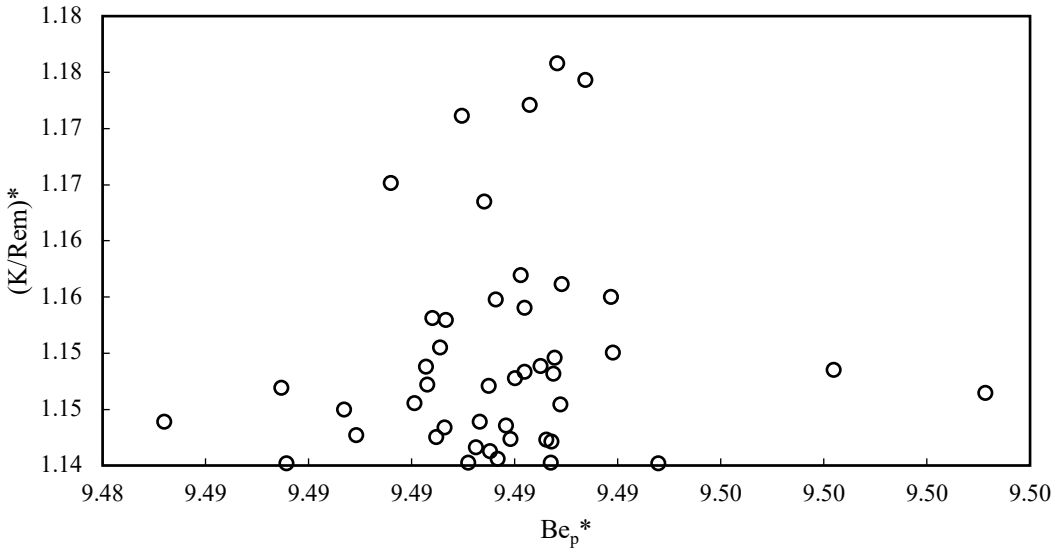

Figure A.37. Case 7 - Combined dimensionless group versus Bejan number in the pipeline (a = 0.7, b = -5.52, $r^2 = 0.016$).

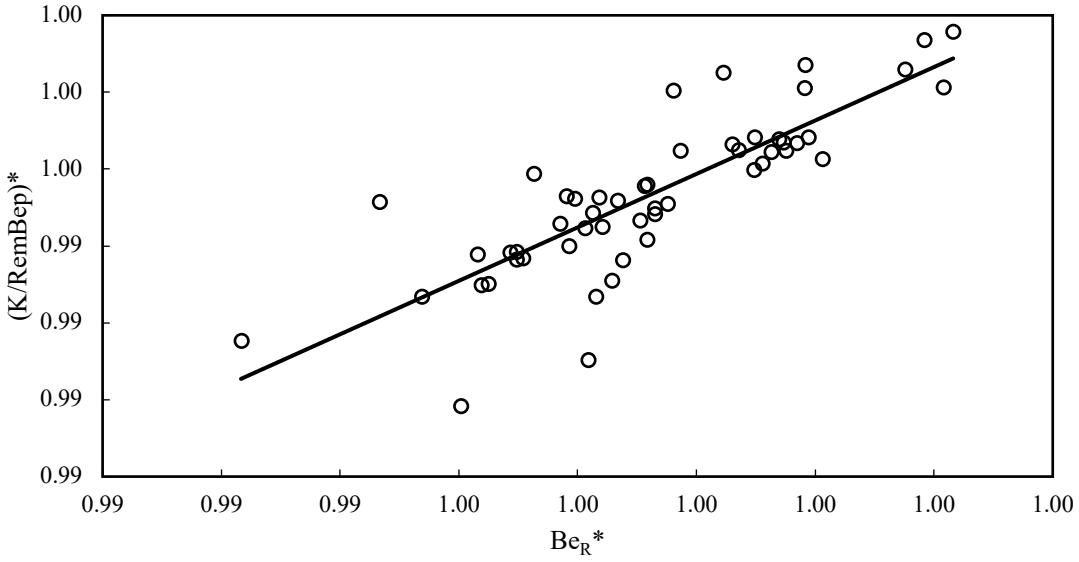

Figure A.38. Case 7 - Combined dimensionless group versus Bejan number in the riser (a = 1.3, b = -0.39, $r^2 = 0.68$).

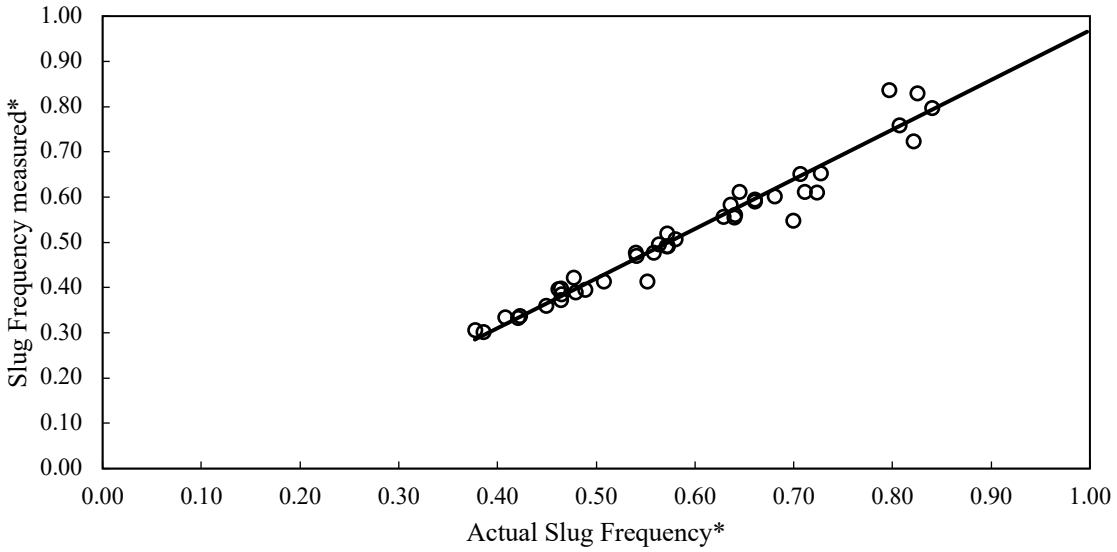

Figure A.39. Comparison of the actual slug frequency measurement with the predicted slug frequency calculated from the new model for Case 7 (a = 1.09, b = -0.13, R^2 = 0.966).

The resulting correlation for a 20% choke opening is given as $Kc^* = Re_i^{1.39} Be_p^{0.7} Be_r^{1.39}$.

C.8. Case 8 - 10% Choke Opening

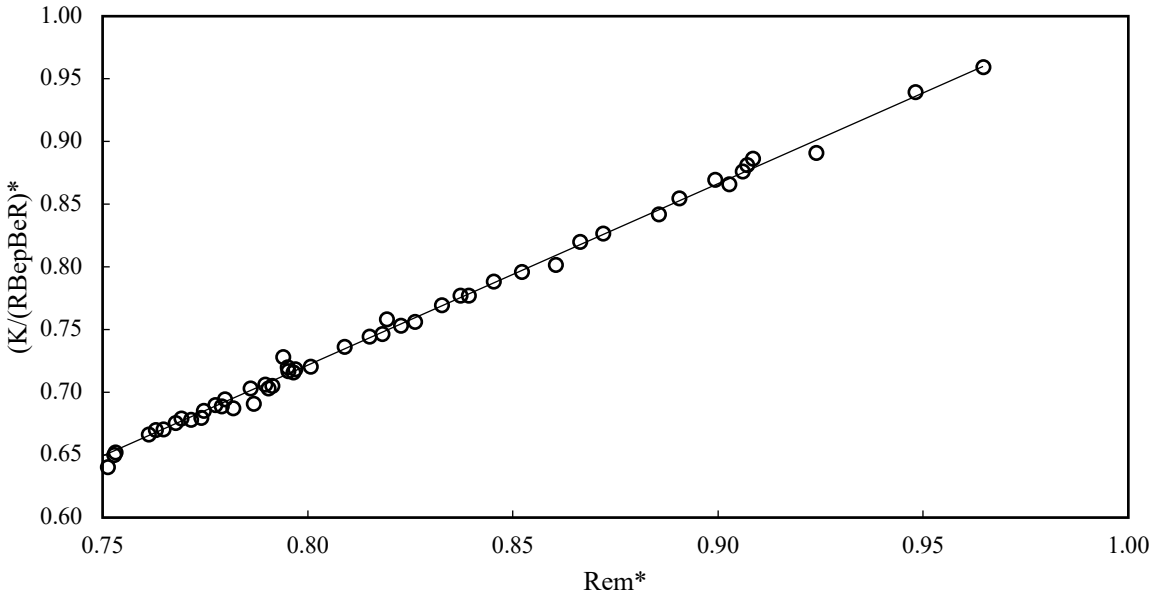

Figure A.40. Combined dimensionless group versus Reynolds number in the pipeline for Case 8 (a = 1.45, b = -0.44, R^2 = 0.99).

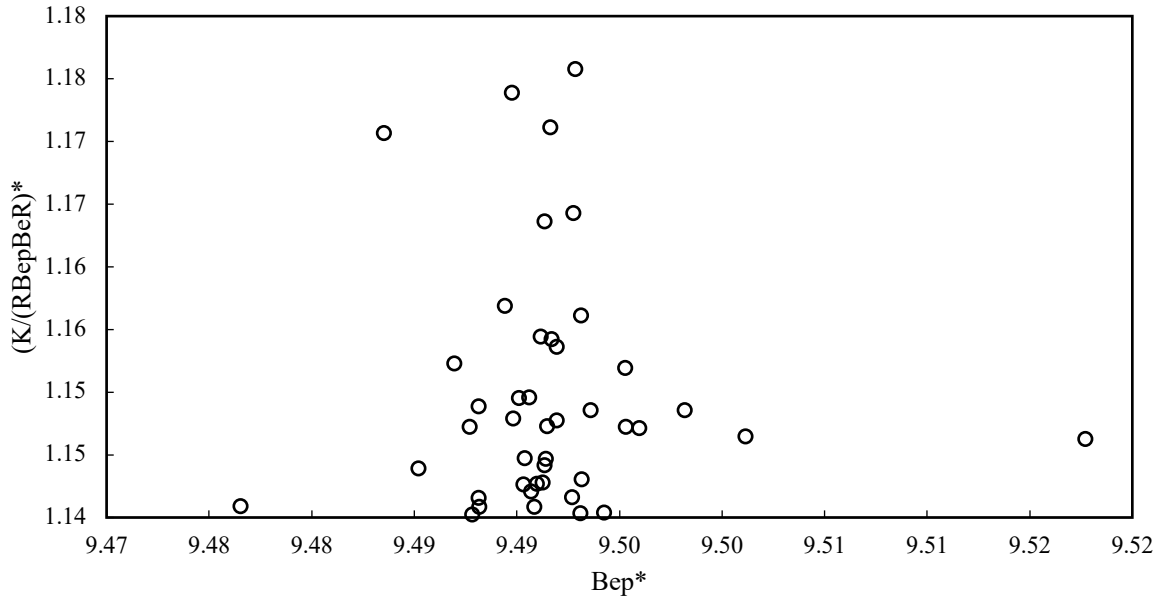

Figure A.41. Combined dimensionless group versus Bejan number in the pipeline for Case 8 (a = 0.071, b = 0.48, $R^2 = 7\times10^{-4}$).

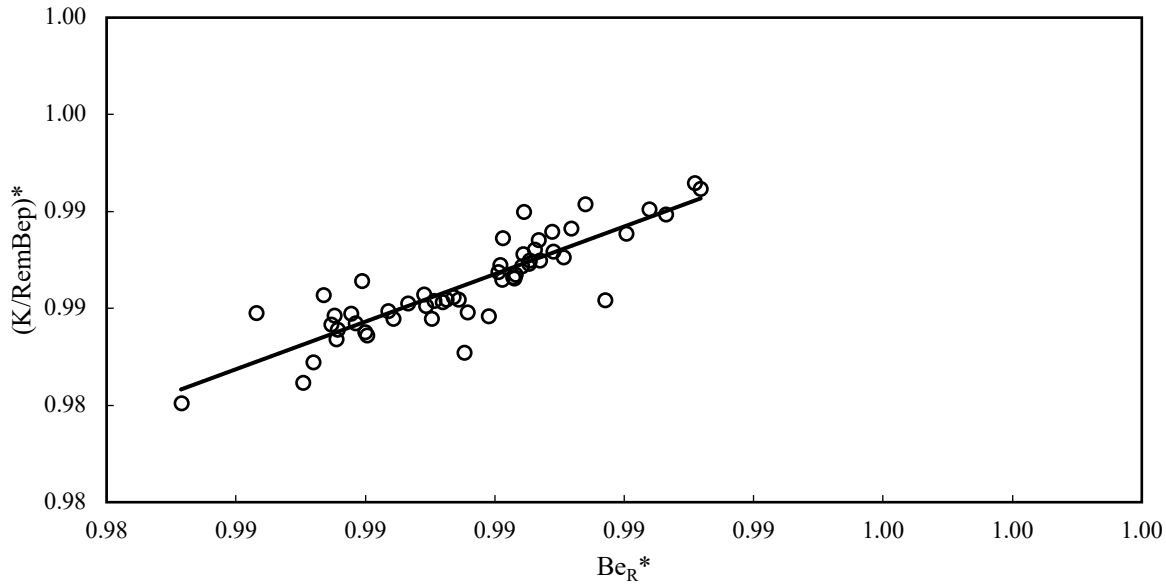

Figure A.42. Combined dimensionless group versus Bejan number in the riser for Case 9 (a = 1.23, b = -0.23, $R^2 = 0.76$).

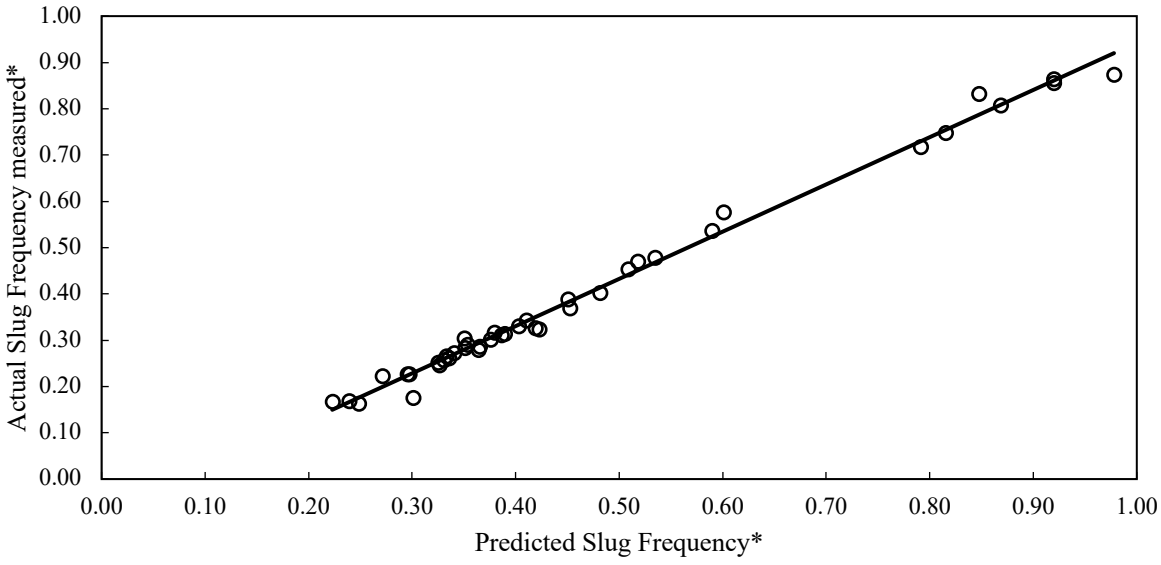

Figure A.43. Comparison of the actual slug frequency measurement with the predicted slug frequency calculated from the new model for Case 8 (a = 1.02, b = -0.078, R^2 = 0.99).

The resulting correlation for 10% choke opening is given as $Kc^* = Re_i^{1.44} Be_p^{0.07} Be_r^{1.23}$.

REFERENCES

Aamo, O. M., Eikrem, G., Siahaan, H., & Foss, B. A. (2005). Observer design for multiphase flow in vertical pipes with gas-lift—theory and experiments. Journal of Process Control, 15(3), 247-257.

Abdul Majeed, G.H., N.B. Abu Al-Soof, and J.R. Alassal (1989) An improved revision to the Hagedorn and Brown liquid holdup correlation. Journal of Canadian Petroleum Technology. **28**(06).

Adeyinka, O.B.; Naterer, G.F. (2005). Experimental uncertainty of measured entropy production with pulsed laser PIV and planar laser-induced fluorescence, International Journal of Heat and Mass Transfer, 2005, **48** (8): p. 1450-1461.

Al-Safran, E. (2008). Slug frequency in gas/liquid horizontal flow. Paper presented at the 6th North American Conference on Multiphase Technology BHR Group, Banff, Canada.

Alvarez, L. P., Mohan, R. S., Shoham, O., & Avila, C. (2010). Multiphase Flow Splitting in Parallel/Looped Pipelines. Paper presented at the SPE Annual Technical Conference and Exhibition.

Andreussi, P., & Bendiksen, K. (1989). An investigation of void fraction in liquid slugs for horizontal and inclined gas-liquid pipe flow. International journal of multiphase flow, 15(6), 937-946.

Andreolli, I., Zortea, M., & Baliño, J. L. (2017). Modeling offshore steady flow field data using drift-flux and black-oil models. Journal of Petroleum Science and Engineering, 157, 14-26.

Arpandi, I., Joshi, A. R., Shoham, O., Shirazi, S., & Kouba, G. E. (1996). Hydrodynamics of two-phase flow in gas-liquid cylindrical cyclone separators. SPE journal, 1(04), 427-436.

Aung, N.Z. and Yuwono T. (2012) Evaluation of Mixture Viscosity Models in the Prediction of Two-phase Flow Pressure Drops. ASEAN Journal on Science and Technology for Development, 29(2).

Azevedo, G., Baliño, J., & Burr, K. (2015). Linear stability analysis for severe slugging in air–water systems considering different mitigation mechanisms. International journal of multiphase flow, 73, 238-250.

Azevedo, G. R. D., Baliño, J. L., & Burr, K. P. (2017). Linear stability analysis for severe slugging: sensitivity to void fraction and friction pressure drop correlations. International Journal of Simulation and Process Modelling, 12(3-4), 235-248.

Awad, M.M. and Muzychyka, Y. (2008). Effective property models for homogeneous two-phase flows, Experimental Thermal and Fluid Science, vol. 33, 106–113.

Baliño, J., Burr, K., & Nemoto, R. (2010). Modeling and simulation of severe slugging in air–water pipeline–riser systems. International journal of multiphase flow, 36(8), 643-660.

Baliño, J., Burr, K., & Pereira, N. (2007). Modeling and simulation of severe slugging in pipeline-riser systems. Paper presented at the Proceedings of COBEM.

Baliño, J. L. (2014). Modeling and simulation of severe slugging in air-water systems including inertial effects. Journal of Computational Science, 5(3), 482-495.

Baliño, J. L., Burr, K., & Nemoto, R. (2010). Modeling and simulation of severe slugging in air–water pipeline–riser systems. International journal of multiphase flow, 36(8), 643-660.

Bendiksen, K. H. (1984). An experimental investigation of the motion of long bubbles in inclinedtubes. International journal of multiphase flow, 10(4), 467-483.

Bennett, M., & Williams, R. A. (2004). Monitoring the operation of an oil/water separator using impedance tomography. Minerals Engineering, 17(5), 605-614.

Bennett, M. A., West, R. M., Luke, S., & Williams, R. A. (2002). The investigation of bubble column and foam processes using electrical capacitance tomography. Minerals Engineering, 15(4), 225-234.

Beggs, D.H and Brill, J.P. (1972), An experimental study of two-phase in inclined pipes, PhD Dissertation, The University of Tulsa.

Beatie, D.H and Whalley, P.B. (1982), Simple two-phase frictional pressure drop calculation method', Int. J. Multiphase Flow, vol. 8, no. 1, pp. 83–87.

Biltoft, J., Hansen, L., Pedersen, S., & Yang, Z. (2013). Recreating riser slugging flow based on an economic lab-sized setup. IFAC Proceedings Volumes, 46(12), 47-52.

Boe, A. (1981). Severe slugging characteristics. Course in Two Phase Flow, NTH, Trondheim, Norway.

Boschee, P. (2013,). Challenges in the Design of Separators. Society of Petroleum Engineers. .

Barnea, D., Luninski, Y., Taitel, Y. (1983). Flow in small diameter pipes. Can. J. Chem. Engng. 61, 617-620.

Brill, J. P. (2010). Modeling multiphase flow in pipes. The Way Ahead, 6(02), 16-17.

Buckingham, E. (1914). On physically similar systems; illustrations of the use of dimensional equations. Physical Review, 4(4), 345.

Bybee, K. (2004). Wellbore Stability in the Compacting and Subsiding Valhall Field. Journal of Petroleum Technology, 56(10), 72-73. doi:10.2118/1004-0072-JPT

Calvert, P., & Davis, J. R. (2010). A Dynamic Business Needs Dynamic Solutions; How Field of the Future Has Turned BP into a Smooth Operator. Paper presented at the SPE Intelligent Energy Conference and Exhibition.

Campos, S. R. V., Baliño, J. L., Slobodcicov, I., & Paz, E. (2014). Orifice plate meter field performance: Formulation and validation in multiphase flow conditions. Experimental Thermal and Fluid Science, 58, 93-104.

Cavallini, G. Censi, D. Del Col, L. Doretti, G.A. Longo, L. Rossetto (2001), Experimental investigation on condensation heat transfer and pressure drop of new HFC refrigerants (R134a, R125, R32, R410A, R236ea) in a smooth horizontal tube, International Journal of Refrigeration, Volume 24, Issue 1, P 73-87, ISSN 0140-7007.

Cavallini, D. Del Col, M. Matkovic, L. Rossetto (2009). Frictional pressure drop during vapour–liquid flow in mini channels: Modelling and experimental evaluation, International Journal of Heat and Fluid Flow, 30 (1) 131-139, ISSN 0142-727X.

Cheng, H., Hills, J., & Azzopardi, B. (2002). Effects of initial bubble size on flow pattern transition in a 28.9 mm diameter column. International journal of multiphase flow, 28(6), 1047-1062.

Chexal, B., Lellouche, G., Horowitz, J., & Healzer, J. (1992). A void fraction correlation for generalized applications. Progress in nuclear energy, 27(4), 255-295.

Chin, R. W., Stanbridge, D. I., & Schook, R. (2002). Increasing Separation Capacity with New and Proven Technologies. Paper presented at the SPE Annual Technical Conference and Exhibition, San Antonio, Texas. https://doi.org/10.2118/77495-MS.

Cicchitti, A., Lombaradi, C., Silversti, M., Soldaini, G. and Zavattarlli, R. (1960). Two-phase cooling experiments – pressure drop heat transfer burnout measurements, Energia Nucleare, 7(6), 407–425.

Chirinos, W. A., Gomez, L. E., Wang, S., Mohan, R., Shoham, O., & Kouba, G. (1999). Liquid Carry-over in Gas-Liquid Cylindrical Cyclone Compact Separators. Paper presented at the SPE Annual Technical Conference and Exhibition, Houston, Texas. https://doi.org/10.2118/56582-MS

Courbot, A. (1996). Prevention of severe slugging in the Dunbar 16-in. multiphase pipeline.

Cozin, C., Pipa, D. R., Barbuto, F. A., Morales, R. E., & da Silva, M. J. (2013). A Comprehensive Analysis on Gas-liquid Slug Flows in Horizontal Pipes. Paper presented at the OTC Brasil.

Carroll, A., et al. Flow Assurance and Production Chemistry for the Na Kika Development. in Offshore Technology Conference. 2005. Offshore Technology Conference.

Dalsmo, M., Halvorsen, E., & Slupphaug, O. (2005). Active feedback control of unstable wells at the brage field.

Davidson, W.F., Hardie, P.H., Humphreys, C.R., Markson, A.A., Mumford, A.R. and

Ravese, T. (1943). Studies of heat transmission through boiler tubing at pressures from 500–3300 Lbs., Trans. ASME, 65 (6), 553–591.

De Henau, V., & Raithby, G. (1996). A study of terrain-induced slugging in two-phase flow pipelines. International journal of multiphase flow, 22(S1), 119-119.

Di Meglio, F., Kaasa, G. O., Petit, N., & Alstad, V. (2012). Model-based control of slugging: advances and challenges. Paper presented at the IFAC Workshop on Automatic Control in Offshore Oil and Gas Production 2012.

Di Meglio, F., Petit, N., Alstad, V., & Kaasa, G.-O. (2012). Stabilization of slugging in oil production facilities with or without upstream pressure sensors. Journal of Process Control, 22(4), 809-822.

Di Meglio, F., Kaasa, and N. Petit (2010). Model-based control of slugging flow: an experimental case study. in American Control Conference (ACC). IEEE.

2005, Hoboken, NJ: John Wiley. xiv, 574 p.

Di Meglio, F., G.-O. Kaasa, N. Petit and Alstad, V. (2009). A first principle model for multiphase slugging flow in vertical risers. in Decision and Control, 2009 held jointly with the 28th Chinese Control Conference. CDC/CCC 2009. Proceedings of the 48th IEEE Conference on. 2009.

Di Meglio, F., G.-O. Kaasa, N. Petit and Alstad, V. (2010). Reproducing slugging oscillations of a real oil well. in Decision and Control (CDC), 2010 49th IEEE Conference on. 2010. IEEE.

Duns, H., Jr., & Ros, N. C. J. (1963). Vertical flow of gas and liquid mixtures in wells. Paper presented at the 6th World Petroleum Congress, Frankfurt am Main, Germany.

Durdevic, P., Pedersen, S., Bram, M., Hansen, D., Hassan, A., Yang, Z. (2015) Control oriented modeling of a de-oiling hydrocyclone. IFAC-PapersOnLine. **48**(28): p. 291-296.

Durdevic, P., S. Pedersen, and Z. Yang. (2016). Evaluation of oiw measurement technologies for deoiling hydrocyclone efficiency estimation and control. in OCEANS 2016-Shanghai. 2016. IEEE.

Durdevic, P., Pedersen, S., Bram, M., Hansen, D., Hassan, A., & Yang, Z. (2015). Control oriented modelling of a de-oiling hydrocyclone. IFAC-PapersOnLine, 48(28), 291-296.

Dukler, A.E., Moye, W. and Cleveland, R.G., (1964). Frictional pressure drop in two-phase flow. Part A: a comparison of existing correlations for pressure loss and holdup, and Part B: an approach through similarity analysis, AIChE J., vol. 10, no. 1, pp. 38–51.

Ehinmowo, A. B., Orodu, O. D., Anawe, P. A., & Ogunleye, O. O. (2016). Attenuating severe slug flow at large valve opening for increased oil production without feedback control signal. Journal of Petroleum Science and Engineering, 146, 1130-1141.

Eikrem, G. O. (2006). Stabilization of gas-lift wells by feedback control. Citeseer,

Eikrem, G. O., Imsland, L., & Foss, B. (2004). Stabilization of gas lifted wells based on state estimation. IFAC Proceedings Volumes, 37(1), 323-328.

El Moniem, A., & El-Banbi, A. H. (2015). Proper selection of multiphase flow correlations. Paper presented at the SPE North Africa Technical Conference and Exhibition.

Enilari, B. and F. Kara. Slug Flow and it's Mitigation Techniques in the Oil and Gas Industry. in SPE Nigeria Annual International Conference and Exhibition. 2015. Society of Petroleum Engineers.

Fabre, J., Peresson, L. L., Corteville, J., Odello, R., & Bourgeois, T. (1990). Severe slugging in pipeline/riser systems. SPE Production Engineering, 5(03), 299-305.

Fard, M. P., Godhavn, J.-M., & Sagatun, S. I. (2006). Modeling of Severe Slug and Slug Control With OLGA. SPE Production & Operations, 21(03), 381-387. doi:10.2118/84685-PA

Fong, Y., G. Groote, and G. Haandrikman (2013). Increasing Production by Applying Simple/Robust, Field Proven Slug Control Technology. in 16th International Conference on Multiphase Production Technology. BHR Group.

Fourar, M. and Bories, S. (1995), Experimental study of air-water two-phase flow through a fracture (narrow channel), Int. J. Multiphase Flow, vol. 21, no. 4, pp. 621–637.

Fowler, A. J., Ledezma, G. A., Bejan, A. (1997). Optimal Geometric Arrangement of Staggered Plates in Forced Convection. International Journal of Heat and Mass Transfer. 40, p. 1795-1805

Fukano, T., Kariyasaki, A., 1993. Characteristics of gas–liquid two-phase flow in a capillary. Nucl. Eng. Des. 141, 59–68.

Frankiewicz, T., Browne, M. M., & Lee, C.-M. (2001). Reducing Separation Train Sizes and Increasing Capacity by Application of Emerging Technologies. Paper presented at the Offshore Technology Conference, Houston, Texas. https://doi.org/10.4043/13215-MS

Gad-el-Hak, M., & Bandyopadhyay, P. R. (1994). Reynolds number effects in wall-

bounded turbulent flows. Applied Mechanics Reviews, 47(8), 307-365.

Gavrilyuk, S., & Fabre, J. (1996). Lagrangian coordinates for a drift-flux model of a gas-liquid mixture. International journal of multiphase flow, 22(3), 453-460.

Godhavn, J.-M., Fard, M. P., & Fuchs, P. H. (2005). New slug control strategies, tuning rules and experimental results. Journal of Process Control, 15(5), 547-557.

Godhavn, J.-M., Strand, S., & Skofteland, G. (2005). Increased oil production by advanced control of receiving facilities. IFAC Proceedings Volumes, 38(1), 567-572.

Gomez, C., Caldentey, J., Wang, S., Gomez, L., Mohan, R., & Shoham, O. (2002). Oil/Water Separation in Liquid/Liquid Hydrocyclones (LLHC): Part 1 - Experimental Investigation. SPE journal, 7(04), 353-372. doi:10.2118/81592-PA

Gomez, L., Shoham, O., Schmidt, Z., Chokshi, R., & Northug, T. (2000). Unified mechanistic model for steady-state two-phase flow: horizontal to vertical upward flow. SPE journal, 5(03), 339-350.

Gong, J., Yang, Z., Ma, L., & Wang, P. (2014). Severe Slugging in Air-Water Hybrid Riser System. Advances in Mechanical Engineering, 6, 953213.

Gokcal, B., Al-Sarkhi, A., Sarica, C., & Al-safran, E. M. (2010). Prediction of slug frequency for high-viscosity oils in horizontal pipes. SPE Projects, Facilities & Construction, 5(03), 136-144.

Gregory, G., & Scott, D. (1969). Correlation of liquid slug velocity and frequency in horizontal co-current gas-liquid slug flow. AIChE Journal, 15(6), 933-935.

Greskovich, E. J., & Shrier, A. L. (1972). Slug frequency in horizontal gas-liquid slug flow. Industrial & Engineering Chemistry Process Design and Development, 11(2), 317-318.

Heywood, N., & Richardson, J. (1979). Slug flow of air-water mixtures in a horizontal pipe: Determination of liquid holdup by γ-ray absorption. Chemical Engineering Science, 34(1), 17-30.

Hagedorn, A. R., & Brown, K. E. (1965). Experimental Study of Pressure Gradients Occurring During Continuous Two-Phase Flow in Small-Diameter Vertical Conduits. doi:10.2118/940-PA

García, F., García, R., Padrino, J.C., Mata, C., Trallero, J.L. and Joseph, D.D. (2003). Power law composite power law friction factor correlations for laminar turbulent gas–liquid flow in horizontal pipelines', Int. J. Multiphase Flow, vol. 29, no. 10, pp. 1605–1624.

Gudimetla, Carroll, A., Havre, K., Christiansen, C., & Canon, J. (2006). Gulf of Mexico Field of the future: subsea flow assurance. in Offshore Technology Conference. 2006 Offshore Technology Conference.

Hassanein, T., & Fairhurst, P. (1998). 'Challenges in the Mechanical and Hydraulic Aspects of Riser Design for Deep Water Developments. Paper presented at the Deepwater Technology Conference, Oslo, Norway.

Havre, K., & Dalsmo, M. (2001). Active feedback control as the solution to severe slugging. Paper presented at the SPE Annual Technical Conference and Exhibition.

Havre, K., Stornes, K. O., & Stray, H. (2000). Taming slug flow in pipelines. ABB review, 4, 55-63.

Hedne, P., & Linga, H. (1990). Suppression of terrain slugging with automatic and manual riser choking. Advances in Gas-Liquid Flows, 155(19), 453-460.

Helgesen, A. H. (2010). Anti-slug control of two-phase flow in risers with: Controllability

analysis using alternative measurements. Master's thesis, NTNU.

Henriot, V., Courbot, A., Heintze, E., & Moyeux, L. (1999). Simulation of process to control severe slugging: Application to the dunbar pipeline. Paper presented at the

Hill, T. (1990). Gas injection at riser base solves slugging flow problems. Oil and Gas Journal;(USA), 88(9).

Hill, T., & Wood, D. (1994). Slug flow: Occurrence, consequences, and prediction. Paper presented at the University of Tulsa Centennial Petroleum Engineering Symposium.

Hubbard, M.G., An analysis of horizontal gas-liquid slug flow. 1965: Tex. University of Houston.

Hudson, J.D., Dutsch, D.B., Lang P.P, Lorimer SL, Stevens KA, (2002). An overview of the Na Kika flow assurance design. in Offshore Technology Conference. 2002 Offshore Technology Conference.

Ing Youn Chen, Kai-Shing Yang, Yu-Julie Chang, Chi-Chung Wang (2001) Two-phase pressure drop of air–water and R-410A in small horizontal tubes, International Journal of Multiphase Flow, 27(7) 1293-1299, ISSN 0301-9322.

Ishii M., Hibiki T. (2011). One-Dimensional Two-Fluid Model. In: Thermo-Fluid Dynamics of Two-Phase Flow. Springer, New York, NY

Jahanshahi, E., & Skogestad, S. (2011). Simplified dynamical models for control of severe slugging in multiphase risers. IFAC Proceedings Volumes, 44(1), 1634-1639.

Jahanshahi, E., Skogestad, S., & Grøtli, E. I. (2013a). Anti-slug control experiments using

nonlinear observers. Paper presented at the American Control Conference (ACC), 2013.

Jahanshahi, E., Skogestad, S., & Grøtli, E. I. (2013b). Nonlinear model-based control of two-phase flow in risers by feedback linearization.

Jahanshahi, E., Backi, C.J. & Skogestad, S. (2017) Anti-slug control based on a virtual flow measurement. Flow Measurement and Instrumentation. **53**: p. 299-307.

Jahanshahi, E., Skogestad, S. & Grøtli, E.I. (2013). Anti-slug control experiments using nonlinear observers. in American Control Conference (ACC). 2013 IEEE.

Jahanshahi, E., Skogestad, S & Helgesen, A.H. (2012). Controllability analysis of severe slugging in well-pipeline-riser systems. IFAC proceedings. **45**(8): p. 101-108.

Jahanshahi, E. & S. Skogestad (2014). Simplified dynamic models for control of riser slugging in offshore oil production. Oil and Gas Facilities. **3**(06): p. 80-88.

Johal, K.S. and Cousins, A.R.(2001) Intelligent production riser. Google Patents.

Jansen, F., & Shoham, O. (1994). Methods for eliminating pipeline-riser flow instabilities. Paper presented at the SPE Western Regional Meeting.

Jansen, F., Shoham, O., & Taitel, Y. (1996). The elimination of severe slugging—experiments and modeling. International journal of multiphase flow, 22(6), 1055-1072.

Kattan, N. (1996), Contribution to the heat transfer analysis of substitute refrigerants in evaporator tubes with smooth or enhanced tube surfaces, PhD thesis, No 1498, Swiss Federal Institute of Technology, Lausanne, Switzerland.

Kandlikar, S.G. (2002) Fundamental issues related to flow boiling in mini-channels and

micro-channels**.** Exp Therm Fluid Sci, 26, pp. 389-407

Keulegan, G. H. (1958). Forces on cylinders and plates in an oscillating fluid. J. Research of the National Bureau of Standards Research Paper, 2857, 423-440.

Kjeldby, T., Henkes, R., & Nydal, O. (2013). Lagrangian slug flow modeling and sensitivity on hydrodynamic slug initiation methods in a severe slugging case. International journal of multiphase flow, 53, 29-39.

Knudsen, B. L., Bjørkhaug, M., Johannesen, B., Ottøy, M., Sørensen, Ø., Eidsmo, G. S., & Bruun, T. (2010). Field Test of Compact Cyclonic Technology for Separation of Gas/liquid and Oil/water at The Gullfaks Field. Paper presented at the Offshore Technology Conference, Houston, Texas, USA. https://doi.org/10.4043/20748-MS

Kristiansen, O., Sørensen, Ø., & Nilssen, O. (2016). CompactSep™-Compact Subsea Gas-Liquid Separator for High-Pressure Wellstream Boosting. Paper presented at the Offshore Technology Conference.

Kristiansen, T. G. (2004). Drilling Wellbore Stability in the Compacting and Subsiding Valhall Field. Paper presented at the IADC/SPE Drilling Conference, Dallas, Texas. https://doi.org/10.2118/87221-MS

Kristiansen, O. (2004). Experiments on the transition from stratified to slug flow in multiphase pipe flow.

Kokal, S. and Stanislav, J. (1989). An experimental study of two-phase flow in slightly inclined pipes—II. Liquid holdup and pressure drop. Chemical Engineering Science. **44**(3): p. 681-693.

Kline, S.J. and McClintock, F. A. (1953). Describing uncertainties in single sample experiments, Mech. Eng., p.3

Kawaji, M., Chung, P.M.Y., Kawahara, A. (2001). Instantaneous velocity profiles and characteristics of pressure-driven flow in microchannels. In: Proceedings of 2001 ASME IMECE, November 11–16, 2001, New York, pp. 1–11.

Lacy, C. E., Groote, G., Chao, R., Osemwinyen, E., Fleyfel, F., & Akinmoladum, O. (2014). Increasing Production by Applying Field-proven Active Slug Suppression Technology. Paper presented at the SPE Annual Technical Conference and Exhibition, Amsterdam, The Netherlands. https://doi.org/10.2118/170731-MS

Lage, A. C. V. M., & Time, R. W. (2000). Mechanistic Model for Upward Two-Phase Flow in Annuli. Paper presented at the SPE Annual Technical Conference and Exhibition, Dallas, Texas. https://doi.org/10.2118/63127-MS

Lawson, C. (2002) Na Kika Operability Review, October in Offshore Technology Conference and Exhibition. Houston. p. 6-9. 3.

Henkes, R. (2011). Fast model based approximation of the closed-loop performance limits of gas/liquid inline separators for accelerated design. IFAC Proceedings Volumes, 44(1), 12307-12312.

Li, W., Guo, L., & Xie, X. (2017). Effects of a long pipeline on severe slugging in an S-shaped riser. Chemical Engineering Science, 171, 379-390.

Lin, S., Kwok, C.C.K., Li, R.Y., Chen, Z.H., Chen, Z.Y., (1991). Local frictional pressure drop during vaporization for R-12 through capillary tubes. Int. J. Multiphase Flow 17, 95–102.

Lieungh, M. (2012). Stabilizing Slug Control Using Subsea Choke Valve. Institutt for

teknisk kybernetikk.

Løhndorf, P. D., Pedersen, S., & Yang, Z. (2018). Efficiency Control in Offshore Deoiling Installations. Computers and Chemical Engineering.

Luo, X., He, L., Liu, X., & Lü, Y. (2014). Influence of separator control on the characteristics of severe slugging flow. Petroleum Science, 11(2), 300-307.

Malekzadeh, R., Henkes, R., & Mudde, R. (2012). Severe slugging in a long pipeline–riser system: Experiments and predictions. International journal of multiphase flow, 46, 9-21.

Malekzadeh, R., Mudde, R., & Henkes, R. (2012). Dependence of severe slugging on the orientation angle of the pipeline upstream of the riser base. Paper presented at the 8th North American Conference on Multiphase Technology.

Marcano, R., Chen, X. T., Sarica, C., & Brill, J. P (1998). A study of slug characteristics for two-phase horizontal flow. in International Petroleum Conference and Exhibition of Mexico. Society of Petroleum Engineers.

Masella, J., Tran, Q., Ferre, D., & Pauchon, C. (1998). Transient simulation of two-phase flows in pipes. International journal of multiphase flow, 24(5), 739-755.

McCain, W. (1990). The properties of Petroeleum Fluids. PennWell Publishing Company. Tulsa Oklahoma.

McAdams, W.H. (1954). Heat Transmission, third ed. McGraw-Hill, New York.

Meringdal, E. H. (2014). Comparative study of different Methods for Slug control. Institutt for produksjons-og kvalitetsteknikk,

Robert J. Moffat (1988). Describing the uncertainties in experimental results, Experimental Thermal and Fluid Science, **1**(1): p. 3-17.

Mo, S., Chen, X., Chen, Y. et al. Korean. (2015). Effect of geometric parameters of liquid-gas separator units on phase separation performance. J. Chem. Eng., 32: 1243. doi: https://doi-org.qe2a-proxy.mun.ca/10.1007/s11814-014-0353-3

Mokhatab, S. (2007). Severe slugging in a catenary-shaped riser: Experimental and simulation studies. Petroleum science and technology, 25(6), 719-740.

Mokhatab, S., & Towler, B. (2007). Severe slugging in flexible risers: Review of experimental investigations and OLGA predictions. Petroleum Science and Technology, 25(7), 867-880.

Movafaghian, S., Jaua-Marturet, J., Mohan, R. S., Shoham, O., & Kouba, G. (2000). The effects of geometry, fluid properties and pressure on the hydrodynamics of gas–liquid cylindrical cyclone separators. International journal of multiphase flow, 26(6), 999-1018.

Minami, K. and Shoham, O. (1994). Transient two-phase flow behavior in pipelines-experiment and modeling. International journal of multiphase flow. **20**(4): p. 739-752.

Mishima, K. Ishii, M (1984). Flow regime transition criteria for upward two-phase flow in vertical tubes**.** Int J Heat Mass Transfer, 27, pp. 723-737

Manolis, I., Mendes-Tatsis, M., & Hewitt, G. (1995). The effect of pressure on slug frequency in two-phase horizontal flow. In Multiphase Flow 1995 (pp. 347-354): Elsevier.

Nada, S.A. (2017). Experimental investigation and empirical correlations of heat transfer

in different flow regimes of air-water two-phase flow in a horizontal tube. Journal of Thermal Science and Engineering Applications. 9. 021004-1. 10.1115/1.4034903

Mukherjee, H. and Brill, J.P. (1985). Pressure Drop Correlations for Inclined Two-Phase Flow, J. Energy Res. Tech. 107,549.

Naterer, G. F. (2018). Advanced Heat Transfer, 2nd Edition, CRC Press, Boca Raton.

Nemoto, R. H., & Baliño, J. L. (2012). Modeling and simulation of severe slugging with mass transfer effects. International journal of multiphase flow, 40, 144-157.

Nemoto, R.H., Baliño, J.L. & K.P. Burr (2009). Characteristic values and compatibility conditions for the no-pressure-wave model applied to petroleum systems. in Proceeding of the 20th International Congress of Mechanical Engineering. Gramado, RS, Brazil, paper code COB09-0748.

Nicklin D.J. and Davidson J.F. (1962) Symp. Two-phase Fluid Flow, 7 February 1962. Proceedings of the Institute of Mechanical Engineers.

Nydal, O., Audibert, M., & Johansen, M. (2001). Experiments and modeling of gas-liquid flow in a S-shaped riser. Paper presented at the Proceedings of the 10th International Conference on Multiphase Technology.

Nydal, O., Pintus, S., & Andreussi, P. (1992). Statistical characterization of slug flow in horizontal pipes. International journal of multiphase flow, 18(3), 439-453.

Ogazi, A. I. (2011). Multiphase severe slug flow control. Ph. D. Thesis, Cranfield University, United Kingdom.

Osman, E.S. A. (2001). Artificial neural networks models for identifying flow regimes and predicting liquid holdup in horizontal multiphase flow. Paper presented at the SPE Middle East Oil Show.

Orkiszewski, J. (1967). Predicting two-phase pressure drops in vertical pipe. JPT. 829-838; Trans., AIME, 240.

Owens, W.L. (1961). Two-phase pressure gradient. Int. Dev. in Heat Transfer, Pt II. ASME, New York.

Park, S., & Nydal, O. J. (2014). Study on severe slugging in an S-shaped riser: small-scale experiments compared with simulations. Oil and Gas Facilities, 3(04), 72-80.

Pedersen, S. (2016). Plant-Wide Anti-Slug Control for Offshore Oil and Gas Processes. Ph. D. Thesis, Aalborg University, Aalborg, Denmark.

Pedersen, S., Durdevic, P., Stampe, K., Pedersen, S. L., & Yang, Z. (2016). Experimental study of stable surfaces for anti-slug control in multiphase flow. International Journal of Automation and Computing, 13(1), 81-88.

Pedersen, S., Durdevic, P., & Yang, Z. (2015). Review of Slug Detection, Modeling and Control Techniques for Offshore Oil & Gas Production Processes∗. IFAC-PapersOnLine, 48(6), 89-96.

Pedersen, S., Durdevic, P., & Yang, Z. (2017). Challenges in slug modeling and control for offshore oil and gas productions: A review study. International journal of multiphase flow, 88, 270-284.

Pedersen, S., Løhndorf, P. D., & Yang, Z. (2017). Influence of riser-induced slugs on the downstream separation processes. Journal of Petroleum Science and Engineering, 154, 337-343.

Pedersen, S., Jahanshahi, E., Skogestad, S., & Yang, Z. (2014). Comparison of Model-Based Control Solutions for Severe Riser-Induced Slugs. Energies, 2017. **10**(12).

Petalas, N., & Aziz, K. (1998). A mechanistic model for multiphase flow in pipes. Paper presented at the Annual Technical Meeting.

Pinder, G. F., Gray, W.G. (2008). Essentials of multi-phase flow and transport in porous media. Hoboken, N.J. Wiley-Inter-science. ISBN 9780470317624.

Pots, B. F., Bromilow, I. G., & Konijn, M. J. (1987). Severe slug flow in offshore flowline/riser systems. SPE Production Engineering, 2(04), 319-324.

Ragab, A.S. (2008). Simulation of hydrodynamic slug formation in multi-phase flowlines and separation devices. PhD Thesis. Multan Universitat, Leoben.

Reynolds, Osborne (1883). An experimental investigation of the circumstances which determine whether the motion of water shall be direct or sinuous, and of the law of resistance in parallel channels. Philosophical Transactions of the Royal Society. **174**: 935–982.

Ruiz-Cárcel, C., Cao, Y., Mba, D., Lao, L., & Samuel, R. (2015). Statistical process monitoring of a multiphase flow facility. Control Engineering Practice, 42, 74-88.

Sarica, C., & Tengesdal, J. Ø. (2000). A new technique to eliminate severe slugging in pipeline/riser systems. Paper presented at the SPE annual technical conference and exhibition.

Sarica, C. t., & Shoham, O. (1991). A simplified transient model for pipeline-riser systems. Chemical Engineering Science, 46(9), 2167-2179.

Schmidt, Z., Brill, J., & Beggs, H. (1979). Choking can eliminate severe pipeline slugging. Oil & gas journal, 77(46), 230-&.

Schmidt, Z., Brill, J. P., & Beggs, H. D. (1980). Experimental study of severe slugging in

a two-phase-flow pipeline-riser pipe system. Society of Petroleum Engineers Journal, 20(05), 407-414.

Schmidt, Z., Doty, D. R., & Dutta-Roy, K. (1985). Severe slugging in offshore pipeline riser-pipe systems. Society of Petroleum Engineers Journal, 25(01), 27-38.

Schmid, P.J. & Henningson, D.S. (2012). Stability and transition in shear flows. Vol. 142: Springer Science & Business Media.

Schulkes, R. (2011). Slug frequencies revisited. Paper presented at the 15th International Conference on Multiphase Production Technology.

Schook, R., & Thierens, D. (2011). Debottlenecking of Mature Field Production through the Use of Very Compact and Efficient Separation Equipment, Topside or Subsea. Paper presented at the Offshore Technology Conference.

Schook, R., & Van Asperen, V. (2005). Compact separation by means of inline technology. Paper presented at the SPE Middle East Oil and Gas Show and Conference, Kingdom of Bahrain. https://doi.org/10.2118/93232-MS

Scibilia, F., Hovd, M., & Bitmead, R. R. (2008). Stabilization of gas-lift oil wells using topside measurements. IFAC Proceedings Volumes, 41(2), 13907-13912.

Shea, R., Eidsmoen, H., Nordsveen, M., Rasmussen, J., Xu, Z., & Nossen, J. (2004). Slug frequency prediction method comparison. Paper presented at the Proceedings of the 4th North American Conference on Multiphase Technology.

Saisorna, S., Wongwises, S. (2006), A review of two-phase gas-liquid adiabatic flow characteristics in microchannels. Renewable and Sustainable Energy R12 pp 824–838.

Saisorn, S., Wongwises, S. (2008), A review of two-phase gas-liquid adiabatic flow

characteristics in microchannels, Renewable and Sustainable Energy Reviews, Volume 12, Issue 3, 2008, P 824-838, ISSN 1364-0321.

Skofteland, G., & Godhavn, J. (2003). Suppression of slugs in multiphase flowlines by active use of topside choke-field experience and experimental results. Proc. of MultiPhase'03, San Remo, Italy, 11-13 June 2003.

Storkaas, E. (2005). Anti-slug control in pipeline-riser systems. PhD thesis, Norwegian University of Science and Technology,

Storkaas, E. (2005). Stabilizing control and controllability. Control solutions to avoid slug flow in pipeline-riser systems.

Storkaas, E., & Skogestad, S. (2004). Cascade control of unstable systems with application to stabilization of slug flow. IFAC Proceedings Volumes, 37(1), 335-340.

Storkaas, E., & Skogestad, S. (2007). Controllability analysis of two-phase pipeline-riser systems at riser slugging conditions. Control Engineering Practice, 15(5), 567-581.

Storkaas, E., Skogestad, S., & Godhavn, J.M. (2003). A low-dimensional dynamic model of severe slugging for control design and analysis. Paper presented at the 11th International Conference on Multiphase flow (Multiphase03).

Smith, J.M., Van, N., Hendrick, C., and Abbot, M. (2001) Introduction to Chemical Engineering Thermodynamics. McGraw-Hill.

Sukubo, I., & Igboanugo, A. (2012). Improved Analytical Model for Predicting Field Production Performance in Vertical Multiphase Flow in Pipes using MATLAB: A Case Study&Part II. Paper presented at the Nigeria Annual International Conference and Exhibition.

Suo, M., Griffith, P. (1964). Two-phase flow in capillary tubes. J. Basic Eng. 86, 576–582.

Swanborn, R., & Egwim, R. C. (2011). Accelerated production and increased recovery of emote (offshore) mature fields through novel methods to design and operate surface production facilities. Paper presented at the Offshore Technology Conference.

Taitel, Y. (1986). Stability of severe slugging. International journal of multiphase flow, 12(2), 203-217.

Taitel, Y., Bornea, D., & Dukler, A. (1980). Modelling flow pattern transitions for steady upward gas-liquid flow in vertical tubes. AIChE journal, 26(3), 345-354.

Taitel, Y., & Dukler, A. E. (1976). A model for predicting flow regime transitions in horizontal and near horizontal gas-liquid flow. AIChE journal, 22(1), 47-55.

Taitel, Y., Vierkandt, S., Shoham, O., & Brill, J. (1990). Severe slugging in a riser system: experiments and modeling. International journal of multiphase flow, 16(1), 57-68.

Taitel, Y. and A. Dukler (1977). A model for slug frequency during gas-liquid flow in horizontal and near horizontal pipes. International Journal of Multiphase Flow. **3**(6): p. 585-596.

Tengesdal, J., Sarica, C., & Thompson, L. (2002). Severe slugging attenuation for deepwater multiphase pipeline and riser systems. Paper presented at the SPE Annual Technical Conference and Exhibition.

Trononi, E. (1990). Prediction of slug frequency in horizontal two-phase slug flow. AIChE Journal, 36(5), 701-709.

Triplett, K.A., Ghiaasiaan, S.M., Abdel-Khalik, S.I., LeMouel, A., McCord, B.N. (1999). Gas–liquid two-phase flow in microchannels. Part II: void fraction and pressure drop. Int. J. Multiphase Flow 25, 395–410.

Tengesdal, J., Thompson, L., & Sarica, C. (2003). A Design Approach for" Self-Lifting"

Method to Eliminate Severe Slugging in Offshore Production Systems. Paper presented at the SPE Annual Technical Conference and Exhibition.

Vierkandt, S. (1988). Severe Slugging in a Pipeline-Riser System. Experiments and Modeling.

Vierkandt, S. J. (1988). Severe Slugging in a Pipeline-riser System: Experiments and Modeling: Tulsa University Fluid Flow Projects.

Williams, J. G. (1994). Composite tubing with low coefficient of expansion for use in marine production riser systems. In: Google Patents.

Wordsworth, C., Das, I., Loh, W., McNulty, G., Lima, P., & Barbuto, F. (1998). Multiphase flow behavior in a catenary shaped riser. CALtec Report No.: CR, 6820.

Wörner, M. (2003). A compact introduction to the numerical modeling of multiphase flows: Forschungszentrum Karlsruhe Karlsruhe, Germany.

Weber, M.E. (1981). Drift in intermittent two-phase flow in horizontal pipes. The Canadian Journal of Chemical Engineering. **59**(3): p. 398-399.

Xiaoming, L., Limin, H., & Huawei, M. (2011). Flow pattern and pressure fluctuation of severe slugging in pipeline-riser system. Chinese Journal of Chemical Engineering, 19(1), 26-32.

Xie, C., Guo, L., Li, W., Zhou, H., & Zou, S. (2017). The influence of backpressure on severe slugging in multiphase flow pipeline-riser systems. Chemical Engineering Science, 163, 68-82.

Yaw, S. Y., Lee, C. Y., Haandrikman, G., Groote, G., Asokan, S., & Malonzo, M. E. (2014). Smart Choke-A Simple and Effective Slug Control Technology to Extend Field Life. Paper presented at the International Petroleum Technology Conference.

Yocum, B. (1973). Offshore riser slug flow avoidance: mathematical models for design and optimization. Paper presented at the SPE European Meeting.

Zakarian, E. (2000). Analysis of two-phase flow instabilities in pipe-riser systems. ASME-PUBLICATIONS-PVP, 414(1), 187-196.

Zabaras, G. (1999). Prediction of slug frequency for gas-liquid flows. Paper presented at the SPE Annual Technical Conference and Exhibition.

Zhou, H., Guo, L., Yan, H., & Kuang, S. (2018). Investigation and prediction of severe slugging frequency in pipeline-riser systems. Chemical Engineering Science, 184, 72-84.

Zuber, N., & Findlay, J. (1967). GEAP-4517 General Electric Company.